PHYSICOCHEMICAL STUDY OF ANTIOXIDANT – SURFACTANT INTERACTION: UTILIZATION IN CLOTRIMAZOLE TOPICAL FORMULATION

A THESIS SUBMITTED IN FULFILLMENT OF THE REQUIREMENTS FOR

THE DEGREE OF DOCTOR OF PHILOSOPHY

IN

PHARMACY

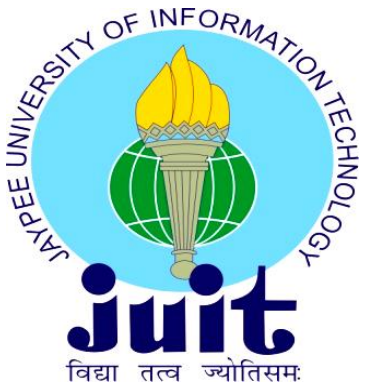

By

VARUN BHARDWAJ

JAYPEE UNIVERSITY OF INFORMATION TECHNOLOGY

WAKNAGHAT

JULY, 2014

JAYPEE UNIVERSITY OF INFORMATION TECHNOLOGY
(Established by H.P. State Legislature vide Act No. 14 of 2002)
P.O. Waknaghat, Teh. Kandaghat, Dis . Solan – 173234 (H.P.) INDIA
Website: www.juit.ac.in
Phone No. +91-01792-257999 (30 Lines).
Fax: +91-01792-245362

CERTIFICATE

This is to certify that the thesis entitled, **"Physicochemical study of antioxidant – surfactant interaction: Utilization in clotrimazole topical formulation"** submitted by **Varun Bhardwaj** to the **Jaypee University of Information Technology, Waknaghat, India** for the award of degree of **Doctor of Philosophy in Pharmacy** is a record of the candidate's own work, carried out by him under our supervision. This work has not been submitted in part or full to any other University or Institute for the award of this or any other degree or diploma.

Supervisor

Dr. Poonam Sharma
Assistant Professor
Department of Biotechnology, Bioinformatics & Pharmacy
Jaypee University of Information Technology
Waknaghat, Solan
Himachal Pradesh, 173234 INDIA
Email : drpoonamsharma@rediffmail.com

poonam.sharma@juit.ac.in

Co-supervisor

Dr. S. Chauhan
Associate Professor
Department of Chemistry
Himachal Pradesh University
Summer hill, Shimla
Himachal Pradesh, 173005 INDIA

DECLARATION

I hereby declare that the work contained in the present PhD thesis entitled **"Physicochemical study of antioxidant – surfactant interaction: Utilization in clotrimazole topical formulation"** submitted at **Jaypee University of Information Technology, Waknaghat, India,** is an authentic record of my original research work, carried out under the supervision of **Dr. Poonam Sharma** and **Dr. S. Chauhan**. This work has not been submitted in part or full for the award of any other degree or diploma in any other university/ Institute.

Signature of the Candidate

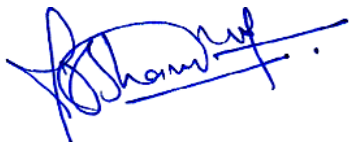

Varun Bhardwaj

Enrolment No.:106755

Department of Pharmacy,

Jaypee University of Information Technology,

Waknaghat, India

Date: 17 July, 2014.

Place: JUIT, Waknaghat.

ACKNOWLEDGEMENT

"I have been bent and broken many of times but every time got molded me into a better shape"

Primarily, I acknowledge this moment of time, which has gone just forever, but made my mind to write some special words for those who have been with me with their ever-whelming gestures throughout my PhD.

Best of my words are for my respected supervisor ***Dr. Poonam Sharma****, Assistant Professor, Department of BT/BI and Pharmacy, Jaypee University of Information Technology, Waknaghat, Solan. Her clarity of mind, intelligence and attitude for quest for perfection encouraged me to put the drop of my hypothesis in the ocean of laws and phenomena. I humbly thank her for the pulls and push, and supporting me to explore.*

I feel lack of vocabulary to express my gratitude and respect towards my co-supervisor ***Dr. S. Chauhan****, Associate Professor, Department of Chemistry, Himachal Pradesh University, Shimla without whom any attempt at any level could not be satisfactorily completed.*

I wish to express my heartiest thanks to Head of department and Dean, ***Prof. (Dr.) R. S. Chauhan****, Department of BT/BI and Pharmacy, Jaypee University of Information Technology, Waknaghat, Solan for his advice and providing me the opportunity and all necessary facilities to accomplish this endeavor successfully. I owe my sincerest thanks to all DPMC members for their kind suggestions and motivation time to time.*

I also want to quote my special thanks to ***Dr. Shailesh Sharma****, Assistant Professor, ASBASJSM College of Pharmacy, Bela and* ***Prof. Singh*** *IMTECH, Chandigarh for sharing useful knowledge and providing facilities during my research work. I also want to thank* ***Prof. (Dr.) M.S. Chauhan****, Department of Chemistry, HPU Shimla, for the guidelines. I also want to thank* ***Mr. Amit Sharma****, PGIMER for collaborative work and support. I am equally thankful to our non teaching staff especially* ***Mr. Amar*** *and* ***Mrs Sonica Gupta*** *for extending help and co-operation.*

Importantly, the man who believed in me few years back and his efforts which describes me the person I am today, ***Prof. (Dr.) Malleshappa N. Noolvi****, whose moral support was always been there. His motivation always made me stronger to accept challenges, get into them and complete them; thank you so much. I express my sincere love and affection towards all those benevolent souls and true friends* **Neeraj Dharma, Sachin Chauhan, Vishal Sharma, Sandeep Sharma, Talwinder Singh Kanwar, Kundan Sharma, Arun Sharma, Rakesh Gaur, Sumit Bansal and Suthar Sharad Kumar.** *I would also like to thank to my beloved juniors; Vikrant Abbot, Saurabh*

Dhiman, and Tanvi Chaudhary for their well wishes. I would like to add heartfelt words for my Seniors ***Dr. Harun M. Patel*** *,* ***Dr. Jitender Monga,*** *Research Associate, PGIMER and* ***Dr. Varun Jaiswal,*** *Assistant Prof., Shoolini University who had always been a motivation for me in my ups and downs and always being there for me, both in good and bad times.*

I would like to offer my sincere thanks to Department of Science and Technology ***(DST) Govt. of India****, New Delhi, for financial grant (ref. no.* ***SR/FT/CS-59/2009****) in the form of major project as well as for* ***Young scientist International travel fellowship*** *to attend an international conference and present my research work as oral lecture. Sincere thanks to* ***SAIF Department*** *Punjab University, Chandigarh, for co-operation in analysis of the samples.*

Above all my heartfelt veneration go to my ***Mother*** *and* ***Father*** *who put me on the path and taught how to take my first step into the journey of life. My younger brother and lab team member* ***Tarun Bhardwaj*** *is the soul of my energy. He always motivated me towards achieving my goals. I cannot repay their silent patience and constant encouragement. Last but not the least a mentor; Ms. Shikha, who wordlessly provided me her moral support and the right impetus to undertake the challenges of this proportion like all other spheres of life. It was like her and my father who dreamt and believed what I am capable of achieving.*

For me, the road towards completion of this thesis was not a bed of roses. On various stages, I felt low and almost lost the hope of accomplishing whatever I had planned theoretically but the support of my well-wishers saw me through the twist and turns of the roads. And So, I again thank the Almighty for providing me an excellent opportunity to be amidst gentle, helpful and virtuous people.

The expertise in this study belongs to those acknowledged above. All errors are mine.

Varun Bhardwaj

DEDICATION

This thesis is dedicated to my parents, my younger brother and my loved ones, who raised me to be the person I am today. You have been with me every step of the way, through good times and bad. Thank you for all the unconditional love, guidance, and support that you have always given me, helping me to succeed and instilling in me the confidence that I am capable of doing anything I put my mind to.

Thank you for everything

LIST OF FIGURES

LIST OF TABLES

Abstract

Micellar systems hold excellent drug delivery applications due to their capability to solubilize a large number of hydrophobic and hydrophilic molecules. In this present work, the mixed micelle formation between three surfactants (SDS, CTAB and Triton X-100) and two synthetic lipophilic antioxidants (BHA and BHT) have been studied in different alcohols and hydroalcoholic mediums i.e. 100%, 70% and 30% of MeOH, EtOH and 1-PrOH. Early micellization was found with critical micelle concentration (CMC) shifting towards lower concentration. In this context, conductance study, CMC, standard thermodynamic parameters of micellization namely ΔH_m^o, ΔG_m^o and ΔS_m^o have been evaluated at different temperatures. Molar volume and compressibility measurements have also been carried out to evaluate the apparent molar volume (ϕ_v) and apparent molar adiabatic compression (ϕ_k) of BHA/BHT – surfactant complex and discussed in terms of the solute – solute and solute – solvent interactions. In addition spectroscopic analysis (FTIR and ^{1}H–NMR) confirmed the presence of intermolecular interaction between antioxidants – surfactant molecules within studied concentration. From spectroscopic studies, the order of shifting suggested the existence of intermolecular interaction especially, in the hydrophilic region of surfactant. However, BHA and BHT have been known as potential antioxidants with antimicrobial property. In an attempt to develop better formulation of clotrimazole (CLZ) with antifungal profile, surfactant aided antioxidants micellar system was dispersed within CLZ gel formulation. Initially, the gel library was prepared (27 formulations) and subjected to *in vitro* evaluation. Based on *in vitro* release and kinetic profile, best three formulations were selected for further analysis. Moreover, *in vitro* antifungal activity (MIC μg/ml) and fractional inhibitory concentration index (FICI) against different drug resistant and susceptible *Candida* isolates were carried and directed to the best among 3 formulations. The optimized best selected formulation was thereafter evaluated via morphology studies and *in vivo* antifungal evaluation. Morphology studies depicted the distribution of micellar structures within the polymeric gel network as well as the contact activity mechanism against *Candida albicans*. The physicochemical characterization showed that average micellar size was lower than ~ 160 nm, low polydispersity index, negative zeta potential and gel pH 6.9. After 60 days, no significant change was observed within the formulation. Photostability studies revealed that antioxidants' eminently inhibits the drug degradation under UV radiations with improved drug stability. In addition, *in vivo* antifungal activity was carried out on experimentally induced cutaneous

infection in immunosuppressed *Sprague Dawley* (SD) rats. Then, *in vivo* study confirmed the maximum therapeutic efficacy, as the lowest number of cfu/ml was recorded. Conclusively, this study provide a good skin targeting effect and may be promising for stable and effective topical delivery of CLZ offering maintained localized effect.

Key words: Physicochemical interaction; Thermodynamics; Micellization; Acoustical study; Spectroscopy; Antioxidants; Surfactants; Clotrimazole; Formulation; *In vitro* analysis; *In vivo* evaluation.

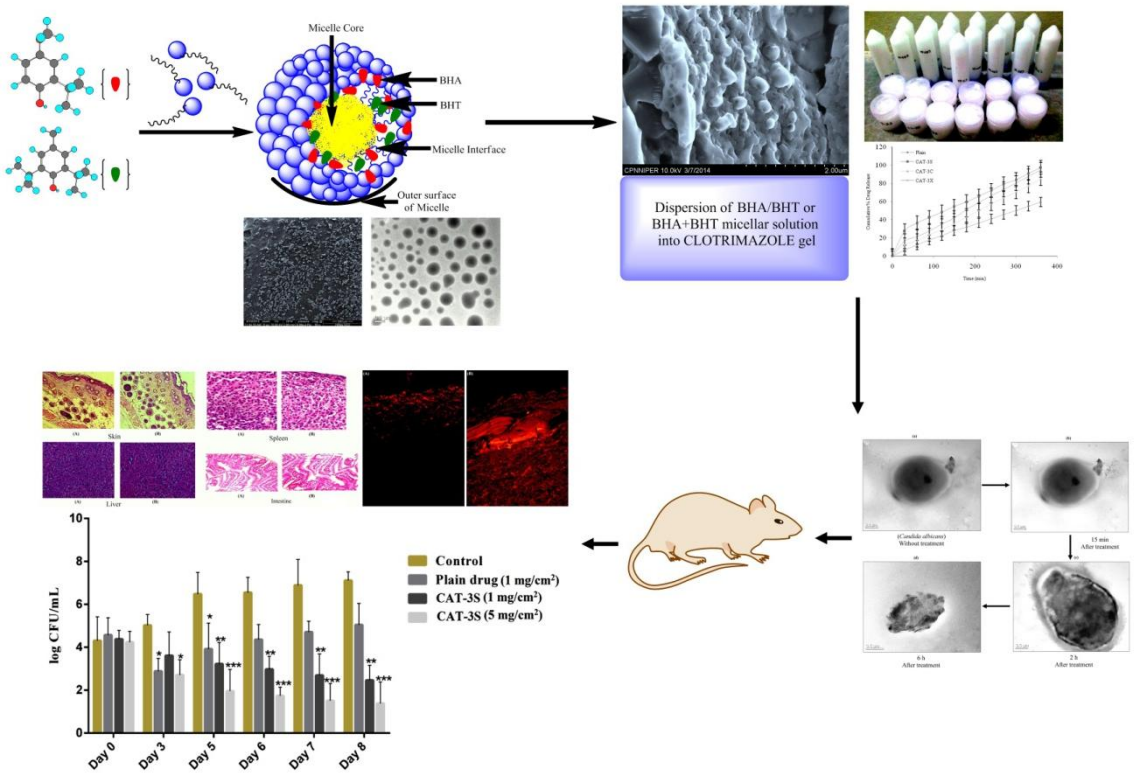

Graphical Abstract

CHAPTER-1

INTRODUCTION

1.1 General Introduction

The best wealth of mankind is good health as it goes "*Health is wealth*". Human put best of his efforts and adopt good habits and life style which enable him to enjoy the health, but, since many ages he gets encountered with various types of diseases affecting his health and well-being [1]. Effort to cure diseases has been leading in the discovery of various drugs, formulations and delivery systems [2]. To get therapeutic response of drug required for treatment of disease different routes of administration are opted. Routes of administration are usually classified by application location (or exposition) which is a matter of pharmacokinetics (concerning the physiological effects of drugs). Factors governing the choice of route are (i) physical and chemical properties of drug (solubility/stability or pH etc.), (ii) site of desired action, (iii) rate and extent of absorption of drug [3].

A most common challenge faced by pharmaceutical scientists is to design and develop drugs or design formulations with good aqueous solubility while simultaneously retaining potency and selectivity. The limited solubility along with metabolic stability and limited permeability across the biological membrane leads to poor bioavailability of drug which in turn affects the drug delivery system [4]. The drugs with poor aqueous solubility necessitate the use of various additives, excipients and co-solvents to produce suitable formulation. In recent decade, antioxidants and surfactants in formulation is one of the most employed classes to attain desired functionality with their additive effects such as synergism and stability. As, the bioactive molecules find their way into biological systems through membranes. These membranes have lipid bilayered structures, which resembles very closely with surfactant molecules [5, 6].

Surfactants are well known to possess self-assembly structure and interactions which acts as an alternative system for the delivery of biological active molecules in order to bring significant change in their pharmacological profile [7]. The fundamental property of surfactant at certain concentration in specific solution medium is commonly known as aggregates, so-called micelles [8]. Thus micellar solution forms an alternative approach in delivery of bioactive compounds. The molecular organization of micellar system depends on the delicate interplay between hydrophobic and hydrophilic interactions which are responsible for structural organization in living systems. So, these physico-chemical interaction such as electrostatic, hydrophilic, hydrogen bonding and hydrophobic interactions etc. play a decisive

role in improvement of formulation and delivery system [9]. In this context, thermo-acoustic parameters can be used to examine the transport property of surfactants in presence of bioactive molecules which can latterly dispersed into specific topical formulation base to gain desired effect.

Now days, antifungal drug resistance is a serious and growing phenomenon in contemporary medicine and has developed as one of the pre-eminent public health concerns of the 21st century, particularly as it pertains to pathogenic organisms [10, 11]. Therefore, new topical prophylactic formulation that exhibit rapid, potent and direct fungicidal activity is in urgent need. Drug tolerant may depend on physiological adaptations without direct connections to drug target activity or to drug uptake, efflux or inactivation [12]. Identifying these adaptations, and targeting them to enhance the activity of existing drugs, is a promising approach to mitigate the public health crisis caused by the scarcity of new drugs. Keeping in mind that antifungal drug resistance is one of the most exigent problems and efforts of many of pharmaceutical chemists to develop new antifungal drug, but due to long span of time going through clinical trials, improving existing drug efficacy or biological profile could be one of the best alternative to overcome the challenges. For such improvement, relevance of combinational/dual delivery against many kinds of micro-organisms [13-15] had already been reported which showed a promising future for medical application.

In this context, we intended our study via employing simple and promising approaches to evaluate interactions, region of micellization in addition to other thermo-acoustic parameters usually called as physico-chemical study and spectroscopic analysis with determination of location of two potential synthetic antioxidants in micellar structure of different types of surfactants. Finally, utilizing the physico-chemical analysis in the formulation of clotrimazole topical gel with dispersion of surfactant aided antioxidants and then lastly, antifungal evaluation of different surfactant aided formulations.

1.2 Antioxidant

An antioxidant is a bioactive moiety that originally can be referred to molecules that retard or prevent the utilization of oxygen by human tissues and known to prevent the oxidative system as a whole. Antioxidants holds two major categories and can be classified either as primary or secondary antioxidants. Primary antioxidants are those which actively inhibit oxidation reaction whereas later one inhibits oxidation indirectly by various mechanisms such as

oxygen-scavenging, binding pro-oxidants etc. They may either delay or inhibit the initiation step by reacting with a free radical or inhibit propagation by reacting with peroxy or alkoxy radicals [16]. Primary antioxidant chemical reaction can be categorized into hydrogen-atom transfer (HAT) and single-electron transfer (SET). Both HAT and SET are quite applicable for phenolic antioxidant action. Secondary antioxidants are also known as preventive antioxidants functionalized by decomposition of peroxides into stable products [17].

It has been proposed that the antioxidant properties of phenolic compounds can be mediated by the following mechanisms: (a) scavenging radical species such as ROS/RNS; (b) suppressing ROS/RNS formation by inhibiting some enzymes or chelating trace metals involved in free radical production; (c) up-regulating or protecting antioxidant defense [139]. The process of oxidation involves the transfer of electrons between molecules to oxidizing agents. This transfer of electrons between molecules gives rise to radicals (free radicals). The important oxidation mechanism is commonly well known as auto-oxidation [17]. The free radical chain reaction and the mechanism of auto-oxidation involve three main steps which are as follows [18-20]:

Initiation

Initiation reaction is initiated by the abstraction of hydrogen radical from allylic methylene group as presented in chemical reaction (Figure 1.1). The formation of lipid radical is mediated by tiny metals, light and heat etc. This is followed by hemolytic cleavage in which hydroperoxides form alkoxy radicals.

Propagation

Propagation of free radical oxidation process occurs by chain reaction that consumes oxygen and yield new radicals i.e. peroxy radicals ($ROO^{\bullet}$) or by following ROOH formation as shown in reaction (Figure 1.1). The existing products $R^{\bullet}$ and $ROO^{\bullet}$ can also propagate further free radical reactions where ROO starts a reaction with other molecules leading to the formation of hydroperoxides and free radicals. This chain reaction can occur repeatedly causing hydroperoxides accumulation.

Termination

Termination reaction is known to interrupt the repetition order of propagation step. When coupling exists between two radicals, the reaction is recognized as dimerization. The

explained flowchart representing initiation, propagation and termination step is presented in Figure 1.1.

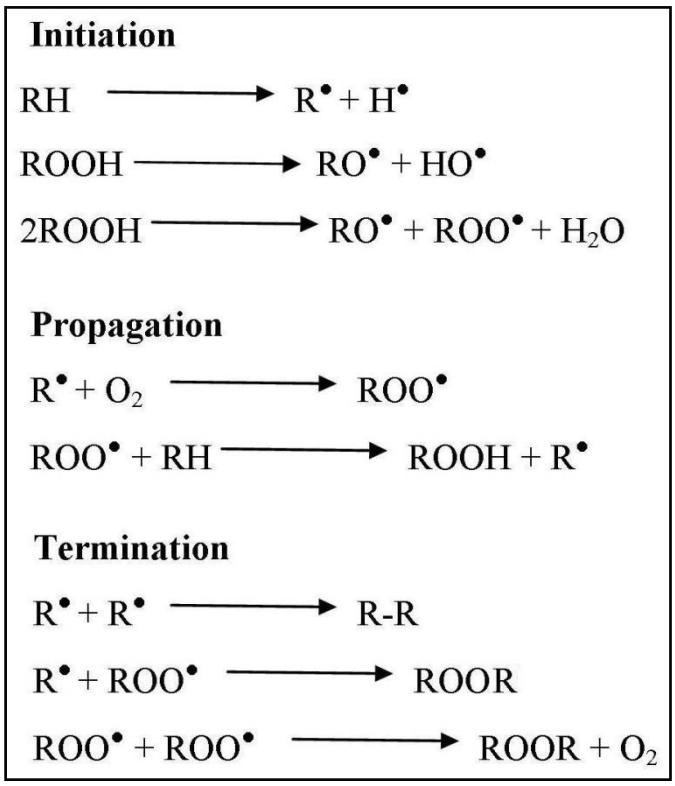

Figure 1.1: Representation of auto-oxidation mechanism.

Historically, Bert Hollet in 1797 and latter Davy, recorded the first scientific observation on oxidation inhibitors. They described their theory as 'catalyst poisoning' in oxidative reactors. Thereafter, report on the use of antioxidants to retard lipid oxidation appeared in 1843 in which Deschamps showed that an ointment containing gum benzoin did not become rancid. Lately, many reports came with the possibility of using antioxidants and phenolic synthetic compounds to retard oxidative decomposition. In 1930s, gum guaiac was the first antioxidant approved for the stabilization of animal fats [21]. Antioxidants with unique properties of enhancing shelf life without any damage to product qualities include tocopherol, β-carotene, vitamins, butylatedhydroxy anisole (BHA), butylatedhydroxy toluene (BHT), TBHQ, rosmarinic acid and many more. Due to a wide and diverse class of bioactive antioxidant molecules [22], we have emphasized on the phenolic synthetic antioxidants i.e. BHA and BHT (Figure 1.2) with their potential use in pharmaceutical sectors. However, BHA is available as isomeric organic compounds i.e. 2-*tert*-butyl-4-hydroxyanisole and 3-*tert*-

butyl-4-hydroxyanisole, whereas, 2-*tert*-butyl-4-hydroxyanisole was undertaken in present investigation.

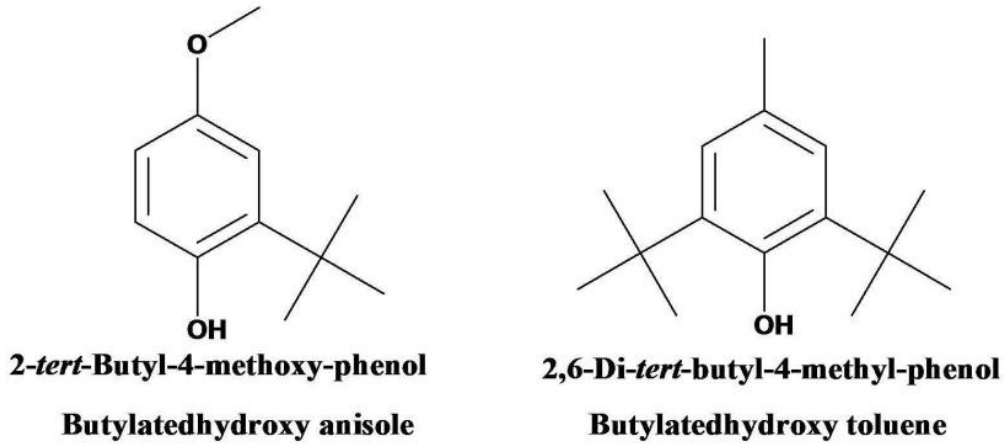

Figure 1.2: Structural representation of BHA and BHT.

The use of synthetic antioxidants such as BHA and BHT as ingredients has received increasing attention as additive. BHA is a synthetic phenolic antioxidant, authorized as an additive (E320) in the European Union for certain products. BHT also stands as another synthetic lipophilic antioxidant authorized as additive individually or in combination with other synthetic antioxidants, for a range of products by European Union. An ADI of 0-0.5mg/kg body weight was established for BHA (WHO, 1989). The lowest ADI (0-0.05mg/kg body weight) for BHT was established in 1989 on the basis of reproduction, thyroid and hematological effects observed in 90-day feeding study in the rat by the Scientific Committee for food (Commission of the European Communities, 1989). It was significant that the ADI established by the Joint Expert Committee on Food Additives (JECFA), on the basis of hepatic enzyme induction in a 22-month feeding study in the rat is six times higher (0-0.3mg/kg body weight) (WHO, 1995). Latterly, in year 2000, WHO revealed the assess intake level of BHA and BHT with certain limits [22, 23].

BHA and BHT are extensively used antioxidants in human health materials. It is interesting to note down that these lipophilic molecules works well when used together and results in synergism with much greater potency. In spite of the primary function of these compounds is to delay autoxidation, they are also reported to exhibit considerable antimicrobial activity. Their activity on bacteria such as *E. coli*, *S. tryhimurin* and *S. aureus* is well documented. They are also known to show total inhibition on *A. parasiticus* and effective against several other species such as *Asperigillus*, *Byssochlamys*, *Penicillium* and *Geotrichum*.

Beside antibacterial and antiviral activity [24] they were also found to be active against some of fungi and yeasts such as *Candida* species and *A. fumigatus* [25-29]. Owing to differences in the molecular structure, BHA and BHT exhibit substantial variation in effectiveness when employed with different types of cosmeceutical products and drug formulations.

1.3 Surfactants

The term surface active agents commonly referred to surfactants. Surfactants are usually organic compounds that are amphiphilic in nature, i.e. they contain both hydrophobic groups (tail) and hydrophilic groups (head). Surfactants have the ability to self assemble into a variety of microstructures including spherical, rod like and inversed micelles, vesicles etc. Generally surfactants are considered as good carriers because they form micelles and can solubilize drugs. It is well known that solubility of predominantly hydrophobic molecules in aqueous solution is enhanced by the addition of surfactants [30, 31]. This phenomenon of solubilization constitutes the basis on which surfactant find useful application in many pharmaceutical and biological systems. Thus, surfactants play an eminent role in many processes of interest in both fundamental as well as in applied science. In particular they are decisively employed in contemporary pharmaceutical biotechnology or pharmaceutical sciences, since they have defined role in various drug dosage forms to control wetting, stability, bioavailability and many more properties. It is important to note down that, lyophobic colloids such as polymers, require certain energy to be applied for their formation and are quite unstable from thermodynamic point of view and frequently known to form large aggregates [32, 33].

In view of diverse types of surfactants, they are generally classified as follows [34-36]:

(i) *Anionic surfactants:* They are the most widely utilized class of surfactants in industrial applications due to their relatively low cost of manufacturer and linear chains which are more effective and more degradable than branched ones. In anionic surfactant, the most commonly used hydrophilic groups are carboxylates, sulfates, sulphonates and phosphates. Carboxylates: C_nH_{2n+1} COO^- X, Sulfates: C_nH_{2n+1} OSO_3^- X, Sulphonates: C_nH_{2n+1} SO_3^- X , and Phosphates: C_nH_{2n+1} OPO (OH) O^- X; with n = 8-16 atoms and counter ion X is usually Na+.

(ii) *Cationic surfactants:* The most common cationic surfactants are the quaternary ammonium compounds with general formula R′ R″ R‴ R⁗ N^+X^-, where X^- is usually

chloride ion and R represents alkyl groups. A common cationic surfactant class is the alkyl trimethyl ammonium chloride where R contains 8-18 carbon atoms e.g. Cetyltrimethylammonium bromide. Because of their chemical stability, the prime use of cationic surfactants is their tendency to adsorb at negative charged surfaces e.g. dispersants for inorganic pigments, antistatic agents, topical formulations and as bactericides.

(iii) *Non-ionic surfactants:* These surfactants are based on ethylene oxide, referred to as ethoxylated surfactants. In non-ionic surfactants, surface active portion do not bear an ionic charge. Owing to their advantageous properties, like their solubility in aqueous and non-aqueous media and dispersion etc., they are used in many industries. A most common example of non-ionic surfactant is Triton X-100.

(iv) *Amphoteric or zwitter ionic surfactants:* These surfactants possess both anionic and cationic groups. Depending on the pH of a media, they can either behave as cationic, anionic or neutral species. Typical example is N-alkyl betaines and sulfobetains.

According to the composition of head the surfactants are pictured in Figure 1.3.

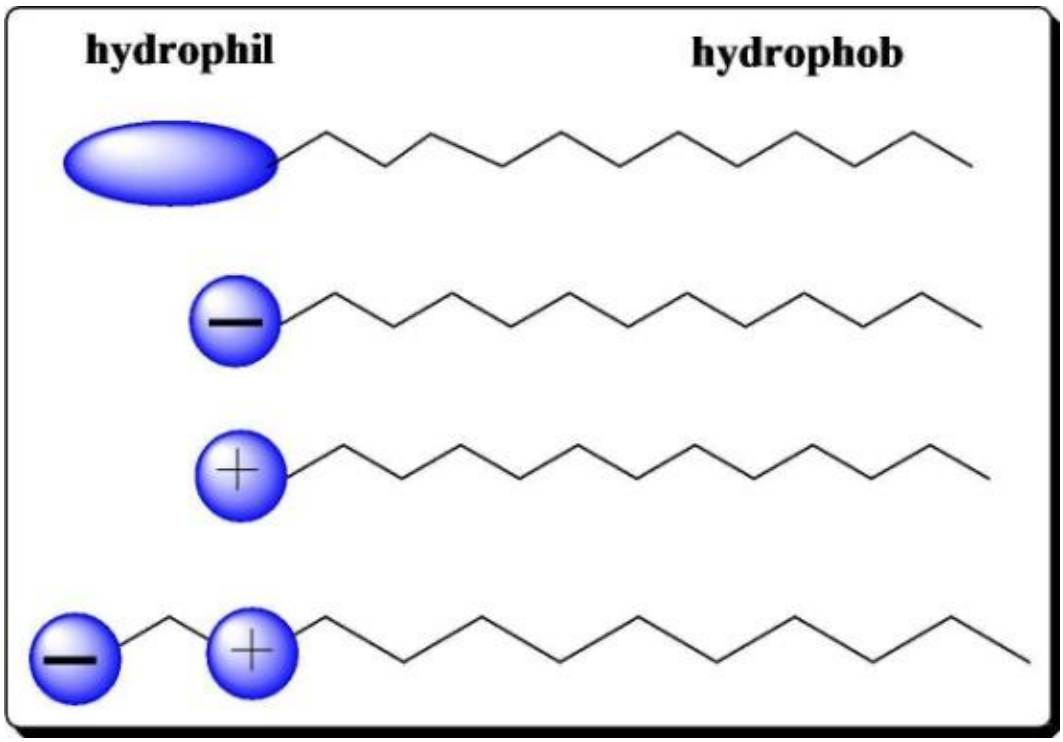

Figure 1.3: Different class of surfactants depending on their head groups.

Keeping in view the applications and ability of surfactants, following surfactants has been used in the present study and presented in Figure 1.4.

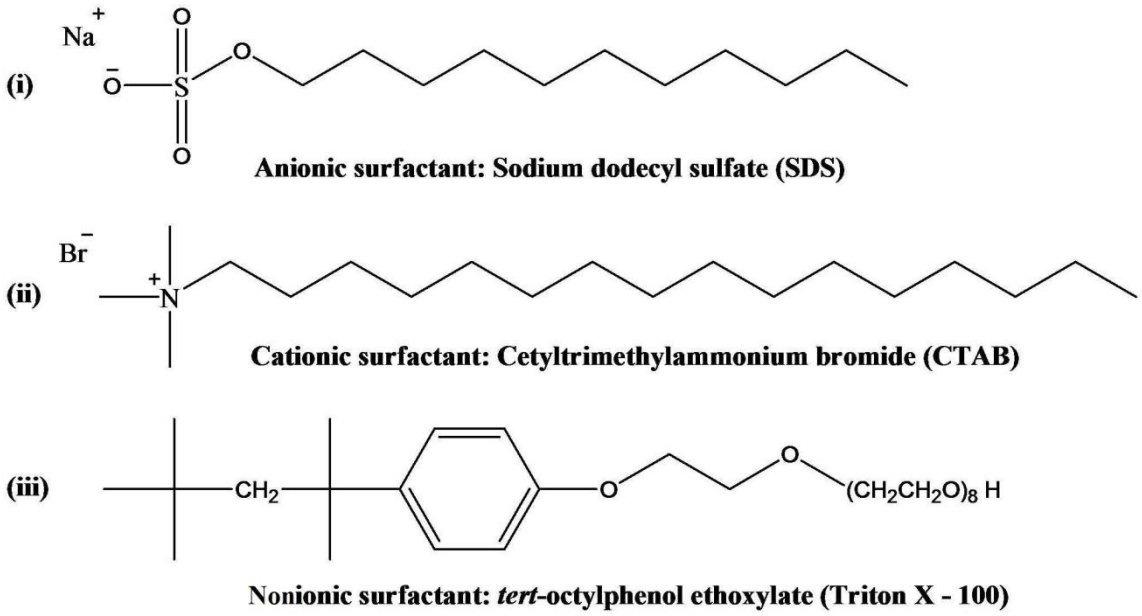

Figure 1.4: Structural representation of surfactants used in the present study.

1.3.1 Micellization

Micelles are stable aggregates of surfactant molecules which form spontaneously in surfactant solutions. In a micelle, the hydrophobic tail flocks to the interior in order to minimize their contact with water and the hydrophilic head remains on the outer surface in order to maximize their contact with water. The compounds that make up a micelle are typically amphiphilic in nature, meaning that they are not only the micelles soluble in protic solvents such as water but also in aprotic solvents as a reverse micelle [37, 38]. The structural presentation of micelle is given in Figure 1.5.

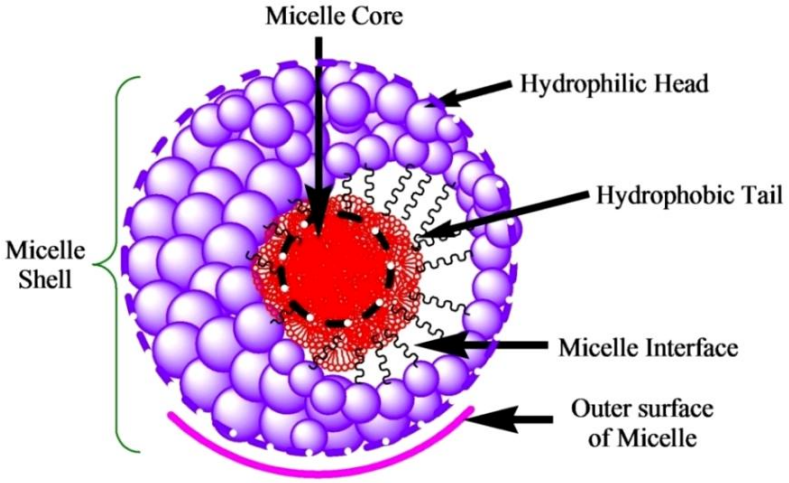

Figure1.5: The representation of micellar structure.

The most important property of amphiphilic molecules are characterized by their tendency to form aggregates, usually called as micelles, above a certain defined concentration. So micelle is defined as "a colloid particle together with its surrounding stabilizing agent". Micellization is not, however, just limited to aqueous solution; it is sometimes observed in non-aqueous polar solvents such as ethylene glycol or alcohols and non-polar solvents e.g. hexane [39, 40]. A surfactant at low concentration in a system adsorbs onto surfaces or interfaces significantly changing the surface or interfacial energy. Moreover, it disrupts the interaction among the molecules resulting distortion of water structure and leading to increase in Gibbs energy of the system [41]. This condition is therefore can be overcome by association of surfactant molecules into micelles. Thus, most often, the energy of adsorption and micelle formation are discussed in terms of various kinds of forces driving among the surfactant and the solvent molecules. The micellization process results from a delicate balance of intermolecular forces, including hydrophobic, steric, electrostatic, hydrogen bonding, and van der Waals interactions. The main attractive forces results from the hydrophobic effects associated with the nonpolar surfactant tails and the main opposing repulsive forces results from steric interactions and electrostatic interactions between the surfactant polar heads [42].

An important property of micelles that has particular significance in pharmaceutical science is their ability to increase the solubility of sparingly soluble substances in water. On the other hand, numerous drug delivery and drug targeting systems have been studied in an attempt to minimize drug degradation and loss, to prevent harmful side effects, and to increase drug bioavailability [43, 44]. Within this context, the utilization of micelles as drug carriers presents some advantages when compared to other alternatives such as soluble polymers and liposomes. Solubilization can be defined as the spontaneous dissolving of a substance by reversible interaction with the micelles of a surfactant in water to form a thermodynamically stable isotropic solution with reduced thermodynamic activity of the solubilized material [45]. If we plot a graph between the solubility of a poorly soluble compound versus the concentration of surfactant, as shown in Figure 1.6, it is observed that the solubility is very low until the surfactant concentration reaches the critical concentration usually known as critical micelle concentration (CMC) and above CMC the solubility increases linearly with the concentration of surfactant, indicating that solubilization is related to micellization [46].

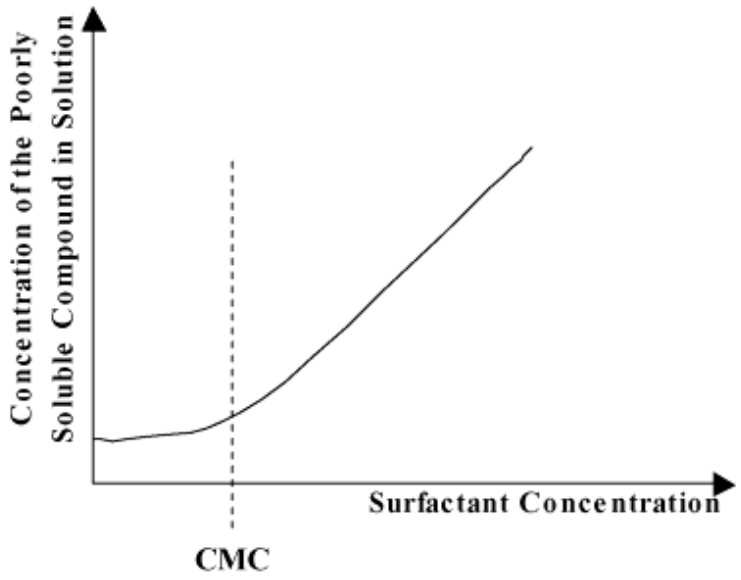

Figure 1.6: Plot of concentration of a poorly soluble molecule as a function of surfactant concentration in aqueous solution.

The variation in surfactant concentration resulting change in properties is a characteristic of most surfactants. Critical micelle concentration is defined as the certain concentration where micelle formation occurs. Surfactant molecules below this concentration (CMC) are monomers whereas above CMC they are self associated. Their shape and size varies depending on structure and medium of solubilization. The determination of a surfactant's critical micelle concentration (CMC) can be made via conductivity [47], capillary electrophoresis [48], voltammetry [49], scattering techniques [50], surface tension [51], UV–Vis and fluorescence spectroscopy [52, 53], which are based on an abrupt change in the physical properties related to micelle formation. In view of above statements, it is a well accepted that CMC of a surfactant is of paramount importance in determination of various characteristic properties and parameters of micelles used in many chemical processes in pharmaceutical science. Therefore, the micellar solutions are one of the medium which is utilized to attain desired functionality depending on the temperature, concentration, pH, and presence of other molecules.

1.3.2 Impact of Additive

The effect of presence of additives on CMC of surfactant has been widely studied. Recently, increasing attention is being devoted to the study of incorporation or solubilization of neutral molecules into micelle in aqueous solution. Self-association property of surfactants to form

self-assembled aggregates, in specific medium has a profound effect on the solubility of some additive such as organic compounds. The solubilization process of additives or so called surfactant aided delivery of bio-active compounds is of importance in many industrial process including food and cosmeceutical industries as well as in a diverse fundamental research oriented studies like micellar modeling of biological membranes [54].

In addition to the solubilization, the viscosity of the micellar interior and the locus of the additive within the micellar structure are also important in many applications of micellar solubilization. The physical behavior of the surfactant micelle can be visualized as the construction model membrane to mimic a biological system. Small amount of additive may produce marked changes in the CMC of the surfactant and therefore results in variation of thermodynamic and other transport related properties [55, 56]. The presence of the additive depresses the CMC of surfactant through strengthening the hydrophobic interactions in aqueous surfactant solution.

The polar additives (alcohols and amides) affect the CMC of aqueous surfactant solution by being incorporated into the micelle, while the non-polar additives involved in the modification of solvent-micelle or solvent-surfactant interaction. Non-polar additives usually increases CMC such as urea and guanidinium salt, by causing disruption of water structure. This may increase the degree of hydration of the hydrophilic group and since hydration of the hydrophilic group opposes micellization [57]. Especially, short chain alcohols are well documented to promote micellization in aqueous solution (decreases CMC) and increasing the flexibility of micellar membranes, which mainly depends on their hydrophobic-hydrophilic character. As mentioned, some of the most studied solubilizate are alcohols because of their diverse role in the preparation of pharmaceutical formulations. It is generally accepted that the alcohol binds to the micelle in the surface region, leading to following principle effects;

a) alcohol molecules intercalate between the surfactants ionic head groups to decrease the micelle surface area per head group and increase of ionization [58]. It seems to be a function of mole fraction of alcohol [59],
b) the dielectric constant at micellar interface decreases probably due to the replacement of water molecules in the interface region by alcohol molecules [59],
c) molecular order of interface region of micelle changes [60].

Hence, the addition of alcohol can strongly influence the behavior of micelles and increase or decrease the micellar size depending on the hydrophilic/hydrophobic character of alcohol. The specific binding involves both electrostatic and hydrophobic interactions, whereas the non-specific binding is dominated by hydrophobic interactions. Also alcohol-water mixtures exhibit a wide range of relative permittivity, viscosity and a high degree of hydrogen bonding effect. Hydrogen bonding between the polar groups of additive and water molecules helps in counter balancing the lateral pressure which tends to push additive into the interior of the micelle, so they remain in the outer core or interface between the surfactant molecules. Therefore, the additives containing more than one group with tendency to form hydrogen bond with water causes more depression in CMC as compared to that with one group [61]. So, depending upon the structural re-arrangement, concentration of the additives, polarity, microviscosity and hydration degree, additives can mainly reside either at the outer surface, interface or the inner core of the micelle [62], as depicted in Figure 1.7.

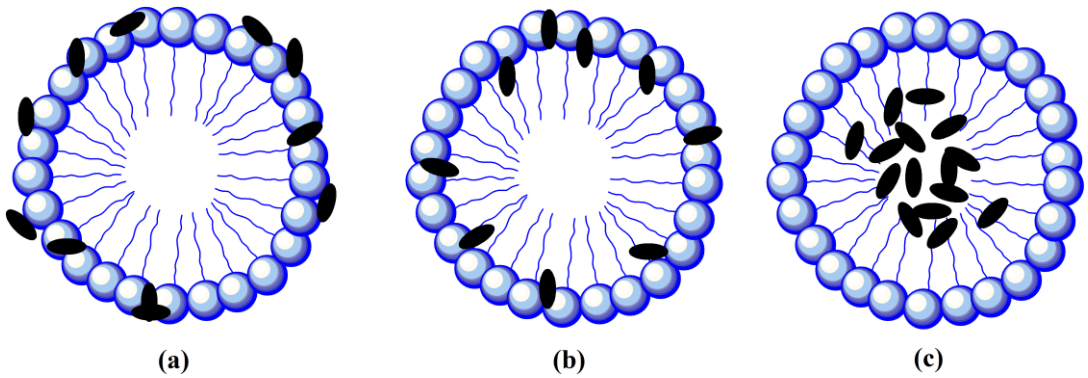

Figure 1.7: Three main regions of micelle where molecules locate itself a) on the surface b) at the interface c) in the core of micelle.

The investigation of interfacial and thermodynamic properties of surfactants in solution, both in the presence and absence of additives, can provide valuable information with regard to solute–solute and solute–solvent interactions in system.

1.4 Physico-chemical Interaction

Drug action, although complex, result from various kinds of physicochemical interactions e.g. ionic, covalent, dipole-dipole interactions, hydrophobic interactions etc [63]. Knowledge of use of drugs involving physiological and biochemical effects and their mechanism of action at macromolecular/ subcellular level involves pharmacokinetics process. About 30% of

pharmacological active molecules are rejected due to pharmacokinetic related failures such as physico-chemical profile. Physical properties related parameters stand one of those which should be analyzed in order to design better formulations [64]. Characteristically, surfactants have a far-ranging use in biomembrane studies. As surfactants are amphiphilic molecules, mimic lipids, some of the same rules governing lipid behavior also apply to the surfactants. Among the membrane models utilized, micellar system can be considered as interesting alternative to study the interactions of different compounds with membranes because of the relative simplicity of these systems and therefore have been used with this purpose [65]. In recent time, there has been growing keen interest in bio-active molecules and surfactant interactions with their potential application in foods, cosmeceutical, and drug delivery as well as in biotechnological processes [66].

In past few years, there have been various numbers of methods and tactical approaches to investigate these interactions [67-72]. It has been proposed and well known that hydrophobic and electrostatic interactions are the two main driving forces used/studied for the association between surfactants and bio-active molecules in aqueous solution. The nature of solvent plays a decisive role and affects the stability of system by distributing itself between aqueous and micellar phase or by accumulating both at polar head groups and inside the micelle hydrophobic core, whereas electrolyte affects the structure of the solvent which also has direct impact on the micellization. The substantial substitutions of the molecule or structure characteristics affect the interaction via change in CMC and thus resulting in variation of thermodynamic parameters. The thermodynamic parameters are quite complex in case of ionic micelles because the interaction process is governed by both hydrophobic and electrostatic interactions, whereas for non-ionic surfactants these parameters are obviously less complex. In early days, the interaction study was limited to aqueous solutions only but in recent time research, multi-component systems can be easily studied and optimized to predict and design processes being used in topical cosmeceutical formulations.

1.5 Fungal Infections

Fungal infections are extensively common in human beings, especially in the tropical regions. Fungi produces broad spectrum of human infections ranging from superficial skin infections affecting the outer layers of skin, hair, nails and mucous membranes to systemic infections [73]. These infections usually occur as a result of decrease in the natural human defenses due

to either immunosuppressive diseases or immune suppressive agents and also in association with opportunistic heavy exposure to the fungus. When fungi infect the skin surface, they invade the stratum corneum to avoid being shed from the skin surface by desquamation, so the management of the superficial fungal infection begins with agent that can penetrate the stratum corneum cells [74].

Historically, the first written descriptions of oral apthous lesions that were probably thrush, date to time of Hippocrates and Galen [75]. In 1839, Langenbeck discovered fungi in the gastrointestinal tract of a patient, and 2 years later Berg demonstrated the fungal etiology of thrush in children [75]. In 1834, Robin microscopically observed budding cells and filaments in epithelial scraping, and named the fungus *Oidium albicans*. Since then, there have been more than 100 synonyms for *Candida albicans*, a denomination first used by Berkhout in 1923, which is currently the accepted name of this species [76]. The first well-documented case of invasive candidiasis was described by Zenker in 1861 and when the widespread use of antibiotics began in the 1940s, the incidence of practically all forms of *Candida* infections rose abruptly. Until the past 2 decades, *Candida* was often regarded as simply a contaminant or "normal flora" in laboratory results, instead of highly prevalent and potentially aggressive pathogen we recognize today [77]. These species are also a component of normal human flora in the majority of healthy individuals and the most common cause of fungal infection worldwide. They are most commonly found in the gastrointestinal tract, on the mucous membranes of the mouth and vagina, and on skin [78].

1.5.1 Targets for antifungal therapy

Briefly, the targets for antifungal therapy [79] and examples of drugs are as follows and pictured in Figure 1.8.

i. Fungal ergosterol synthesis inhibitors, e.g. Azoles; Fluconazole, Itraconazole and Clotrimazole etc.
ii. Squalene epoxidase inhibitors, e.g. Morpholines, Amorolfine and Terbinafine.
iii. Ergosterol disruptors (polyenes antibiotics), e.g. Amphoterecin B and Nystatin.
iv. Glucan synthesis inhibitors, e.g. Caspofungin.
v. Chitin synthesis inhibitors, e.g. Nikkomycin and Polyoxins.
vi. Nucleic acid synthesis inhibitors, e.g. Flucytosine.
vii. Protein synthesis inhibitors, e.g. Sordarins.

viii. Microtubules synthesis inhibitors, e.g. Griseofulvin.

In this present investigation we intend our study on azole derivatives namely, Clotrimazole, because of intrinsic and emerging resistance to azoles which actually represents a major challenge for empirical therapeutic and prophylactic strategies.

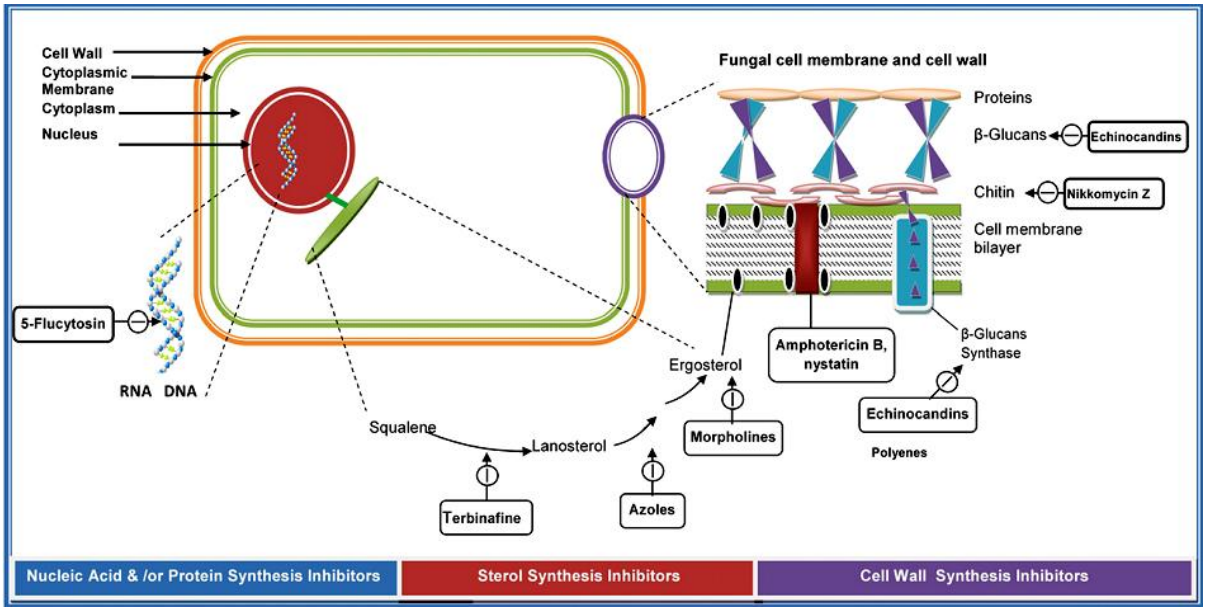

Figure 1.8: Targets for antifungal therapy.

Azole antifungal agents are the largest class of synthetic antimycotics. Some are used topically to treat superficial dermatophytic and yeast infections. Others used systemically to treat severe fungal infections. Clotrimazole (Figure 1.9.) is one of the imidazole derivatives, which is commonly used to treat fungal infections. It inhibits CYP P450 14 α-demethylase in fungi. This enzyme is involved in the conversion of lanosterol to ergosterol. The basic nitrogen of the azole ring forms a tight bond with the heme iron of the fungal P450 preventing the substrate and oxygen binding. Inhibition of C14 α-demethylase results in accumulation of sterols still bearing a C14 methyl group, changing the exact shape and physical properties of the membrane causing further changes in permeability. The intrinsic and emerging resistance to azoles actually represents a major challenge for empirical therapeutic and prophylactic strategies [80].

Antifungal resistance is based on different mechanisms, namely, (i) reduced drug permeability and intracellular accumulation, (ii) decreased target affinity/ processivity for the drug, (iii) counteraction of the drug effect, and, (iv) mutation [80]. The mechanism of

resistance depends on the mode of action of antifungal compounds [81]. Due to problem to combat against resistance, new topical prophylactic formulation that exhibit rapid, stable, potent and direct antifungal activity is in urgent need. Identifying these adaptations, and targeting them to enhance the activity of existing drugs, is a promising approach to mitigate the public health crisis caused by the scarcity of new drugs. So, in order to attain better penetration and accumulation of drug, strategic drug delivery in combination of antioxidants (BHA and BHT) could be of paramount value. Achieving better antifungal response and profile, surfactant aided BHA and BHT as active components having antimicrobial prolife, are likely to provide synergistic effect in combination to clotrimazole gel formulation.

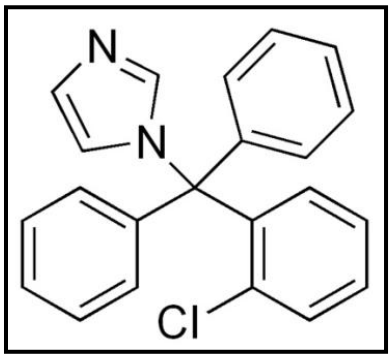

Figure 1.9: Chemical structure of clotrimazole.

1.6 Objectives of the study

At present antifungal drug resistance is one of the major problems and of high concern. Finding new drug is a long time consuming process. Alternatively, for such improvement, relevance of combinational drug delivery against many kinds of micro-organisms had already been reported, which showed a promising future in medical application. Introduction of binding and bounding techniques have marked a new era in targeted research for transdermal drug delivery. Different reports showed a promising future of antioxidants in combination of active pharmaceutical ingredients in making transdermal delivery more effective. Further, research in this area will allow stable formulations, better control over drug release *in vivo*, and allowing physician to make the therapy more effective. The aim of this study was to improve the transdermal permeation of anti-fungal drugs clotrimazole, poorly water-soluble drug, employing conventional gel formulation in combination surfactant aided synthetic antioxidants, which itself holds antimicrobial property. Also, alcohols are well-known permeation enhancer, and mechanisms of these carriers in improving permeation are

explained by their content as penetration enhancers. To achieve this target we intend our study to evaluate the antioxidants-surfactants-alcohols interactions through different thermodynamic and acoustical parameters in addition to spectroscopic studies. These studies provide information with regard to interaction at various concentrations of surfactant and alcohol containing synthetic antioxidants.

Keeping in mind, the rationale of resistance and mechanism, the objectives were designed accordingly. Initially, the emphasis was on thermodynamic micellar and transport studies, and there after release of antioxidants from surfactant binding to inhibit reactive oxygen in term of increasing permeability of membrane.

[1] Physico-chemical interaction study of BHA and BHT with different classes of surfactants (SDS, CTAB and Triton X-100). The study includes; specific conductance with determination of CMC and thermodynamic parameters, Density and ultrasonic sound velocity study with volumetric and compressibility parameters, Viscometric analysis, and FTIR and ^{1}H-NMR analysis with examination of locus of molecules (BHA/BHT) within micellar structure.

[2] Pre-formulation evaluation and formulation of clotrimazole topical gel.

[3] Utilizing the results of physico-chemical studies in terms of interactions, region of micellization and concentration that would guide the dispersion of surfactant aided BHA and BHT or their combination with potential antioxidant ability into clotrimazole containing topical gel formulation.

[4] Broad spectrum antifungal evaluation on *Candida* clinical isolates.

The proposed study with plan of work is presented in Figure 1.10.

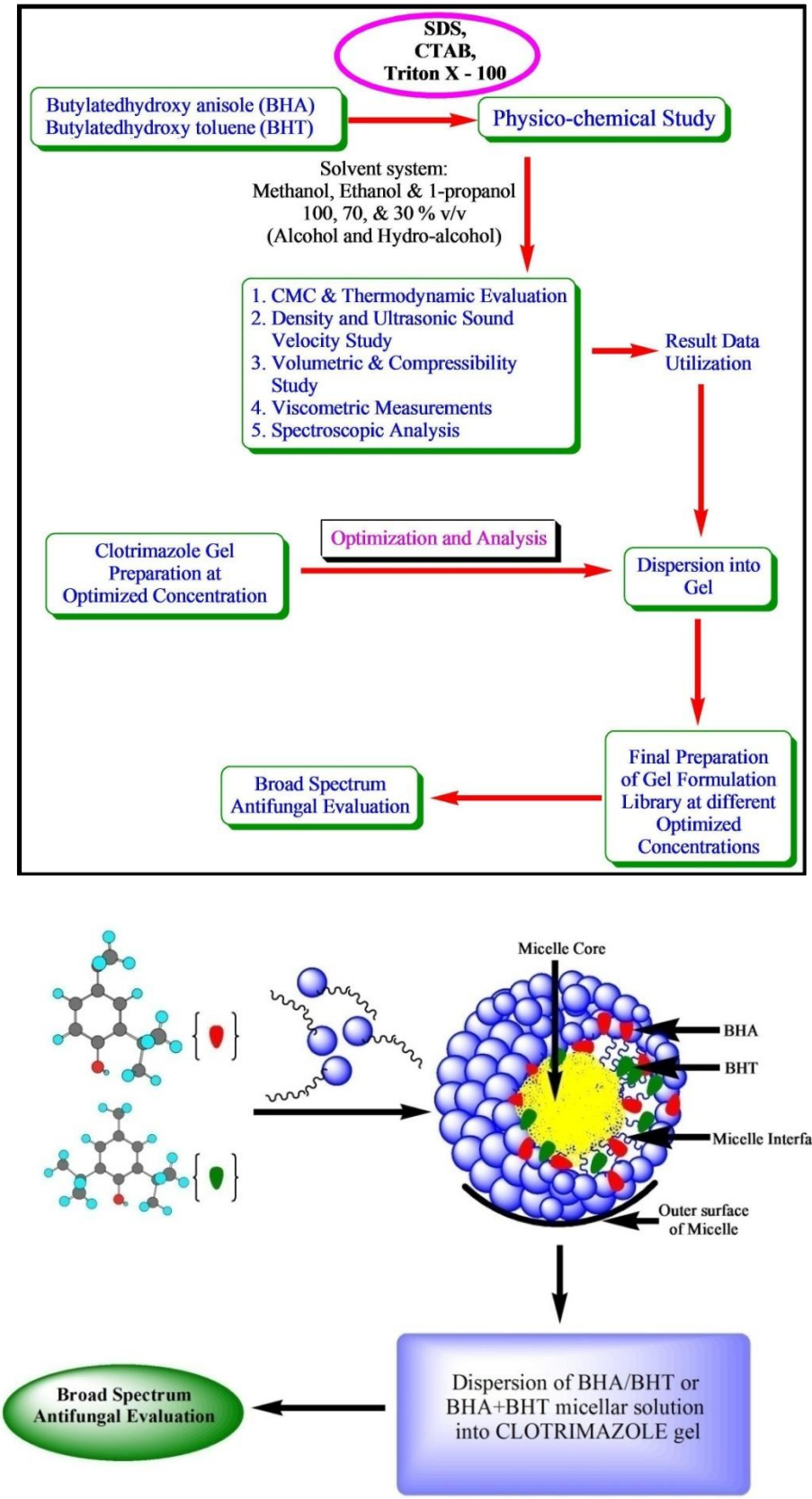

Figure 1.10: Flowchart and graphical representation of proposed study.

References

[1] R. Crawford, "Healthism and the medicalization of everyday life," *International Journal of Health Services,* vol. 10, pp. 365-388, 1980.

[2] T. M. Allen and P. R. Cullis, "Drug delivery systems: entering the mainstream," *Science,* vol. 303, pp. 1818-1822, 2004.

[3] S. Balbach and C. Korn, "Pharmaceutical evaluation of early development candidates “the 100 mg-approach”," *International Journal of Pharmaceutics,* vol. 275, pp. 1-12, 2004.

[4] M. R. Prausnitz and R. Langer, "Transdermal drug delivery," *Nature Biotechnology,* vol. 26, pp. 1261-1268, 2008.

[5] M. Rosen and X. Hua, "Synergism in binary mixtures of surfactants: II. Some experimental data," *Journal of the American Oil Chemists Society,* vol. 59, pp. 582-585, 1982.

[6] G. Sauermann, U. Schonrock, V. Schreiner, and F. Stab, "Synergistic combinations of active substance for the cosmetic or dermatological care of the skin, hair & nails," US 5710177 A, 1998.

[7] S. Karaborni, K. Esselink, P. Hilbers, B. Smit, J. Karthäuser, N. Van Os, and R. Zana, "Simulating the self-assembly of (dimeric) gemini surfactants," *Science,* vol. 266, pp. 254-256, 1994.

[8] M. S. Bakshi, "Micelle formation by anionic and cationic surfactants in binary aqueous solvents," *Journal of the Chemical Society, Faraday Transactions,* vol. 89, pp. 4323-4326, 1993.

[9] M. J. Lawrence, "Surfactant systems: their use in drug delivery," *Chemical Society Reviews,* vol. 23, pp. 417-424, 1994.

[10] M. A. Pfaller, "Antifungal drug resistance: mechanisms, epidemiology, and consequences for treatment," *The American Journal of Medicine,* vol. 125, pp. S3-S13, 2012.

[11] D. P. Kontoyiannis and R. E. Lewis, "Antifungal drug resistance of pathogenic fungi," *The Lancet,* vol. 359, pp. 1135-1144, 2002.

[12] R. E. Hancock and H.-G. Sahl, "Antimicrobial and host-defense peptides as new anti-infective therapeutic strategies," *Nature Biotechnology,* vol. 24, pp. 1551-1557, 2006.

[13] M. J. Nirmala, A. Mukherjee, and N. Chandrasekaran, "Design and Formulation Technique of a Novel Drug Delivery System for Azithromycin and its Anti-Bacterial Activity Against Staphylococcus aureus," *AAPS PharmSciTech,* vol. 14, pp. 1045-1054, 2013.

[14] F. A. Andrews, W. H. Beggs, and G. A. Sarosi, "Influence of antioxidants on the bioactivity of amphotericin B," *Antimicrobial Agents and Chemotherapy,* vol. 11, pp. 615-618, 1977.

[15] A. Ogita, K. Matsumoto, K.-i. Fujita, Y. Usuki, Y. Hatanaka, and T. Tanaka, "Synergistic fungicidal activities of amphotericin B and N-methyl-N ″-dodecylguanidine: a constituent of polyol macrolide antibiotic niphimycin," *The Journal of Antibiotics,* vol. 60, pp. 27-35, 2007.

[16] C. Balsano and A. Alisi, "Antioxidant effects of natural bioactive compounds," *Current Pharmaceutical Design,* vol. 15, pp. 3063-3073, 2009.

[17] B. D. Craft, A. L. Kerrihard, R. Amarowicz, and R. B. Pegg, "Phenol-Based Antioxidants and the In Vitro Methods Used for Their Assessment," *Comprehensive Reviews in Food Science and Food Safety,* vol. 11, pp. 148-173, 2012.

[18] C. A. Rice-Evans, N. J. Miller, and G. Paganga, "Structure-antioxidant activity relationships of flavonoids and phenolic acids," *Free Radical Biology and Medicine,* vol. 20, pp. 933-956, 1996.

[19] E. W. Kellogg and I. Fridovich, "Superoxide, hydrogen peroxide, and singlet oxygen in lipid peroxidation by a xanthine oxidase system," *Journal of Biological Chemistry,* vol. 250, pp. 8812-8817, 1975.

[20] D.-X. Hou, "Potential mechanisms of cancer chemoprevention by anthocyanins," *Current Molecular Medicine,* vol. 3, pp. 149-159, 2003.

[21] P. Wanasundara and F. Shahidi, "Antioxidants: Science, technology, and applications," *Bailey's Industrial Oil and Fat Products,* 2005.

[22] F. Shahidi and Y. Zhong, "Antioxidants: regulatory status," *Bailey's Industrial Oil and Fat Products,* 2005.

[23] L. Soubra, D. Sarkis, C. Hilan, and P. Verger, "Dietary exposure of children and teenagers to benzoates, sulphites, butylhydroxyanisol (BHA) and butylhydroxytoluen (BHT) in Beirut (Lebanon)," *Regulatory Toxicology and Pharmacology,* vol. 47, pp. 68-77, 2007.

[24] K. Kim, H. Moon, V. Sapienza, R. Carp, and R. Pullarkat, "Inactivation of cytomegalovirus and Semliki Forest virus by butylated hydroxytoluene," *Journal of Infectious Diseases,* vol. 138, pp. 91-94, 1978.

[25] D. Thompson, "Inhibition of growth of mycotoxigenic Fusarium species by butylated hydroxyanisole and/or carvacrol," *Journal of Food Protection®,* vol. 59, pp. 412-415, 1996.

[26] H. t. CHANG and A. Branen, "Antimicrobial effects of butylated hydroxyanisole (BHA)," *Journal of Food Science,* vol. 40, pp. 349-351, 1975.

[27] D. Y. FUNG, S. TAYLOR, and J. KAHAN, "Effects of butylated hydroxyanisole (BHA) and butylated hydroxytoluene (BHT) on growth and aflatoxin production of Aspergillus flavus," *Journal of Food Safety,* vol. 1, pp. 39-51, 1977.

[28] L. Shelef and P. Liang, "Antibacterial effects of butylated hydroxyanisole (BHA) against Bacillus species," *Journal of Food Science,* vol. 47, pp. 796-799, 1982.

[29] J. Cupp, P. Wanda, A. Keith, and W. Snipes, "Inactivation of the lipid-containing bacteriophage PM2 by butylated hydroxytoluene," *Antimicrobial Agents and Chemotherapy,* vol. 8, pp. 698-706, 1975.

[30] M. J. Rosen and J. T. Kunjappu, *Surfactants and Interfacial Phenomena*: John Wiley & Sons, 2012.

[31] J. Istraelachvili, "Intermolecular and surface forces, with special applications to colloidal and biological systems," *Academic, London,* vol. 251, 1985.

[32] F. Menger and C. Littau, "Gemini surfactants: a new class of self-assembling molecules," *Journal of the American Chemical Society,* vol. 115, pp. 10083-10090, 1993.

[33] J. M. Ford and W. Hait, "Pharmacology of drugs that alter multidrug resistance in cancer," *Pharmacological Reviews,* vol. 42, pp. 155-199, 1990.

[34] I. Robb and E. Lucassen-Reynders, "Anionic Surfactants-Physical Chemistry of Surfactant Action," *Surfactant Science Series. Dekker, New York,* 1981.

[35] E. Anacker and E. Jungermann, "Cationic surfactants," *Marcel Dekker, New York,* vol. 169, p. 257, 1970.

[36] G. Fernley, "Zwitterionic surfactants: structure and performance," *Journal of the American Oil Chemists' Society,* vol. 55, pp. 98-103, 1978.

[37] F. M. Menger, "The structure of micelles," *Accounts of Chemical Research,* vol. 12, pp. 111-117, 1979.

[38] F. Boschke, *Micelles* vol. 87: Springer, 1980.

[39] M. Foti, M. Piattelli, M. T. Baratta, and G. Ruberto, "Flavonoids, coumarins, and cinnamic acids as antioxidants in a micellar system. Structure-activity relationship," *Journal of Agricultural and Food Chemistry,* vol. 44, pp. 497-501, 1996.

[40] C. J. Drummond, G. G. Warr, F. Grieser, B. W. Ninham, and D. F. Evans, "Surface properties and micellar interfacial microenvironment of n-dodecyl. beta.-D-maltoside," *The Journal of Physical Chemistry,* vol. 89, pp. 2103-2109, 1985.

[41] C. Y. Lee, J. A. McCammon, and P. Rossky, "The structure of liquid water at an extended hydrophobic surface," *The Journal of Chemical Physics,* vol. 80, pp. 4448-4455, 1984.

[42] D. F. Evans and B. Ninham, "Molecular forces in the self-organization of amphiphiles," *The Journal of Physical Chemistry,* vol. 90, pp. 226-234, 1986.

[43] S. Palma, R. Manzo, D. Allemandi, and L. Fratoni, "Lo Nostro, P., 2003. Drugs solubilization in ascorbyl-decanoate micellar solutions," *Colloids Surf. A: Physicochem. Eng. Aspects,* vol. 212, pp. 163-173.

[44] E. Cremophor, "the drawbacks and advantages of vehicle selection for drug formulation Gelderblom, H.; Verweij, J.; Nooter, K.; Sparreboom, A," *European Journal of Cancer,* vol. 37, pp. 1590-1598, 2001.

[45] H. Hoffmann and G. Ebert, "Surfactants, micelles and fascinating phenomena," *Angewandte Chemie International Edition in English,* vol. 27, pp. 902-912, 1988.

[46] M. J. Rosen, "Surfactants and Interface Phenomena," *John Wiley & Sons Inc.: New York,* 1989.

[47] R. S. Kumar, S. Arunachalam, V. Periasamy, C. Preethy, A. Riyasdeen, and M. Akbarsha, "Surfactant–cobalt (III) complexes: synthesis, critical micelle concentration (CMC) determination, DNA binding, antimicrobial and cytotoxicity studies," *Journal of Inorganic Biochemistry,* vol. 103, pp. 117-127, 2009.

[48] J. Jacquier and P. Desbene, "Determination of critical micelle concentration by capillary electrophoresis. Theoretical approach and validation," *Journal of Chromatography A,* vol. 718, pp. 167-175, 1995.

[49] A. B. Mandal, B. U. Nair, and D. Ramaswamy, "Determination of the critical micelle concentration of surfactants and the partition coefficient of an electrochemical probe by using cyclic voltammetry," *Langmuir,* vol. 4, pp. 736-739, 1988.

[50] C. Thévenot, B. Grassl, G. Bastiat, and W. Binana, "Aggregation number and critical micellar concentration of surfactant determined by time-dependent static light scattering (TDSLS) and conductivity," *Colloids and Surfaces A: Physicochemical and Engineering Aspects,* vol. 252, pp. 105-111, 2005.

[51] B. Sarkar, S. Lam, and P. Alexandridis, "Micellization of alkyl-propoxy-ethoxylate surfactants in water− polar organic solvent mixtures," *Langmuir,* vol. 26, pp. 10532-10540, 2010.

[52] B. Tanhaei, N. Saghatoleslami, M. P. Chenar, A. Ayati, M. Hesampour, and M. Mänttäri, "Experimental Study of CMC Evaluation in Single and Mixed Surfactant Systems, Using the UV–Vis Spectroscopic Method," *Journal of Surfactants and Detergents,* vol. 16, pp. 357-362, 2013.

[53] F. Müh and A. Zouni, "Micelle formation in the presence of photosystem I," *Biochimica et Biophysica Acta (BBA)-Biomembranes,* vol. 1778, pp. 2298-2307, 2008.

[54] V. P. Torchilin, "Micellar nanocarriers: pharmaceutical perspectives," *Pharmaceutical Research,* vol. 24, pp. 1-16, 2007.

[55] M. Fanun, "Conductivity, viscosity, NMR and diclofenac solubilization capacity studies of mixed nonionic surfactants microemulsions," *Journal of Molecular Liquids,* vol. 135, pp. 5-13, 2007.

[56] A. Cid, J. Mejuto, P. Orellana, O. López-Fernández, R. Rial-Otero, and J. Simal-Gandara, "Effects of ascorbic acid on the microstructure and properties of SDS micellar aggregates for potential food applications," *Food Research International,* vol. 50, pp. 143-148, 2013.

[57] M. Schick and A. Gilbert, "Effect of urea, guanidinium chloride, and dioxane on the cmc of branched-chain nonionic detergents," *Journal of Colloid Science,* vol. 20, pp. 464-472, 1965.

[58] P. Lianos, J. Lang, C. Strazielle, and R. Zana, "Fluorescence probe study of oil-in-water microemulsions. 1. Effect of pentanol and dodecane or toluene on some properties of sodium dodecyl sulfate micelles," *The Journal of Physical Chemistry,* vol. 86, pp. 1019-1025, 1982.

[59] J. R. Cardinal and P. Mukerjee, "Solvent effects on the ultraviolet spectra of benzene derivatives and naphthalene. Identification of polarity sensitive spectral characteristics," *The Journal of Physical Chemistry,* vol. 82, pp. 1614-1620, 1978.

[60] P. Baglioni and L. Kevan, "Structural effects of alcohol addition to sodium dodecyl sulfate micelles studied by electron spin-echo modulation of 5-doxylstearic acid spin probe," *Journal of Physical Chemistry,* vol. 91, pp. 1516-1518, 1987.

[61] A. Florence, "Surfactant interactions with biomembranes and drug absorption," *Pure Appl. Chem,* vol. 53, pp. 2057-2068, 1981.

[62] G. Mugesh, W.-W. du Mont, and H. Sies, "Chemistry of biologically important synthetic organoselenium compounds," *Chemical Reviews,* vol. 101, pp. 2125-2180, 2001.

[63] D. F. Veber, S. R. Johnson, H.-Y. Cheng, B. R. Smith, K. W. Ward, and K. D. Kopple, "Molecular properties that influence the oral bioavailability of drug candidates," *Journal of Medicinal Chemistry,* vol. 45, pp. 2615-2623, 2002.

[64] P. York, "Solid-state properties of powders in the formulation and processing of solid dosage forms," *International Journal of Pharmaceutics,* vol. 14, pp. 1-28, 1983.

[65] W. Caetano and M. Tabak, "Interaction of chlorpromazine and trifluoperazine with ionic micelles: electronic absorption spectroscopy studies," *Spectrochimica Acta Part A: Molecular and Biomolecular Spectroscopy,* vol. 55, pp. 2513-2528, 1999.

[66] A. N. Martin, J. Swarbrick, and A. Cammarata, "Physical pharmacy: physical chemical principles in the pharmaceutical sciences," Lippincott Williams & Wilkins, 1993.

[67] E. L. Gelamo, R. Itri, A. Alonso, J. V. da Silva, and M. Tabak, "Small-angle X-ray scattering and electron paramagnetic resonance study of the interaction of bovine serum albumin with ionic surfactants," *Journal of Colloid and Interface Science,* vol. 277, pp. 471-482, 2004.

[68] Y. Li, X. Wang, and Y. Wang, "Comparative studies on interactions of bovine serum albumin with cationic gemini and single-chain surfactants," *The Journal of Physical Chemistry B,* vol. 110, pp. 8499-8505, 2006.

[69] M. S. Ali, M. A. Rub, F. Khan, and H. A. Al-Lohedan, "Interaction of amphiphilic drug amitriptyline hydrochloride with β-cyclodextrin as studied by conductometry, surface tensiometry and viscometry," *Journal of Molecular Liquids,* vol. 167, pp. 115-118, 2012.

[70] T. Chakraborty, I. Chakraborty, S. P. Moulik, and S. Ghosh, "Physicochemical and conformational studies on BSA− surfactant interaction in aqueous medium," *Langmuir,* vol. 25, pp. 3062-3074, 2009.

[71] Z. Yan, R. Liu, S. Wu, X. Bai, and J. Wang, "Effect of temperature on the interactions of glycyl dipeptides with sodium perfluorooctanoate in aqueous solution: Volumetric, conductometric, and spectroscopic study," *The Journal of Chemical Thermodynamics,* vol. 57, pp. 360-366, 2013.

[72] Z. Yan, X. Sun, W. Li, Y. Li, and J. Wang, "Interactions of glutamine dipeptides with sodium dodecyl sulfate in aqueous solution measured by volume, conductivity, and fluorescence spectra," *The Journal of Chemical Thermodynamics,* vol. 43, pp. 1468-1474, 2011.

[73] G. Garber, "An overview of fungal infections," *Drugs,* vol. 61, pp. 1-12, 2001.

[74] I. P. Kaur and S. Kakkar, "Topical delivery of antifungal agents," *Expert Opinion on Drug Delivery,* vol. 7, pp. 1303-1327, 2010.

[75] G. C. Ainsworth, *Ainsworth & Bisby's dictionary of the fungi*: Cabi, 2008.

[76] J. E. Mackinnon and R. C. Artagaveytia-Allende, "The so-called genus Candida Berkhout, 1923," *Journal of Bacteriology,* vol. 49, p. 317, 1945.

[77] L. Ostrosky-Zeichner and P. G. Pappas, "Invasive candidiasis in the intensive care unit," *Critical Care Medicine,* vol. 34, pp. 857-863, 2006.

[78] R. López-Martínez, "Candidosis, a new challenge," *Clinics in Dermatology,* vol. 28, pp. 178-184, 2010.

[79] T. Walsh, M.-A. Viviani, E. Arathoon, C. Chiou, M. Ghannoum, A. Groll, and F. Odds, "New targets and delivery systems for antifungal therapy," *Medical Mycology,* vol. 38, pp. 335-347, 2000.

[80] N. H. Georgopapadakou, "Antifungals: mechanism of action and resistance, established and novel drugs," *Current Opinion in Microbiology,* vol. 1, pp. 547-557, 1998.

[81] B. H. Vanden, F. Dromer, I. Improvisi, M. Lozano-Chiu, J. Rex, and D. Sanglard, "Antifungal drug resistance in pathogenic fungi," *Medical Mycology,* vol. 36, pp. 119-128, 1997.

CHAPTER-2

LITERATURE REVIEW

2.1 Introduction

The bioactive molecule – membrane interactions are important in understanding the mechanism of action and also provides insight into more complex biological processes such as passage through cell membrane or topical layer of skin [1]. Owing to the much complex structure of biomembrane, the less intricate models such as surfactant micelles possessing spherical structure have been used to mimic the biomembrane environments [2, 3]. In comparison to other membrane models including polymer and liposomes, the micellar system are considered to be more advantageous, because of their relative simplicity, low toxicity, narrow size distribution, longer residence time in the system and the enhanced bioavailability and stability of the pharmacological active through micelle incorporation [4-6]. These pharmacological or bioactive compounds can be drugs or beneficial molecules with potential functionality. Here, in this present study, we focused on lipophilic synthetic phenolic antioxidants i.e. BHA and BHT.

Many environmental factors have been found to affect the antimicrobial activity of these phenolic antioxidants, e.g. presence of lipid or solubilization in lipid phase and proteins, results in reduced antimicrobial profile. The presence of electrolyte can sometime enhance the activity [7-9]. It was also theorized that low temperature decreases the solubility and availability of BHA and BHT into the lipid of the cell membrane, which in turn decreases the compound's effectiveness. Overall, it would appear that the antimicrobial activity of phenolic antioxidants can be significantly limited by the presence of other components in a formulation, such as topical formulation. The method of application to cosmetic or drug products, however, may increase their activity in products. Accordingly, these compounds should be generally applied by dissolving them in appropriate medium such as alcohols (methanol, ethanol etc.) prior to addition to products [10]. Empirically, the greatest potential for use of phenolic compounds would most likely be in combination with other antimicrobials, to avail better biological action [11].

In this regard, we intend to devote this section to summarize and discuss the relevant representation studies of micellar formation, intermolecular interactions of different drugs in presence of different surfactant as well as studies including topical gel formulation that appeared in literature during the recent past.

Kaushal et al. [12] reported the micellar behavior of anionic surfactant (SDS) in presence of a cardiovascular drug i.e. furosemide at two concentrations i.e. 0.001 and 0.002M in 8.0 mol% aqueous solution of dimethylsulphoxide (DMSO). They employed conductance (κ), densities (ρ), velocities of sound (υ) and viscosities (η) studies in the temperature range 20–40 °C at an interval of 5 °C. The results showed that critical micelle concentration (CMC) values of surfactant decrease with increase in furosemide concentration and rise in temperature. By utilizing CMC data, various thermodynamic parameters like standard enthalpy of micellization (ΔH°_{m}), standard entropy of micellization (ΔS°_{m}) and standard free energy of micellization (ΔG°_{m}), that have direct impact on the consequences of such interactions at the molecular level were calculated. The apparent molar volume (ϕ_v) and apparent molar adiabatic compressibility (ϕ_k) have also determined using densities and sound velocities. The obtained results revealed sensitivity towards the interactions prevailing in furosemide–SDS–DMSO-water systems.

T. Farias et al. [13] utilized the advantages of surfactant micelles as drugs carriers for the solubilization of sulfamethoxazole and metronidazole in aqueous solutions of benzalkonium chloride. The combination of conductivity and proton nuclear magnetic resonance (^{1}H NMR) experiments led to the conclusion that the less soluble drug i.e. sulfamethoxazole, was solubilized in the interior of the surfactant micelles while metronidazole interacted to some extent with the polar head group of the surfactant. However, this interaction was weak since no change in the micellization phenomenon was observed for these experimental conditions.

In view point of pharmaceuticals, one of the characteristic and important properties of micellar system or micelles is their ability to enhance the solubility of poorly soluble drugs in water, thus increasing their bioavailability. In this context, Rangel-Yagui et al. [14] studied the solubilization of an anti-inflammatory drug i.e. ibuprofen in micellar solutions of sodium dodecyl sulfate (SDS), dodecyltrimethylammonium bromide (DTAB), and n-dodecyl octa (ethylene oxide) ($C_{12}EO_8$). Concluding from results, irrespective of the surfactant type, the solubility of ibuprofen increased linearly with increment surfactant concentration, as a consequence of the association between the drug and the micelles. In addition, due to the stronger tendency of the nonionic surfactant in forming micelles in solution, at the same surfactant concentration, the same solubility of ibuprofen in both DTAB and $C_{12}EO_8$ was

obtained. The impact of surfactants on the solubilization as well as dissolution of poorly soluble acidic drugs were compared to identify the most suitable surfactant for conducting an acidic drug dissolution test by Park et al. [15]. Cetyltrimethylammonium bromide (CTAB), SDS and polysorbate 80 were the surfactants used in this study while, the drugs were Mefenamic acid, nimesulide, and ibuprofen. It was observed that the dissolution rates of these acidic drugs were substantially enhanced in cationic surfactant medium (CTAB). Ultraviolet (UV) spectrophotometric analysis confirmed the existence of electrostatic interactions between acidic drugs and CTAB. Mehta et al. [16] reported the micellar properties of cationic surfactants viz. dodecyldimethylethyl ammonium bromide (DDAB) and dodecyltrimethylammonium chloride (DTAC) in aqueous solutions containing diclofenac by spectroscopic and conductometric measurements. The CMC and degree of counter-ion binding of the micelles were determined over different temperatures from conductivity studies. A comparison of CMC and other thermodynamic parameters of surfactant – water with those of surfactant – drug – water revealed considerable changes in the nature of micellization of the surfactant, due to presence of drug. At lower temperatures, the micellization was found to be entropy driven while at higher temperatures it was enthalpy driven. The UV and ^{1}H - NMR studies suggested possible packing of diclofenac molecules within the micellar structure.

One more study on anti-inflammatory drug was reported by Ahmed et al. [17]. They investigated the effects of different surfactants on crystal properties and dissolution behavior of aspirin. Aspirin was crystallized through methanol in presence of surfactants namely cetrimide, SDS and Tween 80. Using Fourier transform infrared spectroscopy (FTIR), dissolution profile of aspirin tablets prepared with surfactant was compared with control aspirin tablets. It was observed that surfactants modified the crystal habit of drug, via affecting the crystal properties likely, density and equilibrium solubility. Presence of SDS in aspirin tablets enhanced the dissolution of aspirin significantly as compared to control aspirin tablets. From these results, it was concluded that the choice and selection of surfactants could prove valuable in manufacturing of drug dosage forms.

Tiwary et al. [18] reported the micellization, aggregation behavior and thermodynamics of CTAB in absence and presence of anticonvulsant drug (Hydantoin) using conductivity, surface tension, UV–visible and fluorescence spectroscopic methods. A strong interaction between the two components was indicated. The fluorescence spectroscopic method was used to calculate the aggregation number and the standard thermodynamic parameters of micellization. The negative values of standard Gibbs free energy change

suggested spontaneous micellization and synergism. One more example includes anticancer drug providing insight on the understanding of physico-chemical studies via spectroscopic analysis. Bakkialakshmi et al. [19] studied the binding of the anticancer drugs, namely, Uracil, 5-Fluorouracil and 5-Chlorouracil at two levels of temperature using fluorescence quenching method. UV - visible, time - resolved fluorescence, FTIR, ^{1}H - NMR and scanning electron microscope (SEM) analysis were conducted. In addition to thermodynamic parameters, binding constants (K_a) and binding sites (n) at various temperatures were thereafter calculated. Change in FTIR absorption intensity, NMR chemical shifts and fluorescence lifetimes of the drugs revealed strong binding of anticancer drugs to BSA. Given below are the chemical structures of the drugs presented in above mentioned literature (Figure 2.1.).

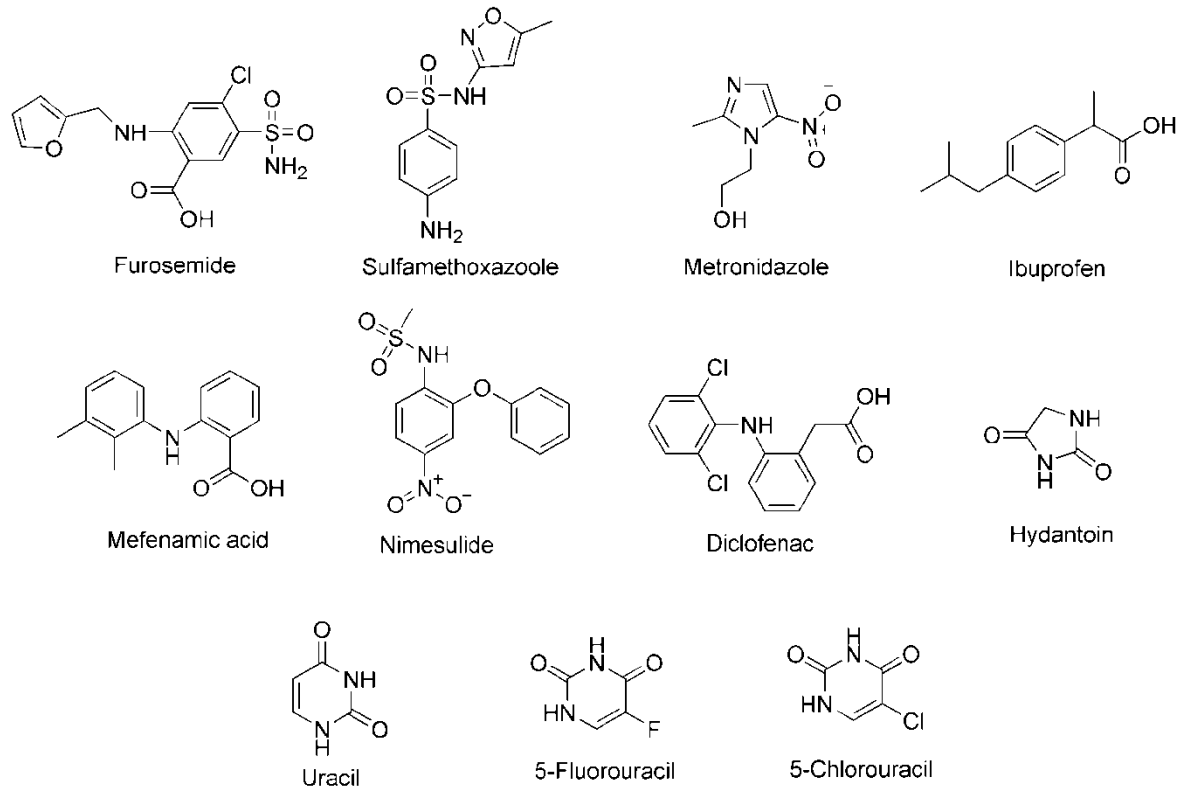

Figure 2.1: Chemical structures of the drugs presented in mentioned literature.

The amphiphilic nature of phenothiazines (Figure 2.2.), due to hydrophobic ring system and hydrophilic side groups, determines their ability to form micelles in aqueous solution and interactions with surfactants, model lipid bilayers, and biomembranes [20-23]. The detailed insights of the self-aggregation behavior and the interactions of phenothiazine drugs with surfactants in aqueous solution is of great significance in the rational design of more efficient drug delivery systems.

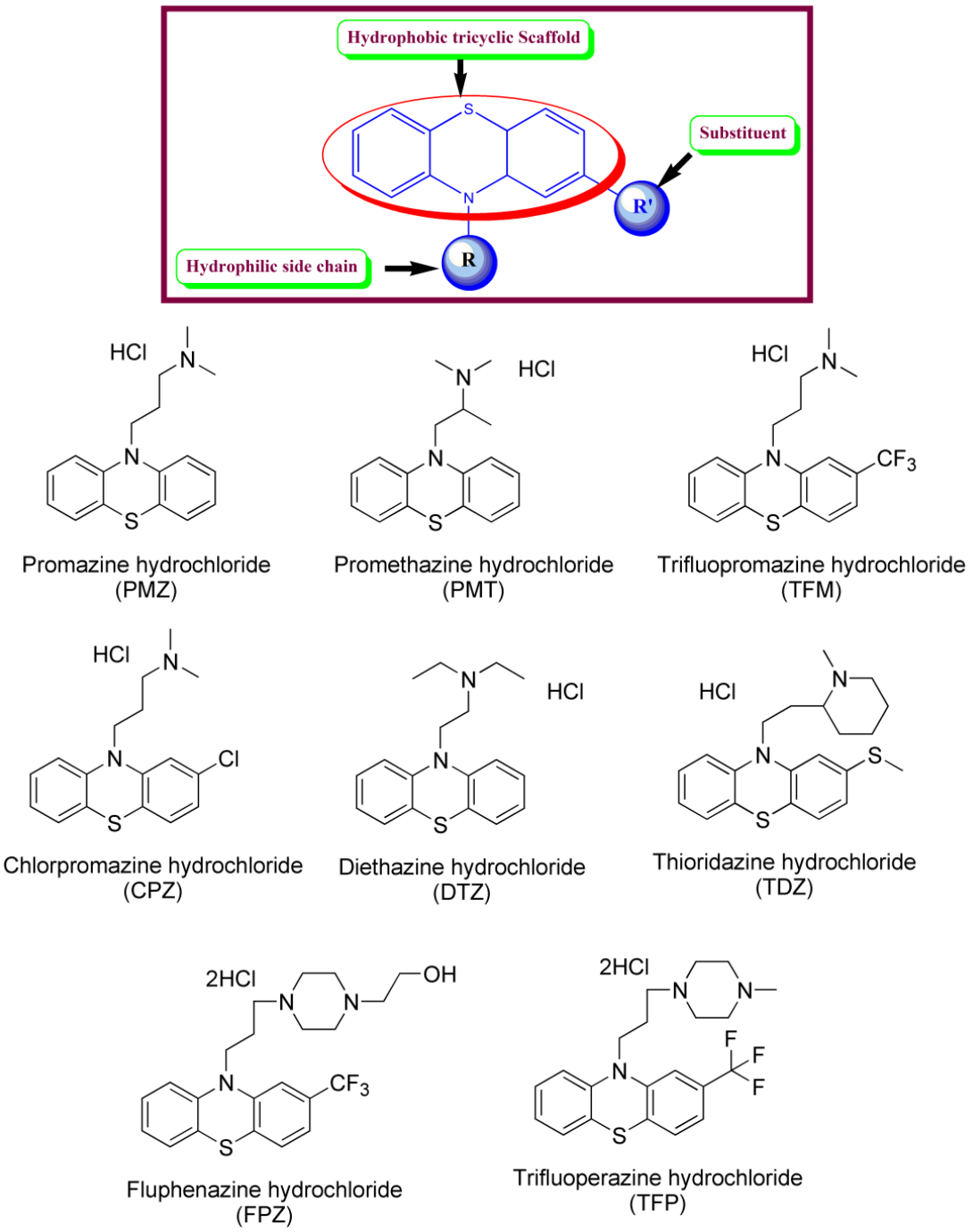

Figure 2.2: Chemical structure of phenothiazine drugs.

Florence and Parfitt [24] studied the micellization of some phenothiazine derivatives by employing NMR, pH and viscosity measurements. The interactions of these tranquillizer drugs with surfactants can contribute to a detailed understanding of transport and receptor binding of phenothiazine derivatives at the molecular level. Owing to the paramount importance of interactions of phenothiazine drugs with surfactants significant progress has

been achieved in exploring their physicochemical aspects. An overview on the studies of these drugs with surfactants is as follows. Rub et al. [25] reported a detailed conductometric study of promethazine hydrochloride (PMT) and conventional (tetradecyltrimethylammonium bromide; TTAB and hexadecyltrimethylammonium bromide; HTAB) surfactants at different temperatures ranging from 293.15 K to 308.15 K. The PMT-surfactant mixed micelles were formed by synergistic interactions as indicated by their lower CMC values than ideal CMC values. The interaction parameter (β) suggested attractive interactions in these drug-surfactant mixed micelles. The standard free energy of micellization (ΔG°_{m}) for the mixed systems became more negative indicating spontaneity of micelle formation in these mixed systems. The standard entropy of micellization (ΔS°_{m}) values were found to be positive at all temperatures for all the mixed systems because of the water structure breaking around the tricyclic hydrophobic portion of PMT.

Using the surface tension measurements, Alam and co-workers [26] evaluated thermodynamic parameters such as the standard free energy of micellization (ΔG°_{m}), the standard free energy of adsorption (ΔG°_{ads}), the free energy of a surface at equilibrium (G^{s}_{min}) and excess free energy of micellization (ΔG_{ex}) of the amphiphilic drugs including phenothiazines (CPZ and PMT) in the presence of different additives such as NaCl, HTAB and TX-100 [27]. The ΔG°_{m} values of drugs in the absence or presence of additives were negative and decreased with increase in additive concentration. This indicated that the micellization is more spontaneous in the presence of the additives. Gokturk et al. [28] spectrophotometrically studied the effect of ethanol on distribution and binding characteristics of poorly soluble model drug, phenothiazine in the presence of SDS and TX-100 [28]. The parameters such as binding constant were found to decrease with an increase in the percentage of ethanol due to the incorporation of ethanol molecules to the micellar surface. This suggested that amount of ethanol reduced the binding and the distribution of drug in micelles, this inhibitory effect being more for SDS than TX-100 micelles. Recently, Gokturk and Var [29] employed absorption spectroscopy to investigate the influence of pharmaceutically important co-solvents such as ethanol, ethyleneglycol and propyleneglycol (PG) on the interactions of promethazine hydrochloride (PMT) and triflupromazine hydrochloride (TFM) with anionic SDS micelles in the concentration range varying from premicellar to postmicellar region [29]. A decrease in absorbance values of the two phenothiazine drugs in the presence of surfactants at the concentration below cmc indicated the complex formation between them

due to electrostatic interactions. On the other hand, at the surfactant concentration above CMC, there has been an increase in the absorbance values signifying drug's binding with SDS micelles. Liao and Wiedmann [30] showed that the hydrophobicity has a significant impact on the solubilization of the bioactive molecules such as drugs e.g. amitriptyline, ethopropazine, imipramine, promazine, promethazine, quinacrine in lung surfactant on the basis of distribution coefficient and temperature measurements. It has also been reported that electrostatic interactions play an important role in addition to hydrophobic interactions. Owing to the wide applications of phenothiazine drugs in pharmacological and biological fields, the physicochemical aspects of their interactions with surfactants have been extensively studied. From the micellization and interfacial studies of phenothiazine drugs with surfactants, it has been observed that the CMC values of these drug-surfactant systems decreased with an increase in the concentration of surfactant which indicated that phenothiazine drugs form mixed micelles with surfactants through synergistic interactions.

In general, the amount of drug solubilized in a micellar system increases with the increase in temperature. Alkhamis et al. [31] studied the solubilization of the drug gliclazide, a second-generation sulfonylurea used in the treatment of non-insulin dependent diabetes mellitus. The drug solubility was determined as a function of the concentration of different surfactants at 25 and 37 °C and, for all the ionic surfactants studied; the solubilization was higher at 37 °C than at 25 °C. This was attributed to the increase in thermal agitation, which results in an increase in the space available for solubilization in the micelle, in addition to the increase of gliclazide solubility in water at higher temperatures. One interesting suggested approach is to combine micellar solubilization with other properties that may be improved in a drug solution. In this context, Palma et al. [32] combined the solubilization properties of a surfactant with the ascorbic acid antioxidant property that protected drugs from degradation by light, heat, dissolved oxygen and other radical producing species, by means of synthesizing an ascorbyl-decanoate surfactant. It was observed that micellar solutions of the surfactant significantly improved the solubility of hydrophobic drugs with respect to pure water, by including these molecules in the hydrophobic micellar core, as well as protected them from degradation. It was also observed that the drug solubilization was more effective for the most hydrophobic drugs (Danthron and Griseofulvin) than for more hydrophilic ones (Phenacetin).

2.2 Topical gel formulation

A gel coined in 19th century by Scottish chemist Thomson Graham is a solid, jelly like material that can have properties ranging from soft and weak to hard and tough [33, 34]. Gels consist of three-dimensional networks of cross-linked polymer chains and these polymers can be linked either through covalent bonds, i.e. by chemical cross-linking, or non-covalent bonds, i.e. by physical cross-linking. Non-covalent cross-linking occurs after polymerization and may be a result of either hydrophobic or electrostatic attractions, or both. Gel formulations are popular pharmaceutical dosage forms and as a result of which, many administrational routes have been suggested for gels but, herein, we concentrate on topical delivery. The contact time of a gel formulation on skin or mucosa is typically much longer than that of an aqueous solution owing to the more favorable adhesive [35, 36] and/or rheological [37-39] properties, which increases the absorption of the drug substance, opening up the possibility of: lower drug dose, longer dosing intervals, or both and importantly high patient compliance.

When applied to skin, the mucoadhesive and rheological properties of a gel may increase the residence time on the tissue. Advantageously, gels have better diffusion rate therefore quickly emptied of the drug, resulting in extended residence time at the site of application. To prolong the release of drug substances for gel formulations many strategies have been suggested; the drug can be formulated as solid particles in the gel, rendering a suspension [40]; the drug substance may interact with the gel polymer or the drug can be distributed to liposomes or micelles [41, 42], which are incorporated in the gel. In recent years the possibility of obtaining prolonged drug release from anionic, cationic or non-ionic aggregates, composed of surface-active molecules or charged surfactants and then incorporating these in gels has been explored [43].

Bachhav et al. [44] reported efficient topical drug administration for the treatment of superficial fungal infections and deliver the therapeutic agent to the target compartment with reducing risk of systemic side effects. The objective was to develop aqueous micelle solutions of clotrimazole (CLZ), econazole nitrate (ECZ) and fluconazole (FLZ) using novel amphiphilic methoxy-poly (ethylene glycol)-hexyl substituted polylactide (MPEG-hexPLA) block copolymers. The CLZ, ECZ and FLZ formulations were characterized with respect to drug loading and micelle size. Penetration pathways and micellar distribution in the skin were visualized using fluorescein loaded micelles and confocal laser scanning microscopy. ECZ

delivery was compared to that from Pevaryl® cream (1% w/w ECZ), a marketed liposomal formulation for topical application. ECZ deposition in porcine skin following 6 h application using the MPEG-dihexPLA micelles was >13-fold higher than that from Pevaryl® cream (22.8 ± 3.8 and 1.7 ± 0.6 μg/cm^2, respectively). A significant enhancement was also observed with human skin; the amounts of ECZ deposited were 11.3 ± 1.6 and 1.5 ± 0.4 μg/cm^2, respectively (i.e., a 7.5-fold improvement in delivery). Conclusively, the significant increase in ECZ skin deposition achieved using the MPEG-dihexPLA micelles demonstrates their ability to improve cutaneous drug bioavailability leading to improved clinical efficacy *in vivo*.

Ahmad et al. [45] studied that thymol (THY) and carvacrol (CARV), the principal chemical components of thyme oil that have long been known for their wide use in medicine due to antimicrobial and disinfectant properties. They drew attention to a possible synergistic antifungal effect of these monoterpenes with azole antimycotic-fluconazole. The inhibition of drug efflux pumps was considered a feasible strategy to overcome clinical antifungal resistance. They investigated the combination effects of these monoterpenes and FLC against 38 clinically obtained FLC-sensitive, and eleven FLC-resistant Candida isolates. Synergism was observed with combinations of THY-FLC and CARV-FLC evaluated by checkerboard microdilution method and nature of the interactions was calculated by FICI. In addition, antifungal activity was assessed using agar-diffusion and time-kill curves. Both monoterpenes inhibited efflux by 70-90%, showing their high potency to block drug transporter pumps.

Verma et al. [46] aimed at developing nanovesicles of econazole nitrate (EN) and formulating them as a suitable dermatological gel for improved therapeutic efficacy, better dispersity, and good storage stability. Optimized ethosomes with vesicle size and entrapment efficiency of 202.85 ± 5.10 nm and 81.05 ± 0.13%, respectively, were formulated as Carbopol 934 NF gels with varied permeation enhancers (G1–G7), and compared with liposomal and hydroethanolic gels. The evaluation of gels demonstrated G6 with a flux rate of 0.46 ± 0.22 μg/cm^2 hr^{½} as the best formulation that was able to exhibit controlled release of EN for 12 h across rat skin, and percent drug diffused from ethosomes was nearly two fold higher than liposomal and hydroethanolic gels. Confocal laser scanning microscopy demonstrated drug permeation as far as the last layer of epidermis (stratum basale). The results collectively suggest that because of the controlled drug release, better antifungal activity, and good storage stability, EN ethosomal gel has tremendous potential to serve as a topical delivery system. Kovacs et al. [47] reported the influence of solubilizers on the aqueous solubility of the

itraconazole, ketoconazole and miconazole in order to enhance their solubility for a possible parenteral dosage form. The solubilizer effect of acetate, phosphate and gluconate solutions were studied, along with ethanol, glycerol, macrogol 400, propylene glycol and surfactants, such as polysorbate 20, 60, 80 and sodium taurocholeate. All of the assessed excipients showed considerable solubility enhancement characteristics, moreover the binary and ternary combinations showed synergistic effects solubilizing more miconazole than what they solubilized separately. Ternary combinations were capable of solubilizing more than 30mg/ml miconazole, and more than 135 mg/ml of ketoconazole. In the same context, Chang et al. [48] developed more effective treatment for vaginal candidasis. Clotrimazole (CT) was formulated in mucoadhesive thermosensitive gels (MTG). Several MTG formulations composed of poloxamers (P) 407, 188, and polycarbophil (PC) were prepared. P188 and PC increased the mucoadhesiveness but reduced the syringebility of liquid forms of the gels. Based on the balance between the mucoadhesiveness and syringebility, MTG composed of P407/P188/PC (15/15/0.2 or 15/20/0.2) were further examined. Out of the two MTG, the formulation with 15% of P188 gelled at higher temperature and revealed lower elastic modulus. In vitro, sustained release of CT from MTG was observed. In vivo antifungal activity of CT, tested against *Candida albicans* vaginitis in female rats, was significantly prolonged after vaginal delivery using MTG. At 10 days post-dose, the cfu of *C. albicans* was more than 10^4 -fold decreased in MTG-treated groups. Moreover, the vaginal delivery of CT in MTG enhanced the viability of epithelial cells without affecting the morphology of vaginal mucosa. These results indicate that CT-containing vaginal MTG might be further developed for safe, convenient, and effective treatment of vaginal candidasis with reduced dosing interval.

Bachhav et al. [49] developed and evaluated microemulsion based gel for the vaginal delivery of fluconazole (FLZ). The solubility of FLZ in oils and surfactants was evaluated to identify components of the microemulsion. The bioadhesive potential and antifungal activity of the FLZ microemulsion based gel (FLZ-MBG) was determined in comparison to the marketed clotrimazole gel (Candid V® gel) by in vitro methods. The vaginal irritation potential of the FLZ-MBG was evaluated in rabbits. The clinical efficacy of the FLZ-MBG and Candid V® gel was evaluated in females suffering from vaginal candidiasis. The FLZ microemulsion exhibited globule size of 24 nm and polydispersity index of 0.98. Carbopol® ETD 2020 could successfully gel the FLZ microemulsion without disturbing the structure. The FLZ-MBG showed significantly higher ($P < 0.05$) in vitro bioadhesion and antifungal

activity as compared to that of Candid V® gel. The FLZ-MBG did not show any signs of vaginal irritation in the rabbits. The small-scale clinical studies indicated that the FLZ-MBG shows faster onset of action than Candid V® gel although no difference was observed in the clinical efficacy.

Liu et al. [50] reported a new strategy for the controlled release of a hydrophobic anticancer drug, camptothecin (CPT), which suffers a limited therapeutical utilization because of its poor water solubility. CPT was first solubilized in the solution of a cationic surfactant, dodecyltrimethylammonium bromide (DTAB). It has been demonstrated that the presence of DTAB has increased the solubility of CPT significantly. In a 50 mM DTAB solution, the drug's solubility was enhanced to 85 μM, 22 times of its solubility in pure water. The micellar drug solution of CPT-DTAB was subsequently used to prepare agarose hydrogels, which act as the drug carriers in the release studies. To take advantage of the cationic property of DTAB, negatively charged κ-carrageenan was added as a guest polymer in some hydrogel samples. The release of CPT from these hydrogel-surfactant systems was performed at 37 °C and the effects of DTAB and κ-carrageenan on the release of CPT were studied respectively. By fitting to the well-known Fickian diffusion model, the diffusion coefficients of CPT were obtained. In one more study, Liu and Li [51] reported the incorporation of CPT into the micelles formed from an ionic surfactant, sodium dodecyl sulfate (SDS) and the micellar drug aqueous solution was then used in preparation of the agarose hydrogel. It was observed that the presence of SDS greatly increased the solubility of CPT in water. For example, in 1mL of 1.0 wt. % SDS water solution, 0.11mg CPT could be solubilized (0.318mM), which was 83 times the solubility in pure water. It was the hydrophobic cores of the SDS micelles that were able to accept the lipophilic drug to form stable drug-immobilized micelles. The formulation of a hydrogel using the drug-immobilized micelles has allowed us to obtain a unique and novel drug release system where the drug molecules are encapsulated by the micelles and the drug-containing micelles are dispersed in the gel network. The release of CPT from the deliberately fabricated agarose hydrogel system has been studied as a function of surfactant concentration at 37 °C. Again, the diffusion coefficients of CPT obtained by fitting to Fick's law ranged from 2.12 to 7.36×10^{-7} $cm^2\,s^{-1}$. The results showed that SDS prolonged the drug release by reducing the diffusion coefficient of CPT in the gel.

D'Auria et al. [52] thoroughly studied the effect of surfactants or other additives on imidazoles biological profile. Initially, Itraconazole antifungal activity was investigated by agar diffusion tests. In this study the authors investigated the influence of sodium dioctyl sulfosuccinate, an anionic surfactant, in Sabouraud dextrose agar at different culture conditions on the itraconazole activity against *Candida albicans*. The results demonstrated that it is possible to obtain cleared and increased zones of inhibition and a good dosage/zone of inhibition correlation in complex medium of Sabouraud dextrose. Afterward, they studied the susceptibility assays of *Candida tropicalis* to miconazole [53]. Their data based on assays of miconazole nitrate and miconazole sulfosalicylate against *C. tropicalis* showed that it is possible to abolish various interference activities on the antimicrobial activity by suitable modifications of some cultural conditions. Thus, a study was carried out to assess miconazole sulfosalicylate activity on *C. tropicalis* throughout experiments performed by contact test and agar diffusion test. The use of these techniques made it possible to display some activity of the imidazoles even against strains of *C. tropicalis*, which were defined as resistant using usual susceptibility assay conditions. Experimental conditions which cause the increase of susceptibility of *C. tropicalis* are related to factors that modify the barrier function and cellular permeability as demonstrated mainly by the effect of electrical conductivity (E.C.), pH of the medium and pretreatment of fungal inoculum with sodium dioctylsulfosuccinate (SDSS).The results suggested that the correlation between drug dosage and inhibitory activity in vitro can be improved by such modifications. One more study by Simonetti et al. [54] reported the enhanced contact activity of fluconazole in association with antioxidants. According to their study, fluconazole alone does not demonstrate any contact activity against resistant organisms. Phenolic antioxidants, such as butylatedhydroxy anisole (BHA), appeared to promote fluconazole activity resulting in the killing of 10^4 cfu/mL of 11 resistant *Candida albicans* strains within 3-15 min and 10^4 cfu/mL of 10 resistant *Escherichia coli* strains within 6-15 min. Fluconazole activity was increased by the addition of ethyl alcohol (20%). Antioxidants appear to promote fluconazole activity by increasing cell membrane permeability. This combination has potential advantages in the administration of topical fluconazole. In one another study [55] , Tioconazole (TCZ) killed resistant *Candida albicans* in less than 3 min, after the addition of BHA, at sub-inhibitory concentrations. The bactericidal activity was also rapid against resistant *Escherichia coli*. BHA increased the TCZ activity in RPMI 1640 medium 18 times against ten strains of resistant *C. albicans* as judged by MIC and increased the activity 43 times against ten resistant *E. coli* strains. BHA at sub-

inhibitory concentrations promoted the reduction of *C. albicans* virulence by reducing 180 times the hyphal cells of TCZ and decreasing hydrophobicity. The synergy could be due to changes in cellular permeability because of increased leakage of cellular enzymes. Strippoli et al. [56] looked at the *in vitro* effect of an antioxidant, propyl gallate (PG), on the antifungal activity of miconazole sulphosalicylate, econazole sulphosalicylate and ketoconazole against 40 clinical isolates of *C. albicans*. The combination of imidazole and PG gave MIC values 10–150 times lower than those of imidazole alone. The optimal conditions for this enhanced activity were pH 6.2–8.0 and a fungal cell concentration lower than 3×10^5 cells/mL. The mechanism of the interaction between imidazole and PG was not known and demonstrated but reported that might be PG had effect on the P-450 cytochrome. Theoretically this combination could reduce the side effects of long treatment with imidazoles and lower the risk of resistance to these antifungal drugs. One more study on *in vitro* activity of propyl gallate-azole drug combination against azole-resistant *C. albicans* strains was reported by D'Auria et al. [57]. They focused on the influence of antioxidant i.e. PG in addition to in vitro antifungal activity of itraconazole and fluconazole in order to determine whether PG could increase the antifungal activity and reduce strain resistance. For this, they performed susceptibility tests against azole-resistant isolates of *C. albicans* by microbroth dilution method in the presence of PG at 400 $\mu g\ ml^{-1}$ PG-triazole combination brought about a marked reduction of inhibitory azole concentration. In particular, the MIC_{90} for itraconazole and fluconazole dropped from 1 $\mu g\ ml^{-1}$ – 0.125 $\mu g\ ml^{-1}$ and from > 64 ml^{-1} – 8 $\mu g\ ml^{-1}$, respectively. Conclusively, synergism was obtained with mechanism likely to be followed as effect on P-450 cytochrome.

Romano et al. [58] reported the antioxidant and antibacterial activity of a methanol rosemary extract (RE) containing 30% carnosic acid (CA), 16% carnosol (COH) and 5% rosmarinic acid (RA) in vitro alone and in combination with the antioxidant food additives butylated hydroxytoluene (BHT) and butylated hydroxyanisole (BHA). The antioxidant efficiency of the extract, CA, and RA, was determined by a kinetic analysis of the 2,2-diphenyl-2-picrylhydrazyl hydrate radical (DPPH) scavenging activity. RE showed two different rate slopes in the reduction of DPPH vs. time curve, which correlated with the distinct behaviours of RA and CA; pure RA reached the plateau more rapidly than CA. A synergistic antioxidant effect between RE and BHT was demonstrated by isobolographic analysis and a synergistic interaction of RE with BHA to inhibit E. *coli* and *Staphylococcus aureus* growth was observed. Therefore, rosemary not only enhances the antioxidant efficiency of BHA and

BHT, but also the antibacterial effect of BHA; allowing a decrease from 4.4 to17 folds in the amounts of the synthetic compounds used.

References

[1] M. A. Cheema, S. Barbosa, P. Taboada, E. Castro, M. Siddiq, and V. Mosquera, "A thermodynamic study of the amphiphilic phenothiazine drug thioridazine hydrochloride in water/ethanol solvent," *Chemical Physics,* vol. 328, pp. 243-250, 2006.

[2] R. Zana, "Surfactant solutions new methods of investigations," Marcel Dekker, New York 1986.

[3] I. M. Banat, R. S. Makkar, and S. Cameotra, "Potential commercial applications of microbial surfactants," *Applied Microbiology and Biotechnology,* vol. 53, pp. 495-508, 2000.

[4] B. E. Rabinow, "Nanosuspensions in drug delivery," *Nature Reviews Drug Discovery,* vol. 3, pp. 785-796, 2004.

[5] C. W. Pouton, "Formulation of poorly water-soluble drugs for oral administration: physicochemical and physiological issues and the lipid formulation classification system," *European Journal of Pharmaceutical Sciences,* vol. 29, pp. 278-287, 2006.

[6] M. J. Lawrence, "Surfactant systems: their use in drug delivery," *Chemical Society Reviews,* vol. 23, pp. 417-424, 1994.

[7] J. Cupp, P. Wanda, A. Keith, and W. Snipes, "Inactivation of the lipid-containing bacteriophage PM2 by butylated hydroxytoluene," *Antimicrobial Agents and Chemotherapy,* vol. 8, pp. 698-706, 1975.

[8] T. Vardaman, J. May, and J. Drott, "Studies on the Effect of Butylated Hydroxytoluene on Mycoplasma synoviae," *Poultry Science,* vol. 57, pp. 1526-1529, 1978.

[9] N. Stern, L. Smoot, and M. Pierson, "Inhibition of Staphylococcus aureus growth by combinations of butylated hydroxyanisole, sodium chloride, and pH," *Journal of Food Science,* vol. 44, pp. 710-712, 1979.

[10] J. J. Kabara and D. S. Orth, *Preservative-free and Self-preserving Cosmetic and Drug Products: Principles and Practices*: CRC Press, 1997.

[11] J. J. Kabara, "Topical antimicrobial pharmaceutical compositions," ed: EP Patent 0,530,861, 1998.

[12] D. Kaushal, D. Rana, M. Chauhan, and S. Chauhan, "A physicochemical study of SDS in aqueous solution of Furosemide: Effect of DMSO on surfactant-Furosemide interaction," *Fluid Phase Equilibria,* vol. 355, pp. 123-129, 2013.

[13] T. Farías, L.-C. De Menorval, J. Zajac, and A. Rivera, "Solubilization of drugs by cationic surfactants micelles: Conductivity and ^{1}H NMR experiments," *Colloids and Surfaces A: Physicochemical and Engineering Aspects,* vol. 345, pp. 51-57, 2009.

[14] C. O. Rangel-Yagui, H. W. L. Hsu, A. Pessoa-Jr, and L. C. Tavares, "Micellar solubilization of ibuprofen: influence of surfactant head groups on the extent of solubilization," *Revista Brasileira de Ciências Farmacêuticas,* vol. 41, pp. 237-246, 2005.

[15] S.-H. Park and H.-K. Choi, "The effects of surfactants on the dissolution profiles of poorly water-soluble acidic drugs," *International Journal of Pharmaceutics,* vol. 321, pp. 35-41, 2006.

[16] S. Mehta, K. Bhasin, A. Kumar, and S. Dham, "Micellar behavior of dodecyldimethylethyl ammonium bromide and dodecyltrimethylammonium chloride in aqueous media in the presence of diclofenac sodium," *Colloids and Surfaces A: Physicochemical and Engineering Aspects,* vol. 278, pp. 17-25, 2006.

[17] M. Ahmed, A. Rhgigh, and F. Shakeel, "Effect of Surfactants on the Crystal Properties and Dissolution Behavior of Aspirin," *Asian J. Research Chem,* vol. 2, pp. 2, 2009.

[18] L. K. Tiwary, A. Mandal, M. S. Alam, S. Thennarasu, and A. B. Mandal, "Thermodynamics studies on tyrosine-hydantoin drug–cetyltrimethylammonium bromide mixed micellar system," *Colloids and Surfaces B: Biointerfaces,* vol. 82, pp. 126-133, 2011.

[19] S. Bakkialakshmi and D. Chandrakala, "A spectroscopic investigations of anticancer drugs binding to bovine serum albumin," *Spectrochimica Acta Part A: Molecular and Biomolecular Spectroscopy,* vol. 88, pp. 2-9, 2012.

[20] M. A. Cheema, M. Siddiq, S. Barbosa, P. Taboada, and V. Mosquera, "Surface and bulk properties of two amphiphilic phenothiazine drugs in different aqueous media," *Journal of Chemical & Engineering Data,* vol. 53, pp. 368-373, 2007.

[21] R. Savic, A. Eisenberg, and D. Maysinger, "Block copolymer micelles as delivery vehicles of hydrophobic drugs: micelle-cell interactions," *Journal of Drug Targeting,* vol. 14, pp. 343-355, 2006.

[22] S. Schreier, S. V. Malheiros, and E. de Paula, "Surface active drugs: self-association and interaction with membranes and surfactants. Physicochemical and biological aspects," *Biochimica et Biophysica Acta (BBA)-Biomembranes*, vol. 1508, pp. 210-234, 2000.

[23] E. J. Kim and D. O. Shah, "Cloud point phenomenon in amphiphilic drug solutions," *Langmuir*, vol. 18, pp. 10105-10108, 2002.

[24] A. Florence and R. Parfitt, "Micelle formation by some phenothiazine derivatives. II. Nuclear magnetic resonance studies in deuterium oxide," *The Journal of Physical Chemistry*, vol. 75, pp. 3554-3560, 1971.

[25] M. A. Rub and A. Z. Naqvi, "Mixed micelles of amphiphilic drug promethazine hydrochloride and surfactants (conventional and gemini) at 293.15 K to 308.15 K: Composition, interaction and stability of the aggregates," *Journal of Colloid and Interface Science*, vol. 354, pp. 700-708, 2011.

[26] M. S. Alam, A. Mandal, and A. B. Mandal, "Effect of KCl on the micellization and clouding phenomenon of the amphiphilic phenothiazine drug promethazine hydrochloride: some thermodynamic properties," *Journal of Chemical & Engineering Data*, vol. 56, pp. 1540-1546, 2011.

[27] M. S. Alam and A. B. Mandal, "Thermodynamics of some amphiphilic drugs in presence of additives," *Journal of Chemical & Engineering Data*, vol. 55, pp. 2630-2635, 2010.

[28] S. Gokturk and U. Var, "Effect of ethanol on partition and binding equilibrium of phenothiazine in anionic and nonionic micellar solutions," *Curr. Res. Chem*, vol. 3, pp. 49-61, 2011.

[29] S. Göktürk and U. Var, "Effect of Pharmaceutically Important Cosolvents on the Interaction of Promethazine and Trifluopromazine Hydrochloride with Sodium Dodecyl Sulfate Micelles," *Journal of Dispersion Science and Technology*, vol. 33, pp. 527-535, 2012.

[30] X. Liao and T. S. Wiedmann, "Solubilization of cationic drugs in lung surfactant," *Pharmaceutical Research*, vol. 20, pp. 1858-1863, 2003.

[31] K. A. Alkhamis, H. Allaboun, and W. a. Y. Al-Momani, "Study of the solubilization of gliclazide by aqueous micellar solutions," *Journal of Pharmaceutical Sciences*, vol. 92, pp. 839-846, 2003.

[32] S. Palma, R. H. Manzo, D. Allemandi, L. Fratoni, and P. Lo Nostro, "Drugs solubilization in ascorbyl–decanoate micellar solutions," *Colloids and Surfaces A: Physicochemical and Engineering Aspects,* vol. 212, pp. 163-173, 2003.

[33] T. Graham, "XXXV.—On the properties of silicic acid and other analogous colloidal substances," *Journal of the Chemical Society,* vol. 17, pp. 318-327, 1864.

[34] D. J. Lloyd, "The problem of gel structure," *Colloid Chemistry,* vol. 1, pp. 767-782, 1926.

[35] K. Edsman and H. Hägerström, "Pharmaceutical applications of mucoadhesion for the non-oral routes," *Journal of Pharmacy and Pharmacology*, vol. 57, pp. 3-22, 2005.

[36] R. B. Gandhi and J. R. Robinson, "Oral cavity as a site for bioadhesive drug delivery," *Advanced Drug Delivery Reviews,* vol. 13, pp. 43-74, 1994.

[37] J. Carlfors, K. Edsman, R. Petersson, and K. Jörnving, "Rheological evaluation of Gelrite® in situ gels for ophthalmic use," *European Journal of Pharmaceutical Sciences,* vol. 6, pp. 113-119, 1998.

[38] K. Edsman, J. Carlfors, and R. Petersson, "Rheological evaluation of poloxamer as an in situ gel for ophthalmic use," *European Journal of Pharmaceutical Sciences,* vol. 6, pp. 105-112, 1998.

[39] N. Peppas, P. Bures, W. Leobandung, and H. Ichikawa, "Hydrogels in pharmaceutical formulations," *European Journal of Pharmaceutics and Biopharmaceutics,* vol. 50, pp. 27-46, 2000.

[40] H. Sjöberg, S. Persson, and N. Caram-Lelham, "How interactions between drugs and agarose-carrageenan hydrogels influence the simultaneous transport of drugs," *Journal of Controlled Release,* vol. 59, pp. 391-400, 1999.

[41] A. Paavola, I. Kilpeläinen, J. Yliruusi, and P. Rosenberg, "Controlled release injectable liposomal gel of ibuprofen for epidural analgesia," *International Journal of Pharmaceutics,* vol. 199, pp. 85-93, 2000.

[42] M. Paulsson and K. Edsman, "Controlled drug release from gels using surfactant aggregates: I. Effect of lipophilic interactions for a series of uncharged substances," *Journal of Pharmaceutical Sciences,* vol. 90, pp. 1216-1225, 2001.

[43] T. Bramer, M. Paulsson, K. Edwards, and K. Edsman, "Catanionic drug–surfactant mixtures: phase behavior and sustained release from gels," *Pharmaceutical Research,* vol. 20, pp. 1661-1667, 2003.

[44] Y. Bachhav, K. Mondon, Y. Kalia, R. Gurny, and M. Möller, "Novel micelle formulations to increase cutaneous bioavailability of azole antifungals," *Journal of Controlled Release,* vol. 153, pp. 126-132, 2011.

[45] A. Ahmad, A. Khan, and M. Nikhat, "Reversal of efflux mediated antifungal resistance underlies synergistic activity of two monoterpenes with fluconazole," *European Journal of Pharmaceutical Sciences,* vol. 48, pp. 80-86, 2013.

[46] P. Verma and K. Pathak, "Nanosized ethanolic vesicles loaded with econazole nitrate for the treatment of deep fungal infections through topical gel formulation," *Nanomedicine: Nanotechnology, Biology and Medicine,* vol. 8, pp. 489-496, 2012.

[47] K. Kovács, G. Stampf, I. Klebovich, I. Antal, and K. Ludányi, "Aqueous solvent system for the solubilization of azole compounds," *European Journal of Pharmaceutical Sciences,* vol. 36, pp. 352-358, 2009.

[48] J. Yun Chang, Y.-K. Oh, H. Soo Kong, E. Jung Kim, D. Deuk Jang, K. Taek Nam, and C.-K. Kim, "Prolonged antifungal effects of clotrimazole-containing mucoadhesive thermosensitive gels on vaginitis," *Journal of Controlled Release,* vol. 82, pp. 39-50, 2002.

[49] Y. G. Bachhav and V. B. Patravale, "Microemulsion based vaginal gel of fluconazole: Formulation, *in vitro* and *in vivo* evaluation," *International Journal of Pharmaceutics,* vol. 365, pp. 175-179, 2009.

[50] J. Liu, L. Li, and Y. Cai, "Immobilization of camptothecin with surfactant into hydrogel for controlled drug release," *European Polymer Journal,* vol. 42, pp. 1767-1774, 2006.

[51] J. Liu and L. Li, "SDS-aided immobilization and controlled release of camptothecin from agarose hydrogel," *European Journal of Pharmaceutical Sciences,* vol. 25, pp. 237-244, 2005.

[52] F. D'Auria, N. Simonetti, and V. Strippoli, "Increased itraconazole antifungal activity by agar diffusion test," *Journal of Microbiological Methods,* vol. 20, pp. 47-54, 1994.

[53] N. Simonetti, G. Simonetti, V. Strippoli, A. Callari, and M. Tecca, "Susceptibility assays of *Candida tropicalis* to miconazole," *Journal of Microbiological Methods,* vol. 30, pp. 221-229, 1997.

[54] G. Simonetti, A. Villa, and N. Simonetti, "Enhanced contact activity of fluconazole in association with antioxidants against fluconazole-resistant organisms," *Journal of Antimicrobial Chemotherapy,* vol. 50, pp. 257-259, 2002.

[55] G. Simonetti, N. Simonetti, and A. Villa, "Increase of activity of tioconazole against resistant microorganisms by the addition of butylated hydroxyanisole," *International Journal of Antimicrobial Agents*, vol. 22, pp. 439-443, 2003.

[56] V. Strippoli, F. D'Auria, M. Tecca, A. Callari, and G. Simonetti, "Propyl gallate increases in vitro antifungal imidazole activity against *Candida albicans*," *International Journal of Antimicrobial Agents*, vol. 16, pp. 73-76, 2000.

[57] F. D'Auria, M. Tecca, R. Strippoli, and N. Simonetti, "*In vitro* activity of propyl gallate–azole drug combination against fluconazole-and itraconazole-resistant Candida albicans strains," *Letters in Applied Microbiology*, vol. 32, pp. 220-223, 2001.

[58] C. S. Romano, K. Abadi, V. Repetto, A. A. Vojnov, and S. Moreno, "Synergistic antioxidant and antibacterial activity of rosemary plus butylated derivatives," *Food Chemistry*, vol. 115, pp. 456-461, 2009.

CHAPTER-3

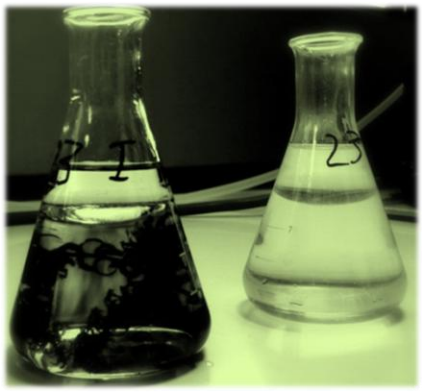

EXPERIMENTAL

In this chapter, a detailed description of chemicals and reagents, apparatus/instruments and experimental procedure has been discussed.

3.1 Chemicals and Reagents

3.1.1 Water Water being one of the major solvent in the study which is also employed in calibration of instruments or apparatus was obtained by double distillation process. By volume, 1000 ml of pure water was collected from the double distillation unit (Harco & Co.) which was further subjected to distillation on acidified $KMnO_4$ over a 750 mm long fractionating column. Different fractions of distilled water were collected and their conductivity, κ (S cm^{-1}) and pH were determined. The sample of κ value ~ 1–3 × 10^{-6} S cm^{-1} was collected for use. The pH of the sample collected in the range 6.75–6.95. Both of these parameters were measured at room temperature. The sample of purified water so obtained was not utilized after two days.

3.1.2 Solvents Absolute alcohols i.e. methanol, ethanol and 1–propanol were obtained from Merck Chemicals with purity ≥ 99.9 %. Other solvents in experimental and lab processes such as acetone, sulfuric acid and hydrochloric acid etc. for complete cleansing of glassware were also obtained from Merck Chemicals. Physico–chemical study of surfactants in presence of BHA/BHT was carried out in three different solvent compositions of alcohols i.e. 100, 70, 30% v/v methanol, ethanol and 1–propanol.

3.1.3 Pharmaceutical Ingredients Butylatedhydroxy anisole (BHA) and butylatedhydroxy toluene (BHT) were obtained from MERCK Chemicals and were used as received. Clotrimazole (CLZ) was obtained as gift sample from Glenmark Pharmaceuticals Pvt. Ltd. Carbopol 940 and triethanol amine were obtained from Himedia and were used as such for gel formulation.

3.1.4 Animals

In present study, male *Sprague Dawley* (SD) rats (160–180 g) were used. Animals were housed in plastic cages in a 12 h dark–light cycle, with controlled temperature (25 °C) and humidity (70%). Water and food were provided ad libitum throughout the study. The animals were housed in Central Animal Facility (CAF) of ASBASJSM college of Pharmacy, Bela, Ropar, India. All protocols were approved by Institutional Animal Ethics Committee (IAEC),

and experiments were performed in accordance with Committee for the Purpose of Control and Supervision on Experiments on Animals (CPCSEA).

3.1.5 Surfactants All the surfactants used in the study were of AR grade and purity > 99.0%. Anionic surfactant; sodium dodecyl sulfate (SDS) was obtained from Merck Chemicals, cationic surfactant; cetyltrimethylammonium bromide (CTAB) was obtained from Sigma, and nonionic surfactant; *tert*– octylphenol ethoxylated or Triton X–100 (TX100) containing 9 units ethylene oxide as the hydrophilic moiety was also obtained from Merck Chemicals.

3.2 Experimental Details (Apparatus and Methods)

3.2.1 pH Measurements

The pH of the purified water was tested using Cyber scan 2500 pH meter (Figure 3.1.). Also, the solutions prepared for investigation were monitored regularly while performing experiments using this apparatus.

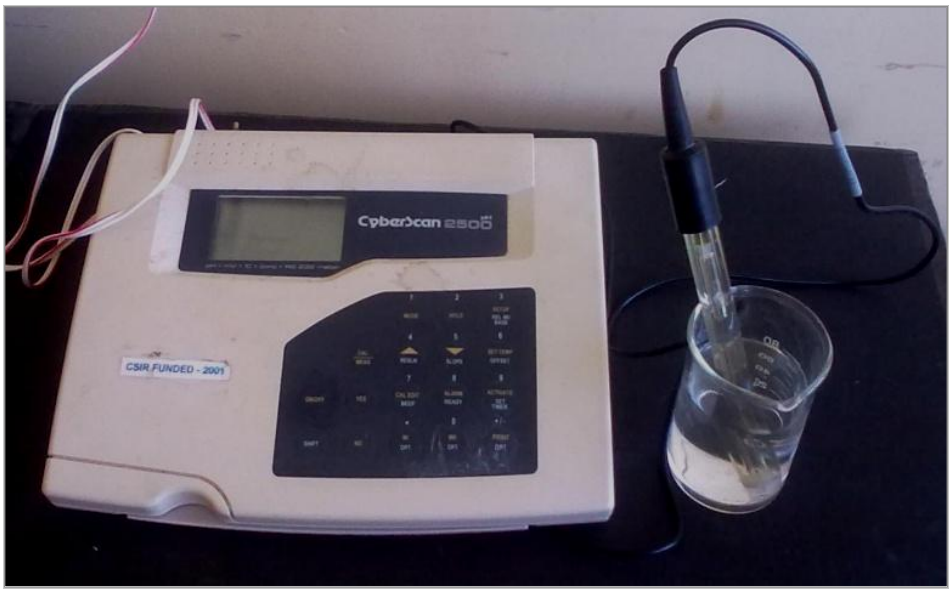

Figure 3.1: Cyber scan 2500 pH meter.

3.2.2 Thermostat

A high precision water thermostat (supplied by Harco & Co.) fitted with a digital temperature controlled device was used for all experimental measurements. The temperature of thermostat was maintained within ± 0.1 °C over the entire temperature range studied. All precautions were taken to protect the heat loss due to convection, especially when the measurements were

carried out at higher temperatures. However, the temperature of bath was continuously monitored with the help of a calibrated thermometer.

3.2.3 Conductivity measurements

Conductivity measurements were carried out with digital conductivity meter Cyber scan CON–510 (Figure 3.2.). It was calibrated at 25 °C by determining the limiting molar conductance, Λ_o values of $NaNO_3$, $AgNO_3$, Bu_4NI, Bu_4NBr and $NaBPh_4$ in DMSO at 25 °C. Λ_o values of these electrolytes were found to be 41.1, 44.0, 36.0 and 35.8 S cm^2 mol^{-1} , respectively which were in good agreement with those reported in literature [1]. The temperature of the solution was maintained ± 0.1 °C by circulating water from thermostat through a double walled vessel containing the solution. The circulation was done with the help of a high power digital water circulator supplied by Riviera Pvt. Ltd., Mumbai. The sample was allowed to attain the temperature of thermostat before taking the measurements.

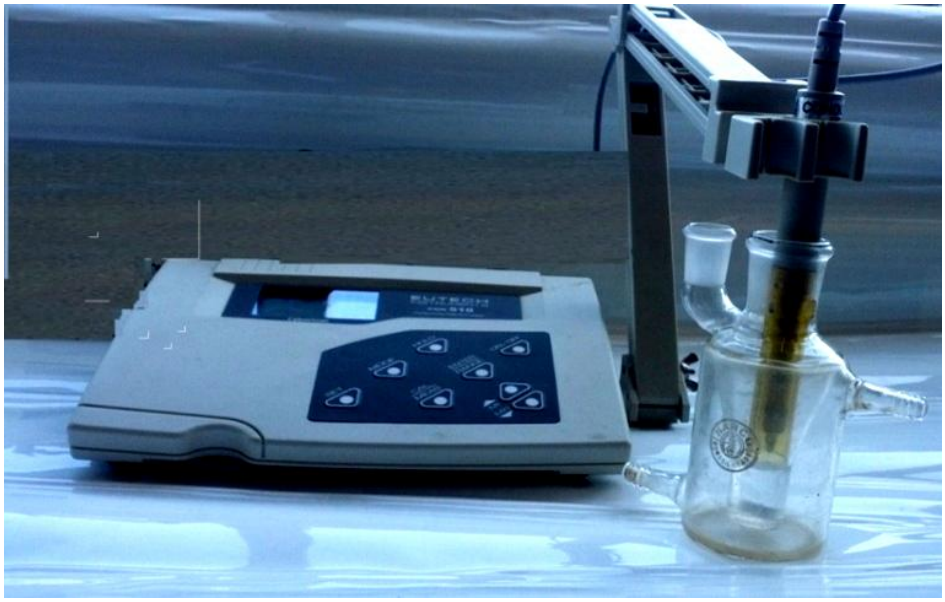

Figure 3.2: Cyber scan CON– 510 conductivity meter.

3.2.3.1 Determination of Critical Micelle Concentration (CMC)

The critical micelle concentration (CMC) was obtained at different temperatures (25–35) °C by measuring the specific conductance of SDS, CTAB and TX–100 at fixed concentrations of BHA and BHT i.e., (0.03 and 0.02) mol kg^{-1}, respectively. The choice of temperature was based on standard temperature, i.e. 25 °C, and relevance to body temperature, which remains at about 35 °C. The concentration of the solution was varied by adding aliquots of

concentrated stock solution of surfactants to the known volume of solution in the double walled vessel by means of a 10–100 μL eppendorf micropipette. The experiments were repeated twice with two different stock solutions of surfactants. The specific conductivity data were plotted against molar concentration of surfactants and CMC was estimated from the intersection point by drawing tangents in the resultant graph [2, 3]. The reproducibility of individual points was reasonably good and the standard deviation of the mean in the CMC was found to be < ± 2 %. This deviation was calculated from the CMC data obtained from two different runs.

3.2.3.2 Thermodynamics

The CMC values were thereafter utilized to evaluate and calculate the thermodynamic parameters. The *d* ln (X_{cmc})/dT was accounted as the slope of the straight line obtained by plotting lnX_{cmc} against temperature, α (degree of counter ion dissociation) was calculated from the relation, $\alpha = S_2/S_1$, where, S_1 and S_2 are the slopes in the pre micellar and post micellar regions. The relations [4, 5] used for standard enthalpy change, standard entropy (ΔS°_m) and Gibbs free energy change (ΔG°_m) for micellization are as follows.

$$\Delta H^o_m = -RT^2(2-\alpha)[d(\ln X_{CMC})/dT] \qquad \text{(Eq. 3.1)}$$

$$\Delta S^o_m = \frac{\Delta H^o_m - \Delta G^o_m}{T} \qquad \text{(Eq. 3.2)}$$

$$\Delta G^o_m = (2-\alpha)RT\ln(X_{CMC}) \qquad \text{(Eq. 3.3)}$$

3.2.4 Density and ultrasonic sound velocity Measurements

Density (ρ) and ultrasonic sound velocity (*u*) measurements were performed on a high–precision digital Density and Sound Analyzer–5000 (DSA–5000) as shown in Figure 3.3, at different temperatures (25–35) °C. It was supplied by Anton Paar Gmbh, Graz, Austria. The instrument was calibrated periodically with distilled water over a temperature range (20–50 °C). The precision in the density data was found to be better than ± 2 × 10^{-6} g·cm^{-3} and that of velocity data, it was better than ± 0.20 m s^{-1}. The precision in temperature of the DSA–5000 is ± 0.001 °C.

Figure 3.3: Density and sound analyzer (DSA–5000).

3.2.4.1 Volumetric and compressibility parameters

The obtained data from density (ρ) and ultrasonic sound velocity (*u*) was utilized to calculate the apparent molar volume (ϕ_v) and apparent molar adiabatic compression (ϕ_κ) values. These parameters were calculated using following relation [6, 7].

$$\phi_V = \frac{M}{\rho} + \frac{[\rho_o - \rho]}{m\rho\rho_o} \qquad \text{(Eq. 3.4)}$$

$$\phi_\kappa = \phi_v\kappa_s + \frac{[\kappa_s - \kappa_o]}{m\rho_o} \qquad \text{(Eq. 3.5)}$$

where m (mol kg^{-1}) is the molality of the solution calculated from the molar concentration data using m = 1/[d/C–M/1000], here m (mol kg^{-1}) stands for molal concentration and M (g mol^{-1}) for relative molar mass of surfactant, ρ (kg m^{-3}) is the density of the solution, ρ_o (kg m^{-3}) is the density of the solvent system. κ_s (TPa^{-1}) stands for isentropic compressibility of the solution and κ_s was determined by using relation as $\kappa_s = 1/\rho u^2$.[6]

3.2.5 Viscosity Measurements

The viscosity (η) measurements [8] for various alcoholic/ hydroalcoholic solutions were carried out in a calibrated jacketed ubbelohde viscometer using calibrated stopwatch. The

viscosity (η) measurements for surfactants in presence of BHA and BHT at fixed concentration were determined at three temperatures (25–35) °C with an interval of 5 °C and accounted for 100%, 70% and 30% (v/v) alcohol (methanol, ethanol and 1–propanol) compositions with water. The ubbelohde viscometer was periodically cleaned by treating with chromic acid and distilled water and finally washed with alcohol and dried in oven for ~ 2 hrs. After drying, the ubbelohde viscometer was filled with fixed volume of the test solution. The approximate flow time of water was 460 sec at 25 °C. The viscometer was always placed vertically in a water thermostat having a digital temperature controller of accuracy ± 0.05 °C. The samples were kept imperturbable within viscometer for about 10 minutes before every measurement just to settle time dependent effect. The average deviation for three measurements of a single concentration of the solution did not exceed ± 0.03 sec. The precision achieved in viscosity measurement was well within ± 0.01%.

However, the viscometer was calibrated with DMSO and MeOH (both of A.R. Grade) at 298.15 K using viscosity coefficient, n_o = 0.008903 poise and density, d = 0.99707 g cm^{-3} for water. The viscosity coefficients of DMSO and MeOH were found to be 0.02 and 0.0055 poise, respectively which were found in good agreement with the literature values [9]. The precision achieved in viscosity measurements in flow time was estimated to be better than $\pm$ 3 %. The entire work was concerned solely with relative viscosities which were determined by using the equation [10] (3.6).

$$\eta_r = \eta / \eta_o = (t \times d)/(t_o \times d_o) \qquad \text{(Eq. 3.6)}$$

where, t_o, d_o and n_o refers to the flow time, density and viscosity of solvents and t, d of solution, respectively.

3.3 Pre–formulation Drug analysis

3.3.1 Determination of melting point

Capillary fusion method was used to determine the melting point of clotrimazole using Remi's melting point apparatus. The melting point was determined and compared with the literature value [11].

3.3.2 Determination of absorption maxima

A solution of clotrimazole (10µg/ml) in methanol was scanned between 200–400 nm, using Shimadzu 1700 spectrophotometer. The scanned λ_{max} was in good agreement with literature value [11].

3.3.3 Determination of solubility

Solubility studies of drug sample were carried out in pure methanol as well as optimized ratio of phosphate buffer (pH 7.4) and methanol i.e. 6:4. An excess amount of drug was added to screw capped vials containing 10 ml of solution, in each. The vials were kept in water bath shaker at 25 °C and shaken for 24 hours until the equilibrium was attained. The saturated solution then filtered through whatmann filter paper and was analyzed on UV Spectrophotometer at λ_{max} of each solvent.

3.4 Drug – excipient compatibility studies

While preparing a formulation for the development of final dosage form, it is mandatory to confirm the compatibility between the drug and polymer to be utilized and to ensure that the drug is not interacting with polymer. FTIR technique was been used to determine the interaction of drug with excipients.

3.4.1 Fourier Transform Infra Red spectral analysis

The Fourier Transform Infra – Red (FTIR) analysis of the drug and polymer were carried out for qualitative compound identification using Perkin Elmer 1600. The pellets were prepared on KBr – press (Spectra Lab., India). The spectra were scanned over wave number range of 4000 cm^{-1} – 400 cm^{-1}. Since FTIR is related to covalent bonds or hydrogen bonds, the spectra provide detailed information about the structural arrangements of molecular compounds. FTIR confirm the functional identity of the drug and to detect the interaction of the drug with excipients [12].

3.5 Preparation of standard plots

Standard plots of clotrimazole were prepared in:

1. Methanol
2. Methanol: Phosphate buffer (pH 7.4)

3.5.1 Standard plot of clotrimazole in methanol and methanol: phosphate buffer (pH 7.4)

50 mg of clotrimazole was dissolved in small volume of methanol in 100 ml volumetric flask and volume was made up to 100 ml with methanol to get a concentration of 500 µg/ml. From this stock solution, aliquots were withdrawn into a series of 10 ml volumetric flask and volume was made with methanol to get a concentration ranging from 10–500 µg/ml. Due to precipitation and hydrophobic nature of drug, the optimized concentration of buffer and methanol was defined in order to prepare standard calibration curve. Same amount of clotrimazole was dissolved in optimized methanol : phosphate buffer pH 7.4 (4 : 6) system in 100 ml volumetric flask and volume was made up to 100 ml with methanol: phosphate buffer 7.4 (4 : 6) to get a concentration of 500 µg/ml. Similarly, from this stock solution, aliquots were withdrawn into a series of 10 ml volumetric flask and volume was made with methanol to get a concentration ranging from 10–500 µg/ml. The absorbance of the resulting solutions was then measured at 261 nm using UV spectrophotometer against parent solvent as reference [13].

3.6 Formulation of gel

3.6.1 Preparation of micellar solution with SDS, CTAB and TX100

From our previous thermo–physical analysis studies, the critical micelle concentration (CMC) with most feasible and thermodynamic stable concentration was taken into consideration. Among them, 30% v/v EtOH was found to be the most feasible and thermodynamically controlled system which was lately utilized in the present formulation studies. It was found and reported that the presence of additives facilitated the micellization process, resulting early micelle formation. In context of this, three optimized surfactant's (SDS, CTAB and TX100) concentrations near/ above CMCs were selected, respectively.

Likely, for SDS (6.0, 7.0 and 8.0 mmol kg^{-1}), CTAB (0.8, 0.9 and 1.0 mmol kg^{-1}) and TX100 (0.20, 0.22 and 0.24 mmol kg^{-1}) were the selected concentrations of surfactants. Optimized concentration was utilized for BHA and BHT with respect to obtained CMC values of surfactant in 30% v/v EtOH. All the calculate concentrations based on thermo–physical analysis are presented in Table 3.2. Accordingly, BHA (5 mg) and BHT (4 mg) were added to surfactant hydroethanolic solutions (30% v/v EtOH). The mixture was stirred at room

temperature at 700 rpm for 24 h. Afterward the mixture was centrifuged at 10000 rpm at 25 °C for 15 min and then upper solution was filtered through a nylon syringe filter (pore size 0.2 μm, Whatman Inc., USA). The prepared micellar solution was dispersed into the gel. The list of instruments used in present study has been provided in Table 3.1.

Table 3.1: List of other instruments used in the study

S. No.	Equipments	Manufacturer/Model
1	U.V. Visible Equipments	Nanodrop, Schimadzu UV–1700
2	Diffusion cell apparatus	Orchid scientific & innovative India Pvt. Ltd.
3	Humidity control chamber	Narang scientific works NSW–175
4	Electronic weighing balance	Shimadzu A × 200
5	Hot air oven	Narang scientific works NSW–143
6	Magnetic stirrer	Harco & Co.
7	Melting point apparatus	Remi's Equipment Pvt. Ltd.

3.6.2 Preparation of clotrimazole gel

The gel base was prepared by dispersing the polymer (carbopol 940) in distilled water. Carbopol 940 was chosen due to its hydrophilic nature and bioadhesive property, which may result in an increased residence time of a drug at the site of absorption by interacting with the topical membrane. The polymer was weighed accordingly for each formulation and then soaked in distilled water for 2 h prior to use. Afterward, it was dispersed in distilled water under magnetic stirring for 1 h so as to obtain a homogenous gel base of 1% w/w. Thereafter, SDS/CTAB/TX100 immobilized BHA, BHT and BHA + BHT were added to the gel base. Triethanolamine (TEA), pH = 7.0 was added drop–wise to obtain neutralized carbopol gels and were further subjected to constant stirring. The concentration of employed ingredients has been presented in **Table 3.2**.

3.7 Evaluation of gel

3.7.1 Homogeneity and grittiness

All the gel formulations were tested for homogeneity by visual inspection after the gels have been stabilized in the container. They were tested for their appearance and presence of any aggregates. All the formulations were evaluated microscopically for the presence of particles and no appreciable particulate matter was seen under light microscope. Hence the gel preparation fulfils the requirement as desired for any topical preparation.

3.7.2 pH measurement

Further, the pH of gel formulations was determined. The measurement of pH of each formulation was done in triplicate and average values were calculated.

Table 3.2: Formulations containing different concentration additives and excipients.

S. No.	Codes	CLZ (%)	BHA (mg)	BHT (mg)	SDS (mg)	CTAB (mg)	TritonX–100 (mg)
1	CA–1S	1	5	–	17	–	–
2	CA–2S	1	5	–	20	–	–
3	CA–3S	1	5	–	23	–	–
4	CT–1S	1	–	4	17	–	–
5	CT–2S	1	–	4	20	–	–
6	CT–3S	1	–	4	23	–	–
7	CAT–1S	1	5	4	17	–	–
8	CAT–2S	1	5	4	20	–	–
9	CAT–3S	1	5	4	23	–	–
10	CA–1C	1	5	–	–	3	–
11	CA–2C	1	5	–	–	4	–
12	CA–3C	1	5	–	–	4.5	–
13	CT–1C	1	–	4	–	3	–
14	CT–2C	1	–	4	–	4	–
15	CT–3C	1	–	4	–	4.5	–
16	CAT–1C	1	5	4	–	3	–
17	CAT–2C	1	5	4	–	4	–
18	CAT–3C	1	5	4	–	4.5	–
19	CA–1X	1	5	–	–	–	1
20	CA–2X	1	5	–	–	–	2
21	CA–3X	1	5	–	–	–	3
22	CT–1X	1	–	4	–	–	1
23	CT–2X	1	–	4	–	–	2
24	CT–3X	1	–	4	–	–	3
25	CAT–1X	1	5	4	–	–	1
26	CAT–2X	1	5	4	–	–	2
27	CAT–3X	1	5	4	–	–	3

CLZ = Clotrimazole; **CA**= CLZ+BHA; **CT**= CLZ+BHT; **CAT**= CLZ+BHA+BHT; **S**= SDS; **C**= CTAB; **X**= Triton X–100. In all the formulations ethanol absolute, triethanolamine and water were used as q.s.

3.7.3 Drug content

The drug content uniformity was determined for all the formulations by UV spectrophotometric method. A 500 mg of clotrimazole gel was taken and dissolved in 50 ml of methanol. The volumetric flask were kept for 2 hours and shaken well in a shaker to mix it properly and then filtered. The drug content was measured spectrophotometrically at 261 nm.

3.7.4 Viscosity study

The measurement of viscosity of the prepared gel was done with a Brookfield Viscometer. The gels were rotated at 20 rpm using spindle no. 64 and the corresponding dial reading was noted.

3.7.5 Spreadability

One of the criteria for a gel to meet the ideal quantities is that it should possess good spreadability. It is the term expressed to denote the extent of area to which gel readily spreads on application to skin. The therapeutic efficacy of a formulation also depends upon its spreading value. Spreadability is expressed in terms of time in seconds taken by two slides to slip off from gel which is placed in between the slides under the direction of certain load, lesser the time taken for separation of two slides, better the spreadability.

It is calculated by using the formula: $S = M. L / T$ (Eq. 3.7)

where, M = weight tied to upper slide

L = length of glass slides

T = time taken to separate the slides

3.7.6 *In vitro* release study

The diffusion studies of the prepared gels were carried out using Franz diffusion cell with the diameter of 0.50 cm. For studying the dissolution release profile of formulated gels, a cellullose membrane (pores size 0.22µm) was used which was hydrated in phosphate buffer pH 7.4 prior to use for 24 h before placing them between donor and receptor compartments. The receptor compartment contained 18 ml phosphate buffer at pH 7.4, under magnetic stirring. The temperature of the Franz diffusion cells was maintained at 37 ± 0.5 °C. Gel sample (0.5 g) was taken in cellophane membrane and the diffusion studies were carried out at

37 ± 1 °C. Samples were withdrawn periodically at 0.5, 1, 2, 3, 4, 5, and 6 h and then each sample was replaced with equal volume of fresh dissolution medium to maintain the sink conditions. Then the samples were analyzed spectrophometrically by using phosphate buffer pH 7.4 as reference. The amount of drug permeated into the receptor solution was determined by removing 1 ml of sample hourly for 6 h. The withdrawn volume was replaced with an equal volume of buffer solution. The absorbance was measured at 261 nm. The result of *in vitro* permeation study can be represented by plotting graphs between;

i. cumulative percent permeated versus time
ii. cumulative percent permeated versus √time
iii. log cumulative percent permeated versus time
iv. log cumulative percent permeated versus log time

3.7.7 Mathematical modeling of release profile

Mathematical modeling [14], whose development requires the comprehension of all the phenomena affecting drug release kinetics, has a very important value in the process of optimization of such formulation. The use of mathematical modeling turns out to be very useful as this approach enables, the prediction of release kinetics before the release systems are realized. More often, it allows the measurement of some important physical parameters, such as the drug diffusion coefficient and resorting to model fitting on experimental release data.

The data from the *in vitro* study was fitted to the following kinetic models to determine the kinetics of drug release. The suitability of equation is judged on the basis of best fit to the equation using statistical indicators like R^2 [15].

3.7.7.1 Zero–order model

Drug dissolution from dosage forms that do not disaggregate and release the drug slowly can be represented by the equation [16]:

$$Q_t = Q_0 + K_0 t \qquad \text{(Eq. 3.8)}$$

Where, Q_t is the amount of drug dissolved in time t, Q_0 is the initial amount of drug in the solution (most times, $Q_0 = 0$), and K_0 is the zero order release constant expressed in units of concentration/time.

To study the release kinetics, data obtained from *in vitro* drug release studies were plotted as cumulative amount of drug released versus time. This relationship can be used to describe the drug dissolution of several types of modified release pharmaceutical dosage forms, as in the case of some transdermal systems, as well as matrix tablets with low soluble drugs in coated forms, osmotic systems, etc [17].

3.7.7.2 First order model

This model has also been used to describe absorption and/or elimination of some drugs, although it is difficult to conceptualize this mechanism on a theoretical basis. The release of the drug which followed first order kinetics can be expressed by the equation:

$$\text{Log } C = \log C_0 - Kt / 2.303 \qquad \text{(Eq. 3.9)}$$

Where, C_0 is the initial concentration of drug, k is the first order rate constant, and t is the time.

The data obtained are plotted as log cumulative percentage of drug remaining vs. time which would yield a straight line with a slope of K/2.303. This relationship can be used to describe the drug dissolution in pharmaceutical dosage forms such as those containing water – soluble drugs in porous matrices [18].

3.7.7.3 Higuchi model

The first example of a mathematical model aimed to describe drug release from a matrix system was proposed by Higuchi. Initially conceived for planer systems, it was then extend to different geometrics and porous systems.

This model is based on the hypothesis that

i. Initial drug concentration in the matrix is much higher than drug solubility
ii. Drug diffusion takes place only in one dimension (edge effect must be negligible)
iii. Drug particles are much smaller than system thickness
iv. Matrix swelling and dissolution are negligible
v. Drug diffusivity is constant
vi. Perfect sink conditions are always attained in the release environment.

Accordingly, model expression is given by the equation:

$$F_t = Q = A\,[D\,(2C - C_s)\,C_s t]^{1/2} \qquad \text{(Eq. 3.10)}$$

Where, Q is the amount of drug released in time t per unit area A, C is the drug initial concentration, C_s is the drug solubility in the matrix media, and D is the diffusivity of the drug molecules (diffusion coefficient) in the matrix substance

In a general way it is possible to simplify the Higuchi model as (generally known as the simplified Higuchi model):

$$F_t = Q = K_H t^{1/2} \qquad \text{(Eq. 3.11)}$$

where, K_H is the Higuchi dissolution constant. The data obtained were plotted as cumulative percentage drug release versus square root of time. This relationship can be used to describe the drug dissolution from several types of modified release pharmaceutical dosage forms, as in the case of some transdermal systems and matrix tablets with water soluble drugs [19].

3.7.7.4 Korsmeyer–Peppas model

Korsmeyer et al. (1983) [20] developed a simple, semi–empirical model, relating exponentially the drug release to the elapsed time (t). To find out the mechanism of drug release, first 60% drug release data were fitted in Korsmeyer Peppas model.

$$M_t / M_\infty = Kt^n \qquad \text{(Eq. 3.12)}$$

Where, M_t / M_∞ is a fraction of drug released at time t, K is the release rate constant, and *n* is used to characterize different release for cylindrical shaped matrices.

In this model, the value of n characterizes the release mechanism of drug as described in Table 3.3. For the case of cylindrical tablets, $0.5 \leq n$ corresponds to a Fickian diffusion mechanism, $0.5 < n < 1.0$ to non–Fickian transport, $n = 1.0$ to Case II (relaxational) transport, and $n > 1.0$ to super case II transport. To find out the exponent of n the portion of the release curve, where $M_t / M_\infty < 0.6$ should only be used. To study the release kinetics, data obtained from in vitro drug release studies were plotted as log cumulative percentage drug release.

Table 3.3: Interpretation of diffusion release mechanism from polymeric films.

Release exponent (*n*)	Drug release mechanism	Rate as a function time
0.5	Fickian diffusion	$t^{-0.5}$
$0.5 < n > 1.0$	Anomalous transport	t^{n-1}
1.0	Case II transport	Zero order release
Higher than 1.0	Super case II transport	t^{n-1}

3.8 *In vitro* antifungal activity against *Candida* isolates

3.8.1 Fungal strains

Fungal strains; *Candida* clinical isolates, used in the present study were collected from Department of Medical Microbiology, Postgraduate Institute of Medical Education and Research, Chandigarh, India and Indra Gandhi Medical College, Shimla, Himachal Pradesh, India. Among obtained 30 clinical isolates, 11 were fluconazole (FLZ) resistant *C. albicans*, 4 miconazole (MLZ) resistant *C. albicans*, 3 FLZ susceptible *C. albicans*, 8 FLZ susceptible *C. tropicalis*, and 4 FLZ susceptible *C. glabrata* clinical isolates.

3.8.2 *In vitro* antifungal activity

Standardized protocol M27–A2, CLSI (Clinical and Laboratory Standards Institute) was followed to perform the experiment [21]. The inocula were performed after growth (48 h/ 35 °C) on Sabouraud dextrose agar. The colonies were suspended in 0.85% sterile saline and this suspension was homogenized in a vortex mixer for 15 s; after that, cell density was set in a spectrophotometer and transmittance (λ = 630 nm) was adjusted to match standard 0.5 on the McFarland scale (1×10^6 to 5×10^6 cells/ ml). In the sequence, a 1:50 dilution in water was done, followed by a 1:20 dilution in RPMI 1640 medium, resulting in a final concentration of $1.5 \pm 1.0 \times 10^3$ cells/ml [22]. The micro–dilution technique [23] was performed in polystyrene sterile plates with flat–bottom, disposable, with 96 wells diluted in RPMI 1640 buffered broth. 100 µl of the standardized inoculum was added to each micro – dilution plate. The plates were incubated at 35 °C for 48 hrs and then 10 ml of 0.5% 2,3,5–triphenyltetrazolium chloride dye was added to all wells, and the plates were re–incubated at 35 °C for 20 min. Afterward, the minimum inhibitory concentration (MIC µg/ml) was determined.

To assess the interaction of drug combinations (BHA+BHT and CLZ) the obtained data was further analyzed using the Fractional Inhibitory Concentration Index (FICI), which is

based on the zero–interaction theory of Loewe additivity. The drug interactions were classified as synergic (FICI ≤ 0.5), additive (FICI 0.5 – 1.0), showing no interaction between FICI = >0.5 – 4, and antagonistic (FICI > 4) [24].

3.9 Morphological study

The surface morphology was characterized by scanning electron microscope (S–3400N, Hitachi, Japan). The gel sample was deposited on a glass cover slip previously adhered to a metallic stub by a bio–adhesive carbon tape. Afterward, the sample was air–dried before analysis and coated with gold to obtain a conducting surface. Finally, the sample was analyzed by scanning electron microscopy in vacuum. Transmission electron microscope (Hitachi H–7500 80 kV; Ibaraki, Japan) was further used to visualize the dispersed micellar structures within the gel.

The visualization of morphology of *C. albicans* was carried out by TEM [25, 26]. Initially untreated *C. albicans* was visualized and afterward, it was treated with the optimized best formulation at a concentration of 10 μg/ml. The images were taken at different interval of time likely; 15 min, 2 h and 6 h in order to gain information on the action of formulation on infection site.

3.10 Physical and photo–stability studies

The formulation was stored for 3 months after preparation in order to evaluate changes in drug content, pH, viscosity, and spreadability. Photo–stability study for CLZ was performed to quantify the drug after exposure to UV light for 14 h. Quartz cuvettes were filled with CLZ methanolic solution (C–1) and CAT–3S (CLZ with dispersed BHA + BHT micelles) and exposed to UV radiation (TUV lamp – 30 W) in a chamber at a fixed distance from each other for 14 h. In order to compare, the CLZ methanolic solution was covered with aluminium paper as dark control. The protection of CLZ against the UV radiations was evaluated by quantifying the remaining drug using HPLC.

3.11 Skin Irritation study and toxicity profiling

Healthy male *Sprague Dawley* (SD) rats with average weight of 160–180 g were selected. Initially, hair were removed from the dorsal side of rats (2 cm × 3 cm) with the help of electric clipper without damaging the skin. The control group was treated with normal saline and gel

was applied to the treatment group three times a day for three days consecutively (n = 3). The visual observations were carried out at regular intervals of 12, 24, 48, and 72 h for various symptoms such as erythema, flakiness, dryness, erythema or edema. The irritation scores of the test area were obtained by judging the extent of erythema and edema according to the literature [27]. Erythema and edema were graded as follows: 0 for no visible reaction, 1 for just present reaction (barely perceptible–light pink), 2 for slight reaction (light red), 3 for moderate reaction (moderate red), and 4 for severe reaction (extreme redness).

In vivo toxicity test was conducted to gain better perspective or perception. Twelve animals were randomly divided into two groups. The first group (untreated) served as control, whilst second group received the treatment (CAT–3S). The treatments were given via topical application. After 24 h of treatment, the remnants of the gels were gently washed away from the skin surface using adsorbent cotton dipped in physiological saline. Again the dorsal sites of treated animals were inspected for any erythema or edema. Thereafter, animals were sacrificed. Major organs likely, skin, liver, kidney, and intestine were taken out. The excised skin sample and isolated organs were presented in 10% formalin for histopathological examination. Sections were fixed and blocks were made following the procedure as reported in literature [28]. The sections were stained with eosin–hematoxylin (H and E) to determine gross histopathology.

3.12 Confocal laser scanning microscopy (CLSM)

The depth and mechanism of the skin permeation of Rhodamine B within prepared gel system was investigated in absence of drug using CLSM [29]. The formulation was applied to the dorsal skin of rats for 8 h. The rat was then sacrificed by heart puncture and dorsal area was excised and cleaned with a thin stream of water to remove any residual gel. Afterward, the skin was placed on aluminium foil and adhering fat was removed. The excised skin was sliced and examined with CLSM (FV fluoview 1000; Olympus, Tokyo, Japan).

3.13 *In vivo* antifungal study

3.13.1 Preparation of Inoculum

Clinical isolate of *Candida albicans* (PGI/DML54) was used to infect the animals. Cultures were revived from glycerol stock onto sabouraud dextrose agar (SDA) slants for 48 h at 35 °C before use. Cells were suspended by vortexing a single pure colony in pyrogen free normal

saline and subsequently diluted to a final concentration of 2×10^6 cells/ml. The colonies were pure as identified from the morphology, and none of the cell suspensions were contaminated with any other organism.

3.13.2 Cutaneous infection

Each animal's back was shaved with an electric clipper and an approximately 3.0 cm^2 area was marked on each animal's back. The marked area was infected with 10^7 cfu/ml suspensions by gently rubbing onto the skin for 3 days with the help of a sterile, cotton–tipped swab until no more visible fluid was observed [30]. Infection was produced under an occlusive dressing and the infected area was covered with a sterile adhesive bandage, held in place with extra–adherent tape for 48 h before treatment began [31]. Control animals were infected in the same manner; however, they did not receive any formulation treatment.

3.13.3 *In vivo* efficacy

In vivo antifungal activity for the most potent formulation was carried out by using male SD rats (160–180 g). All animals were rendered immunosuppressed by injecting cyclophosphamide (150 mg/kg) intraperitoneally 4 days and 1 day before experimental infection. Treatment began 24 h after the infection was induced and test formulation was topically applied once daily for 3 consecutive days. The experimental animals were divided into four groups each containing 6 animals and the test animals were treated topically. Group 1 was treated with plain drug (1 mg/cm^2), group 2 with formulation CAT–3S at dose level of 1 mg/cm^2; group 3 with formulation CAT–3S at dose level of 5 mg/cm^2; and group 4 served as the control. All animals were sacrificed 48 h following the last treatment and 3.0 cm^2 of skin from the infected sites was excised. The infected skin samples were collected, washed and then plated into SDA culture media and incubated for 48 h at 37 ± 1 ºC, and then viable CFUs were counted [32].

3.14 Statistics

The antifungal efficacy against *C. albicans* was analyzed with two–way ANOVA and followed by a Bonferroni test using graph pad prism software.

References

[1] D. J. McLaughlin, D. S. Hibbett, F. Lutzoni, J. W. Spatafora, and R. Vilgalys, "The search for the fungal tree of life," *Trends in Microbiology,* vol. 17, pp. 488-497, 2009.

[2] M. Debreczeny, V. Ball, F. Boulmedais, B. Szalontai, J.-C. Voegel, and P. Schaaf, "Multilayers built from two component polyanions and single component polycation solutions: a way to engineer films with desired secondary structure," *The Journal of Physical Chemistry B,* vol. 107, pp. 12734-12739, 2003.

[3] Y. Moroi, H. Takagi, S. Nagadome, Y. Hirata, and G. Sugihara, "Micelle formation and phase behavior of dodecylammonium heptafluorobutyrate in a water-ethanol mixture," *Journal of Colloid and Interface Science,* vol. 149, pp. 252-255, 1992.

[4] S. Chauhan, K. Sharma, D. Rana, G. Kumar, and A. Umar, "Conductance, apparent molar volume and compressibility studies of cetyltrimethylammonium bromide in aqueous solution of leucine," *Journal of Molecular Liquids,* vol. 175, pp. 103-110, 2012.

[5] S. Chauhan, K. Sharma, D. Rana, G. Kumar, and A. Umar, "Volumetric and Conductance Studies of Cetyltrimethyl Ammonium Bromide in Aqueous Glycine," *Journal of Solution Chemistry,* vol. 42, pp. 634-656, 2013.

[6] S. Chauhan, K. Sharma, K. Kumar, and G. Kumar, "A comparative study of micellization behavior of an ethoxylated alkylphenol in aqueous solutions of glycine and leucine," *Journal of Surfactants and Detergents,* vol. 17, pp. 161-168, 2014.

[7] V. Syal, S. Chauhan, P. K. Gupta, and P. Sharma, "Physico-chemical studies of some bivalent electrolytes in aqueous mixtures of DMSO at different temperatures by transport property measurements," *Electrochem. Soc. Ind,* vol. 53, p. 1, 2004.

[8] S. Chauhan, V. Syal, M. Chauhan, and P. Sharma, "Viscosity studies of some narcotic–analgesic drugs in aqueous–alcoholic mixtures at 25° C," *Journal of Molecular Liquids,* vol. 136, pp. 161-164, 2007.

[9] K. Sharma and S. Chauhan, "Apparent Molar Volume, Compressibility and Viscometric Studies of Sodium Dodecyl Benzene Sulfonate (SDBS) and Dodecyltrimethylammonium Bromide (DTAB) in Aqueous Amino Acid Solutions: A Thermo–Acoustic Approach," *Thermochimica Acta,* vol. 568, pp. 15-27, 2014.

[10] S. Chauhan, M. Chauhan, D. Kaushal, V. Syal, and J. Jyoti, "Study of micellar behavior of SDS and CTAB in aqueous media containing furosemide—a cardiovascular drug," *Journal of Solution Chemistry,* vol. 39, pp. 622-638, 2010.

[11] R. J. Ekiert and J. Krzek, "Determination of azole antifungal medicines using zero-order and derivative UV spectrophotometry," *Acta Poloniae Pharmaceutica,* vol. 66, pp. 19-24, 2009.

[12] F. Monajjemzadeh, D. Hassanzadeh, H. Valizadeh, M. R. Siahi-Shadbad, J. S. Mojarrad, T. A. Robertson, and M. S. Roberts, "Compatibility studies of acyclovir and lactose in physical mixtures and commercial tablets," *European Journal of Pharmaceutics and Biopharmaceutics,* vol. 73, pp. 404-413, 2009.

[13] R. Ekiert, J. Krzek, and P. Talik, "Chromatographic and electrophoretic techniques used in the analysis of triazole antifungal agents—a review," *Talanta,* vol. 82, pp. 1090-1100, 2010.

[14] S. Dash, P. N. Murthy, L. Nath, and P. Chowdhury, "Kinetic modeling on drug release from controlled drug delivery systems," *Acta Pol Pharm,* vol. 67, pp. 217-223, 2010.

[15] Y. N. Kalia and R. H. Guy, "Modeling transdermal drug release," *Advanced Drug Delivery Reviews,* vol. 48, pp. 159-172, 2001.

[16] S. Jose, J. Fangueiro, J. Smitha, T. Cinu, A. Chacko, K. Premaletha, and E. Souto, "Predictive modeling of insulin release profile from cross-linked chitosan microspheres," *European Journal of Medicinal Chemistry,* vol. 60, pp. 249-253, 2013.

[17] C. G. Varelas, D. G. Dixon, and C. A. Steiner, "Zero-order release from biphasic polymer hydrogels," *Journal of Controlled Release,* vol. 34, pp. 185-192, 1995.

[18] B. Mukherjee, S. Mahapatra, R. Gupta, B. Patra, A. Tiwari, and P. Arora, "A comparison between povidone-ethylcellulose and povidone-eudragit transdermal dexamethasone matrix patches based on in vitro skin permeation," *European journal of pharmaceutics and biopharmaceutics,* vol. 59, pp. 475-483, 2005.

[19] K. Knutson, S. Krill, W. Lambert, and W. Higuchi, "Physicochemical aspects of transdermal permeation," *Journal of Controlled Release,* vol. 6, pp. 59-74, 1987.

[20] R. W. Korsmeyer, R. Gurny, E. Doelker, P. Buri, and N. A. Peppas, "Mechanisms of solute release from porous hydrophilic polymers," *International Journal of Pharmaceutics,* vol. 15, pp. 25-35, 1983.

[21] A. Espinel-Ingroff, A. Fothergill, M. Ghannoum, E. Manavathu, L. Ostrosky-Zeichner, M. Pfaller, M. Rinaldi, W. Schell, and T. Walsh, "Quality control and reference

guidelines for CLSI broth microdilution susceptibility method (M38-A document) for amphotericin B, itraconazole, posaconazole, and voriconazole," *Journal of Clinical Microbiology*, vol. 43, pp. 5243-5246, 2005.

[22] R. Cruz, S. Werneck, C. Oliveira, P. Santos, B. Soares, D. Santos, and P. Cisalpino, "Conditions for determining the minimal inhibitory concentration (MIC) of seven antifungal agents against Paracoccidioides brasiliensis by microdilution: influence of different media, incubation times and temperatures," *Journal of Clinical Microbiology*, pp. 02231-12, 2012.

[23] A. Aller, E. Martin-Mazuelos, F. Lozano, J. Gomez-Mateos, L. Steele-Moore, W. Holloway, M. Gutierrez, F. Recio, and A. Espinel-Ingroff, "Correlation of fluconazole MICs with clinical outcome in cryptococcal infection," *Antimicrobial Agents and Chemotherapy*, vol. 44, pp. 1544-1548, 2000.

[24] M. D. Johnson, C. MacDougall, L. Ostrosky-Zeichner, J. R. Perfect, and J. H. Rex, "Combination antifungal therapy," *Antimicrobial Agents and Chemotherapy*, vol. 48, pp. 693-715, 2004.

[25] K. S. Kim, Y.-S. Kim, I. Han, M.-H. Kim, M. H. Jung, and H.-K. Park, "Quantitative and qualitative analyses of the cell death process in *Candida albicans* treated by antifungal agents," *PLoS ONE*, vol. 6, pp. e28176, 2011.

[26] R. K. Basniwal, H. S. Buttar, V. Jain, and N. Jain, "Curcumin nanoparticles: preparation, characterization, and antimicrobial study," *Journal of Agricultural and Food Chemistry*, vol. 59, pp. 2056-2061, 2011.

[27] S. D. Mandawgade and V. B. Patravale, "Development of SLNs from natural lipids: application to topical delivery of tretinoin," *International Journal of Pharmaceutics*, vol. 363, pp. 132-138, 2008.

[28] S. Khurana, N. Jain, and P. Bedi, "Nanoemulsion based gel for transdermal delivery of meloxicam: physico-chemical, mechanistic investigation," *Life Sciences*, vol. 92, pp. 383-392, 2013.

[29] P. Verma and K. Pathak, "Nanosized ethanolic vesicles loaded with econazole nitrate for the treatment of deep fungal infections through topical gel formulation," *Nanomedicine: Nanotechnology, Biology and Medicine*, vol. 8, pp. 489-496, 2012.

[30] K. Maebashi, T. Itoyama, K. Uchida, N. Suegara, and H. Yamaguchi, "A novel model of cutaneous candidiasis produced in prednisolone-treated guinea-pigs," *Medical Mycology*, vol. 32, pp. 349-359, 1994.

[31] M. M. Abdel-Mottaleb, N. Mortada, A. El-Shamy, and G. Awad, "Physically cross-linked polyvinyl alcohol for the topical delivery of fluconazole," *Drug Development and Industrial Pharmacy*, vol. 35, pp. 311-320, 2009.

[32] M. Ning, Y. Guo, H. Pan, X. Chen, and Z. Gu, "Preparation, in vitro and in vivo evaluation of liposomal/niosomal gel delivery systems for clotrimazole," *Drug Development and Industrial Pharmacy*, vol. 31, pp. 375-383, 2005.

CHAPTER-4

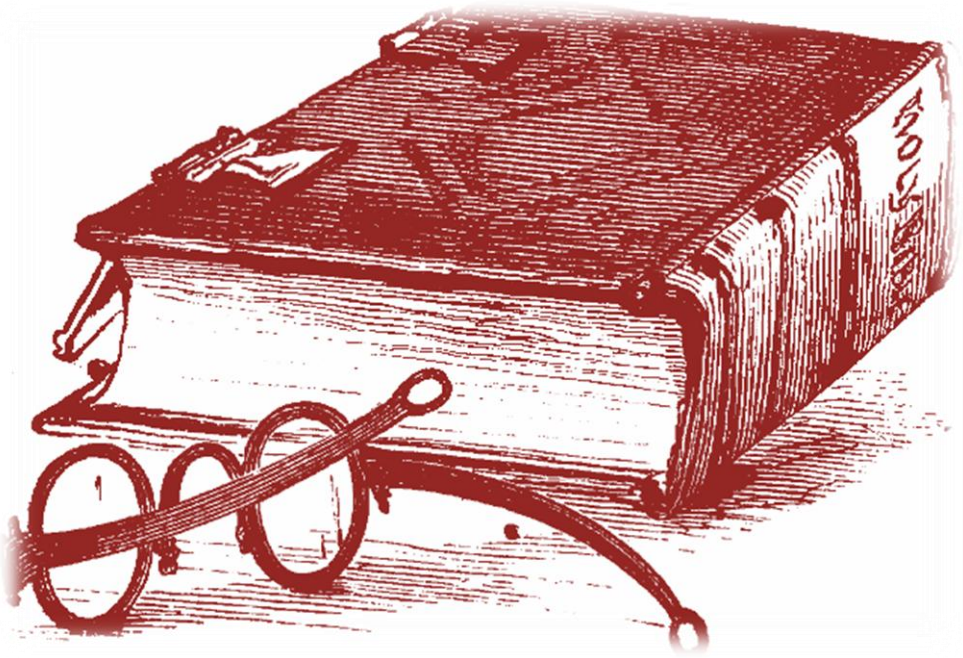

RESULT & DISCUSSION-I

This chapter is based on our findings published in peer reviewed journals [1-7]. The experimental results of specific conductance, transport measurements and their interpretation in terms of thermo–acoustical and spectroscopic parameters of SDS, CTAB and TX100 in presence of BHA and BHT in pure alcohols (with carbon chain length 1 – 3) and their aqueous – alcoholic composite solutions have been reported in this chapter.

4.1 Specific conductance and micellization study

The specific conductivity (κ) data of SDS, CTAB and Triton X 100 at Temperature 'T' = (25, 30, and 35) °C for all the alcohols and hydroalcoholic solution containing BHA and BHT have been summarized in *APPENDIX–A*. The plots between κ and surfactant concentration of SDS, CTAB and Triton X 100 in alcohol containing 2 carbon chain length (EtOH) and their hydroalcoholic concentrations (100%, 70% and 30% v/v) have been shown respectively. All the κ values were found to increase with increment in temperature. The determination of CMC value is obtained by drawing two tangents for the plot of κ versus surfactant concentration and the intersection point between the two straight lines was considered as the CMC value (mmol kg^{-1}). The obtained CMC

values were converted into their mole fraction unit, X_{CMC} before subjecting them further to determine the thermodynamic parameters of micellization.

To interpret the impact of antioxidants (BHA and BHT) on surfactants (SDS, CTAB and Triton X 100) as well as their interaction, it is necessary to know the critical micelle concentration (CMC) of respective surfactants in pure water. According to the literature, CMC for SDS is 8.3 mmol kg^{-1}, CTAB is 0.92 mmol kg^{-1} and Triton X 100 is 0.22 mmol kg^{-1} in water at 25 °C [8-10]. Since the variation in the specific conductance of surfactant is quite linear before and after the break, a comparison among the monomeric and the micellar species over the whole concentration range can be made by computing the pre–micellar (S_1) and post–micellar (S_2) slopes. Both S_1 and S_2 values were determined from the linear regression analysis of the conductivity data with a correlation factor always greater than 0.995. The slope in the pre–micellar region has always been found greater than that in the post–micellar region. A similar kind of surfactant combinations in which the breakpoint in the conductivity curve is not sharp can be generally explained on the basis of two situations: first, when instead of an instantaneous micelle formation process, stepwise micellization occurs as in the case of all bile salts or in the presence of organic additives ; second, when apart from the ordinary spherical micelles, bilayer assembly or insoluble salt formation takes place, for example, as in the case of binary combinations of oppositely charged ionic surfactants [11, 12]. The short chain alcohols are solubilized mainly in aqueous phase and affect the micellization process by modifying the solvent properties. The influence of MeOH, EtOH and 1–PrOH on the micellar behavior of the surfactants can be explained on the basis of several different roles of alcohols in the case of surfactants. It is generally accepted that the alcohol binds to the micelle in the surface region, leading to principle effects [13].

4.1.1 BHA and BHT impact on SDS properties

Specific conductance (κ) was found to be concentration dependent of surfactants (anionic; SDS) in all studied alcohols and their hydroalcoholic solution containing BHA and BHT. Specific conductivity 'κ' was found to increase with increase in surfactant concentration and temperature. The specific conductivity plots have been presented in Figure 4.1 – 4.2.

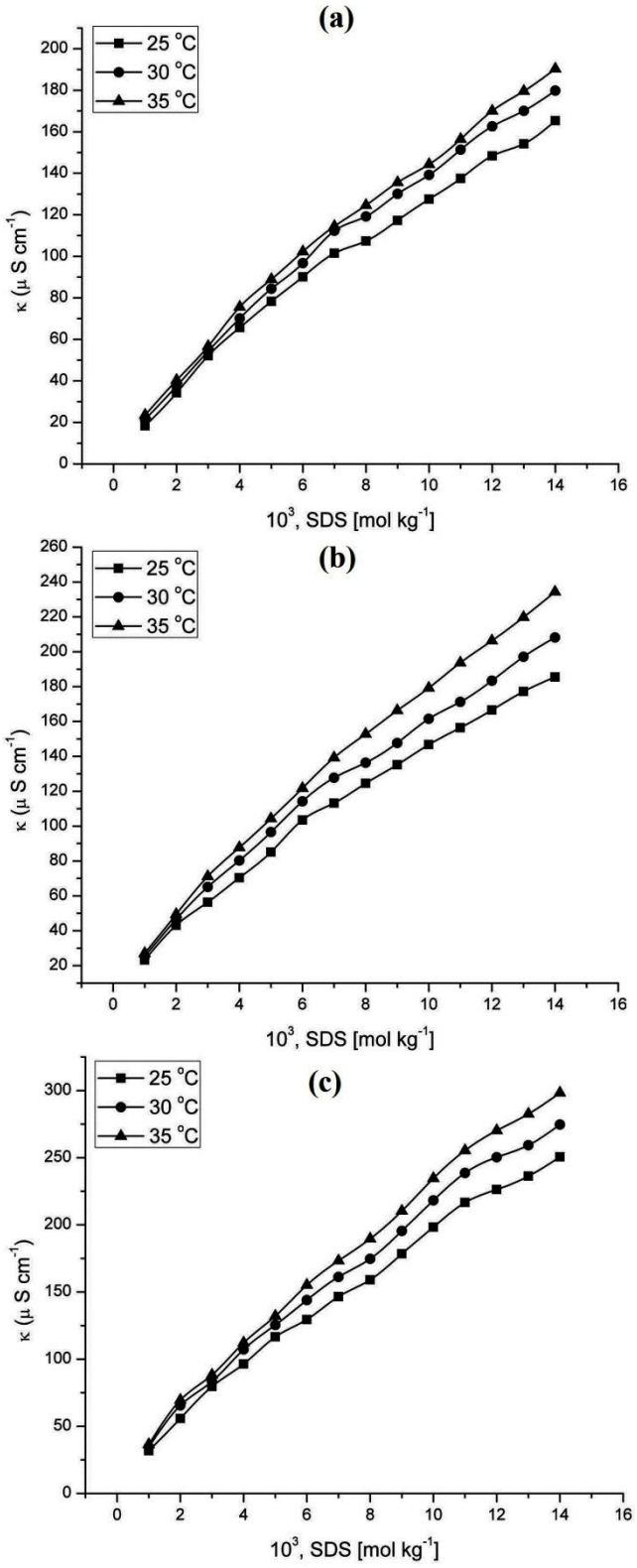

Figure 4.1: Conductivity vs. concentration plots of SDS in (a) 100% v/v, (b) 70% v/v, and (c) 30% v/v EtOH solutions containing BHA (0.03 mol kg^{-1}) at different temperatures.

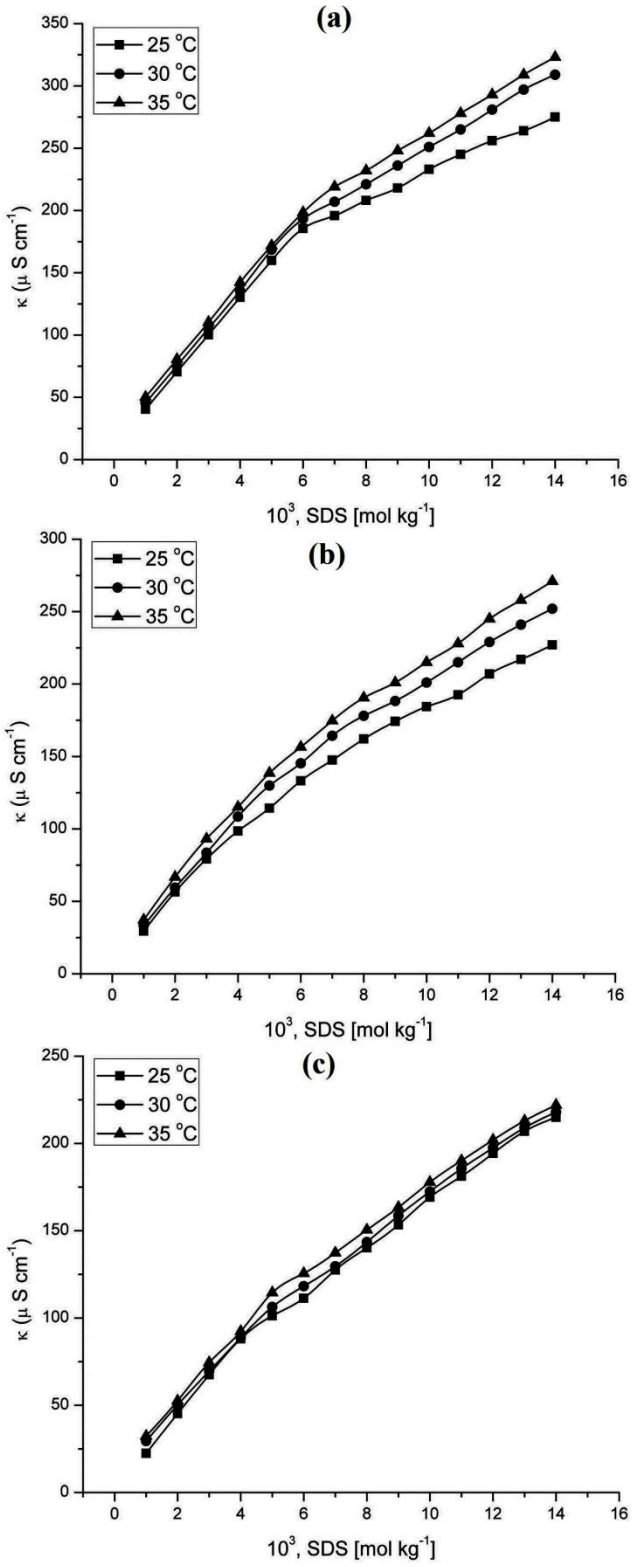

Figure 4.2: Conductivity vs. concentration plots of SDS in 30 % v/v (a) MeOH, (b) EtOH, and (c) 1–PrOH solutions containing BHT (0.02 mol kg^{-1}) at different temperatures.

In all the studied solutions, CMC was found lower than that of standard CMC value in pure water. This is due to presence of the bulkier moiety as *tert*–butyl substitution and moreover hydroxy group (BHA and BHT) contributing eminently for better interaction and therefore causing micellization much earlier. Lowering of repulsion between surfactant head group and also the hydrophobic nature of CH_3^+ must have provided some surface for the micellization. Also, the hydration of intermolecular aggregation of molecules which is favoring their limited aqueous solubilization and therefore affecting the aggregation tendency with the addition of non–aqueous components [14]. Thus, the group substitutions on molecules significantly have impact on interactions, causing micellization much earlier. However in comparison to BHA, in case of BHT, the CMC values of SDS were found marginally lower but substantial. Whereas CMC increase with temperature is related to increase in thermal motion of solvents and their favorable nature for micellization. Alcohols as the most commonly used co–surfactants, which are added to surfactant in order to improve their properties. Nevertheless, some studies reveal that short chain alcohols behave like surfactants in many respects [15, 16].

In context of different alcoholic systems, the CMC values variations was observed. At all compositions (100%, 70% and 30% v/v) the CMC values for SDS in presence of BHA containing MeOH were found to lie in a range of 5.5 – 7.0 mmol kg^{-1}, for EtOH 5.5 – 6.9 mmol kg^{-1}, and for 1–PrOH 4.3 – 5.7 mmol kg^{-1}, respectively (Table 4.1). Whereas, in case of BHT, the CMC values for SDS in MeOH were found to lie in a range of 5.5 – 6.8 mmol kg^{-1}, for EtOH 4.7 – 7.7 mmol kg^{-1}, and for 1–PrOH 4.1 – 5.6 mmol kg^{-1}, respectively as shown in Table 4.2.

Table 4.1: Thermodynamic parameters data CMC, X_{CMC}, α, ΔH°_m, ΔG°_m, and ΔS°_m values of SDS containing BHA in different compositions at temperature T = 25, 30 and 35 °C.

Compositions	T °C	CMC (10^3)	X_{CMC} (10^3)	α	ΔH°_m (kJ mol^{-1})	ΔG°_m (kJ mol^{-1})	ΔS°_m (J mol^{-1} K^{-1})
100% v/v MeOH	25	5.5	12.8	0.518	–10.94	–15.97	16.88
	30	6.6	13.9	0.525	–11.25	–15.86	15.21
	35	7.0	15.1	0.538	–11.53	–15.67	13.49
70% v/v MeOH	25	6.0	10.2	0.540	–10.78	–16.60	19.54
	30	6.4	10.9	0.565	–10.95	–16.34	17.77
	35	6.8	11.6	0.578	–11.22	–16.24	16.32
30% v/v MeOH	25	5.0	5.4	0.505	–11.04	–19.33	27.84
	30	5.4	5.8	0.522	–11.28	–19.28	26.05
	35	5.6	6.1	0.544	–11.48	–18.98	24.33
100% v/v EtOH	25	5.5	11.0	0.93	–7.89	–11.92	13.52
	30	6.6	13.2	0.96	–7.94	–11.34	11.24
	35	7.0	14.0	0.99	–7.96	–11.04	9.99
70% v/v EtOH	25	6.1	8.4	0.44	–10.59	–18.44	26.31
	30	6.3	8.9	0.45	–10.88	–18.43	24.90
	35	6.9	9.6	0.46	–11.17	–18.34	23.26
30% v/v EtOH	25	5.8	5.3	0.44	–10.59	–20.25	32.40
	30	6.0	5.5	0.48	–10.67	–19.91	30.48
	35	6.8	6.2	0.49	–10.96	–19.64	28.20
100% v/v 1–PrOH	25	4.3	15.6	0.615	–10.22	–14.27	13.58
	30	4.6	16.7	0.634	–10.42	–14.07	12.03
	35	4.9	17.8	0.652	–10.63	–13.87	10.53
70% v/v 1–PrOH	25	4.8	11.4	0.635	–10.08	–15.25	17.36
	30	5.5	12.6	0.769	–9.39	–13.55	13.71
	35	5.7	13.1	0.790	–9.54	–13.45	12.67
30% v/v 1–PrOH	25	4.4	5.2	0.537	–10.80	–18.99	27.48
	30	4.7	5.6	0.563	–10.96	–18.75	25.68
	35	5.0	5.9	0.566	–11.31	–18.80	24.32

Table 4.2: Thermodynamic parameters data CMC, X_{CMC}, α, ΔH°_m, ΔG°_m, and ΔS°_m values of SDS containing BHT in different compositions at temperature T = 25, 30 and 35 °C.

Compositions	T °C	CMC (10^3)	X_{CMC} (10^3)	α	ΔH°_m (kJ mol^{-1})	ΔG°_m (kJ mol^{-1})	ΔS°_m (J mol^{-1} K^{-1})
100% v/v MeOH	25	5.5	12.9	0.516	–10.95	–15.99	16.90
	30	5.8	13.6	0.523	–11.27	–15.96	15.47
	35	6.2	14.5	0.535	–11.55	–15.86	14.00
70% v/v MeOH	25	5.8	10.0	0.538	–10.79	–16.66	19.69
	30	6.1	10.5	0.554	–11.03	–16.57	18.27
	35	6.7	11.6	0.569	–11.28	–16.30	16.29
30% v/v MeOH	25	5.9	6.4	0.502	–11.06	–18.74	25.78
	30	6.2	6.7	0.518	–11.31	–18.66	24.27
	35	6.8	7.4	0.536	–11.54	–18.40	22.27
100% v/v EtOH	25	6.2	12.2	0.401	–11.81	–17.43	18.87
	30	7.2	14.1	0.451	–11.82	–16.62	15.84
	35	7.7	15.1	0.461	–12.13	–16.51	14.20
70% v/v EtOH	25	5.9	8.1	0.723	–9.42	–15.24	19.53
	30	6.4	8.7	0.761	–9.45	–14.79	17.61
	35	7.1	9.7	0.797	–9.48	–14.29	15.60
30% v/v EtOH	25	4.7	4.3	0.508	–11.01	–20.14	30.63
	30	5.6	5.1	0.547	–11.09	–19.32	27.18
	35	5.8	5.3	0.555	–11.39	–19.38	25.94
100% v/v 1–PrOH	25	4.1	14.9	0.618	–10.20	–14.41	14.13
	30	4.4	16.0	0.642	–10.36	–14.12	12.41
	35	4.8	17.4	0.656	–10.60	–13.93	10.83
70% v/v 1–PrOH	25	4.7	10.8	0.738	–9.31	–14.16	16.26
	30	5.2	11.9	0.778	–9.32	–13.63	14.22
	35	5.6	12.8	0.796	–9.49	–13.44	12.81
30% v/v 1–PrOH	25	4.3	5.1	0.758	–9.16	–16.21	23.64
	30	4.6	5.5	0.788	–9.25	–15.87	21.86
	35	4.9	5.8	0.798	–9.48	–15.85	20.68

4.1.1.1 Thermodynamics of micellization of SDS

4.1.1.1.1 Temperature and alcohol compositions dependence of X_{CMC}

The effect of temperature on X_{CMC} values of SDS containing BHA and BHT have been presented in Table 4.1 – 4.2 and Figures 4.3 – 4.4 indicating an increase with temperature increment, while in case of alcoholic compositions, X_{CMC} values decreases with increase in hydration within the solvent system i.e. aqueous rich solution. The temperature dependence of X_{CMC} can be employed to compute the thermodynamic parameters of micellization for amphiphiles. In general, the effect of temperature on the X_{CMC} value of surfactant in aqueous–alcoholic medium is complex and is analyzed in terms of hydrophobic and hydrophilic hydrations [17]. In monomeric form of surfactant, both the hydrophobic as well as hydrophilic hydrations are possible whereas only hydrophilic hydration is possible for micellized surfactant system. Both types of hydrations are known to decrease with increase in temperature [18]. At lower temperature, a hydrophilic dehydration favours the micelle formation while with the increase in temperature; hydrophobic dehydration does not favour the micelle formation. Thus the magnitude of these two factors determines whether the *CMC* (X_{CMC}) values increase or decrease over a particular temperature range. The change in X_{CMC} is predominantly caused by the penetration of different alcohol molecules in the micelles. To explain the trend in the micellization enthalpies, we must look at the interactions that occur between the different components in solution. Normally, these include interactions that occur between the components in the micellar phase i.e. SDS–SDS interactions and BHA/BHT–SDS interactions, as well as interactions that occur between the alcohol and SDS–water. As methanol contains only one hydroxyl atom with one carbon atom, so the interaction in the micellar interior would be dominated by the interaction with the SDS alkyl chain [19]. BHT having bulkier group (CH_3^+), will tends to provide better site for interaction. The difference between short–chain and medium chain alcohols is due to the fact that there is less penetration of short chain alcohols in the micelles and is usually considered as co–solvents which act on the micellization process by modifying the properties of water as well as chemical potential of the free surfactant. While a decrease in X_{CMC} values, with decrease in alcohol concentration was observed in addition to difference in obtained α value was noticed due to alcohol penetration in micelles thereby suggesting that the system with less alcohol concentration was found to be the most favorable and feasible. This might be also due to the difference of

structure making/breaking ability of alcohol in water [20]. Moreover, alcohol molecule acting as ligand replaces the water in the sphere and thus binding to the surfactant molecule producing co–solvent effect as it is known that alcohol at higher concentration surrounds surfactant molecule completely.

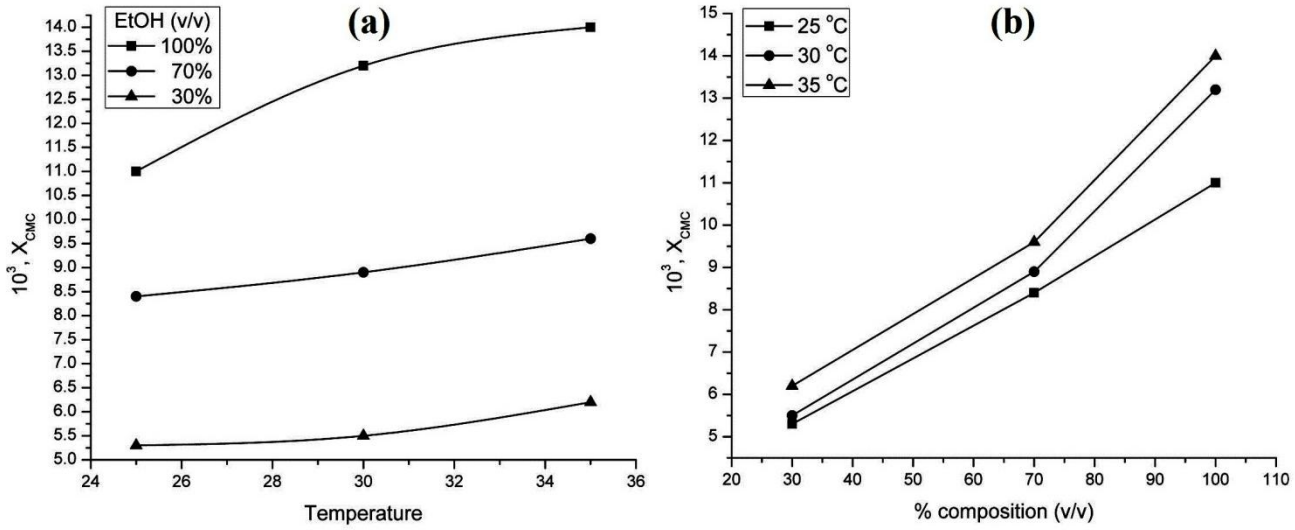

Figure 4.3: Plots of X_{CMC} vs. (a) temperature and (b) EtOH % composition (v/v) in solution for SDS containing BHA 0.03 mol kg^{-1}.

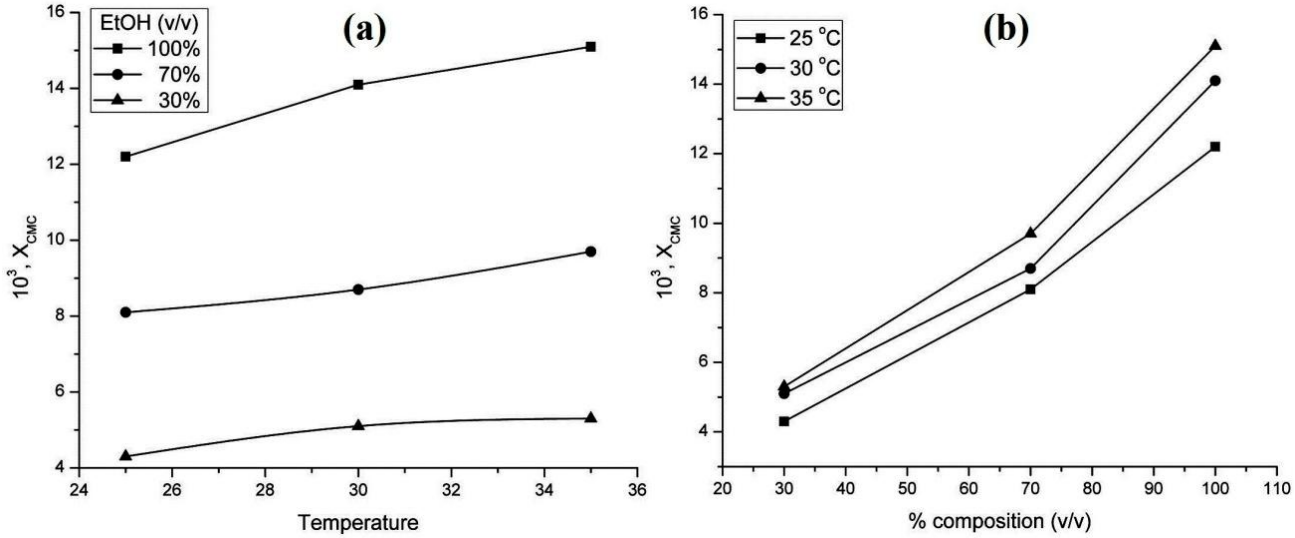

Figure 4.4: Plots of X_{CMC} vs. (a) temperature and (b) EtOH % composition (v/v) in solution for SDS containing BHT 0.02 mol kg^{-1}.

4.1.1.2 Thermodynamic parameters

The X_{CMC} data reported in Table 4.1–4.2 was further used to calculate various thermodynamic parameters. The standard enthalpy change (ΔH°_{m}), standard entropy change (ΔS°_{m}) and standard Gibbs free energy change for micellization (ΔG°_{m}) were obtained from the equations provided in experimental section 3.2.3.2. The uncertainty in the temperature and thermodynamic measurements for SDS are: 0.01 K in temperature, ± 0.03 kJ mol^{-1} in ΔH°_{m}, ± 0.02 kJ mol^{-1} in ΔG°_{m} and ± 2 J mol^{-1} K^{-1} in ΔS°_{m}, respectively.

The obtained values have been presented in Table 4.1 – 4.2 along with CMC and X_{CMC} values. On interpreting the data reported in Table 4.1 – 4.2, it has been found that ΔH°_{m} values for SDS in alcohol and hydroalcoholic solution containing BHA and BHT are negative over the entire temperature range studied. This observation clearly depicts that the micellization of SDS is in spontaneous process over the entire temperature range and moreover is energy driven and exothermic in nature. However, all the values of ΔG°_{m} and ΔH°_{m} are found negative where ΔS°_{m} with positive magnitude. The values of ΔG°_{m} suggested that the process of micellization is spontaneous which was confirmed by negative values of ΔH°_{m}. As shown in Table 4.1 – 4.2 and Figure 4.5 – 4.6, ΔG°_{m} values were found less negative at higher alcoholic concentration (EtOH) which can be attributed to steric hindrance of micelle formation. It is also suggested that as the number of carbon atom in the alkyl chains of various alcohols increases, the Gibbs free energy of micellization decreases. With increase in temperature ΔH°_{m} values do not vary significantly. Here it can be understood by assuming that London dispersion interactions represent the main attractive force for micelle formation [21, 22]. The values of ΔS°_{m} indicate that micelle formation in these studied systems is entropically controlled. The micelle formation is facilitated by the presence of lipophilic organic molecule with regard to temperature and solvent composition dependence. Keeping in view that the composition with higher negative value of ΔG°_{m} are solubilized to a greater extent and have greater tendency to transfer from dispersed to micellar phase as in case of 30% v/v among all three alcohols (MeOH, EtOH and 1–PrOH).

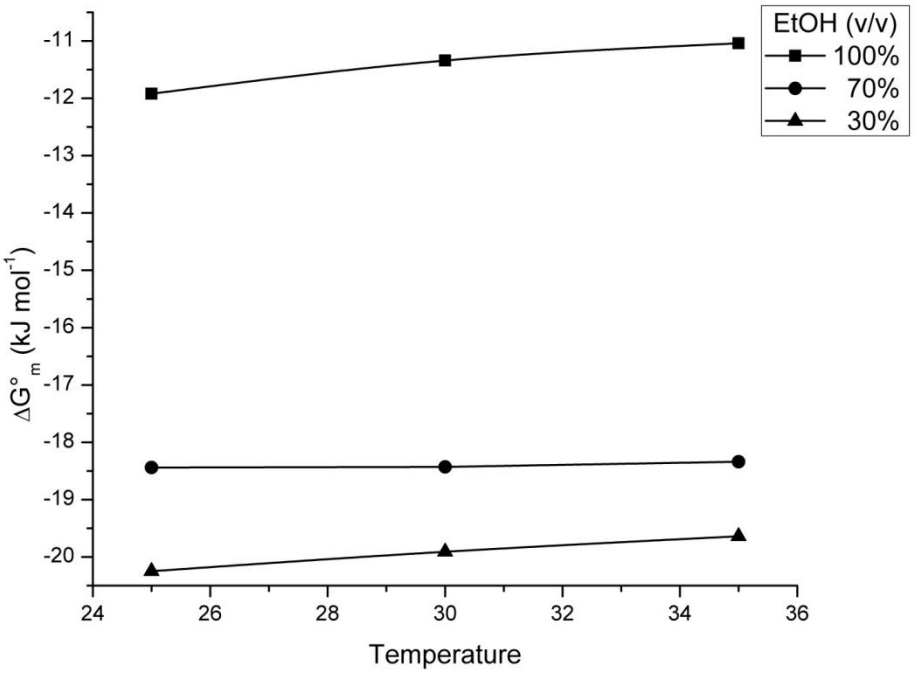

Figure 4.5: Plot of ΔG°_{m} versus temperature of SDS in presence of BHA (0.03 mol kg^{-1}) containing different compositions of EtOH.

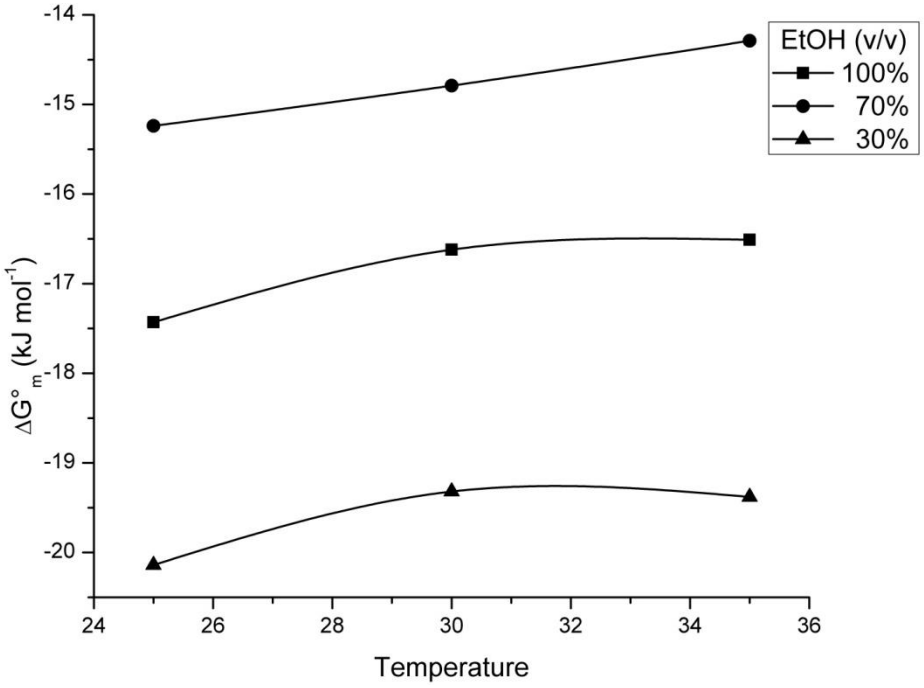

Figure 4.6: Plot of ΔG°_{m} versus temperature of SDS in presence of BHT (0.02 mol kg^{-1}) containing different compositions of EtOH.

4.1.2 BHA and BHT impact on CTAB properties

In another study the impact of antioxidants were analyzed on cationic surfactant micellar properties. CTAB was the choice of surfactant in this investigation with concentration ranging from 0.1 – 1.8 mmol kg^{-1} in different alcohols and hydro–alcoholic composite solutions. With respect to the CTAB concentration, specific conductance was found to increase with CTAB concentration as well as with temperature increment. Specific conductivity plots have been presented in Figure 4.7 – 4.8 and complete data presented in *APPENDIX– A*. In all studied compositions and concentrations CMC was found to decrease in comparison to the standard CMC value of CTAB in water at T = 25 °C i.e. 0.92 mmol kg^{-1}. This provided a clear suggestion presence of additives favor the micellization process via existing decisive intermolecular interaction within surfactant molecule and the additives. At all compositions (100%, 70% and 30% v/v) the CMC values for CTAB in presence of BHA containing MeOH were found to lie in a range of 0.71 – 0.84 mmol kg^{-1}, for EtOH 0.70 – 0.86 mmol kg^{-1}, and for 1–PrOH 0.61 – 0.76 mmol kg^{-1}, respectively (Table 4.3). Whereas, in case of BHT, the CMC values for CTAB in MeOH were found to lie in a range of 0.70 – 0.82 mmol kg^{-1}, for EtOH 0.68 – 0.84 mmol kg^{-1}, and for 1–PrOH 0.60 – 0.75 mmol kg^{-1}, respectively as shown in Table 4.4.

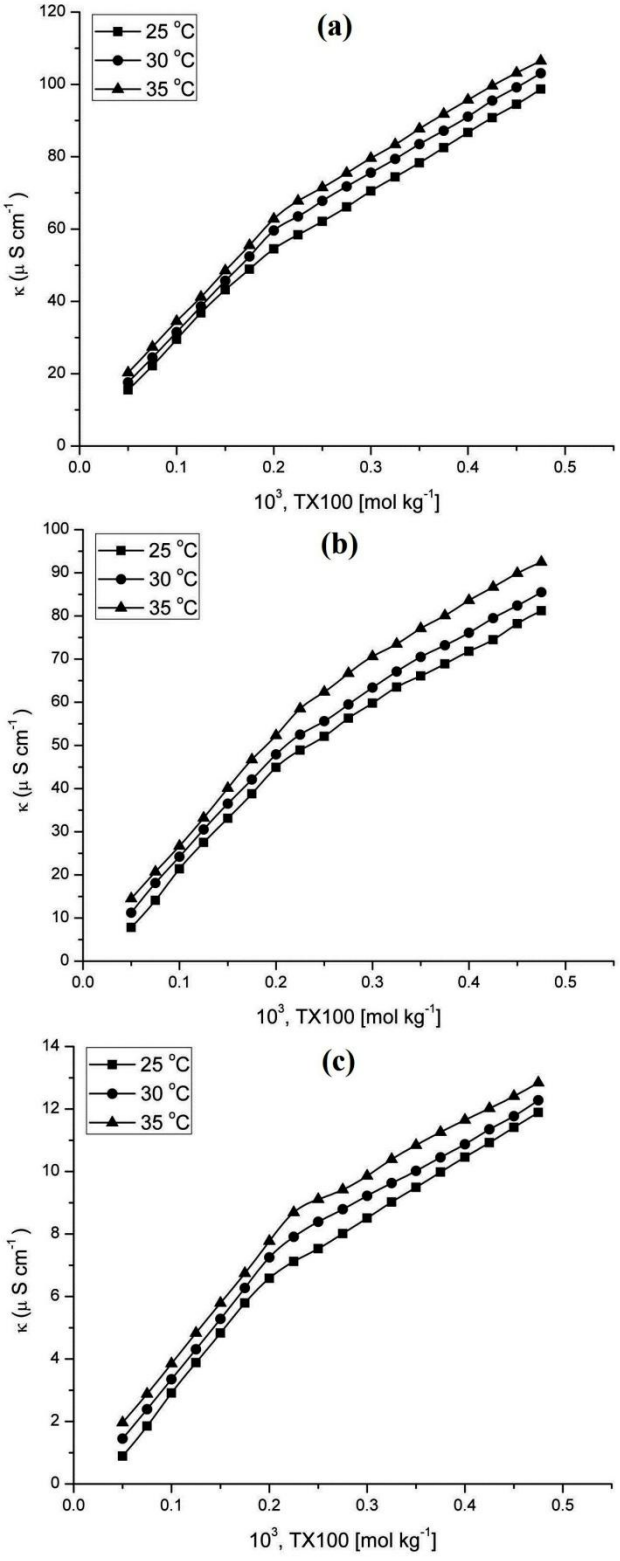

Figure 4.7: Conductivity vs. concentration plots of CTAB in (a) 100% v/v, (b) 70% v/v, and (c) 30% v/v EtOH solutions containing BHA (0.03 mol kg^{-1}) at different temperatures.

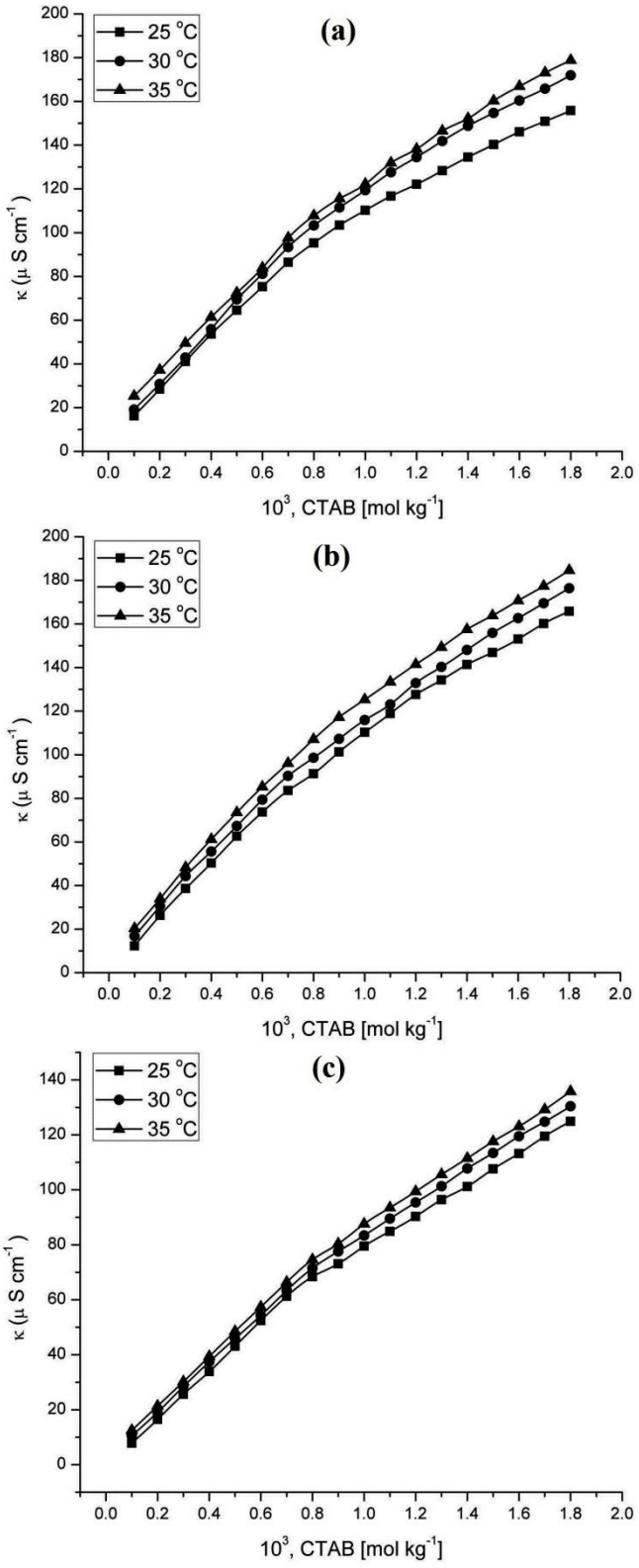

Figure 4.8: Conductivity vs. concentration plots of CTAB in 30% v/v (a) MeOH, (b) EtOH, and (c) 1–PrOH solutions containing BHT (0.02 mol kg^{-1}) at different temperatures.

Table 4.3: Thermodynamic parameters data CMC, X_{CMC}, α, ΔH°_m, ΔG°_m, and ΔS°_m values of CTAB containing BHA in different compositions at temperature T = 25, 30 and 35 °C.

Compositions	T °C	CMC (10^3)	X_{CMC} (10^3)	α	ΔH°_m (kJ mol^{-1})	ΔG°_m (kJ mol^{-1})	ΔS°_m (J mol^{-1} K^{-1})
100% v/v MeOH	25	0.71	16.4	0.320	–12.40	–26.97	48.18
	30	0.74	17.1	0.337	–12.69	–26.86	46.17
	35	0.76	17.6	0.358	–12.95	–26.67	44.50
70% v/v MeOH	25	0.72	12.4	0.303	–12.52	–28.12	52.34
	30	0.75	12.9	0.322	–12.80	–28.11	50.50
	35	0.80	13.7	0.341	–13.08	–27.99	48.41
30% v/v MeOH	25	0.74	8.0	0.292	–12.61	–30.17	58.93
	30	0.78	8.4	0.309	–12.90	–30.15	56.93
	35	0.84	9.1	0.323	–13.22	–30.06	54.65
100% v/v EtOH	25	0.70	14.8	0.356	–12.13	–26.51	48.24
	30	0.76	16.1	0.372	–12.42	–26.37	46.01
	35	0.84	17.8	0.389	–12.70	–26.27	44.06
70% v/v EtOH	25	0.71	10.1	0.322	–12.38	–28.64	54.54
	30	0.78	11.1	0.338	–12.68	–28.47	52.09
	35	0.81	11.5	0.356	–12.96	–28.45	50.29
30% v/v EtOH	25	0.76	7.0	0.264	–12.81	–31.22	61.77
	30	0.80	7.4	0.284	–13.09	–31.16	59.63
	35	0.86	7.9	0.297	–13.43	–31.13	57.48
100% v/v 1–PrOH	25	0.61	22.5	0.294	–12.59	–25.74	44.11
	30	0.64	23.6	0.315	–12.86	–25.63	42.16
	35	0.68	25.1	0.327	–13.19	–25.61	40.33
70% v/v 1–PrOH	25	0.65	15.0	0.252	–12.90	–28.15	51.15
	30	0.68	15.7	0.269	–13.21	–28.12	49.21
	35	0.70	16.2	0.290	–13.48	–28.11	47.48
30% v/v 1–PrOH	25	0.68	8.1	0.242	–12.97	–30.96	60.36
	30	0.71	8.5	0.262	–13.26	–30.95	58.37
	35	0.76	9.1	0.284	–13.53	–30.75	55.92

Table 4.4: Thermodynamic parameters data CMC, X_{CMC}, α, ΔH°_m, ΔG°_m, and ΔS°_m values of CTAB containing BHT in different compositions at temperature T = 25, 30 and 35 °C.

Compositions	T °C	CMC (10^3)	X_{CMC} (10^3)	α	ΔH°_m (kJ mol^{-1})	ΔG°_m (kJ mol^{-1})	ΔS°_m (J mol^{-1} K^{-1})
100% v/v MeOH	25	0.70	16.6	0.320	–12.23	–26.27	47.11
	30	0.72	17.1	0.337	–12.48	–26.25	45.42
	35	0.75	17.8	0.358	–12.76	–26.22	43.72
70% v/v MeOH	25	0.72	12.6	0.302	–12.53	–28.06	52.09
	30	0.75	13.1	0.325	–12.78	–28.01	50.27
	35	0.80	14.0	0.338	–13.10	–27.96	48.22
30% v/v MeOH	25	0.75	8.2	0.281	–12.69	–30.28	59.02
	30	0.79	8.6	0.296	–13.00	–30.26	56.95
	35	0.82	9.0	0.315	–13.28	–30.24	55.05
100% v/v EtOH	25	0.68	14.7	0.365	–12.07	–26.41	48.12
	30	0.72	15.6	0.378	–12.38	–26.39	46.25
	35	0.80	17.3	0.392	–12.68	–26.14	43.71
70% v/v EtOH	25	0.70	10.1	0.328	–12.34	–28.54	54.35
	30	0.75	10.8	0.345	–12.63	–28.47	52.28
	35	0.81	11.7	0.366	–12.88	–28.24	49.85
30% v/v EtOH	25	0.79	7.3	0.302	–12.53	–30.37	59.85
	30	0.80	7.4	0.326	–12.77	–30.36	58.03
	35	0.84	7.8	0.342	–13.07	–30.35	56.10
100% v/v 1–PrOH	25	0.60	23.0	0.314	–12.44	–25.35	43.31
	30	0.63	24.1	0.330	–12.74	–25.32	41.51
	35	0.68	26.0	0.342	–13.07	–25.26	39.56
70% v/v 1–PrOH	25	0.61	14.5	0.284	–12.66	–27.76	50.64
	30	0.65	15.4	0.298	–12.99	–27.74	48.67
	35	0.70	16.6	0.312	–13.31	–27.66	46.59
30% v/v 1–PrOH	25	0.67	8.1	0.266	–12.80	–30.54	59.54
	30	0.70	8.5	0.291	–13.04	–30.52	57.68
	35	0.75	9.1	0.308	–13.34	–30.32	55.14

4.1.2.1 Thermodynamics of micellization of CTAB

4.1.2.1.1 Temperature and alcohol compositions dependence of X_{CMC}

Before calculating the thermodynamic parameters we again intend to analyze the temperature and alcohol concentration effect on X_{CMC} values. As the X_{CMC} is the CMC values expression in mole fraction, these values were found to increase with temperature elevation. In case of CTAB also, the values of X_{CMC} were found to decrease with increment in water concentration within the solvent system i.e. 30% v/v hydro–alcoholic media. The variation in X_{CMC} values with regard to temperature and alcohol composite solutions have been presented in Figures 4.9 – 4.10. With respect to three different alcohols i.e. MeOH, EtOH and1–PrOH, X_{CMC} values were found to increase marginally as provided in Tables 4.3 – 4.4. With increase in carbon chain length of alcohols X_{CMC} values increases. Comparatively, X_{CMC} values obtained in 1–PrOH composite media were at higher side. This might be because of change in micellization process and suggestive of that the system is significantly hydrophobic causing penetration into the micellar system via linking H–Bond with hydroxyl group present on BHA/BHT molecules.

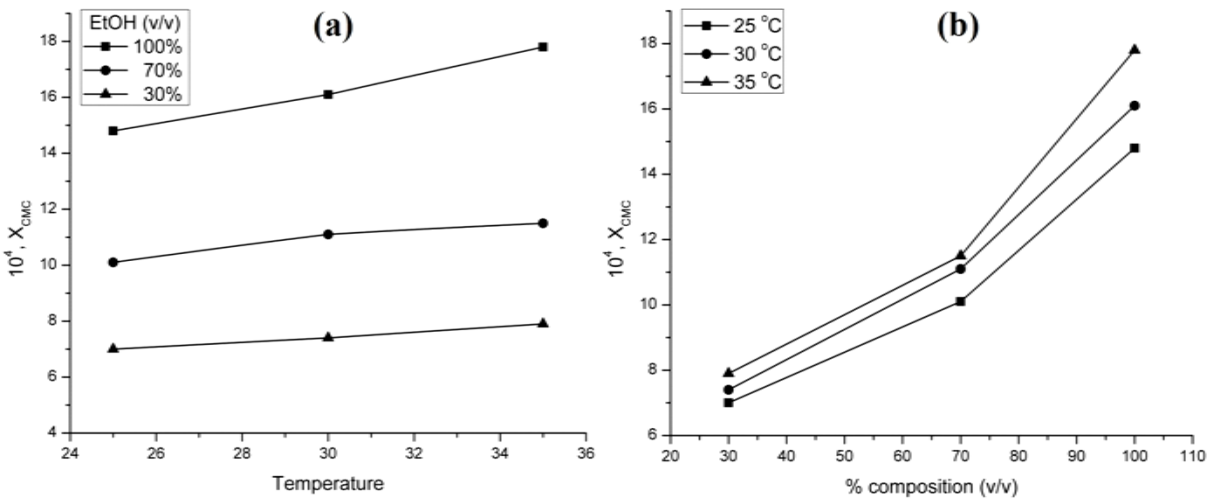

Figure 4.9: Plots of X_{CMC} vs. (a) temperature and (b) EtOH % composition (v/v) in solution for CTAB containing BHA 0.03 mol kg^{-1}.

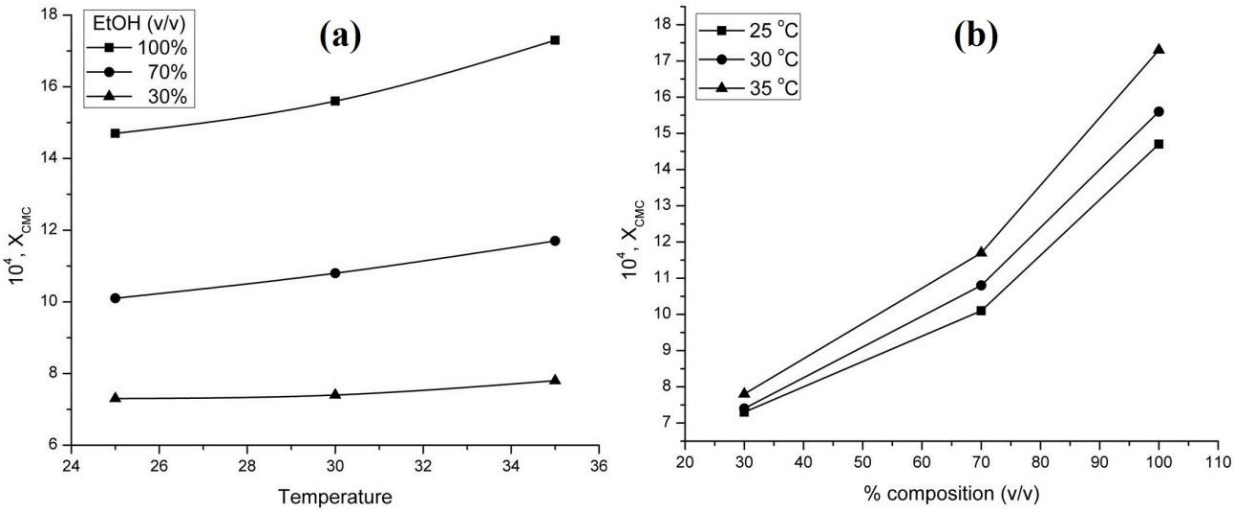

Figure 4.10: Plots of X_{CMC} vs. (a) temperature and (b) EtOH % composition (v/v) in solution for CTAB containing BHT 0.02 mol kg^{-1}.

4.1.2.2 Thermodynamic parameters

The thermodynamic parameters were determined by utilizing X_{CMC} data. Equations provided in experimental section 3.2.3.2 were used to determine the values of standard enthalpy change (ΔH°_m), standard entropy change (ΔS°_m) and standard Gibbs free energy change for micellization (ΔG°_m). The applied method resulted values has been presented in Table 4.3 – 4.4 along with α and X_{CMC} values. The uncertainty in the thermodynamic measurements for CTAB are: 0.01 K in temperature, ± 0.03 kJ mol^{-1} in ΔH°_m, ± 0.02 kJ mol^{-1} in ΔG°_m and ± 2 J mol^{-1} K^{-1} in ΔS°_m, respectively. Interpreting the data reported in Table 4.3 – 4.4, over the entire studied temperature range, values of ΔH°_m and ΔG°_m for CTAB in all alcohol and hydroalcoholic composite solutions containing BHA and BHT were found negative where as ΔS°_m with positive values. The values of ΔS°_m indicated that micellization in these studied systems is entropically controlled. In comparison to the earlier studied surfactant (SDS), values of ΔG°_m suggested that micellization is more spontaneous and energy driven. Again the ΔG°_m values were found less negative at higher alcoholic concentration which can be attributed to steric hindrance of micelle formation as shown in Figure 4.11 – 4.12. This also provided an assurance that compositions with higher negative value of ΔG°_m are solubilized to a greater extent with greater tendency to transfer from dispersed to micellar phase as in case of 30% v/v all three alcohols.

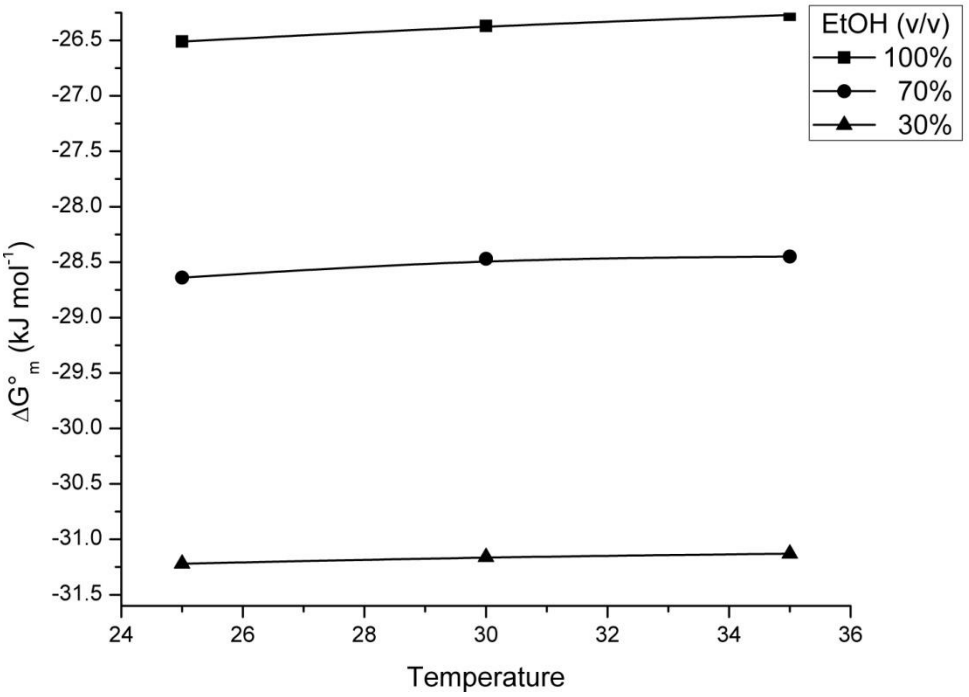

Figure 4.11: Plot of ΔG°_{m} versus temperature of CTAB in presence of BHA (0.03 mol kg^{-1}) containing different compositions of EtOH.

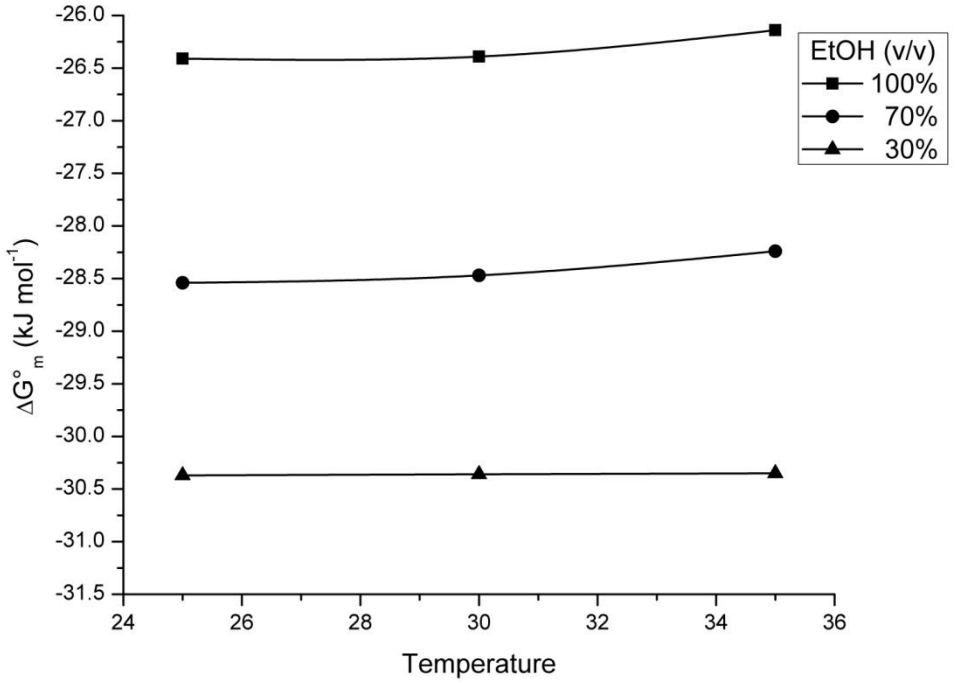

Figure 4.12: Plot of ΔG°_{m} versus temperature of CTAB in presence of BHT (0.02 mol kg^{-1}) containing different compositions of EtOH.

In addition ΔH°_{m} values do not vary significantly with temperature increment assuring that London dispersion interactions represent the main attractive force for micelle formation [21]. Therefore, presence substantial antioxidant molecules facilitated the micellization with respect to temperature and solvent composition dependence.

4.1.3 BHA and BHT impact on TX 100 properties

Nonionic surfactants represent an important class of amphiphiles which find extensive applications in pharmaceutical formulations [23, 24]. The effectiveness and applicability depend on their structural and solution properties. The presence of additives such as co–solute affects the physicochemical properties of a surfactant and provides valuable information with regard to structural change and interactions in the solution [25]. The mechanism by which nonionic surfactants adsorb onto a hydrophobic surface is based on a strong hydrophobic attraction between the solid surface and the surfactant's hydrophobic tail.

In continuation of our work, we studied the effect of two hydrophobic synthetic antioxidants on TX 100 (*tert*–octylphenol ethoxylate) micellar thermodynamic properties. Specific conductivity plots presented in Figure 4.13 – 4.14 and tabulated in *APPENDIX–A*, depicted the TX100 concentration (0.050 – 0.475 mmol kg^{-1}) dependence as well as different alcohol compositions reliance. Specific conductance was found to increase with temperature and TX 100 concentration supporting our previous conducted studies. In addition a marginal but considerable decrement in determined CMC values were observed in all the studied systems in comparison to standard CMC of TX100 in water i.e. 0.22 mmol kg^{-1}.

Considering these values as CMC, the decrease reflects the early micellization which might be due to the additional hydrophobicity offered by alcohol molecules [40] and BHA/BHT. At all compositions (100%, 70% and 30% v/v) the CMC values for TX100 in presence of BHA containing MeOH were found to lie in a range of 0.18 – 0.24 mmol kg^{-1}, for EtOH 0.17 – 0.24 mmol kg^{-1}, and for 1–PrOH 0.15 – 0.21 mmol kg^{-1}, respectively (Table 4.5). Whereas, in case of BHT, the CMC values for CTAB in MeOH were found to lie in a range of 0.16 – 0.23 mmol kg^{-1}, for EtOH 0.18 – 0.23 mmol kg^{-1}, and for 1–PrOH 0.16 – 0.23 mmol kg^{-1}, respectively as shown in Table 4.6.

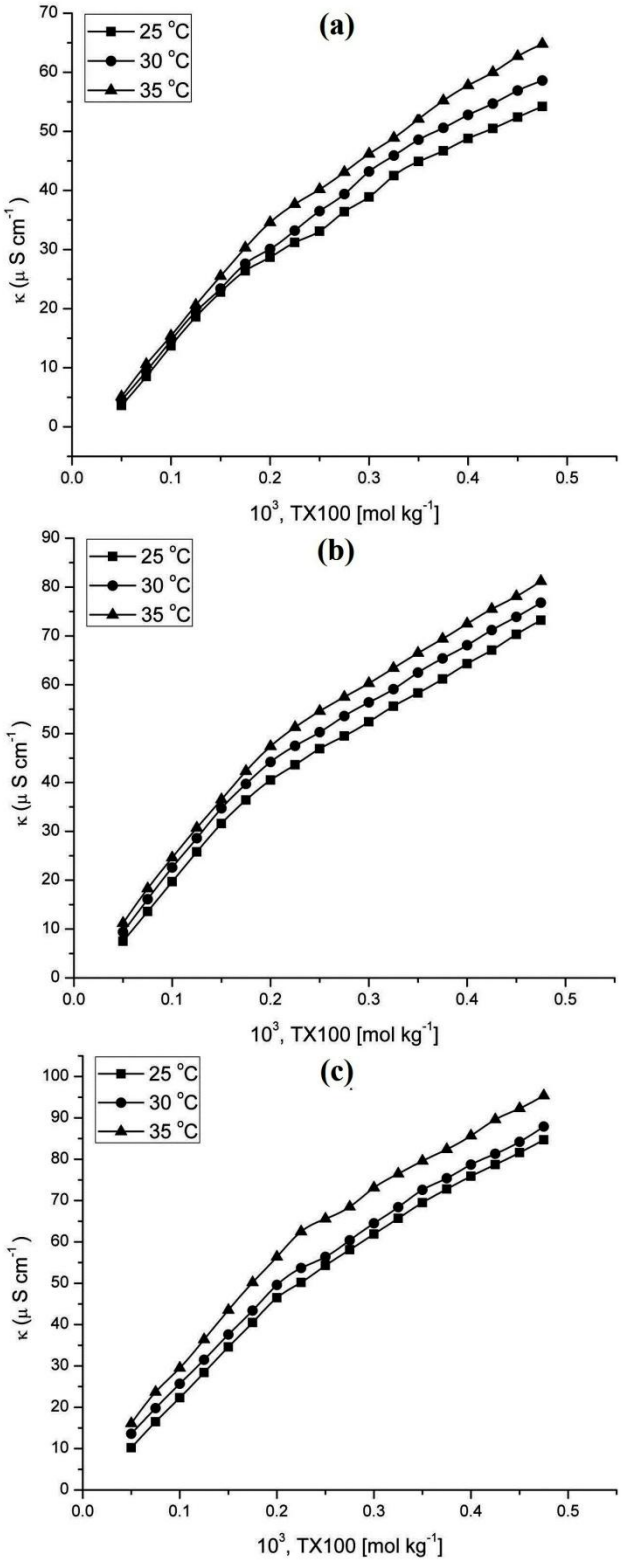

Figure 4.13: Conductivity vs. concentration plots of TX100 in (a) 100% v/v, (b) 70% v/v, and (c) 30% v/v EtOH solutions containing BHA (0.03 mol kg^{-1}) at different temperatures.

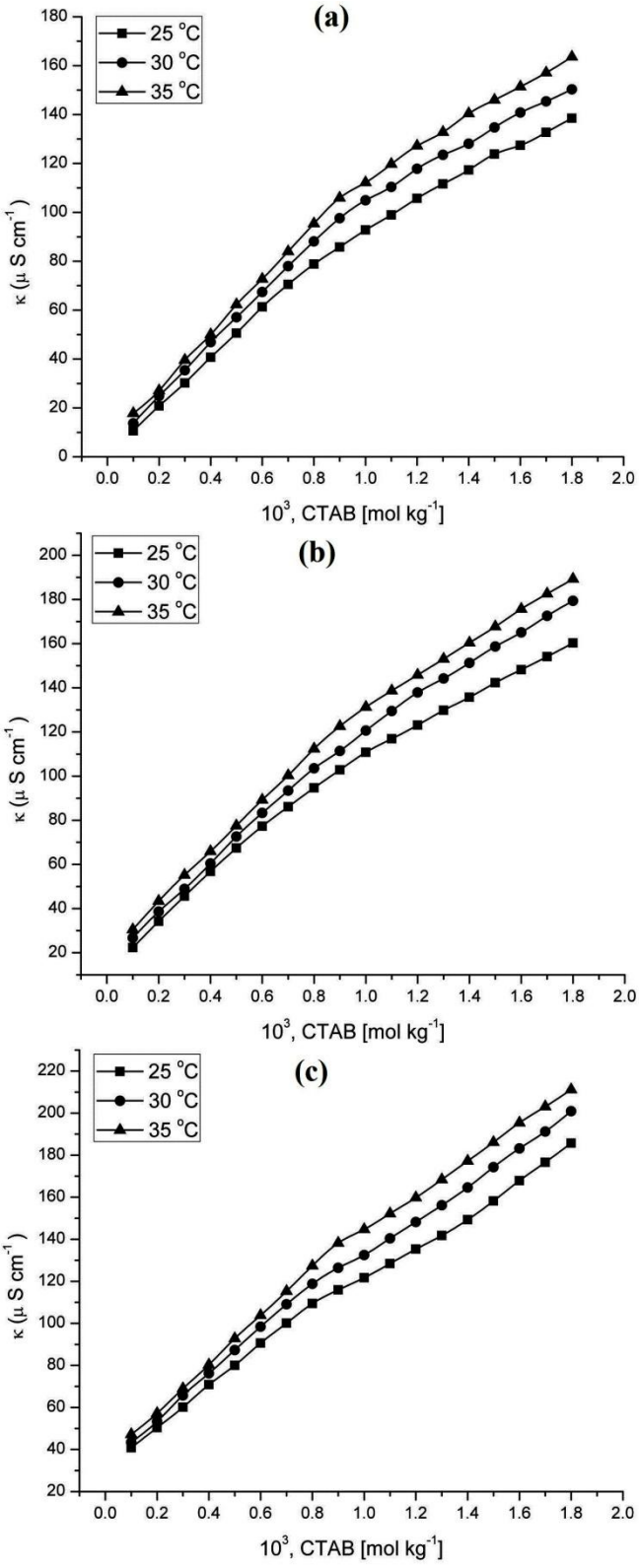

Figure 4.14: Conductivity vs. concentration plots of TX100 in (a) 100% v/v, (b) 70% v/v, and (c) 30% v/v EtOH solutions containing BHT (0.02 mol kg^{-1}) at different temperatures.

Table 4.5: Thermodynamic parameters data CMC, X_{CMC}, α, ΔH°_{m}, ΔG°_{m}, and ΔS°_{m} values of TX 100 containing BHA in different compositions at temperature T = 25, 30 and 35 °C.

Compositions	T °C	CMC (10^3)	X_{CMC} (10^3)	α	ΔH°_{m} (kJ mol^{-1})	ΔG°_{m} (kJ mol^{-1})	ΔS°_{m} (J mol^{-1} K^{-1})
100% v/v MeOH	25	0.18	4.1	0.607	–10.28	–26.88	55.70
	30	0.20	4.6	0.621	–10.52	–26.67	53.31
	35	0.21	4.8	0.634	–10.77	–26.72	51.78
70% v/v MeOH	25	0.20	3.4	0.558	–10.64	–28.50	59.94
	30	0.22	3.7	0.566	–10.94	–28.53	58.06
	35	0.23	3.9	0.582	–11.18	–28.46	56.11
30% v/v MeOH	25	0.21	2.2	0.498	–11.08	–31.48	68.43
	30	0.22	2.3	0.512	–11.35	–31.56	66.68
	35	0.24	2.6	0.524	–11.64	–31.48	64.42
100% v/v EtOH	25	0.17	3.7	0.492	–11.13	–29.51	61.68
	30	0.20	4.2	0.526	–11.25	–28.85	58.08
	35	0.22	4.6	0.539	–11.52	–28.73	55.87
70% v/v EtOH	25	0.19	2.7	0.392	–11.87	–32.70	69.91
	30	0.21	3.0	0.426	–12.01	–32.15	66.47
	35	0.23	3.2	0.439	–12.31	–32.13	64.37
30% v/v EtOH	25	0.20	1.8	0.358	–12.12	–35.06	76.99
	30	0.22	2.0	0.371	–12.43	–34.92	74.21
	35	0.24	2.2	0.392	–12.68	–34.67	71.38
100% v/v 1–PrOH	25	0.15	5.5	0.612	–10.24	–25.79	52.16
	30	0.17	6.2	0.619	–10.54	–25.60	49.71
	35	0.18	6.6	0.637	–10.75	–25.54	48.04
70% v/v 1–PrOH	25	0.17	3.9	0.584	–10.45	–27.50	57.21
	30	0.19	4.4	0.596	–10.71	–27.30	54.74
	35	0.20	4.6	0.608	–10.97	–27.37	53.23
30% v/v 1–PrOH	25	0.19	2.2	0.522	–10.91	–30.83	66.84
	30	0.20	2.4	0.531	–11.21	–30.82	64.73
	35	0.21	2.5	0.549	–11.44	–30.80	62.85

Table 4.6: Thermodynamic parameters data CMC, X_{CMC}, α, ΔH°_m, ΔG°_m, and ΔS°_m values of TX 100 containing BHT in different compositions at temperature T = 25, 30 and 35 °C.

Compositions	T °C	CMC (10^3)	X_{CMC} (10^3)	α	ΔH°_m (kJ mol^{-1})	ΔG°_m (kJ mol^{-1})	ΔS°_m (J mol^{-1} K^{-1})
100% v/v MeOH	25	0.16	3.8	0.615	–10.22	–27.00	56.30
	30	0.18	4.2	0.628	–10.47	–26.85	54.06
	35	0.20	4.7	0.644	–10.69	–26.59	51.63
70% v/v MeOH	25	0.18	3.1	0.562	–10.61	–28.75	60.85
	30	0.19	3.3	0.573	–10.89	–28.79	59.08
	35	0.22	3.8	0.594	–11.08	–28.33	55.99
30% v/v MeOH	25	0.20	2.2	0.522	–10.91	–30.83	66.84
	30	0.21	2.3	0.538	–11.15	–30.82	64.90
	35	0.23	2.5	0.555	–11.39	–30.67	62.59
100% v/v EtOH	25	0.18	3.9	0.578	–10.49	–27.62	57.45
	30	0.20	4.3	0.586	–10.79	–27.60	55.48
	35	0.22	4.7	0.603	–11.01	–27.40	53.19
70% v/v EtOH	25	0.20	2.9	0.516	–10.95	–29.92	63.66
	30	0.23	3.3	0.523	–11.27	–29.80	61.15
	35	0.25	3.6	0.544	–11.48	–29.52	58.58
30% v/v EtOH	25	0.20	1.8	0.488	–11.16	–32.29	70.89
	30	0.22	2.0	0.499	–11.45	–32.17	68.38
	35	0.23	2.1	0.521	–11.66	–32.04	66.15
100% v/v 1–PrOH	25	0.16	6.1	0.616	–10.21	–25.37	50.85
	30	0.17	6.5	0.629	–10.46	–25.31	49.01
	35	0.18	6.9	0.643	–10.70	–25.26	47.27
70% v/v 1–PrOH	25	0.17	4.0	0.535	–10.81	–28.38	58.95
	30	0.18	4.2	0.548	–11.08	–28.42	57.22
	35	0.21	5.0	0.571	–11.27	–27.81	53.70
30% v/v 1–PrOH	25	0.19	2.3	0.488	–11.16	–31.35	67.75
	30	0.20	2.4	0.509	–11.38	–31.28	65.69
	35	0.23	2.8	0.525	–11.63	–30.89	62.54

In general, when surfactants are added to an aqueous solution of any solvent having hydrophobic segments then, due to hydrophobic effect, it becomes thermodynamically favorable for the surfactant to form aggregates with hydrophobic portion of that solvent moiety preferentially. Therefore, this additional hydrophobicity offered by the alcohol molecule for the studied surfactants may be responsible for the earlier micellization of the surfactant. It is well known that London dispersion forces are the main attractive forces in the formation of the micelles and that the formation of micelles is supposed to be the result of hydrophobic interaction [26]. Whereas, in case of BHT a marginal decrease in all the studied surfactant CMC values was observed. The observed anomalous behavior in specific conductance is associated with some kind of hydrophobic clustering of alcohol molecules [27].

4.1.3.1 Thermodynamics of micellization of TX 100

4.1.3.1.1 Temperature and alcohol compositions dependence of X_{CMC}

Following the basic parameters, we determined X_{CMC} values and analyzed the impact of temperature and alcohol composite solutions. Supporting the previous conductance studies, X_{CMC} values of TX100 in presence of alcohol and hydro–alcohol solutions (100, 70 and 30% v/v; MeOH, EtOH and 1–PrOH) were found to follow the same trend. Likely, with increase in temperature, X_{CMC} values were found augmented revealing temperature dependence. On the other hand, X_{CMC} values were again found to decrease moving from pure alcoholic condition to aqueous rich solution state. The change obtained in the respective magnitude of X_{CMC} values with regard to temperature and alcohol compositions is shown in Figure 4.15 – 4.16 and also provided in Table 4.5 – 4.6. Owing to the difference between the structural categorization of anionic, cationic and non–ionic surfactants, the X_{CMC} values of TX100 were found much lower in comparison to SDS and CTAB suggesting role of different hydrophobic and hydrophilic part in micellization process as well as the approach or extent of getting interacted.

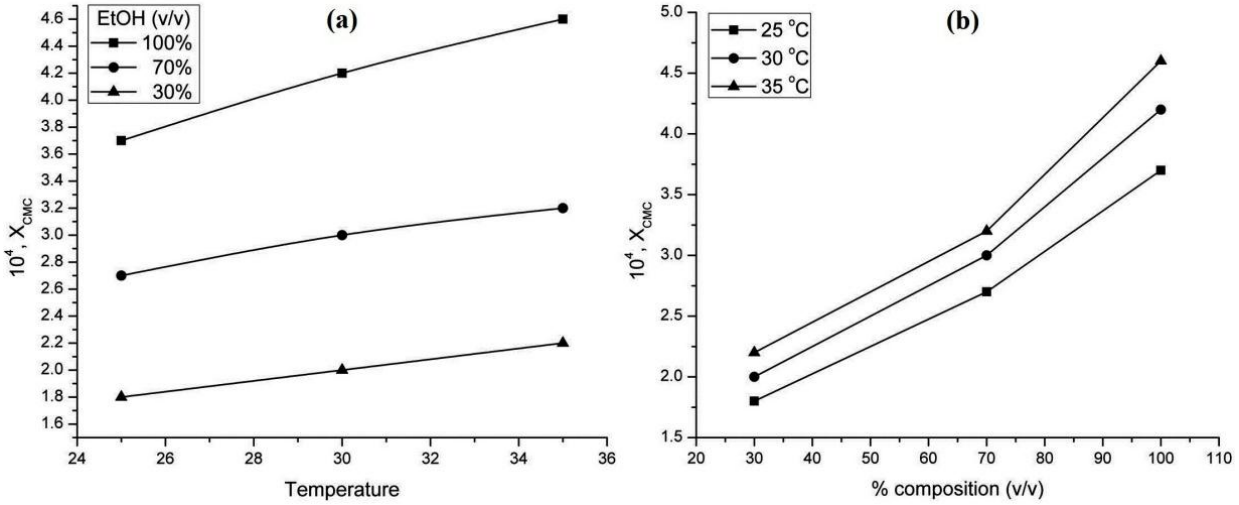

Figure 4.15: Plots of X_{CMC} vs. (a) temperature and (b) EtOH % composition (v/v) in solution for TX100 containing BHA 0.03 mol kg^{-1}.

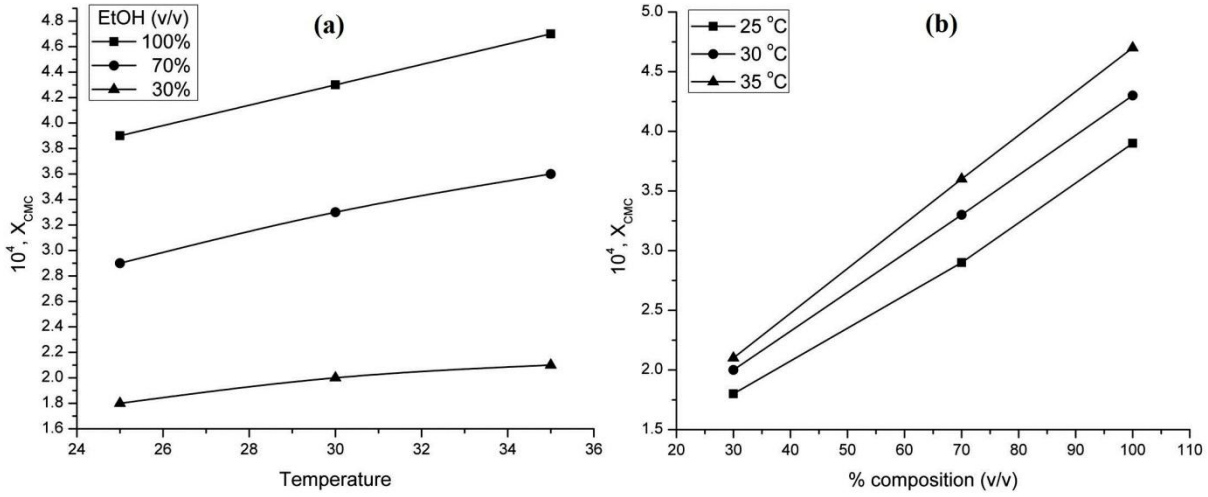

Figure 4.16: Plots of X_{CMC} vs. (a) temperature and (b) EtOH % composition (v/v) in solution for TX100 containing BHT 0.02 mol kg^{-1}.

4.1.3.2 Thermodynamic parameters

The obtained X_{CMC} values were employed to calculate further thermodynamic parameters; standard enthalpy change (ΔH°_m), standard entropy change (ΔS°_m) and standard Gibbs free energy change for micellization (ΔG°_m) (Table 4.5 – 4.6). The equations used are provided in experimental section 3.2.3.2. The uncertainty in the thermodynamic measurements for CTAB are: 0.01 K in temperature, ± 0.03 kJ mol^{-1} in ΔH°_m, ± 0.02 kJ mol^{-1} in ΔG°_m and ± 2 J mol^{-1} K^{-1} in ΔS°_m, respectively.

Analyzing the magnitude and the data obtained, the values of ΔH°_{m} and ΔG°_{m} for CTAB in all alcohol composite solutions containing BHA and BHT were found negative where as ΔS°_{m} were positive indicating micellization is entropically controlled. Comparing three surfactants, it suggested that the surfactants in same solution systems and antioxidants do not vary but significantly showed variations in view point of level of interaction.

Interesting, when compared to the earlier studied two surfactants (SDS and CTAB), values of ΔG°_{m} suggested that micellization is far more spontaneous and driven via energy. Moreover the ΔG°_{m} and ΔS°_{m} values were found more negative and positive, respectively revealed a favorable and stable system for micellization. In TX100, ΔG°_{m} values were again found less negative at higher alcoholic concentration (MeOH, EtOH and 1–PrOH) indicated steric hindrance of micelle formation and assured that compositions with higher negative ΔG°_{m} value solubilizes with much greater tendency to get transferred from dispersed to micellar phase as in case of aqueous rich solutions (Table 4.5 – 4.6 and Figure 4.17 – 4.18). Optimizing ΔH°_{m} variation, London dispersion interactions represented an alternative and additional attractive force in micellization process.

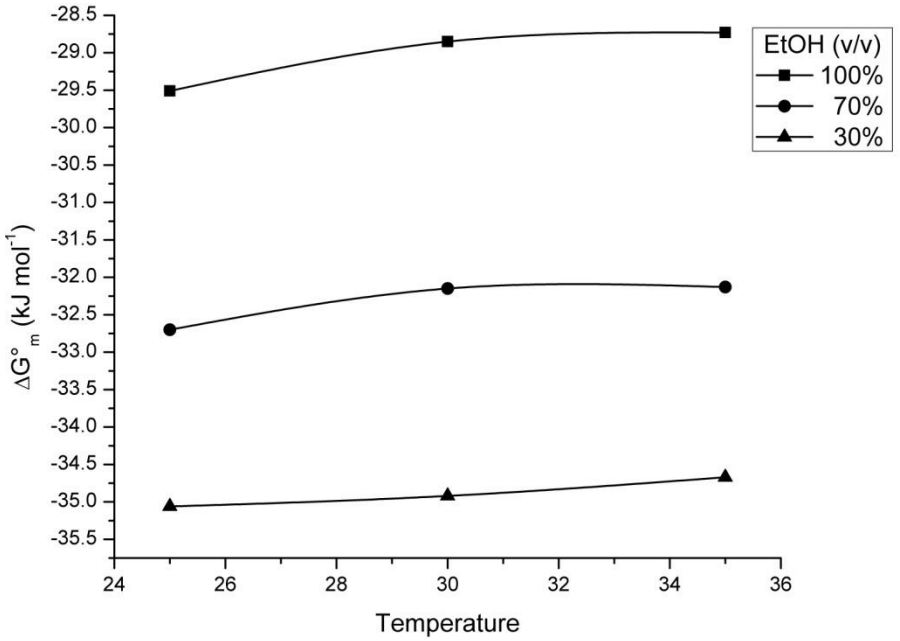

Figure 4.17: Plot of ΔG°_{m} versus temperature of TX100 in presence of BHA (0.03 mol kg^{-1}) containing different compositions of EtOH.

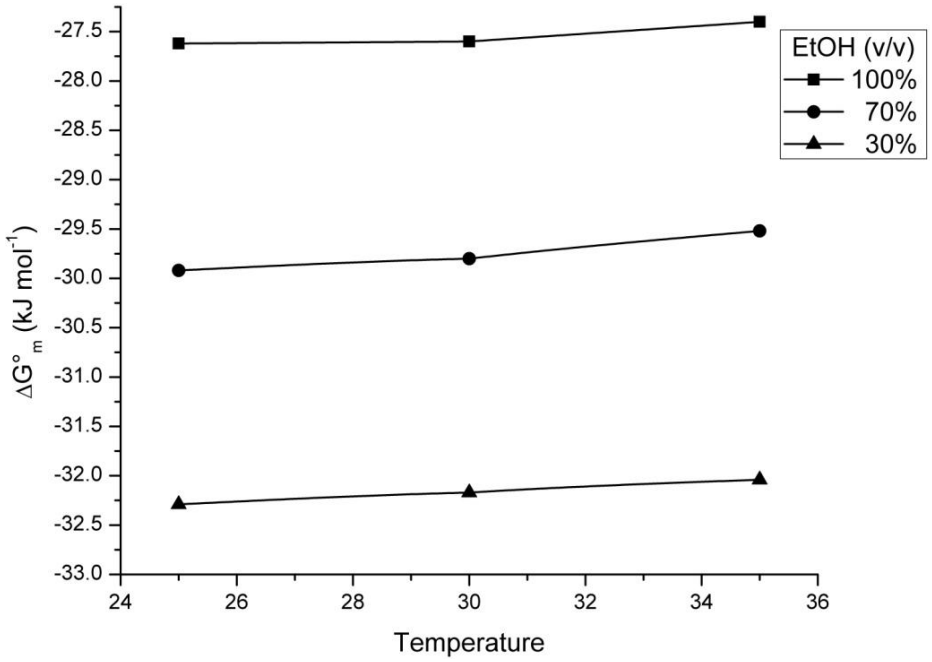

Figure 4.18: Plot of ΔG°_{m} versus temperature of TX100 in presence of BHT (0.02 mol kg^{-1}) containing different compositions of EtOH.

4.2 Viscosity measurement

The present investigation was extended with viscosity measurements with rationale based on competent utility of hydroalcoholic system in topical formulation to disperse active pharmaceutical ingredient (API) and to hold desired viscosity of formulations [28]. Empirically, it has been found that the viscosities of the surfactant solutions have great thermal dependency. Surfactant solutions have their own characteristics depending on their milieu, however, the viscosity of all the composite solutions decreases with temperature increment. The variation in viscosity values could be well attributed to change in micellization process [27].

Initially, the viscosity measurements of SDS in pure alcohol, alcohol rich and water rich compositions (100%, 70%, and 30% alcohol composition with water) were conducted. The concentration dependence of SDS viscosity (η) in different solution of BHA and BHT is presented in Figure 4.19–4.20 and Table 4.7–4.8, at all compositions of alcohol (MeOH, EtOH and 1–PrOH). Viscosity measurements performed in different alcohol composite solutions showed that η decreases initially with increase in concentration of SDS up to 8 mmol kg^{-1} SDS concentration and thereafter, interestingly increases with progressive increase in SDS concentration. Region with a sharp decrease ~ 6–7 mmol kg^{-1} corresponds to the micellization of SDS, which however tends to change prominently as the concentration of SDS increases. A decrease at low SDS concentration is an unexpected observation [29] whereas non–linearity in η with SDS concentration suggests a clear fact that there might be a significant contribution of SDS–BHA/BHT interaction. In view of this, a possible reason for this kind of magnitude in η values is because of hydrophobic groups exerting their effects predominantly via hydrophobic interactions within higher alcoholic concentration [30], moreover the observed minima express the region of micellization which in full support with conductance study. Differences in region of micellization in comparison to conductance can be attributed to the presence of dodecanol in SDS [31] which could increase surfactant dispersion by increasing the hydrophobicity leading to higher micellar values. Furthermore, positive values also suggest the strong interaction between water and alcohol molecules [32]. It might be because of hydrophobic groups which predominantly exert their effect within the solution environment. The region of micellization thus is in complete agreement with the conductance study reported earlier.

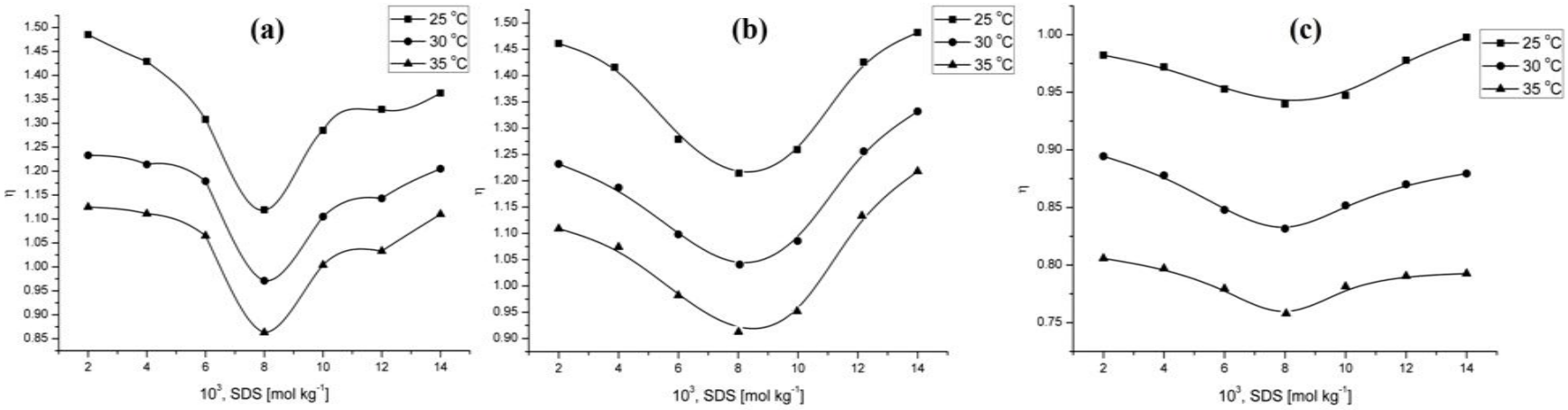

Figure 4.19: Plots of viscosity, η (centipoise) of SDS in compositions of EtOH (a) 100%, (b) 70%, and (c) 30% v/v containing BHA (0.03 mol kg^{-1}) at T = 25, 30 and 35 °C.

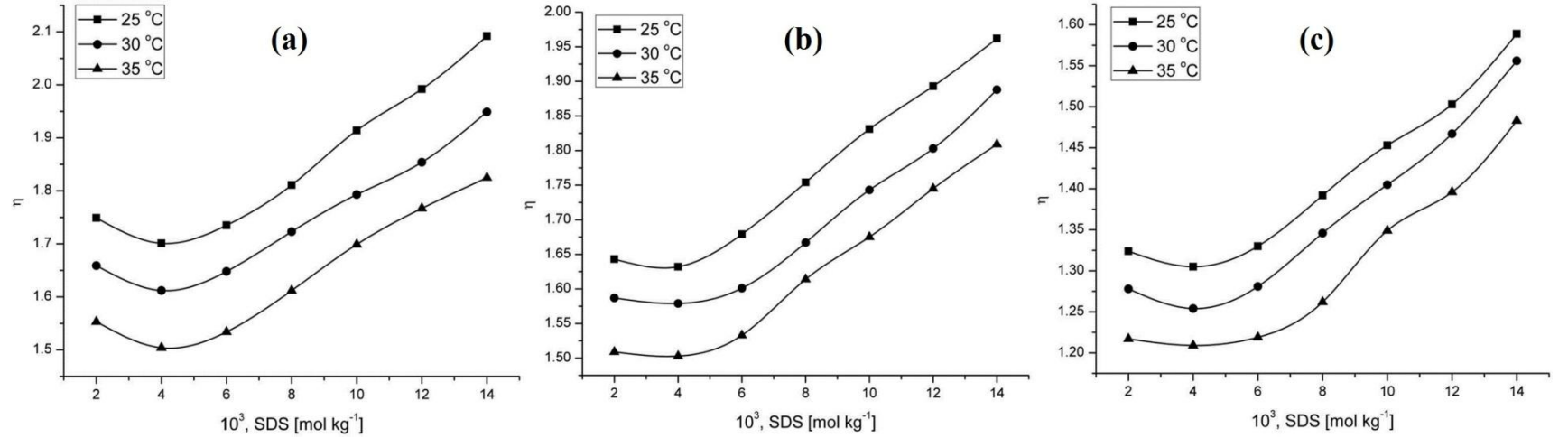

Figure 4.20: Plots of viscosity, η (centipoise) of SDS in compositions of EtOH (a) 100%, (b) 70%, and (c) 30% v/v containing BHT (0.02 mol kg^{-1}) at T = 25, 30 and 35 °C.

Table 4.7: Viscosity, η (centipoise) of SDS (1.0–14.0 mmol kg^{-1}) in various compositions of MeOH, EtOH and 1–PrOH containing BHA (0.03 mol kg^{-1}) at T = 25, 30 and 35 °C.

[SDS] mmol kg^{-1}	**100% v/v MeOH**			**70% v/v MeOH**			**30% v/v MeOH**		
	25 °C	**30 °C**	**35 °C**	**25 °C**	**30 °C**	**35 °C**	**25 °C**	**30 °C**	**35 °C**
2.0	1.335	1.185	1.098	0.9736	0.8468	0.7682	0.7469	0.6802	0.5911
4.0	1.285	1.134	1.044	0.9437	0.8246	0.7392	0.7313	0.6733	0.5908
6.0	1.223	1.085	0.998	0.9368	0.8130	0.7214	0.7224	0.6674	0.5832
8.0	1.314	1.128	1.068	0.9636	0.8409	0.7614	0.7498	0.6834	0.6022
10.0	1.376	1.235	1.135	0.9771	0.8599	0.7697	0.7562	0.6962	0.6189
12.0	1.421	1.298	1.223	0.9908	0.8683	0.7774	0.7668	0.7033	0.6294
14.0	1.462	1.325	1.268	0.9991	0.8770	0.7837	0.7739	0.7116	0.6382
	100% v/v EtOH			**70% v/v EtOH**			**30% v/v EtOH**		
2.0	1.485	1.233	1.125	1.461	1.232	1.109	0.9822	0.8945	0.8058
4.0	1.429	1.214	1.111	1.423	1.187	1.074	0.9720	0.8778	0.7970
6.0	1.308	1.179	1.065	1.279	1.098	0.982	0.9528	0.8479	0.7795
8.0	1.119	0.971	0.863	1.198	1.025	0.906	0.9398	0.8245	0.7494
10.0	1.285	1.105	1.004	1.240	1.072	0.928	0.9473	0.8518	0.7814
12.0	1.329	1.143	1.033	1.431	1.256	1.134	0.9778	0.8701	0.7905
14.0	1.363	1.205	1.110	1.482	1.332	1.218	0.9977	0.8795	0.7926
	100% v/v 1–PrOH			**70% v/v 1–PrOH**			**30% v/v 1–PrOH**		
2.0	2.536	2.452	2.322	2.241	2.183	2.005	1.798	1.632	1.540
4.0	2.512	2.401	2.299	2.230	2.143	2.001	1.721	1.629	1.506
6.0	2.474	2.368	2.232	2.168	2.031	1.986	1.627	1.536	1.418
8.0	2.598	2.444	2.318	2.049	1.932	1.894	1.516	1.429	1.332
10.0	2.646	2.502	2.366	2.293	2.201	2.091	1.787	1.638	1.552
12.0	2.698	2.564	2.412	2.364	2.296	2.132	1.846	1.793	1.681
14.0	2.754	2.602	2.484	2.421	2.379	2.265	1.946	1.872	1.759

Table 4.8: Viscosity, η (centipoise) of SDS (1.0 – 14.0 mmol kg^{-1}) in various compositions of MeOH, EtOH and 1–PrOH containing BHT (0.02 mol kg^{-1}) at T = 25, 30 and 35 °C.

[SDS]	100% v/v MeOH			70% v/v MeOH			30% v/v MeOH		
mmol kg^{-1}	25 °C	30 °C	35 °C	25 °C	30 °C	35 °C	25 °C	30 °C	35 °C
2.0	1.374	1.198	1.106	0.9784	0.8482	0.7694	0.7482	0.6814	0.5925
4.0	1.296	1.148	1.058	0.9445	0.8258	0.7406	0.7328	0.6748	0.5918
6.0	1.245	1.099	1.007	0.9378	0.8142	0.7228	0.7244	0.6688	0.5847
8.0	1.332	1.152	1.076	0.9649	0.8418	0.7626	0.7508	0.6846	0.6038
10.0	1.396	1.248	1.152	0.9786	0.8610	0.7708	0.7578	0.6988	0.6198
12.0	1.432	1.308	1.238	0.9914	0.8698	0.7790	0.7686	0.7048	0.6322
14.0	1.478	1.342	1.284	0.9998	0.8788	0.7852	0.7754	0.7129	0.6402
	100% v/v EtOH			70% v/v EtOH			30% v/v EtOH		
2.0	1.749	1.659	1.553	1.643	1.587	1.509	1.324	1.278	1.217
4.0	1.701	1.612	1.504	1.632	1.579	1.503	1.305	1.254	1.209
6.0	1.735	1.648	1.534	1.679	1.601	1.533	1.330	1.281	1.219
8.0	1.811	1.723	1.612	1.754	1.667	1.614	1.392	1.346	1.262
10.0	1.914	1.793	1.699	1.831	1.743	1.675	1.453	1.405	1.349
12.0	1.992	1.854	1.767	1.893	1.803	1.745	1.503	1.467	1.396
14.0	2.092	1.949	1.825	1.962	1.888	1.809	1.589	1.556	1.483
	100% v/v 1–PrOH			70% v/v 1–PrOH			30% v/v 1–PrOH		
2.0	2.552	2.483	2.344	2.268	2.198	2.084	1.808	1.646	1.558
4.0	2.528	2.422	2.308	2.246	2.154	2.025	1.732	1.642	1.522
6.0	2.489	2.385	2.248	2.182	2.042	1.992	1.644	1.548	1.434
8.0	2.608	2.468	2.330	2.064	1.946	1.906	1.532	1.444	1.358
10.0	2.660	2.522	2.376	2.306	2.214	2.110	1.798	1.655	1.568
12.0	2.712	2.588	2.428	2.388	2.312	2.188	1.856	1.808	1.698
14.0	2.778	2.616	2.499	2.446	2.394	2.278	1.968	1.892	1.776

The viscosity measurements were thereafter obtained for a cationic surfactant belonging to different class (CTAB) at a concentration range of 0.2–1.8 mmol kg^{-1} in alcoholic and hydro–alcoholic solutions (MeOH, EtOH and 1–PrOH). The variation in viscosity with regard to BHA and BHT in 100%, 70%, 30 % v/v alcoholic and hydro–alcoholic solutions (EtOH) is presented in Figure 4.21–4.22, whereas the complete data for viscometric study is reported in Table 4.9–4.10. The viscosity values were found to increase with increase in CTAB concentration and decreases with temperature increment. Interestingly, an inflection point was observed at a certain point with respect to CTAB concentration region (~ 0.8–1.0) mmol kg^{-1} and thereafter a linear increment in the viscosity magnitude was obtained. Therefore, this certain point of variation within the region was assumed as region of micelle formation. No second inflection was observed in the studied surfactant concentration range, indicating no structural transition in micelles. Latterly, the study was further extended to include non–ionic surfactant i.e. TX100 in same studied solutions containing BHA and BHT. The variation and concentration dependence of TX100 viscosity in different composite solutions in addition to BHA and BHT is presented in Figure 4.23–4.24 and Table 4.11–4.12. It was again found that the viscosities of the surfactant solutions depend greatly on temperature. Moreover, in this case again a slight linear increase was observed up to a certain concentration (~ 0.20 mmol kg^{-1}) thereafter a sharp increase was noticed. Therefore, this point of variation was assumed as the region of micelle formation. The viscosity of all the composite solutions decreases with increment in temperature. It was observed that BHA and BHT significantly increases the viscosity of the TX100 solution indicating that they are sufficiently hydrophobic in nature to penetrate micelles and link via hydrogen bonds due to hydroxyl group substitution on molecules, providing a clear indication of inducing micellar transition. On the basis of earlier report [33], this could be explained that presence of *tert*–butyl groups provides an extra hydrophobic force toward the micelle.

As cohesive forces increases with increment in additive's concentration, all the values were found to increase with increment in surfactant molecules. Initially, In general, this variation also suggests a solute–solvent interaction which is a measure of cohesiveness i. e. intermolecular forces present between the molecular ions or solvent molecules within the various solution systems. The observed increase in the viscosity values with increase in all surfactant concentration reveals the existence of cohesive forces due to addition molecules.

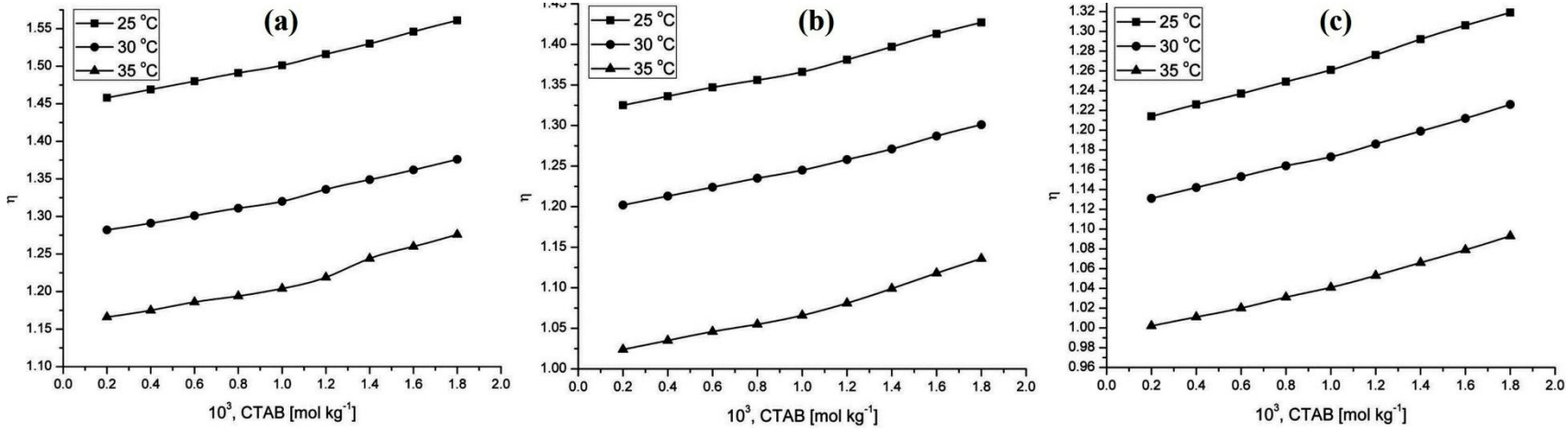

Figure 4.21: Plots of viscosity, η (centipoise) of CTAB in compositions of EtOH (a) 100%, (b) 70%, and (c) 30% v/v containing BHA (0.03 mol kg^{-1}) at T = 25, 30 and 35 °C.

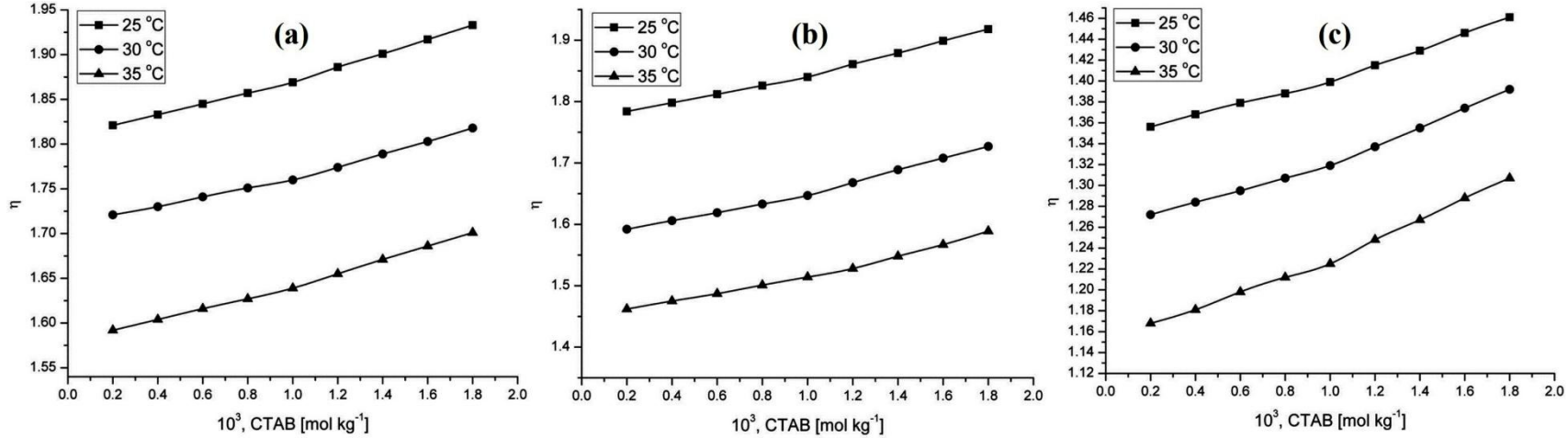

Figure 4.22: Plots of viscosity, η (centipoise) of CTAB in compositions of EtOH (a) 100%, (b) 70%, and (c) 30% v/v containing BHT (0.02 mol kg^{-1}) at T = 25, 30 and 35 °C.

Table 4.9: Viscosity, η (centipoise) of CTAB (0.2 – 1.8 mmol kg^{-1}) in various compositions of MeOH, EtOH and 1–PrOH containing BHA (0.03 mol kg^{-1}) at T = 25, 30 and 35 °C.

[CTAB]	100% v/v MeOH			70% v/v MeOH			30% v/v MeOH		
mmol kg^{-1}	25 °C	30 °C	35 °C	25 °C	30 °C	35 °C	25 °C	30 °C	35 °C
0.2	1.124	1.042	0.9855	0.9615	0.8368	0.7712	0.7512	0.6624	0.6022
0.4	1.138	1.054	0.9982	0.9762	0.8596	0.7825	0.7644	0.6717	0.6146
0.6	1.151	1.065	1.008	0.9823	0.8732	0.7904	0.7774	0.6804	0.6228
0.8	1.168	1.076	1.021	0.9979	0.8974	0.8048	0.7882	0.6915	0.6335
1.0	1.182	1.089	1.038	1.024	0.9132	0.8158	0.7978	0.7008	0.6478
1.2	1.212	1.114	1.059	1.054	0.9421	0.8399	0.8162	0.7132	0.6637
1.4	1.236	1.136	1.081	1.078	0.9686	0.8566	0.8356	0.7374	0.6892
1.6	1.258	1.154	1.101	1.099	0.9839	0.8714	0.8598	0.7524	0.7088
1.8	1.282	1.172	1.125	1.134	0.9988	0.8968	0.8786	0.7772	0.7296
	100% v/v EtOH			70% v/v EtOH			30% v/v EtOH		
0.2	1.458	1.282	1.166	1.325	1.202	1.024	1.214	1.131	1.002
0.4	1.469	1.291	1.175	1.336	1.213	1.035	1.226	1.142	1.011
0.6	1.480	1.301	1.186	1.347	1.224	1.046	1.237	1.153	1.020
0.8	1.491	1.311	1.194	1.356	1.235	1.055	1.249	1.164	1.031
1.0	1.501	1.320	1.204	1.366	1.245	1.066	1.261	1.173	1.041
1.2	1.516	1.336	1.219	1.381	1.258	1.081	1.276	1.186	1.053
1.4	1.530	1.349	1.244	1.397	1.271	1.099	1.292	1.199	1.066
1.6	1.546	1.362	1.260	1.413	1.287	1.118	1.306	1.212	1.079
1.8	1.561	1.376	1.276	1.427	1.301	1.136	1.319	1.226	1.093
	100% v/v 1–PrOH			70% v/v 1–PrOH			30% v/v 1–PrOH		
0.2	2.812	2.654	2.469	2.215	2.146	2.002	1.825	1.706	1.612
0.4	2.826	2.664	2.481	2.228	2.161	2.015	1.839	1.712	1.614
0.6	2.838	2.675	2.493	2.245	2.175	2.028	1.853	1.717	1.625
0.8	2.849	2.684	2.505	2.262	2.191	2.041	1.864	1.727	1.634
1.0	2.862	2.694	2.517	2.279	2.205	2.054	1.877	1.739	1.646
1.2	2.882	2.711	2.535	2.305	2.226	2.073	1.898	1.759	1.664
1.4	2.901	2.726	2.553	2.328	2.244	2.092	1.921	1.777	1.682
1.6	2.916	2.741	2.571	2.352	2.265	2.109	1.942	1.796	1.701
1.8	2.931	2.757	2.589	2.376	2.286	2.127	1.963	1.815	1.719

Table 4.10: Viscosity, η (centipoise) of CTAB (0.2 – 1.8 mmol kg^{-1}) in various compositions of MeOH, EtOH and 1–PrOH containing BHT (0.02 mol kg^{-1}) at T = 25, 30 and 35 °C.

[CTAB] mmol kg^{-1}	100% v/v MeOH			70% v/v MeOH			30% v/v MeOH		
	25 °C	30 °C	35 °C	25 °C	30 °C	35 °C	25 °C	30 °C	35 °C
0.2	1.254	1.145	1.066	1.024	0.8652	0.8024	0.7828	0.6926	0.6225
0.4	1.266	1.155	1.078	1.048	0.8854	0.8134	0.7942	0.7018	0.6328
0.6	1.278	1.166	1.09	1.069	0.9051	0.8247	0.8031	0.7108	0.6431
0.8	1.291	1.176	1.102	1.088	0.9262	0.8351	0.8124	0.7193	0.6542
1.0	1.305	1.187	1.115	1.114	0.9441	0.8488	0.8206	0.7291	0.6654
1.2	1.326	1.202	1.129	1.145	0.9694	0.8642	0.8348	0.7463	0.6802
1.4	1.343	1.221	1.146	1.176	0.9885	0.8824	0.8491	0.7632	0.7004
1.6	1.359	1.234	1.162	1.199	1.007	0.9028	0.8664	0.7774	0.7205
1.8	1.376	1.248	1.178	1.242	1.022	0.9199	0.8823	0.7912	0.7401
	100% v/v EtOH			70% v/v EtOH			30% v/v EtOH		
0.2	1.821	1.721	1.592	1.784	1.592	1.462	1.356	1.272	1.168
0.4	1.833	1.730	1.604	1.798	1.606	1.475	1.368	1.284	1.181
0.6	1.845	1.741	1.616	1.812	1.619	1.487	1.379	1.295	1.198
0.8	1.857	1.751	1.627	1.826	1.633	1.501	1.388	1.307	1.212
1.0	1.869	1.760	1.639	1.840	1.647	1.514	1.399	1.319	1.225
1.2	1.886	1.774	1.655	1.861	1.668	1.528	1.415	1.337	1.248
1.4	1.901	1.789	1.671	1.879	1.689	1.548	1.429	1.355	1.267
1.6	1.917	1.803	1.686	1.899	1.708	1.567	1.446	1.374	1.288
1.8	1.933	1.818	1.701	1.918	1.727	1.589	1.461	1.392	1.307
	100% v/v 1–PrOH			70% v/v 1–PrOH			30% v/v 1–PrOH		
0.2	2.928	2.782	2.535	2.342	2.205	2.136	1.965	1.822	1.739
0.4	2.939	2.793	2.546	2.352	2.216	2.145	1.976	1.834	1.748
0.6	2.950	2.804	2.556	2.363	2.227	2.156	1.988	1.846	1.759
0.8	2.961	2.815	2.565	2.372	2.238	2.167	1.997	1.855	1.770
1.0	2.972	2.826	2.576	2.384	2.247	2.178	2.008	1.864	1.781
1.2	2.991	2.845	2.598	2.405	2.269	2.199	2.027	1.885	1.799
1.4	3.011	2.864	2.624	2.426	2.291	2.220	2.048	1.904	1.821
1.6	3.031	2.883	2.643	2.456	2.313	2.241	2.069	1.925	1.842
1.8	3.051	2.903	2.662	2.477	2.334	2.262	2.085	1.946	1.863

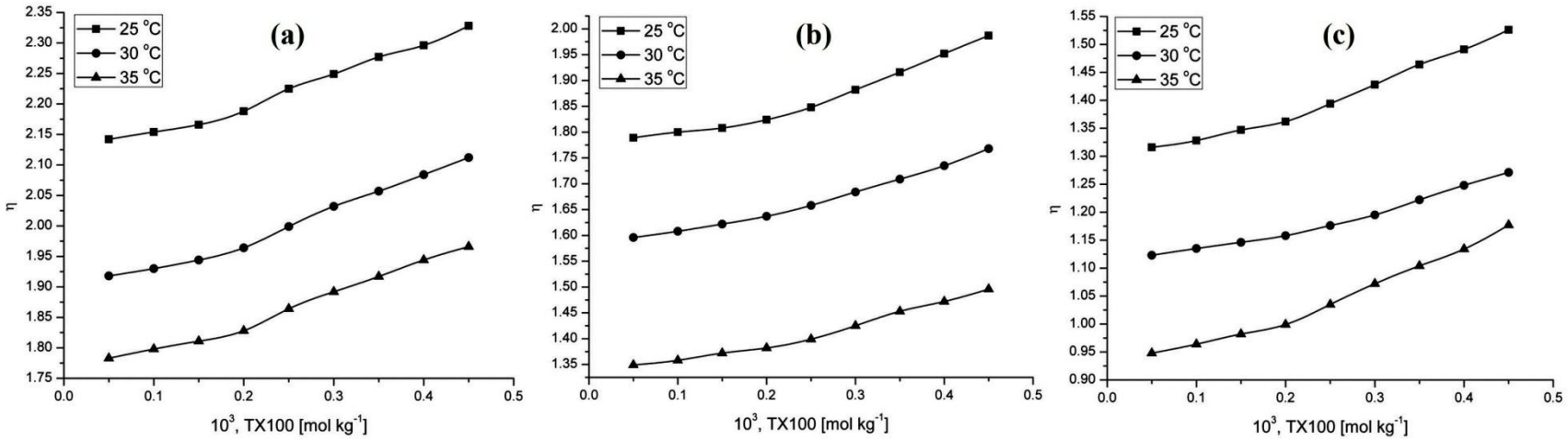

Figure 4.23: Plots of viscosity, η (centipoise) of TX100 in compositions of EtOH (a) 100%, (b) 70%, and (c) 30% v/v containing BHA (0.03 mol kg^{-1}) at T = 25, 30 and 35 °C.

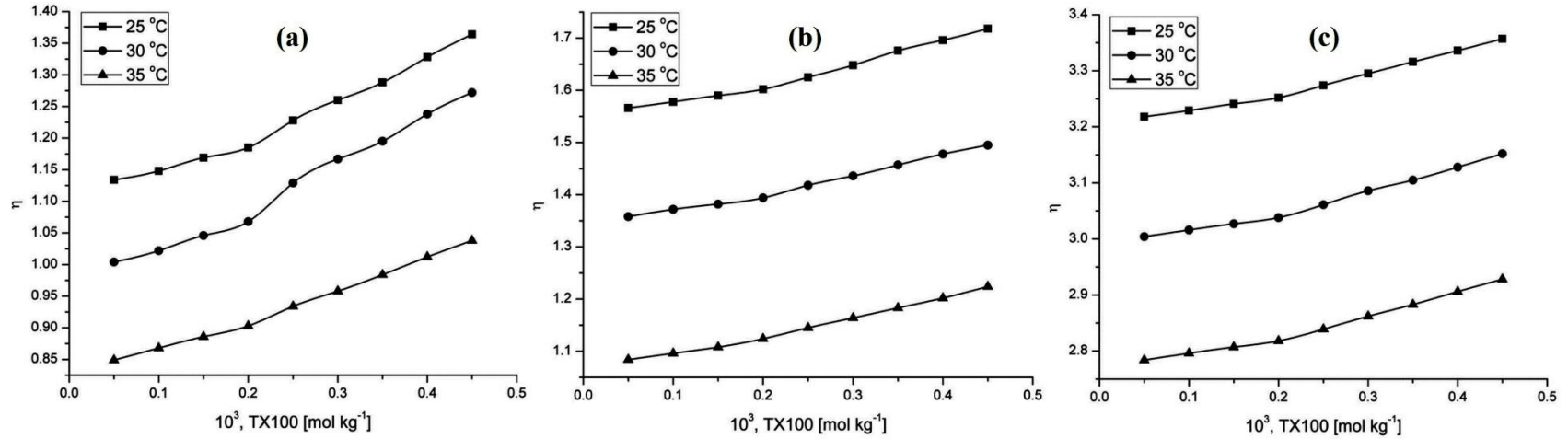

Figure 4.24: Plots of viscosity, η (centipoise) of TX100 in 30 % v/v compositions of (a) MeOH, (b) EtOH, and (c) 1–PrOH containing BHT (0.02 mol kg^{-1}) at T = 25, 30 and 35 °C.

Table 4.11: Viscosity, η (centipoise) of TX100 (0.05 – 0.45 mmol kg^{-1}) in various compositions of MeOH, EtOH and 1–PrOH containing BHA (0.03 mol kg^{-1}) at T = 25, 30 and 35 °C.

[TX100] mmol kg^{-1}	100% v/v MeOH			70% v/v MeOH			30% v/v MeOH		
	25 °C	30 °C	35 °C	25 °C	30 °C	35 °C	25 °C	30 °C	35 °C
0.05	1.545	1.404	1.238	1.246	1.139	0.823	0.916	0.805	0.712
0.10	1.558	1.435	1.252	1.263	1.154	0.844	0.938	0.824	0.728
0.15	1.578	1.466	1.275	1.284	1.165	0.865	0.956	0.84	0.746
0.20	1.594	1.502	1.302	1.302	1.187	0.888	0.978	0.862	0.765
0.25	1.654	1.582	1.351	1.347	1.224	0.934	1.022	0.898	0.802
0.30	1.698	1.632	1.414	1.383	1.265	0.965	1.057	0.925	0.845
0.35	1.746	1.668	1.471	1.413	1.296	1.006	1.095	0.958	0.887
0.40	1.788	1.704	1.513	1.445	1.344	1.043	1.124	0.975	0.914
0.45	1.824	1.742	1.542	1.483	1.376	1.084	1.156	0.998	0.946
	100% v/v EtOH			70% v/v EtOH			30% v/v EtOH		
0.05	2.142	1.918	1.783	1.789	1.596	1.349	1.316	1.123	0.948
0.10	2.154	1.930	1.798	1.800	1.608	1.358	1.328	1.135	0.964
0.15	2.166	1.944	1.811	1.808	1.622	1.372	1.347	1.146	0.982
0.20	2.188	1.964	1.828	1.824	1.637	1.382	1.362	1.158	0.999
0.25	2.225	1.999	1.864	1.848	1.658	1.399	1.394	1.176	1.035
0.30	2.249	2.032	1.892	1.882	1.684	1.425	1.428	1.195	1.072
0.35	2.277	2.057	1.917	1.916	1.709	1.453	1.464	1.222	1.104
0.40	2.296	2.084	1.944	1.952	1.735	1.472	1.491	1.248	1.134
0.45	2.328	2.112	1.966	1.987	1.768	1.496	1.526	1.271	1.177
	100% v/v 1–PrOH			70% v/v 1–PrOH			30% v/v 1–PrOH		
0.05	3.423	3.258	3.023	3.128	2.936	2.766	2.682	2.384	2.122
0.10	3.436	3.272	3.035	3.141	2.948	2.779	2.694	2.395	2.134
0.15	3.446	3.283	3.044	3.154	2.961	2.788	2.704	2.406	2.145
0.20	3.464	3.294	3.058	3.166	2.974	2.802	2.719	2.418	2.156
0.25	3.492	3.319	3.080	3.189	2.995	2.821	2.744	2.441	2.177
0.30	3.514	3.345	3.102	3.208	3.018	2.844	2.768	2.462	2.198
0.35	3.537	3.366	3.125	3.234	3.042	2.865	2.791	2.484	2.220
0.40	3.562	3.390	3.148	3.258	3.061	2.880	2.813	2.505	2.243
0.45	3.585	3.411	3.176	3.281	3.082	2.899	2.834	2.527	2.265

Table 4.12: Viscosity, η (centipoise) of TX100 (0.05 – 0.45 mmol kg^{-1}) in various compositions of MeOH, EtOH and 1–PrOH containing BHT (0.02 mol kg^{-1}) at T = 25, 30 and 35 °C.

[TX100] mmol kg^{-1}	100% v/v MeOH			70% v/v MeOH			30% v/v MeOH		
	25 °C	30 °C	35 °C	25 °C	30 °C	35 °C	25 °C	30 °C	35 °C
0.05	1.662	1.528	1.384	1.365	1.208	0.946	1.134	1.004	0.849
0.10	1.678	1.542	1.403	1.382	1.226	0.962	1.148	1.022	0.868
0.15	1.692	1.565	1.426	1.394	1.238	0.980	1.169	1.046	0.886
0.20	1.716	1.585	1.448	1.414	1.255	0.999	1.185	1.068	0.903
0.25	1.756	1.626	1.488	1.452	1.294	1.036	1.228	1.129	0.934
0.30	1.794	1.662	1.531	1.484	1.334	1.071	1.260	1.167	0.958
0.35	1.818	1.694	1.561	1.514	1.368	1.098	1.288	1.195	0.984
0.40	1.845	1.733	1.594	1.542	1.399	1.134	1.328	1.238	1.012
0.45	1.878	1.768	1.622	1.572	1.436	1.166	1.364	1.272	1.038
	100% v/v EtOH			70% v/v EtOH			30% v/v EtOH		
0.05	2.222	2.094	1.884	1.856	1.642	1.464	1.566	1.358	1.084
0.10	2.234	2.112	1.896	1.870	1.654	1.478	1.578	1.372	1.096
0.15	2.243	2.124	1.908	1.885	1.666	1.489	1.590	1.382	1.108
0.20	2.258	2.135	1.920	1.899	1.677	1.504	1.602	1.394	1.124
0.25	2.284	2.162	1.944	1.922	1.699	1.528	1.625	1.418	1.145
0.30	2.308	2.188	1.965	1.943	1.717	1.558	1.648	1.436	1.164
0.35	2.326	2.211	1.985	1.972	1.734	1.584	1.676	1.457	1.183
0.40	2.346	2.238	2.008	1.998	1.752	1.606	1.696	1.478	1.202
0.45	2.369	2.256	2.034	2.030	1.775	1.632	1.718	1.495	1.224
	100% v/v 1–PrOH			70% v/v 1–PrOH			30% v/v 1–PrOH		
0.05	3.645	3.458	3.232	3.422	3.216	2.976	3.218	3.004	2.784
0.10	3.658	3.469	3.245	3.435	3.228	2.986	3.229	3.016	2.796
0.15	3.668	3.479	3.257	3.446	3.239	2.994	3.241	3.027	2.807
0.20	3.684	3.490	3.270	3.458	3.252	3.006	3.252	3.038	2.818
0.25	3.706	3.512	3.292	3.481	3.273	3.022	3.274	3.061	2.839
0.30	3.729	3.535	3.314	3.502	3.295	3.043	3.295	3.086	2.862
0.35	3.752	3.559	3.337	3.525	3.318	3.064	3.316	3.105	2.883
0.40	3.774	3.584	3.360	3.548	3.341	3.087	3.336	3.128	2.906
0.45	3.796	3.608	3.384	3.574	3.364	3.111	3.357	3.152	2.928

Whereas, the decrease in viscosity values with temperature increase is attributed to the increased kinetic energy of various constituents in solution. Also, at the molecular level the decrease in viscosity with increase in temperature is due to extra vibration between the particles breaking down the intermolecular forces as well as adhesion between the molecules. So, all the values showed fair agreement with respect to region of micelle formation obtained via conductance study and were found supportive with regard to BHA and BHT.

4.3 Density and ultrasonic sound velocity measurements

Density (ρ) in combination with ultrasonic sound velocity (u) were further measured to furnish the information arising from different kind of interactions with respect to behaviour of solute space in composite solutions of short chain alcohols [100%, 70% and 30% v/v (MeOH, EtOH and 1– PrOH)]. The study was carried out for SDS (2.0–14.0 mmol kg^{-1}), CTAB (0.2–1.80 mmol kg^{-1}) and TX100 (0.05–0.45 mmol kg^{-1}) in presence of fixed concentration of BHA (0.03 mol kg^{-1}) and BHT (0.02 mol kg^{-1}) at three different temperature at an interval of 5 °C. In all three surfactants, density and ultrasonic sound velocity were completely found to be concentration and temperature dependent in all solution systems. In addition, the temperature increment favors the increase of kinetic energy and expansion of volume, therefore, resulting in decrease in density. This also suggests that thermal energy is quite higher than the interaction energy at higher temperatures causes the destruction of iceberg structure. On the other hand, decrease in ultrasonic sound velocity with increase in temperature is suggestive of cohesive forces due to existing molecular interactions within the environment.

4.3.1 Volumetric and compressibility measurements

The data obtained from density and ultrasonic sound velocity (*APPENDIX– A*) was further employed to calculate the apparent molar volume (ϕ_v) and apparent molar adiabatic compression (ϕ_κ) values. These parameters were calculated using the relation given in experimental section 3.24.1 (Eq. 3.4 and 3.5). In addition, isentropic compressibility (κ_s) of the solution and solvent, respectively was determined by using relation as $\kappa_s = 1/\rho u^2$ [34] is reported in *APPENDIX– A* . Since these properties are highly sensitive to extrinsic experimental conditions and therefore are suggested to be relevant to gain information, prominently with respect to the existence of solute – solute and solute – solvent interactions [30]. The κ_s values decreases with increase in alcohol and in alcohol rich solutions containing BHA/BHT with slight non – linear increase was observed. This kind of behavior can be rationalized in terms of the strength of existing intermolecular interactions within the system. Also, this kind of non – linear trend further confirms solute – solvent interactions. The κ_s values showed a regular increase with increase in temperature and surfactant (SDS, CTAB and TX100) concentration in pure alcohol solution (100% v/v MeOH, EtOH and 1–PrOH)

and alcohol rich solution (70% v/v). In contrast to this behavior; in water rich solution of alcohols (30% v/v), κ_s values showed a decrease with increase in surfactant concentration and temperature. An increase in κ_s values within 100% and 70% v/v alcohol solutions is indicative of complex system as well as a decrease in κ_s values within water rich solutions suggest compactness introduced into the solution system as a result of BHA/BHT–surfactant (SDS, CTAB and TX100) interactions. However, in 30% v/v alcohol–antioxidant–surfactant system, change in compressibility is attributed to the structural factor which is in support with temperature dependence.

Further, overlook into the nature and level of interaction of surfactant in the presence of BHA and BHT in different alcohols and hydroalcoholic solutions was obtained from the behavior of apparent molar volume, ϕ_v, and apparent molar adiabatic compression, ϕ_κ. The data could not be analyzed in terms of limiting apparent molar volume, (ϕ_v^o) and slope (S_v^*) values of the Masson's equation ($\phi_v = \phi_v^o + S_v^* C^{1/2}$), for the reason that ϕ_v dependence on SDS concentration is found to be non – linear which is not a characteristic feature of electrolytic solutions [35]. With regard to all three surfactants, the values for ϕ_v and ϕ_κ were found to be positive at all temperatures and concentrations in presence of BHA/BHT. Surprisingly, an anomalous trend was observed in pure alcohol solutions which might be because of structure breaking and making effect caused by the solvent system comprising alcohols. In case of SDS and as shown in Figure 4.25–4.26 and Table (4.13–4.14), the ϕ_v values decreases sharply at lower concentration ~ 2 – 6 mmol Kg^{-1}, thereafter, the decrease is almost linear. This change in trend at ~ 6 mmol Kg^{-1} can be considered as the region of micellization or proper micelle formation. Since, BHA/BHT are lipophilic organic molecules, it seems that initially at lower concentration of SDS, the binding seems to be governed by electrostatic forces whereas with subsequent addition of surfactant, the pattern indicated the dominance of hydrophobic interactions as BHA/BHT are believed to expose only the CH_3^+ sites to the medium. It appears that the position of hydroxyl group on alcohol has significant impact on the electrostatic and hydrophobic contribution. Hydrophobic, electrostatic interaction and favorable conditions for micellization were found for SDS because of its anionic nature. Therefore linear consistence at higher surfactant concentration can be attributed to strong hydrophobic interactions. Moreover, at higher SDS concentration, the interchange in level of

interactions among these molecules increases causing formation of SDS micelles. Moreover, higher ϕ_v and ϕ_κ values in alcohol are in good support of previous studies [36].

The variation in ϕ_v values for CTAB in presence of BHA and BHT in 30% v/v hydro–alcoholic solutions (EtOH) is presented in Figure 4.27–4.28 and Table 4.15–4.16, respectively. From the plots and the data obtained, four pertinent features in the trends of ϕ_v for CTAB are as follows:

(i) with increase in temperature, increase in ϕ_v values was attained over the studied temperature range,

(ii) with increase in CTAB concentration, the ϕ_v values decreases significantly in all alcoholic solution systems as well as in the presence of antioxidants,

(iii) the observed change in magnitude i.e. curved shape appearance of ϕ_v values at certain low CTAB concentrations (Figure 4.27–4.28) and thereafter the decrease in ϕ_v is almost linear reveals absolute dominance of hydrophobic – hydrophobic interactions and also indicating the region of micelle formation.

(iv) from one of the well established volumetric properties of surfactant [37], the ϕ_v results, thus also imply that in the concentration region > 1.0 mmol kg^{-1}, the ϕ_v values are practically independent of CTAB concentration and attributed to region of micellization whereas, for concentration < 1.0 mmol kg^{-1} is due to pre–micellar effect,

From the plots shown in Figure 4.29–4.30 and Table 4.17–4.18, we find three relevant features in ϕ_v trend of TX100:

(i) the ϕ_v values decreases significantly with increase in TX100 concentration in case of all alcoholic compositions and in the presence of both the additives (BHA and BHT),

(ii) the effect of temperature is seen to increase the ϕ_v values over the studied temperature range,

(iii) from the Figure 4.29–4.30, the change in trend of ϕ_v values can be attributed to region of micelle formation showing that the micellization region shifts with increase in length of alcohol chain (in case of ethanol when compared to methanol) but decreases in case of 1–propanol which is in support of earlier reports [38].

In context of the observed behavior of ϕ_v and ϕ_κ values in different alcohols and hydro–alcoholic solutions, it could also be explained that due to the addition of surfactant in an aqueous solution containing hydrophobic segments the system becomes thermodynamically favorable for the surfactant to form aggregates with hydrophobic portion of that solvent moiety preferentially. Therefore, this additional hydrophobicity offered by the alcohol molecule may be responsible for the trend obtained. With regard to alcohol – water solutions, evidence from a wide range of data on water/alcohol mixtures at low concentration suggests the formation of cages of fairly regular and longer – lived hydrogen bonds located around hydrophobic groups [39]. Also, BHA, BHT and alcohol molecules are characterized by the presence of hydrophobic and hydrophilic centers leading to two different types of hydration. When two non–polar regions come closer together, these regions are shielded to a greater extent from interactions with water molecules leading to the collapse of the quasi–crystalline structure of water. Since the nature of the interacting groups is different, the changes in thermodynamic properties are expected. The changes can be attributed to specific solvation effects and hydrophobic effects that act in opposite directions. Specific solvation effects are dependent mainly on the composition of the solvent mixture, being greatest for strongly solvated molecules. The hydrophobic effect, on the other hand, increases with the size of solute – solvent molecules [43]. The observed anomalous behavior can be associated to some kind of hydrophobic clustering of alcohol molecules. In all the studied solution systems the effect of ϕ_v values was also reflected in ϕ_κ values, thus supporting each other.

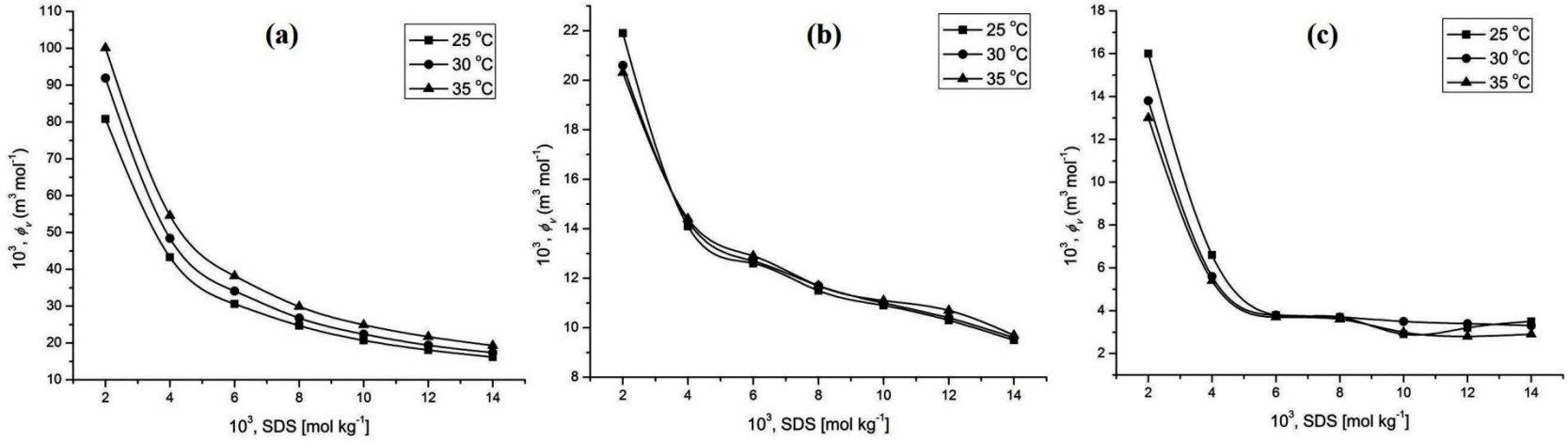

Figure 4.25: Apparent molar volume (ϕ_v) versus SDS in EtOH (a) 100% v/v, (b) 70% v/v, and (c) 30% v/v containing BHA (0.03 mmol kg^{-1}) at different temperatures.

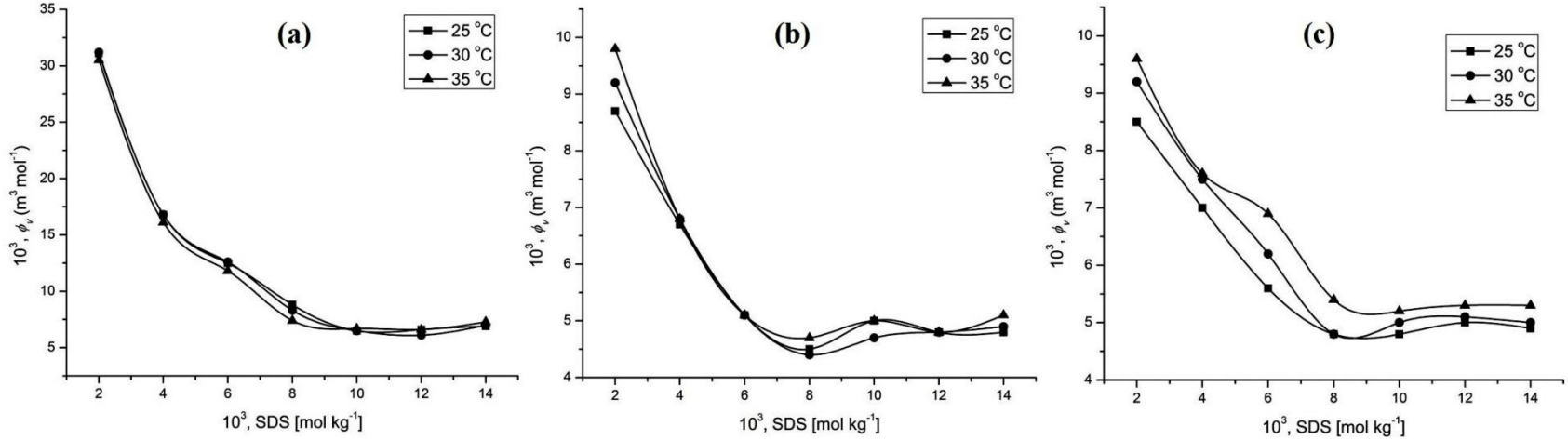

Figure 4.26: Apparent molar volume (ϕ_v) versus SDS in EtOH (a) 100% v/v, (b) 70% v/v, and (c) 30% v/v containing BHT (0.02 mmol kg^{-1}) at different temperatures.

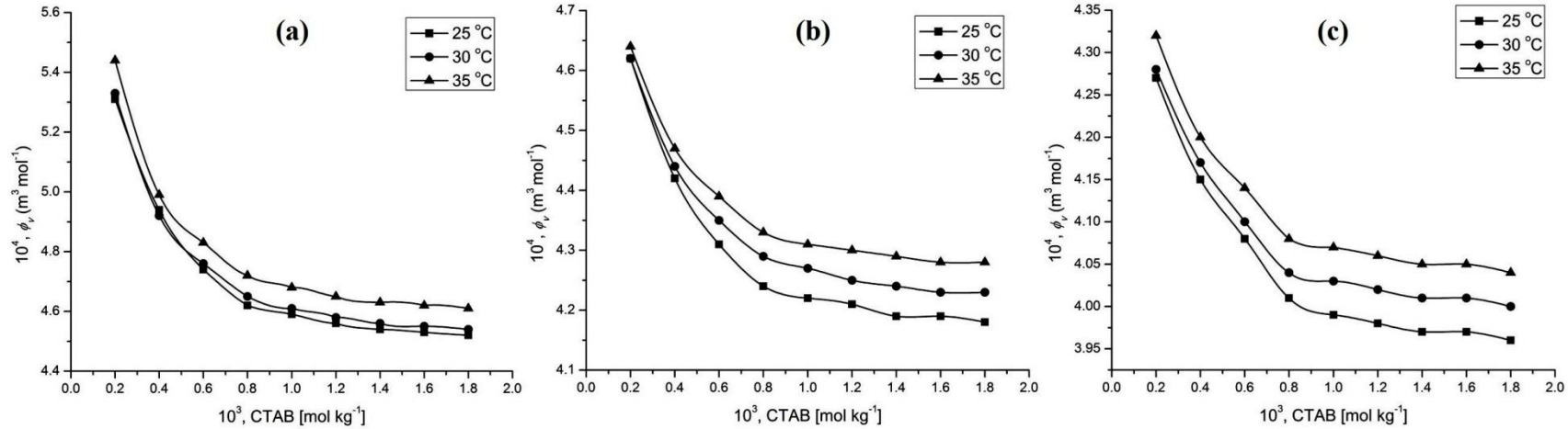

Figure 4.27: Apparent molar volume (ϕ_v) versus CTAB in EtOH (a) 100% v/v, (b) 70% v/v, and (c) 30% v/v containing BHA (0.03 mmol kg^{-1}) at different temperatures.

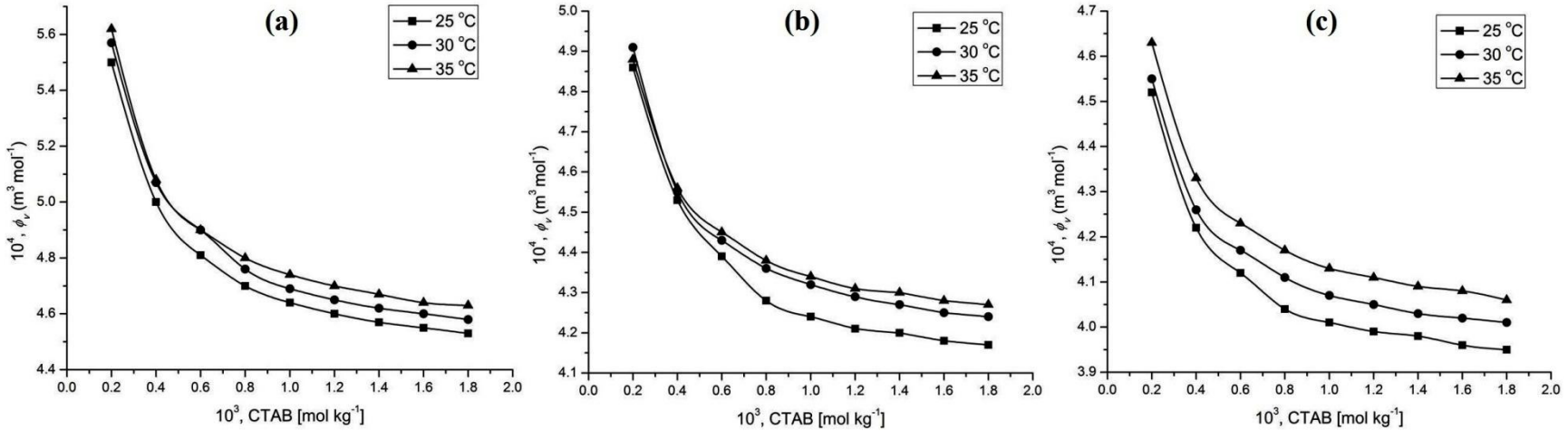

Figure 4.28: Apparent molar volume (ϕ_v) versus CTAB in EtOH (a) 100% v/v, (b) 70% v/v, and (c) 30% v/v containing BHT (0.02 mmol kg^{-1}) at different temperatures.

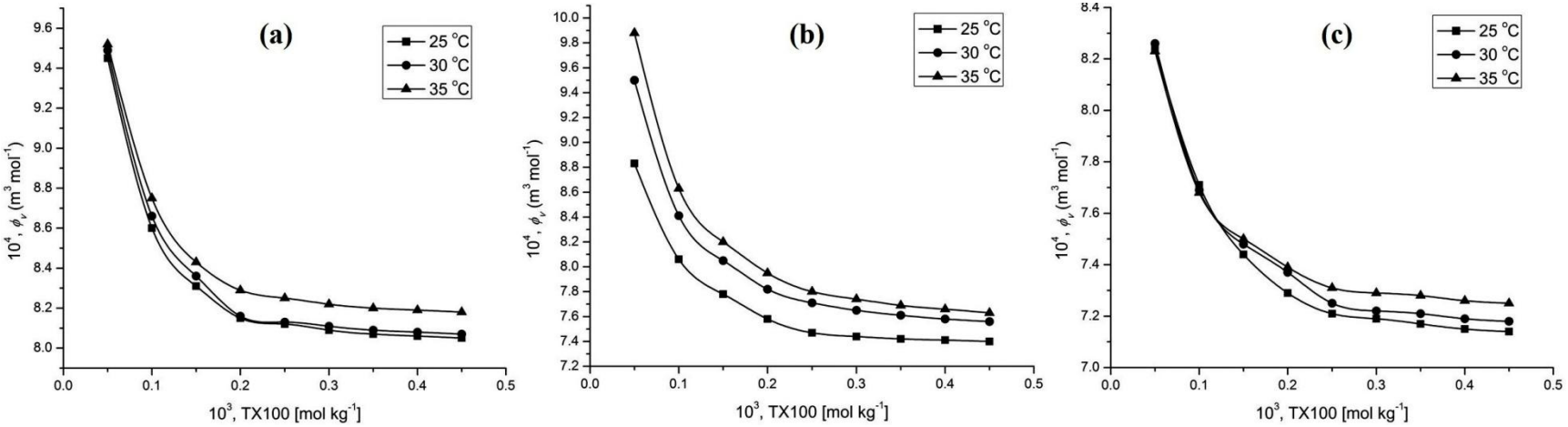

Figure 4.29: Apparent molar volume (ϕ_v) versus TX100 in EtOH (a) 100% v/v, (b) 70% v/v, and (c) 30% v/v containing BHA (0.03 mmol kg^{-1}) at different temperatures.

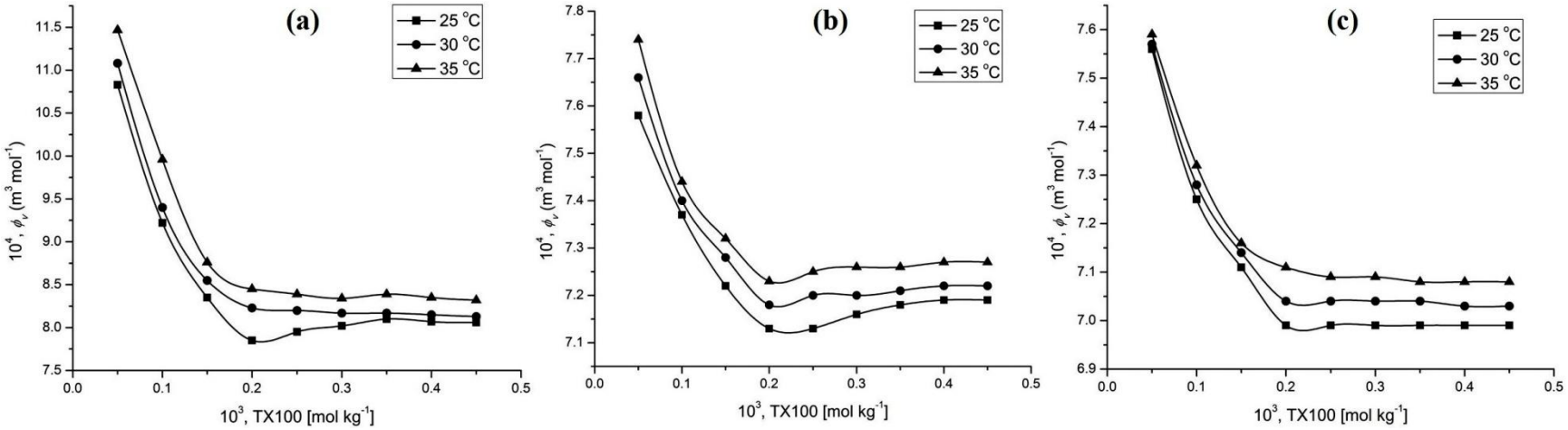

Figure 4.30: Apparent molar volume (ϕ_v) versus TX100 in EtOH (a) 100% v/v, (b) 70% v/v, and (c) 30% v/v containing BHT (0.02 mmol kg^{-1}) at different temperatures.

Table 4.13: Apparent molar volume (ϕ_v) (m^3mol^{-1}) × 10^3 of SDS (2.0–14.0 mmol kg^{-1}) in various compositions of MeOH, EtOH and 1–PrOH containing 0.03 mol kg^{-1} BHA over three different temperatures.

[SDS] mmol kg^{-1}	100% v/v MeOH			70% v/v MeOH			30% v/v MeOH		
	25 °C	**30 °C**	**35 °C**	**25 °C**	**30 °C**	**35 °C**	**25 °C**	**30 °C**	**35 °C**
2.0	33.73	36.28	37.94	10.3	13.4	13.4	8.5	10.7	14.0
4.0	16.47	17.75	18.26	3.8	4.2	4.6	3.7	4.6	4.9
6.0	13.03	13.92	14.54	4.1	4.7	4.9	3.4	3.9	4.1
8.0	10.75	11.52	11.44	3.8	4.5	5.0	4.1	4.3	4.7
10.0	10.74	10.84	11.11	4.5	4.9	4.9	4.1	4.2	4.7
12.0	10.31	10.35	10.55	4.3	4.8	4.8	4.1	4.2	4.7
14.0	9.48	9.55	9.73	4.4	4.7	4.8	4.2	4.2	4.5
	100% v/v EtOH			**70% v/v EtOH**			**30% v/v EtOH**		
2.0	80.8	91.9	100.1	21.9	20.6	20.3	16.0	13.8	13.0
4.0	43.3	48.4	54.6	14.1	14.3	14.4	6.6	5.6	5.4
6.0	30.6	34.1	38.2	12.6	12.7	12.9	3.8	3.8	3.7
8.0	24.7	26.8	29.9	11.5	11.7	11.7	3.7	3.7	3.6
10.0	20.7	22.4	24.9	10.9	11.0	11.1	2.9	3.5	3.0
12.0	18.1	19.4	21.7	10.3	10.4	10.7	3.2	3.4	2.8
14.0	16.2	17.4	19.3	9.5	9.6	9.7	3.5	3.3	2.9
	100% v/v 1–PrOH			**70% v/v 1–PrOH**			**30% v/v 1–PrOH**		
2.0	20.3	32.1	40.5	12.0	15.2	18.3	10.1	11.9	13.4
4.0	11.5	16.3	21.3	9.9	10.8	12.3	6.8	7.8	8.5
6.0	10.9	13.3	16.3	7.1	8.1	8.7	5.3	6.0	6.4
8.0	9.5	11.5	13.4	6.3	6.9	7.5	4.8	5.5	5.9
10.0	9.2	10.2	11.7	6.1	6.7	7.0	4.9	5.3	5.5
12.0	9.1	9.3	10.6	5.8	6.4	6.7	4.8	5.1	5.3
14.0	9.2	8.7	9.9	5.6	6.1	6.3	4.7	4.9	5.2

Table 4.14: Apparent molar volume (ϕ_v) (m^3mol^{-1}) × 10^4 of SDS (2.0–14.0 mmol kg^{-1}) in various compositions of MeOH, EtOH and 1–PrOH containing 0.02 mol kg^{-1} BHT over three different temperatures.

[SDS]	**100% v/v MeOH**			**70% v/v MeOH**			**30% v/v MeOH**		
mmol kg^{-1}	**25 °C**	**30 °C**	**35 °C**	**25 °C**	**30 °C**	**35 °C**	**25 °C**	**30 °C**	**35 °C**
2.0	24.3	24.9	25.7	8.6	9.1	9.5	7.5	7.8	8.1
4.0	13.2	13.7	14.9	6.4	7.1	7.3	6.1	6.2	6.3
6.0	10.2	10.6	11.4	4.6	6.4	6.5	5.4	5.5	5.7
8.0	6.5	6.6	6.9	4.3	5.3	5.4	4.3	4.6	4.7
10.0	6.2	6.1	6.8	3.6	4.7	4.8	3.9	4.1	4.5
12.0	5.8	6.0	6.7	3.5	4.5	4.6	3.7	4.0	4.4
14.0	5.7	5.9	6.5	3.4	4.6	4.5	3.6	3.9	4.3
	100% v/v EtOH			**70% v/v EtOH**			**30% v/v EtOH**		
2.0	31.1	31.2	30.5	8.7	9.2	9.8	8.5	9.2	9.6
4.0	16.8	16.8	16.1	6.7	7.8	6.8	7.0	7.5	7.6
6.0	12.5	12.6	11.8	5.1	5.1	5.1	5.6	6.2	6.9
8.0	8.8	8.3	7.4	4.5	4.4	4.7	4.8	4.8	5.4
10.0	6.5	6.5	6.7	5.0	4.7	5.0	4.8	5.0	5.2
12.0	6.6	6.1	6.6	4.8	4.8	4.8	5.0	5.1	5.3
14.0	6.9	7.0	7.3	4.8	4.9	5.1	4.9	5.0	5.3
	100% v/v 1–PrOH			**70% v/v 1–PrOH**			**30% v/v 1–PrOH**		
2.0	20.4	23.6	24.8	9.2	9.9	10.7	8.3	8.5	8.8
4.0	12.6	13.1	14.5	8.4	8.5	9.6	7.4	7.6	7.8
6.0	11.3	12.5	12.9	7.1	7.2	7.8	6.5	6.6	6.7
8.0	10.2	11.8	12.5	6.5	6.6	6.9	5.4	5.5	5.8
10.0	9.7	11.7	12.1	5.6	5.7	5.9	5.2	5.4	5.6
12.0	9.6	10.6	11.6	5.4	5.5	5.7	5.1	5.3	5.5
14.0	9.4	10.2	11.1	5.3	5.4	5.6	4.8	5.1	5.3

Table 4.15: Apparent molar volume (ϕ_v) (m^3 mol^{-1}) $\times 10^4$ of CTAB (0.2–1.8) mmol kg^{-1} in various compositions of MeOH, EtOH and 1–PrOH containing BHA (0.03 mol kg^{-1}) over different temperatures.

[CTAB]	100% v/v MeOH			70% v/v MeOH			30% v/v MeOH		
mmol kg^{-1}	25 °C	30 °C	35 °C	25 °C	30 °C	35 °C	25 °C	30 °C	35 °C
0.2	5.19	5.31	5.52	4.68	4.72	4.73	4.45	4.47	4.50
0.4	4.90	4.96	5.14	4.49	4.52	4.54	4.23	4.26	4.31
0.6	4.81	4.82	4.99	4.38	4.44	4.48	4.16	4.20	4.25
0.8	4.65	4.69	4.78	4.28	4.34	4.38	4.08	4.12	4.17
1.0	4.60	4.64	4.73	4.26	4.31	4.36	4.05	4.10	4.15
1.2	4.59	4.60	4.70	4.24	4.30	4.34	4.04	4.08	4.13
1.4	4.57	4.58	4.68	4.23	4.29	4.33	4.02	4.07	4.12
1.6	4.55	4.57	4.66	4.22	4.28	4.32	4.02	4.06	4.12
1.8	4.54	4.56	4.65	4.22	4.27	4.32	4.01	4.06	4.11
	100% v/v EtOH			70% v/v EtOH			30% v/v EtOH		
0.2	5.31	5.33	5.44	4.62	4.62	4.64	4.27	4.28	4.32
0.4	4.94	4.92	4.99	4.42	4.44	4.47	4.15	4.17	4.20
0.6	4.74	4.76	4.83	4.31	4.35	4.39	4.08	4.10	4.14
0.8	4.62	4.65	4.72	4.24	4.29	4.33	4.01	4.04	4.08
1.0	4.59	4.61	4.68	4.22	4.27	4.31	3.99	4.03	4.07
1.2	4.56	4.58	4.65	4.21	4.25	4.30	3.98	4.02	4.06
1.4	4.54	4.56	4.63	4.19	4.24	4.29	3.97	4.01	4.05
1.6	4.53	4.55	4.62	4.19	4.23	4.28	3.97	4.01	4.05
1.8	4.52	4.54	4.61	4.18	4.23	4.28	3.96	4.00	4.04
	100% v/v 1–PrOH			70% v/v 1–PrOH			30% v/v 1–PrOH		
0.2	5.90	5.96	5.98	4.66	4.67	4.68	4.54	4.57	4.68
0.4	5.13	5.17	5.20	4.38	4.41	4.43	4.25	4.28	4.35
0.6	4.89	4.90	4.96	4.28	4.31	4.34	4.15	4.19	4.25
0.8	4.66	4.71	4.75	4.23	4.26	4.30	4.08	4.14	4.19
1.0	4.58	4.62	4.67	4.21	4.23	4.27	4.05	4.11	4.16
1.2	4.53	4.57	4.61	4.19	4.21	4.26	4.03	4.09	4.14
1.4	4.50	4.53	4.57	4.18	4.20	4.25	4.02	4.08	4.12
1.6	4.47	4.50	4.54	4.17	4.19	4.24	4.01	4.07	4.11
1.8	4.45	4.48	4.52	4.16	4.18	4.23	4.00	4.06	4.10

The experimental uncertainties calculate for $\phi_v = \pm 0.18 \times 10^4$ m^3 mol^{-1}.

Table 4.16: Apparent molar volume (ϕ_v) (m^3 mol^{-1}) $\times 10^4$ of CTAB (0.2–1.8) mmol kg^{-1} in various compositions of MeOH, EtOH and 1–PrOH containing BHT (0.02 mol kg^{-1}) over different temperatures.

[CTAB]	100% v/v MeOH			70% v/v MeOH			30% v/v MeOH		
mmol kg^{-1}	25 °C	30 °C	35 °C	25 °C	30 °C	35 °C	25 °C	30 °C	35 °C
0.2	5.20	5.36	5.71	4.84	4.85	5.06	4.66	4.79	4.82
0.4	4.88	4.93	5.15	4.51	4.54	4.65	4.39	4.41	4.43
0.6	4.78	4.80	4.96	4.40	4.42	4.51	4.24	4.27	4.30
0.8	4.68	4.71	4.85	4.32	4.36	4.45	4.15	4.20	4.24
1.0	4.59	4.66	4.78	4.27	4.33	4.40	4.11	4.16	4.20
1.2	4.56	4.63	4.74	4.25	4.30	4.37	4.08	4.13	4.17
1.4	4.54	4.61	4.71	4.23	4.28	4.35	4.06	4.11	4.16
1.6	4.53	4.59	4.68	4.21	4.27	4.34	4.04	4.09	4.14
1.8	4.51	4.57	4.67	4.20	4.26	4.32	4.03	4.08	4.13
	100% v/v EtOH			70% v/v EtOH			30% v/v EtOH		
0.2	5.50	5.57	5.62	4.86	4.91	4.88	4.52	4.55	4.63
0.4	5.00	5.07	5.08	4.53	4.55	4.56	4.22	4.26	4.33
0.6	4.81	4.90	4.90	4.39	4.43	4.45	4.12	4.17	4.23
0.8	4.70	4.76	4.80	4.28	4.36	4.38	4.04	4.11	4.17
1.0	4.64	4.69	4.74	4.24	4.32	4.34	4.01	4.07	4.13
1.2	4.60	4.65	4.70	4.21	4.29	4.31	3.99	4.05	4.11
1.4	4.57	4.62	4.67	4.20	4.27	4.30	3.98	4.03	4.09
1.6	4.55	4.60	4.64	4.18	4.25	4.28	3.96	4.02	4.08
1.8	4.53	4.58	4.63	4.17	4.24	4.27	3.95	4.01	4.06
	100% v/v 1–PrOH			70% v/v 1–PrOH			30% v/v 1–PrOH		
0.2	6.51	6.55	6.67	5.44	5.53	5.70	5.29	5.30	5.36
0.4	5.39	5.44	5.53	4.73	4.80	4.91	4.62	4.65	4.71
0.6	5.04	5.07	5.15	4.49	4.56	4.65	4.36	4.41	4.49
0.8	4.77	4.81	4.89	4.37	4.44	4.53	4.20	4.25	4.35
1.0	4.66	4.70	4.77	4.30	4.37	4.45	4.13	4.18	4.28
1.2	4.58	4.63	4.70	4.25	4.32	4.40	4.08	4.14	4.23
1.4	4.53	4.57	4.64	4.21	4.29	4.37	4.04	4.11	4.20
1.6	4.49	4.53	4.60	4.19	4.26	4.34	4.02	4.08	4.17
1.8	4.45	4.50	4.57	4.17	4.24	4.32	4.00	4.06	4.15

The experimental uncertainties calculate for $\phi_v = \pm 0.17 \times 10^4$ m^3 mol^{-1}.

Table 4.17: Apparent molar volume (ϕ_v) (m^3mol^{-1}) × 10^4 of TX100 (0.05–0.45 mmol kg^{-1}) in various compositions of MeOH, EtOH and 1–PrOH containing 0.03 mol kg^{-1} BHA over three different temperatures.

[TX100]	100% v/v MeOH			70% v/v MeOH			30% v/v MeOH		
mmol kg^{-1}	25 °C	30 °C	35 °C	25 °C	30 °C	35 °C	25 °C	30 °C	35 °C
0.05	8.40	8.45	8.61	8.07	8.10	8.12	7.56	7.61	7.68
0.10	8.06	8.09	8.14	7.66	7.71	7.75	7.33	7.35	7.36
0.15	7.88	7.96	8.01	7.45	7.59	7.59	7.18	7.20	7.24
0.20	7.88	7.93	7.95	7.45	7.57	7.59	7.16	7.19	7.22
0.25	7.89	7.92	7.96	7.46	7.57	7.59	7.15	7.18	7.22
0.30	7.92	7.97	7.97	7.46	7.56	7.58	7.14	7.18	7.22
0.35	7.93	7.97	7.97	7.46	7.56	7.58	7.14	7.17	7.21
0.40	7.93	7.97	7.97	7.46	7.56	7.58	7.13	7.17	7.21
0.45	7.93	7.97	7.97	7.46	7.55	7.58	7.13	7.17	7.21
	100% v/v EtOH			70% v/v EtOH			30% v/v EtOH		
0.05	9.45	9.49	9.52	8.83	9.50	9.88	8.24	8.26	8.23
0.10	8.60	8.66	8.75	8.06	8.41	8.63	7.71	7.69	7.68
0.15	8.31	8.36	8.43	7.78	8.05	8.20	7.44	7.48	7.50
0.20	8.15	8.16	8.29	7.58	7.82	7.95	7.29	7.37	7.39
0.25	8.12	8.13	8.25	7.47	7.71	7.80	7.21	7.25	7.31
0.30	8.09	8.11	8.22	7.44	7.65	7.74	7.19	7.22	7.29
0.35	8.07	8.09	8.20	7.42	7.61	7.69	7.17	7.21	7.28
0.40	8.06	8.08	8.19	7.41	7.58	7.66	7.15	7.19	7.26
0.45	8.05	8.07	8.18	7.40	7.56	7.63	7.14	7.18	7.25
	100% v/v 1–PrOH			70% v/v 1–PrOH			30% v/v 1–PrOH		
0.05	9.81	9.94	10.05	9.37	9.29	9.41	8.14	8.24	8.38
0.10	8.70	8.79	8.91	8.19	8.23	8.32	7.46	7.52	7.63
0.15	8.41	8.49	8.60	7.89	7.94	8.03	7.28	7.36	7.44
0.20	8.26	8.35	8.46	7.73	7.80	7.89	7.19	7.27	7.34
0.25	8.17	8.26	8.38	7.64	7.71	7.80	7.14	7.21	7.29
0.30	8.11	8.20	8.32	7.58	7.65	7.75	7.11	7.18	7.25
0.35	8.07	8.15	8.27	7.53	7.61	7.70	7.08	7.15	7.22
0.40	8.04	8.12	8.24	7.50	7.58	7.67	7.07	7.13	7.20
0.45	8.01	8.10	8.22	7.47	7.56	7.65	7.05	7.11	7.18

Table 4.18: Apparent molar volume (ϕ_v) (m^3mol^{-1}) × 10^4 of TX100 (0.05–0.45 mmol kg^{-1}) in various compositions of MeOH, EtOH and 1–PrOH containing 0.02 mol kg^{-1} BHT over three different temperatures.

[TX100] mmol kg^{-1}	100% v/v MeOH			70% v/v MeOH			30% v/v MeOH		
	25 °C	30 °C	35 °C	25 °C	30 °C	35 °C	25 °C	30 °C	35 °C
0.05	8.23	8.30	8.32	7.74	7.74	7.78	7.26	7.29	7.31
0.10	7.84	7.92	7.99	7.49	7.51	7.54	7.15	7.15	7.17
0.15	7.74	7.80	7.83	7.39	7.43	7.47	7.09	7.11	7.14
0.20	7.73	7.78	7.84	7.37	7.41	7.43	7.09	7.12	7.15
0.25	7.76	7.81	7.86	7.36	7.40	7.43	7.09	7.12	7.16
0.30	7.78	7.82	7.87	7.35	7.40	7.42	7.09	7.12	7.16
0.35	7.79	7.84	7.89	7.35	7.39	7.42	7.09	7.12	7.16
0.40	7.80	7.85	7.90	7.34	7.39	7.42	7.09	7.12	7.16
0.45	7.80	7.87	7.91	7.34	7.39	7.42	7.09	7.12	7.16
	100% v/v EtOH			70% v/v EtOH			30% v/v EtOH		
0.05	10.83	11.08	11.47	7.58	7.66	7.74	7.56	7.57	7.59
0.10	9.22	9.40	9.96	7.37	7.40	7.44	7.25	7.28	7.32
0.15	8.35	8.55	8.76	7.22	7.28	7.32	7.11	7.14	7.16
0.20	7.85	8.23	8.45	7.13	7.18	7.23	6.99	7.04	7.11
0.25	7.95	8.20	8.39	7.13	7.20	7.25	6.99	7.04	7.09
0.30	8.02	8.17	8.34	7.16	7.20	7.26	6.99	7.04	7.09
0.35	8.10	8.17	8.39	7.18	7.21	7.26	6.99	7.04	7.08
0.40	8.07	8.15	8.35	7.19	7.22	7.27	6.99	7.03	7.08
0.45	8.06	8.13	8.32	7.19	7.22	7.27	6.99	7.03	7.08
	100% v/v 1–PrOH			70% v/v 1–PrOH			30% v/v 1–PrOH		
0.05	8.66	8.64	8.78	8.18	8.54	8.89	7.74	7.99	8.02
0.10	8.05	8.07	8.14	7.57	7.80	8.06	7.22	7.35	7.37
0.15	7.77	7.84	8.01	7.45	7.58	7.78	7.05	7.14	7.18
0.20	7.75	7.82	7.95	7.41	7.50	7.67	6.99	7.07	7.12
0.25	7.72	7.80	7.95	7.37	7.45	7.61	6.96	7.03	7.08
0.30	7.72	7.79	7.94	7.35	7.42	7.57	6.94	7.01	7.06
0.35	7.72	7.78	7.91	7.33	7.40	7.54	6.93	6.99	7.04
0.40	7.71	7.78	7.91	7.31	7.38	7.52	6.92	6.97	7.03
0.45	7.70	7.77	7.91	7.30	7.37	7.50	6.91	6.96	7.02

Table 4.19: Apparent molar adiabatic compression (ϕ_k) ($m^3mol^{-1}TPa^{-1}$) × 10^2 of SDS (2.0–14.0 mmol kg^{-1}) in various compositions of MeOH, EtOH and 1–PrOH containing 0.03 mol kg^{-1} BHA over three different temperatures.

[SDS]	100% v/v MeOH			70% v/v MeOH			30% v/v MeOH		
mmol kg^{-1}	25 °C	30 °C	35 °C	25 °C	30 °C	35 °C	25 °C	30 °C	35 °C
2.0	286.3	318.5	343.4	68.80	93.26	97.28	38.07	48.57	63.98
4.0	140.2	156.2	166.1	25.39	29.01	33.46	16.47	21.01	22.21
6.0	110.8	122.5	132.3	27.41	32.89	35.87	15.13	17.55	18.95
8.0	91.52	101.4	104.1	25.56	31.36	36.26	18.05	19.53	21.47
10.0	90.97	94.86	100.5	30.45	34.29	35.18	18.65	19.11	21.53
12.0	87.97	91.34	96.29	28.78	33.53	35.33	18.47	18.84	21.51
14.0	80.86	84.19	88.71	29.57	32.92	34.63	18.69	19.08	20.75
	100% v/v EtOH			70% v/v EtOH			30% v/v EtOH		
2.0	773.0	910.2	1027.0	129.0	124.7	125.9	64.46	56.49	53.84
4.0	414.8	480.5	561.7	83.63	86.91	90.35	26.33	22.72	22.53
6.0	293.5	338.6	392.6	74.96	77.83	80.88	15.04	15.32	15.60
8.0	236.7	265.7	308.0	68.75	71.36	74.14	14.67	14.90	14.69
10.0	198.6	222.3	256.9	65.28	67.78	70.39	11.79	13.69	12.38
12.0	173.8	193.0	223.8	62.20	63.86	68.18	13.03	13.97	11.39
14.0	156.3	172.4	199.4	56.92	59.20	61.34	14.13	13.71	12.00
	100% v/v 1–PrOH			70% v/v 1–PrOH			30% v/v 1–PrOH		
2.0	129.5	235.3	334.2	68.25	82.45	100.25	34.67	41.27	47.05
4.0	73.1	120.1	175.5	52.55	58.67	67.71	23.31	27.10	30.04
6.0	69.8	98.3	133.8	37.49	43.68	47.72	18.06	20.83	22.54
8.0	60.7	84.4	110.9	33.56	37.47	41.11	16.50	18.94	20.68
10.0	58.8	74.8	96.4	32.20	36.45	38.35	16.92	18.20	19.45
12.0	63.1	68.4	87.7	30.58	34.46	36.48	16.50	17.52	18.68
14.0	58.7	64.0	82.1	29.40	32.74	34.58	16.13	17.13	18.16

Table 4.20: Apparent molar adiabatic compression (ϕ_k) ($m^3mol^{-1}TPa^{-1}$) × 10^2 of SDS (2.0–14.0 mmol kg^{-1}) in various compositions of MeOH, EtOH and 1–PrOH containing 0.02 mol kg^{-1} BHT over three different temperatures.

[SDS]	100% v/v MeOH			70% v/v MeOH			30% v/v MeOH		
mmol kg^{-1}	25 °C	30 °C	35 °C	25 °C	30 °C	35 °C	25 °C	30 °C	35 °C
2.0	121.4	137.5	146.7	54.5	56.7	59.4	32.5	35.6	37.5
4.0	97.3	102.7	109.4	39.3	43.3	48.5	14.3	16.2	18.4
6.0	88.5	92.5	98.3	35.6	38.4	43.5	13.2	15.4	16.8
8.0	75.4	86.3	91.2	32.2	34.2	42.1	12.1	15.1	16.1
10.0	66.5	72.4	83.4	31.4	33.7	40.2	11.6	14.8	15.4
12.0	61.2	69.5	78.4	30.7	32.2	39.4	11.2	13.2	14.6
14.0	60.3	68.2	77.3	29.3	31.8	38.2	10.9	12.7	13.8
	100% v/v EtOH			70% v/v EtOH			30% v/v EtOH		
2.0	299.1	311.1	315.1	52.17	56.62	61.19	33.68	37.03	39.12
4.0	161.3	167.9	165.8	40.13	41.48	41.96	27.95	30.31	32.12
6.0	119.7	124.9	121.8	30.48	31.17	31.37	22.32	25.02	28.11
8.0	84.89	82.22	76.87	27.17	26.88	29.11	19.02	19.34	21.97
10.0	62.31	64.22	69.54	30.16	29.17	31.19	19.45	20.48	21.37
12.0	62.79	59.88	67.52	29.12	29.46	29.65	19.93	20.95	21.85
14.0	66.33	69.08	75.43	29.15	30.80	32.10	19.39	20.33	21.81
	100% v/v 1–PrOH			70% v/v 1–PrOH			30% v/v 1–PrOH		
2.0	111.2	119.3	124.5	50.2	53.1	55.4	27.4	29.4	32.5
4.0	88.5	93.5	97.4	28.3	29.6	31.5	12.4	14.2	15.1
6.0	76.5	88.1	91.3	23.8	26.4	27.6	11.7	13.6	14.4
8.0	72.3	83.4	85.6	22.1	25.6	26.3	11.2	12.9	13.9
10.0	69.7	76.6	79.4	21.2	25.1	25.9	10.6	12.3	13.2
12.0	68.4	72.2	75.4	20.6	24.7	25.1	10.1	11.6	12.5
14.0	67.2	69.4	71.2	19.4	24.0	24.6	9.8	11.1	12.1

Table 4.21: Apparent molar adiabatic compression (ϕ_k) (m^3 $mol^{-1}TPa^{-1}$) × 10^2 of CTAB (0.2–1.8) mmol kg^{-1} in various compositions of MeOH, EtOH and 1–PrOH containing BHA (0.03 mol kg^{-1}) over different temperatures.

[CTAB] mmol kg^{-1}	100% v/v MeOH			70% v/v MeOH			30% v/v MeOH		
	25 °C	30 °C	35 °C	25 °C	30 °C	35 °C	25 °C	30 °C	35 °C
0.2	51.47	54.24	58.73	34.01	35.49	36.84	22.18	22.89	23.85
0.4	48.74	50.71	54.75	32.76	34.04	35.40	21.11	21.83	22.85
0.6	47.88	49.32	53.28	31.93	33.42	34.89	20.76	21.53	22.56
0.8	46.14	47.88	50.74	31.14	32.58	34.04	20.31	21.08	22.06
1.0	45.60	47.31	50.25	30.96	32.39	33.87	20.19	20.95	21.95
1.2	45.49	46.91	49.93	30.84	32.27	33.75	20.11	20.87	21.88
1.4	45.29	46.71	49.68	30.75	32.18	33.66	20.05	20.82	21.82
1.6	45.14	46.56	49.51	30.68	32.12	33.60	20.01	20.77	21.78
1.8	45.04	46.45	49.37	30.63	32.07	33.56	19.98	20.74	21.74
	100% v/v EtOH			70% v/v EtOH			30% v/v EtOH		
0.2	50.85	52.98	57.41	32.97	34.24	35.74	20.85	21.48	22.38
0.4	47.39	48.95	52.56	31.59	32.92	34.44	20.28	20.93	21.77
0.6	45.41	47.27	50.92	30.82	32.24	33.84	19.94	20.62	21.44
0.8	44.21	46.13	49.58	30.30	31.72	33.27	19.55	20.27	21.13
1.0	43.86	45.71	49.15	30.12	31.55	33.13	19.46	20.19	21.05
1.2	43.57	45.42	48.86	30.01	31.44	33.05	19.4	20.14	20.99
1.4	43.38	45.22	48.65	29.93	31.36	32.97	19.36	20.10	20.95
1.6	43.25	45.08	48.49	29.87	31.30	32.92	19.34	20.07	20.92
1.8	43.11	44.97	48.36	29.82	31.25	32.88	19.31	20.05	20.90
	100% v/v 1–PrOH			70% v/v 1–PrOH			30% v/v 1–PrOH		
0.2	48.78	50.10	52.60	29.64	30.63	31.45	20.92	21.87	22.87
0.4	42.50	43.53	45.75	27.87	28.88	29.74	19.60	20.48	21.29
0.6	40.55	41.30	43.67	27.23	28.26	29.16	19.15	20.06	20.76
0.8	38.46	39.53	41.71	26.92	27.86	28.88	18.81	19.82	20.49
1.0	37.81	38.84	40.99	26.80	27.69	28.69	18.67	19.68	20.33
1.2	37.38	38.37	40.51	26.66	27.57	28.58	18.57	19.59	20.23
1.4	37.10	38.03	40.16	26.57	27.49	28.50	18.51	19.52	20.15
1.6	36.88	37.79	39.90	26.50	27.43	28.44	18.46	19.49	20.09
1.8	36.70	37.60	39.71	26.45	27.39	28.39	18.42	19.45	20.05

The experimental uncertainties values calculate for $K_{\phi,S}$ = 0.05 × 10^2 m^3 mol^{-1} TPa^{-1}.

Table 4.22: Apparent molar adiabatic compression (ϕ_k) ($m^3\ mol^{-1}TPa^{-1}$) × 10^2 of CTAB (0.2–1.8) mmol kg^{-1} in various compositions of MeOH, EtOH and 1–PrOH containing BHT (0.02 mol kg^{-1}) over different temperatures.

[CTAB] mmol kg^{-1}	100% v/v Methanol			70% v/v Methanol			30% v/v Methanol		
	25 °C	30 °C	35 °C	25 °C	30 °C	35 °C	25 °C	30 °C	35 °C
0.2	48.82	52.39	58.70	34.65	35.60	38.00	22.63	23.96	24.87
0.4	45.91	48.20	52.93	32.35	33.37	34.93	21.39	22.07	22.86
0.6	45.06	46.93	51.04	31.56	32.53	33.90	20.66	21.38	22.18
0.8	44.14	46.09	49.88	30.99	32.09	33.44	20.24	21.02	21.88
1.0	43.14	45.58	49.20	30.67	31.81	33.11	20.02	20.80	21.67
1.2	42.87	45.25	48.74	30.47	31.63	32.88	19.87	20.65	21.54
1.4	42.67	45.01	48.41	30.31	31.49	32.70	19.78	20.55	21.43
1.6	42.54	44.83	48.14	30.18	31.39	32.58	19.70	20.47	21.36
1.8	42.41	44.68	47.94	30.10	31.30	32.49	19.64	20.41	21.30
	100% v/v Ethanol			70% v/v Ethanol			30% v/v Ethanol		
0.2	50.80	52.50	54.68	33.41	34.99	36.35	21.14	21.75	23.04
0.4	46.24	47.87	49.51	31.20	32.44	33.98	19.71	20.41	21.55
0.6	44.46	46.30	47.82	30.19	31.61	33.14	19.28	19.95	21.06
0.8	43.48	44.93	46.81	29.35	31.10	32.65	18.88	19.66	20.75
1.0	42.88	44.30	46.18	29.09	30.77	32.33	18.73	19.49	20.55
1.2	42.47	43.88	45.76	28.90	30.56	32.13	18.63	19.37	20.43
1.4	42.19	43.58	45.46	28.78	30.40	31.98	18.55	19.29	20.34
1.6	41.98	43.34	45.24	28.68	30.29	31.86	18.50	19.23	20.27
1.8	41.81	43.17	45.07	28.60	30.20	31.78	18.45	19.18	20.22
	100% v/v 1–propanol			70% v/v 1–propanol			30% v/v 1–propanol		
0.2	51.20	53.26	57.22	32.67	34.64	37.01	23.29	24.34	25.35
0.4	42.41	44.27	47.46	28.40	30.11	31.85	20.38	21.36	22.29
0.6	39.70	41.26	44.26	26.98	28.60	30.20	19.27	20.29	21.28
0.8	37.50	39.09	41.91	26.26	27.84	29.38	18.48	19.51	20.60
1.0	36.59	38.16	40.89	25.82	27.38	28.89	18.17	19.19	20.24
1.2	35.98	37.53	40.22	25.52	27.07	28.56	17.95	18.98	20.01
1.4	35.54	37.09	39.74	25.31	26.85	28.33	17.80	18.83	19.85
1.6	35.22	36.76	39.37	25.15	26.69	28.15	17.68	18.72	19.73
1.8	34.96	36.50	39.10	25.03	26.56	28.01	17.59	18.63	19.64

The experimental uncertainties values calculate for $\phi_k = 0.04 \times 10^2\ m^3\ mol^{-1}\ TPa^{-1}$.

Table 4.23: Apparent molar adiabatic compression (ϕ_k) ($m^3mol^{-1}TPa^{-1}$) × 10^2 of TX100 (0.05–0.45 mmol kg^{-1}) in various compositions of MeOH, EtOH and 1–PrOH containing 0.03 mol kg^{-1} BHA over three different temperatures.

[TX100]	100% v/v MeOH			70% v/v MeOH			30% v/v MeOH		
mmol kg^{-1}	25 °C	30 °C	35 °C	25 °C	30 °C	35 °C	25 °C	30 °C	35 °C
0.05	84.94	87.83	93.93	58.32	59.70	60.93	35.52	36.65	37.64
0.10	81.35	84.22	88.40	55.09	56.80	58.13	34.45	35.39	36.08
0.15	79.43	82.56	86.87	53.39	55.75	56.84	33.68	34.59	35.45
0.20	79.41	82.07	86.10	53.42	55.65	56.80	33.58	34.54	35.35
0.25	79.56	81.77	86.13	53.44	55.59	56.78	33.53	34.50	35.32
0.30	79.72	82.18	86.14	53.42	55.54	56.75	33.48	34.46	35.30
0.35	79.73	82.16	86.15	53.45	55.49	56.71	33.47	34.43	35.27
0.40	79.65	82.09	86.19	53.47	55.46	56.69	33.45	34.41	35.25
0.45	79.63	82.09	86.21	53.46	55.44	56.68	33.43	34.40	35.24
	100% v/v EtOH			70% v/v EtOH			30% v/v EtOH		
0.05	92.90	94.82	98.77	69.67	77.52	84.94	43.56	44.99	45.78
0.10	84.46	86.43	90.71	63.55	68.62	74.15	40.75	41.89	42.73
0.15	81.51	83.41	87.25	61.32	65.61	70.43	39.31	40.71	41.71
0.20	79.84	81.28	85.71	59.61	63.70	68.18	38.47	40.11	41.08
0.25	79.51	80.89	85.27	58.76	62.74	66.90	38.03	39.37	40.62
0.30	79.25	80.65	84.96	58.49	62.27	66.33	37.88	39.23	40.49
0.35	79.06	80.47	84.76	58.32	61.91	65.92	37.77	39.12	40.40
0.40	78.92	80.33	84.62	58.21	61.64	65.60	37.69	39.05	40.32
0.45	78.81	80.24	84.46	58.12	61.45	65.36	37.64	38.98	40.27
	100% v/v 1–PrOH			70% v/v 1–PrOH			30% v/v 1–PrOH		
0.05	83.30	89.14	98.48	54.53	57.07	60.75	36.40	38.27	40.13
0.10	73.83	78.80	87.16	47.62	50.53	53.63	33.31	34.89	36.51
0.15	71.30	76.07	84.20	45.85	48.74	51.79	32.52	34.13	35.58
0.20	70.02	74.79	82.79	44.95	47.87	50.86	32.12	33.69	35.11
0.25	69.25	73.93	81.94	44.40	47.32	50.26	31.89	33.43	34.83
0.30	68.75	73.38	81.32	44.03	46.93	49.88	31.73	33.25	34.64
0.35	68.38	72.97	80.88	43.77	46.67	49.60	31.61	33.11	34.49
0.40	68.09	72.66	80.52	43.58	46.48	49.40	31.53	33.02	34.40
0.45	67.86	72.43	80.27	43.42	46.33	49.25	31.47	32.93	34.32

Table 4.24: Apparent molar adiabatic compression (ϕ_k) ($m^3mol^{-1}TPa^{-1}$) × 10^2 of TX100 (0.05–0.45 mmol kg^{-1}) in various compositions of MeOH, EtOH and 1–PrOH containing 0.02 mol kg^{-1} BHT over three different temperatures.

[TX100]	100% v/v MeOH			70% v/v MeOH			30% v/v MeOH		
mmol kg^{-1}	25 °C	30 °C	35 °C	25 °C	30 °C	35 °C	25 °C	30 °C	35 °C
0.05	82.29	85.83	89.12	53.25	54.29	56.42	32.58	33.48	34.42
0.10	78.14	81.59	85.24	51.47	52.63	54.66	32.05	32.81	33.73
0.15	76.76	78.69	81.75	50.78	52.03	54.10	31.77	32.60	33.59
0.20	75.90	78.99	80.64	50.61	51.91	53.82	31.76	32.64	33.62
0.25	75.76	78.59	80.47	50.52	51.84	53.78	31.78	32.65	33.65
0.30	75.72	78.59	80.45	50.45	51.80	53.76	31.78	32.65	33.66
0.35	75.82	78.64	80.42	50.38	51.78	53.74	31.77	32.65	33.61
0.40	75.86	78.76	80.47	50.36	51.76	53.72	31.77	32.66	33.64
0.45	75.90	78.93	80.61	50.32	51.74	53.70	31.77	32.67	33.65
	100% v/v EtOH			70% v/v EtOH			30% v/v EtOH		
0.05	102.64	108.78	116.70	58.87	61.45	64.24	39.21	40.24	41.03
0.10	87.14	92.26	101.50	57.20	59.27	61.61	37.58	38.72	39.51
0.15	78.70	83.51	88.73	55.88	58.19	60.49	36.83	37.91	38.62
0.20	72.94	80.00	85.26	55.08	57.30	59.65	36.19	37.36	38.29
0.25	74.07	79.63	84.60	54.91	57.36	59.72	36.18	37.33	38.22
0.30	74.52	79.28	83.98	55.23	57.19	59.75	36.18	37.32	38.20
0.35	75.30	79.42	84.69	55.25	57.24	59.82	36.18	37.27	38.16
0.40	75.06	79.01	84.22	55.27	57.24	59.71	36.18	37.26	38.13
0.45	74.86	78.84	83.77	55.28	57.21	59.72	36.17	37.27	38.13
	100% v/v 1–PrOH			70% v/v 1–PrOH			30% v/v 1–PrOH		
0.05	69.89	74.19	82.77	46.63	51.26	56.90	33.81	36.01	37.27
0.10	64..81	69.24	76.57	43.11	46.72	51.58	31.50	33.09	34.22
0.15	62.46	67.15	75.31	42.40	45.42	49.72	30.76	32.17	33.29
0.20	62.34	67.00	74.77	42.22	44.94	49.04	30.51	31.84	33.00
0.25	62.09	66.83	74.83	41.98	44.64	48.64	30.37	31.66	32.84
0.30	62.09	66.72	74.65	41.82	44.45	48.36	30.26	31.52	32.72
0.35	62.02	66.64	74.37	41.71	44.28	48.17	30.18	31.44	32.64
0.40	61.90	66.55	74.34	41.62	44.18	48.04	30.14	31.37	32.58
0.45	61.84	66.52	74.32	41.56	44.10	47.92	30.09	31.32	32.53

4.4 Spectroscopic analysis

4.4.1 Fourier transform infrared spectroscopy (FTIR)

The FTIR spectrum is known to provide significant information about the existing functional groups which can be substantially influenced by the surrounding environment. Hence, FTIR study has been employed to investigate structural and physical information about the intermolecular interactions present in the system [40]. Interpretation of the structural changes has been carried out in terms of wave number shift and band width. With regard to SDS system, the effects of the hydrophobic alkyl chain and spacer chain lengths of the anionic surfactant were taken into account to explain the variation in the systems. Initially, the samples were lyophilized to avoid the peaks of alcohol molecules.

The spectrum of pure BHA showed intense band at ~ 3299 cm^{-1} (stretching) corresponding to –OH– group of BHA. The methylene anti symmetric and symmetric vibrations at ~ 2901 cm^{-1}, ~ 2927 cm^{-1} and ~ 2974 cm^{-1} (C–H stretching) for *t*–butyl group in BHA. The peak at ~ 1383 cm^{-1} is might be because of C–H deformation mode of methyl of *t*–butyl group. The spectrum of pure SDS showed peaks at ~ 1217 cm^{-1} and ~ 1086 cm^{-1}, corresponding to –S=O stretching vibrational modes of sulphonic acid group in SDS. The band at 1217 cm^{-1} and 1086 cm^{-1} due to –S=O stretching vibrations in SDS molecule, shifted to ~ 1219 cm^{-1} and ~ 1080 cm^{-1} in presence of BHA, moreover C–H vibrations were observed at ~ 2923 cm^{-1}. The decrease in the frequency of –CH– stretching band corresponds to more hydrophobic environment [41].

From the spectrum of BHT, prominent band at 3626 cm^{-1} correspond to phenolic –OH– group at position–1, in addition, the band at 3062 cm^{-1} (–CH– stretching) and 1246 cm^{-1} (–CH– bending) correspond to butyl substitution present at position–2 and position–6. The methylene anti – symmetric and symmetric vibrations have been clearly observed at 2957 cm^{-1}, 2851 cm^{-1}, and 2919 cm^{-1} for alkyl –CH– stretching and 1469 cm^{-1} for alkyl –CH– deformation, respectively. The band due to –S=O stretching vibrations in pure SDS shifted to 1213 cm^{-1} and 1080 cm^{-1} in presence of BHT, in addition, –CH– vibrations were observed at 2927 cm^{-1} and 2871 cm^{-1}. The shifting of the band is presented in Table 4.25 and spectra are given in *APPENDIX – B.*

Table 4.25: FTIR band shift obtained in SDS in absence and in the presence of 0.03 mol kg^{-1} BHA and 0.02 mol kg^{-1} BHT in various composite samples.

Codes	–CH– (Stretching)	C–H (bending)	(S=O)
S	2976, 2851	1469	1222
SAM	2922, 2871	1451	1211
STM	2924, 2873	1448	1211
SAE	2923, 2872	1452	1212
STE	2927, 2871	1449	1213
SAP	2921, 2873	1452	1210
STP	2922, 2872	1451	1211

S stands for SDS, A stands for BHA, T stands for BHT, M stands for MeOH, E stands for EtOH and P stands for 1–PrOH. All vibrations were recorded in cm^{-1}

On the other side, FTIR was obtained for cationic surfactant and in presence of BHA/BHT in different medium. The asymmetric –CH– vibrations were recorded at 2918.1 and 2849.4 cm^{-1} whereas, –CH– bending was recorded at 961.36 cm^{-1}. It was difficult to gain much information regarding the change in band because of presence of only –CH– group in CTAB molecules. The substantial shifting was observed in the presence of BHA and BHT. The shifting of the band is presented in Table 4.26 and spectra are given in *APPENDIX – B.*

Table 4.26: FTIR band shift obtained in CTAB in absence and in the presence of 0.03 mol kg^{-1} BHA and 0.02 mol kg^{-1} BHT in various composite samples.

Codes	–CH– (Stretching)	C–H (bending)
C	2918.1, 2849.4	961.36
CAM	2920.3, 2853.2	963.46
CTM	2921.1, 2852.19	963.62
CAE	2919.7, 2854.36	964.73
CTE	2919.63, 2853.62	964.30
CAP	2920.28, 2853.26	963.70
CTP	2919.65, 2854.36	963.98

C stands for CTAB, A stands for BHA, T stands for BHT, M stands for MeOH, E stands for EtOH and P stands for 1–PrOH. All vibrations were recorded in cm^{-1}

From the spectrum of *tert*–octylphenol ethoxylate i.e. TX100, the phenolic vibrations were recorded at 3431.19 cm^{-1}. The asymmetric ($–CH_2–$) stretching vibrations were interpreted at 2950.17 and 2874.14 cm^{-1}, respectively, but the vibrations were not easy to distinguish or correspond for TX100 hydrophobic and hydrophilic region. In addition, broad band at 1107.20 cm^{-1} (C –O– C) can be explained owing the C–O (ester bond) stretching vibration, whereas the broad band at 951.37 cm^{-1} is due to bending of C–H, moreover intense

band at 1456 cm^{-1} can also be attributed to alkyl –CH– deformation. The substantial shifting was observed in the presence of BHA and BHT within the provided system. The shifting of the band is presented in Table 4.27 and spectra are given in *APPENDIX – B*. The order of shifting suggests that the environment is tightly packed and existence of intermolecular interaction especially in hydrophilic region of TX100.

Table 4.27: FTIR band shift obtained in TX100 in absence and in the presence of 0.03 mol kg^{-1} BHA and 0.02 mol kg^{-1} BHT in various composite samples.

Codes	Asymmetric $–CH_2–$ (Stretching)	C–H (bending)	(C–O–C)	Phenolic (O–H)
X	2950.17, 2874.14	951.37	1107.20	3431.19
XAM	2957.13, 2879.22	956.13	1109.07	3436.12
XTM	2758.26, 2879.28	956.10	1111.31	3437.25
XAE	2957.13, 2879.22	956.13	1109.07	3436.12
XTE	2758.43, 2879.37	955.48	1110.19	3436.50
XAP	2957.15, 2879.35	956.46	1110.18	3436.40
XTP	2759.20, 2880.23	956.15	1111.30	3438.63

X stands for TX100, A stands for BHA, T stands for BHT, M stands for MeOH, E stands for EtOH and P stands for 1–PrOH. All vibrations were recorded in cm^{-1}

4.4.2 Proton nuclear magnetic resonance spectroscopy (^{1}H NMR)

Proton nuclear magnetic resonance (^{1}H NMR) is a useful technique to gain more understanding and observe the change of environment in micellization and to predict the locus of the molecules via chemical shift caused due to significant interactions [42]. There are various ways in which an additive can organize itself within the micellar structure. With regard to the possibilities, additive may reside at the micellar surface or can selectively interact with aliphatic chain of the surfactant most often known to be the interface part or can gets completely incorporated in the hydrophobic core up to certain depth depending on site and the type of existing interaction. So, to gain more insight and better perspective, the study was extended to ^{1}H–NMR spectroscopy. Due to the precision of the NMR spectrometer, a change of ~ 0.01 ppm or greater is considered a significant change. The chemical shift was observed in the presence of BHA and BHT revealing significant intermolecular interaction.

The intense resonances at ~ 3.83 ppm and ~ 1.57 ppm corresponding to α $–CH_2–$ and β $–CH_2–$ as shown in structure of SDS. However, moving toward hydrophobic region of SDS,

the resonance at ~ 1.29 ppm and ~ 0.87 ppm with integral of 18 protons and 3 protons correspond to bulkier chain $–(CH_2)_9–$ of SDS and methyl group, respectively (Fig. 4.31). This is due to less shielding of adjoining, thus the hydrophilic part absorbed at down field. The addition of BHA makes substantial changes in chemical shift of α $–CH_2–$ of SDS. The α $–CH_2–$ showed upfield movement with a shift of ~ 0.07 ppm. The β $–CH_2–$, $–(CH_2)_9–$ and $–CH_3–$ segments of SDS were found with no movements as shown in Table 4.28. The spectra have been provided In *APPENDIX – B (B1–B2).*

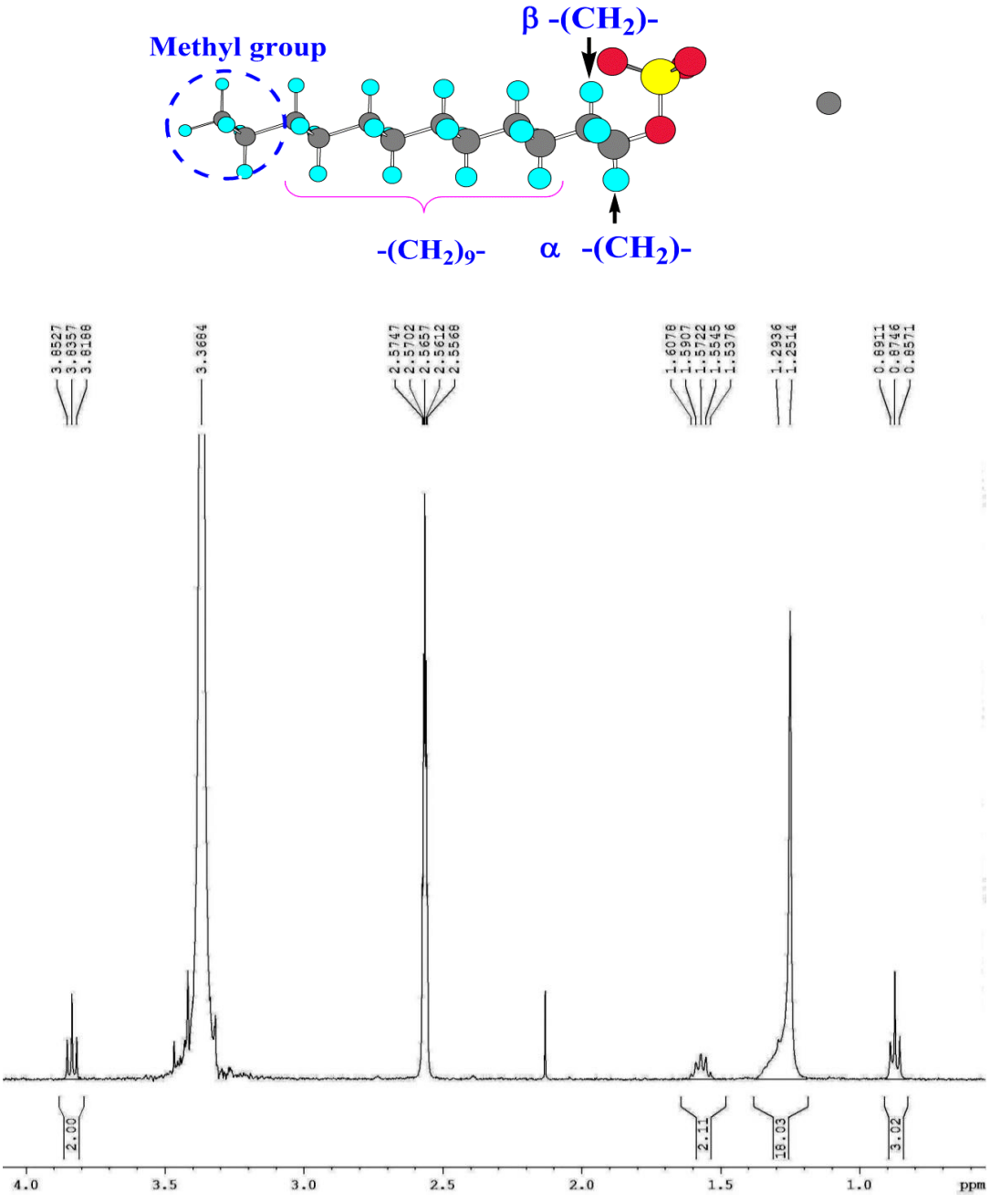

Fig. 4.31: The ^{1}H NMR spectrum of SDS molecule.

Table 4.28: Proton chemical shifts obtained in SDS in absence and presence of 0.03 mol kg^{-1} BHA and 0.02 mol kg^{-1} BHT in various composite samples.

	α –CH_2–	**β –CH_2–**	**–$(CH_2)_9$–**	**–CH_3–**
SAM	0.07	0.01	0.02	–
STM	0.03	0.02	0.01	–
SAE	0.07	0.01	0.02	–
STE	0.03	0.02	0.01	–
SAP	0.06	0.01	0.02	–
STP	0.02	0.02	0.01	–

(–) No proton movement was obtained, S stands for SDS, A stands for BHA, and T stands for BHT, M = MeOH, E = EtOH, P=1– PrOH

Figure 4.32 depicts the structural features and substitutions of cationic surfactant used in the present study i.e. CTAB as well as the ^{1}H NMR spectrum.

A close perusal of various proton signals of pure surfactant and the change in the position of these signals in presence of BHA and BHT in various composite solutions was determined. The intense peaks at ~ 0.85 ppm correspond to the aliphatic methyl group, while at ~ 3.26, ~ 1.65 and ~ 1.42 ppm correspond to α, β and γ –(CH_2)– respectively. The signal at ~ 3.04 ppm correspond to three methyl protons [N^+ $(CH_3)_3$] with integration of ~ 9 protons. The peak for hydrocarbon chain [–$(CH_2)_{12}$–] was obtained at ~ 1.24 ppm with integration ~ 24 protons. The spectrum in presence of BHA and BHT in various composite solutions has been provided in *APPENDIX – B (B3–B4)*.

The chemical shift was observed in the presence of BHA and BHT revealing significant intermolecular interaction. In particular, up field shift was observed in all the samples. This noticeable up field shift in protons has been shown in Table 4.29. The α and β –(CH_2)– were observed with up field shift of signals ~ 0.03 and ~ 0.02 ppm respectively, whereas [N^+ $(CH_3)_3$] and [–$(CH_2)_{12}$–] protons showed ~ 0.02 and 0.04 ppm up field shift. The merging of peaks especially, γ –(CH_2)– and [–$(CH_2)_{12}$–] was observed which is attributed to micelle growth [43]. Moreover, negligible shift of –(CH_3)– protons indicated that BHA and BHT had no intermolecular interaction within the hydrophobic region of the surfactant.

Therefore, at the studied BHA and BHT concentration within CTAB medium, it was observed that they interact with less hydrophobic region i.e. shell region and cooperating up to interface region.

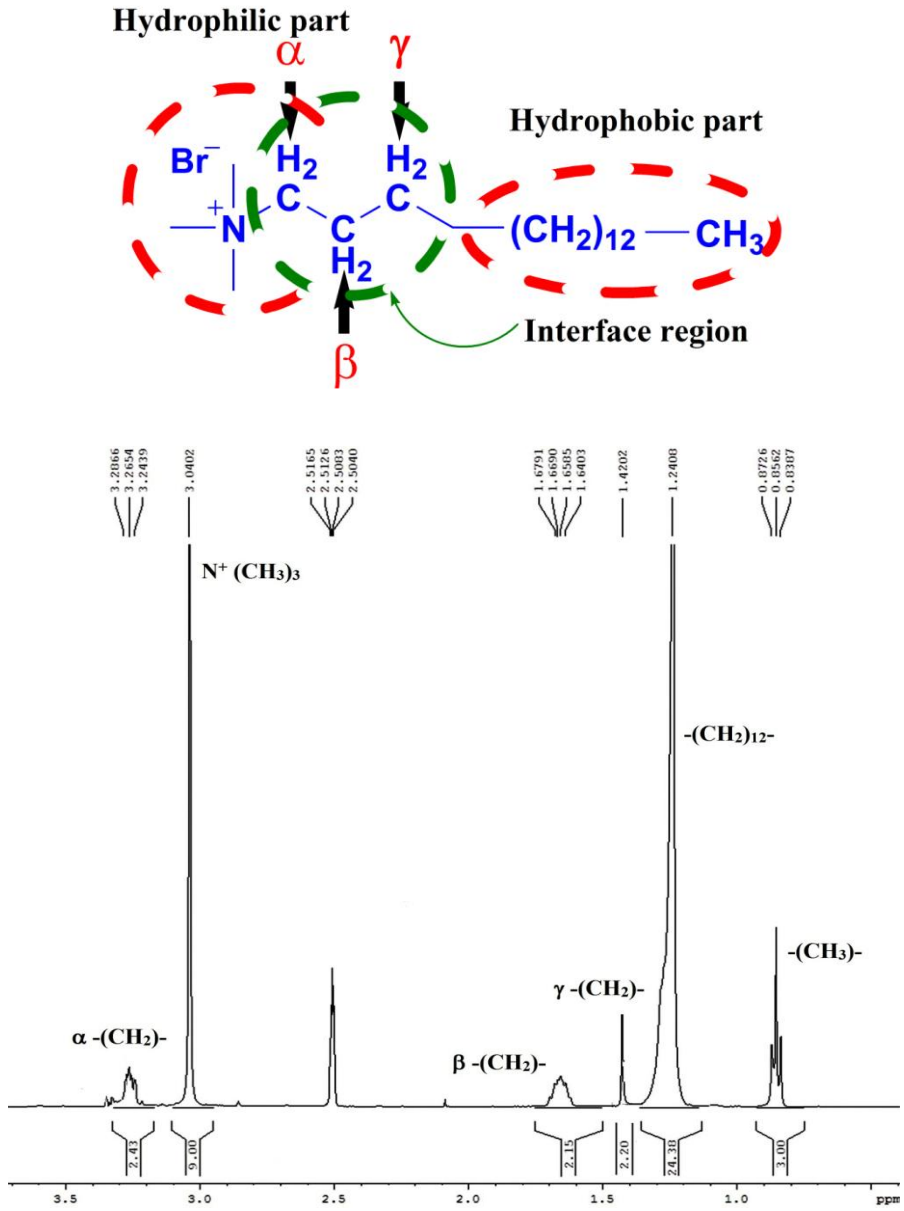

Fig. 4.32: The ^{1}H NMR spectrum of CTAB molecule.

Table 4.29: Proton chemical shifts obtained in CTAB in absence and presence of 0.03 mol kg^{-1} BHA and 0.02 mol kg^{-1} BHT in various composite samples.

	–CH_3–	**– $(CH_2)_{13}$–**	**N^+ –$(CH_3)_3$–**	**β –(CH_2) –**	**α –(CH_2) –**
CAM	–	0.02	0.04	0.02	0.03
CTM	–	0.03	0.03	0.02	0.03
CAE	–	0.02	0.04	0.02	0.03
CTE	–	0.02	0.04	0.02	0.03
CAP	–	0.02	0.04	0.02	0.03
CTP	–	0.03	0.04	0.02	0.03

(–) No proton movement was obtained, C stands for CTAB, A stands for BHA, and T stands for BHT. M = MeOH, E = EtOH, P=1– PrOH

Further, the protons of TX100 has been pictured and presented in the Figure 4.33. An intense resonance at ~ 0.66 pp and ~ 1.66 ppm corresponds to the terminal and internal methyl group protons (T_1 and T_3) of the alkyl chain of TX100 which forms hydrophobic core region of the micellar structure. The resonance at ~ 1.28 ppm (T_2) represents the aliphatic methylene group protons of the chain. However, moving toward the hydrophilic part (shell), long chain protons (T_4, T_5 and T_6) become less shielded and absorb at quite downfield i.e. ~ 3.54, 3.72 and 4.03 ppm. Protons of phenyl ring protons (T_7 and T_8) resonated at ~ 6.81 and 7.23 ppm respectively.

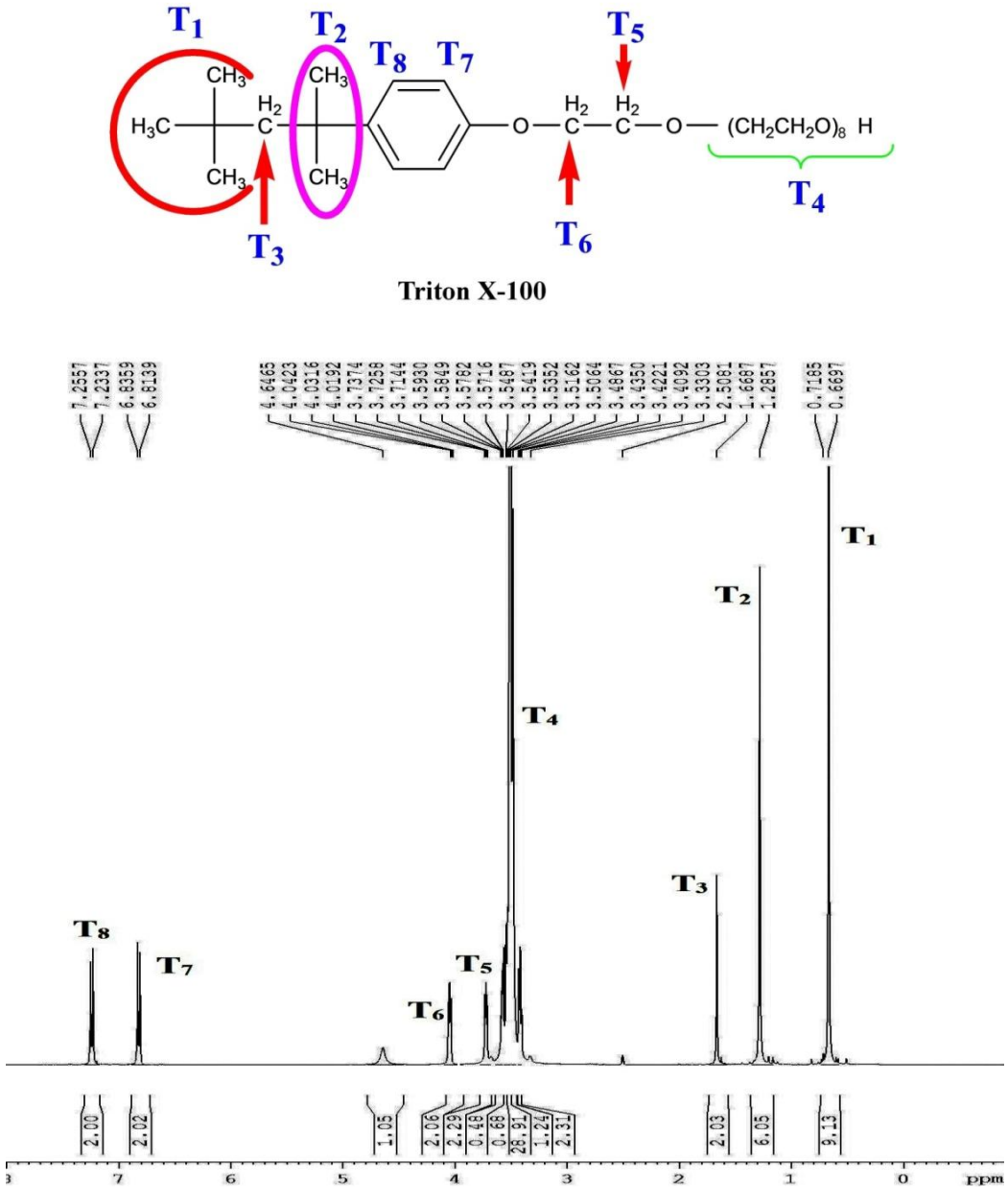

Fig. 4.33: The ^{1}H NMR spectrum of TX100 molecule.

The ^{1}H NMR spectrum in presence of BHA ad BHT has been presented in *APPENDIX – B (B5–B7)*. The chemical shift was observed in the presence of BHA and BHT revealing significant intermolecular interaction. In particular, up field movement was observed in all the samples. The T_4 and T_5 protons resonated with an up field movement of ~ 0.035 ppm and ~ 0.04 ppm, respectively. The T_6 and T_7 showed the movement with an average chemical shift of ~ 0.02 and ~ 0.01 ppm, whereas T_8 protons were resonated with higher up field movement as shown in Table 4.30. This noticeable up field movement in phenyl ring protons points out that BHA and BHT are located nearby outer surface and interface of the micellar structure. This might be because of hydrophobic attraction between nonpolar –CH_3– (*tert*– butyl group in BHA and BHT) and the micellar interface. The merging of peaks especially, T_4 and T_5 was observed which is attributed to micelle growth. Moreover, negligible movement of T_1, T_2 and T_3 protons also indicated that BHA and BHT do not penetrate into the micellar core.

Table 4.30: Proton chemical shifts obtained in TX100 in absence and presence of 0.03 mol kg^{-1} BHA and 0.02 mol kg^{-1} BHT in various composite samples.

	T_1	**T_2**	**T_3**	**T_4**	**T_5**	**T_6**	**T_7**	**T_8**
XAM	–	–	–	0.04	0.03	0.02	0.01	0.13
XTM	–	–	–	0.03	0.04	0.02	0.01	0.09
XAE	–	–	–	0.03	0.04	0.02	0.01	0.11
XTE	–	–	–	0.04	0.05	0.02	0.02	0.12
XAP	–	–	–	0.03	0.02	0.02	0.01	0.12
XTP	–	–	–	0.04	0.04	0.02	0.02	0.11

(–) No proton movement was obtained, X stands for TX100, A stands for BHA, and T stands for BHT. M = MeOH, E = EtOH, P=1– PrOH

Conclusively, ^{1}H NMR spectroscopic analysis revealed the locus of BHA and BHT within all three surfactant systems i.e. outer surface or the interface of the micellar structure.

CHAPTER-5

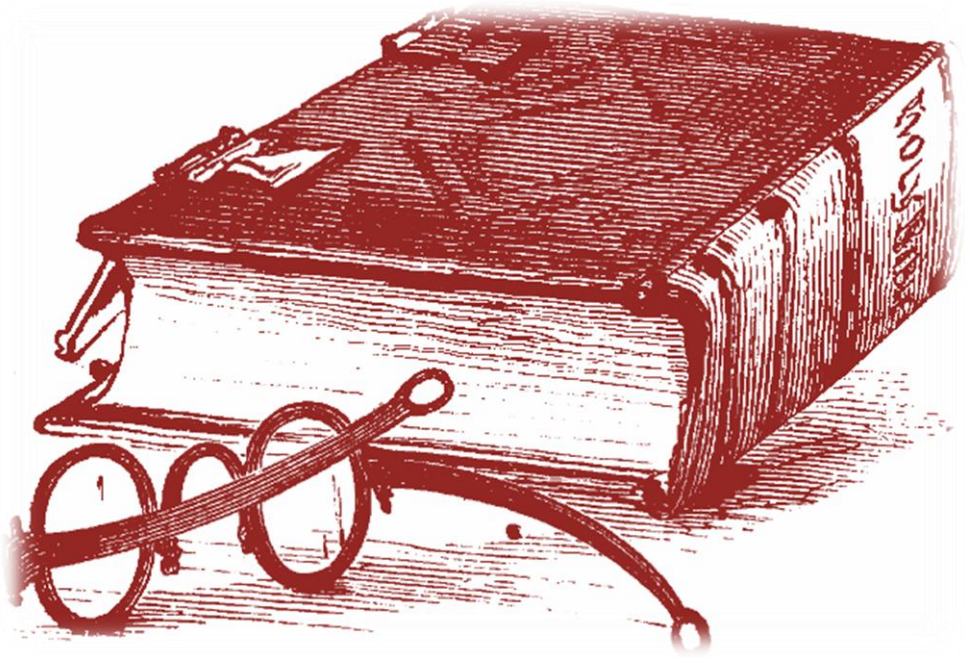

RESULT & DISCUSSION-II

5. Formulation, characterization and evaluation

This chapter is based on utilization of earlier studies in development and formulation of gel library with characterization in order to get best formulation and then, further *in vitro* and *in vivo* evaluation of best selected formulation.

5.1 Physicochemical characterization

5.2 *In vitro* antifungal activity

5.3 Morphological study

5.4 Stability studies

5.5 Skin irritation and *in vivo* toxicity study

5.6 Confocal laser scanning microscopy

5.7 *In vivo* antifungal study (mouse model)

5.1 Physicochemical characterization

5.1.1 Preliminary characterization of gel formulation library

After preparation, the total number of formulations was subjected to preliminary physicochemical examination like pH, viscosity, drug release and spreadability as presented in Table 5.1. All the gels were found with white opaque to translucent appearance. No visible precipitation was observed in all the formulations, whilst smooth and homogeneous texture was obtained. Given that pH of skin can vary according to age which might affects the permeation rate of the drug, the pH was found close to neutral value i.e. 7.0 which can provide better bioadhesive property. Considering pH determination of all 27 formulations, the values were found to lie within a range of $6.8 \pm 0.2 – 7.3 \pm 0.1$, thus lying in the normal pH range of skin. The viscosity values of all the gels were found in the range of 46719 ± 19 to 47839 ± 27 centipoise (cP). Interestingly, the increase of rotation speed did not significantly change the viscosity of the gels, revealing the formation of stable gel structure. This might be because carbopol 940 forms a physically bonded network in which movement of the dispersion medium is restricted by intercalating three dimensional network of solvated particles. Also, this polymer consists of twisted strands often tied together by stronger types of Vander Waals Forces to form stable network throughout the system. From a patient compliance perspective,

spreadability is a pivot for topical gel formulation. The formulations were found to exhibit good spreadability by weight (in a range of 11.00 ± 0.32 – 15.53 ± 0.12 g.cm/s).

Chemical interaction for CLZ and carbopol 940 was carried out via FTIR analysis. Initially the substantial peaks were characterized and analyzed for individual compound, in addition to that, FTIR was obtained for the admixture of CLZ and polymer used in this present study. Comparative FTIR revealed the absence of any kind of chemical interaction, which was attributed that CLZ and carbopol 940 are compatible within the system. All of the characteristic peaks remained unaffected in the obtained spectrum of CLZ + carbopol 940 admixture sample (Figure 5.1).

5.1.2 *In vitro* drug release and mathematic modeling

The ability of gel formulations to deliver CLZ was examined by determining the drug release rate. *In vitro* release study was conducted in optimized ratio of phosphate buffer (pH 7.4) and

Table 5.1: Physicochemical characterization data representing pH, viscosity, drug release, and spreadability.

S. No.	Codes	pH	Viscosity (cP)	Cumulative % drug release (6h)	Spreadability (g.cm/s)
1	CA–1S	6.9	46884 ± 24	82.44 ± 0.52	12.53 ± 0.15
2	CA–2S	6.8	46719 ± 19	87.23 ± 0.36	14.75 ± 0.21
3	CA–3S	7.1	47839 ± 27	94.33 ± 0.60	14.00 ± 0.32
4	CT–1S	6.9	46738 ± 25	82.74 ± 0.26	12.75 ± 0.13
5	CT–2S	7.2	46814 ± 18	87.63 ± 0.43	13.75 ± 0.17
6	CT–3S	6.8	47473 ± 31	94.63 ± 0.31	13.15 ± 0.22
7	CAT–1S	6.8	47249 ± 22	83.82 ± 0.44	14.33 ± 0.16
8	CAT–2S	7.0	47399 ± 20	88.40 ± 0.29	13.33 ± 0.23
9	CAT–3S	7.2	47392 ± 37	95.68 ± 0.50	14.85 ± 0.34
10	CA–1C	6.9	46984 ± 30	79.02 ± 0.34	13.53 ± 0.12
11	CA–2C	7.3	47008 ± 29	81.33 ± 0.42	14.33 ± 0.14
12	CA–3C	6.8	46953 ± 18	83.95 ± 0.54	14.03 ± 0.25
13	CT–1C	7.0	46896 ± 36	79.49 ± 0.57	13.52 ± 0.19
14	CT–2C	7.2	47255 ± 28	81.82 ± 0.31	13.64 ± 0.11
15	CT–3C	6.9	46949 ± 31	84.47 ± 0.30	12.53 ± 0.18
16	CAT–1C	7.1	47391 ± 40	81.05 ± 0.48	14.15 ± 0.27
17	CAT–2C	6.9	47195 ± 27	82.21 ± 0.35	14.53 ± 0.20
18	CAT–3C	6.8	46849 ± 35	85.18 ± 0.43	13.75 ± 0.17
19	CA–1X	7.3	46988 ± 36	85.92 ± 0.26	13.53 ± 0.29
20	CA–2X	7.0	47105 ± 25	88.82 ± 0.35	13.33 ± 0.33
21	CA–3X	7.2	46966 ± 31	93.38 ± 0.25	13.53 ± 0.16
22	CT–1X	6.9	47227 ± 29	86.14 ± 0.36	13.85 ± 0.23
23	CT–2X	7.1	47310 ± 34	89.07 ± 0.29	14.00 ± 0.17
24	CT–3X	6.8	46794 ± 30	94.00 ± 0.42	13.75 ± 0.26
25	CAT–1X	6.9	47399 ± 23	87.05 ± 0.52	14.15 ± 0.18
26	CAT–2X	7.3	47118 ± 28	89.50 ± 0.46	13.45 ± 0.21
27	CAT–3X	7.1	47284 ± 27	94.98 ± 0.23	13.70 ± 0.33

CA= CLZ+BHA; **CT**= CLZ+BHT; **CAT**= CLZ+BHA+BHT; **S**= SDS; **C**= CTAB; **X**= TX100

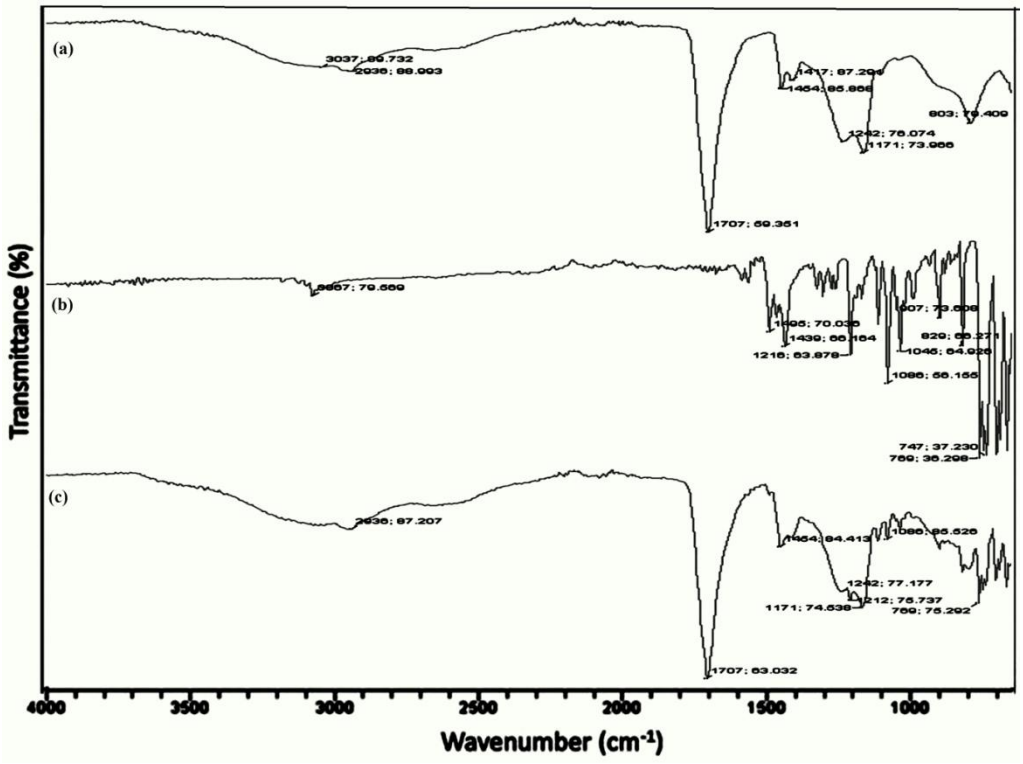

Figure 5.1: FTIR representing drug–polymer compatibility; (a) carbopol 940, (b) clotrimazole and (c) carbopol+clotrimazole.

methanol (6:4). Figure 5.2**,** shows the cumulative percent release of reduced best three formulations containing antioxidants' micellar system with different surfactant i.e. SDS, CTAB and TX100. For all the formulations, the release data has been presented in Table 5.1 and release kinetics for best three in Table 5.2 whereas for all 27 formulations, has been provided in *APPENDIX – C*. The study was initially optimized and then conducted for 6 h to gain better comparison. In comparison to plain drug, CAT–3S and CAT–3X showed higher release with initial slight burst then controlled, which might be because of the present additives providing additional driving force and afterward controlled by polymeric network structure of gel. It is important to note down that higher localized release is required in treatment of superficial localized infections.

In order to describe the drug release profiles from the gel, the *in vitro* release data were fitted into mathematic models and analyzed. The *in vitro* release data were fitted into Zero order, First order, Higuchi and Korsmeyer–Peppas kinetic equations. It was found that all the formulations had a good fit to the zero order equation, likely, R^2 = 0.956 for CAT–3S, R^2 = 0.997 for CAT–3C, and R^2 = 0.9995 for CAT–3X, respectively. Interestingly, CAT–3S was found to have maximum R^2 in case of Higuchi as well as Korsmeyer–peppas model.

Korsmeyer–peppas model suggested that the release followed diffusion controlled mechanism (n = 0.3). Results showed release exponent n values of about 0.3 attributing that drug release is driven by diffusion transport, following Fick's law of diffusion, in other words, drug release is concentration dependent. This kind of obtained release is known to reduce the induction of fungi tolerance to the antifungal drug.

Table 5.2: *In vitro* release rate profile with model kinetics for best three formulations.

Formulations	Zero order		First order		Higuchi		Korsmeyer–Peppas	
	R^2	K	R^2	K	R^2	K	R^2	n
CAT–3S	0.956	0.231	0.506	0.001	0.986	4.637	0.972	0.33
CAT–3C	0.997	0.227	0.693	0.001	0.929	4.637	0.994	0.32
CAT–3X	0.995	0.252	0.653	0.001	0.942	5.207	0.995	0.33

CAT= CLZ+BHA+BHT; **S**= SDS; **C**= CTAB; **X**= TX100

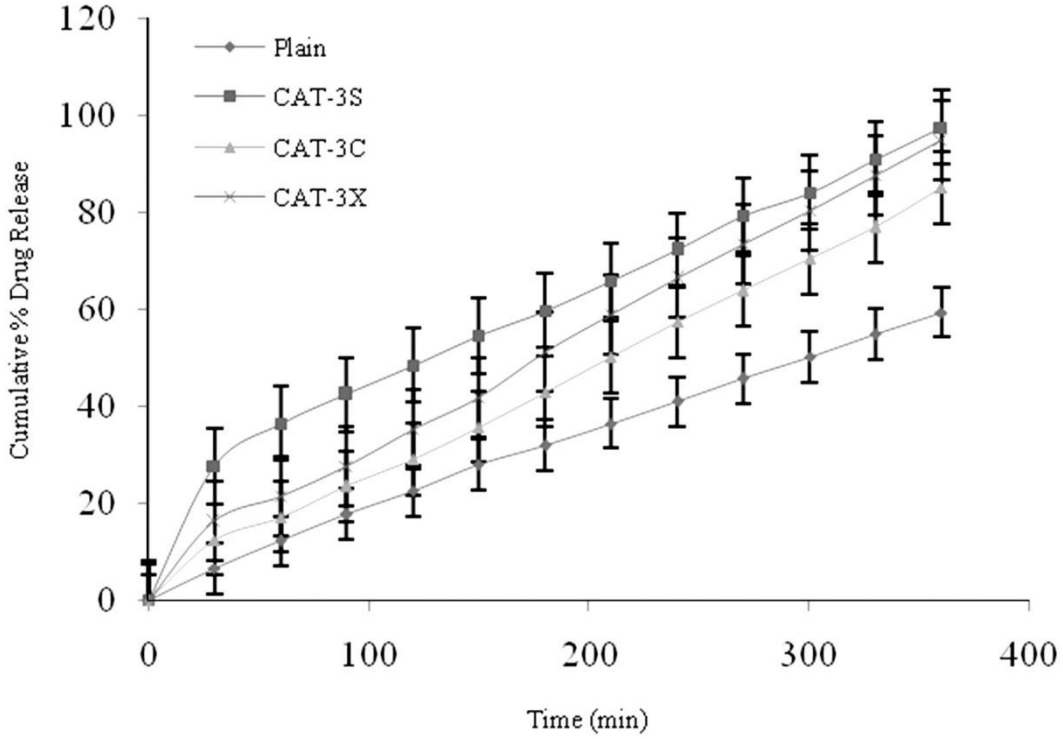

Figure 5.2: Plot representing cumulative % drug release as function of time.

5.2 *In vitro* antifungal activity

The *in vitro* antifungal activity of optimized best three formulations viz., CAT–3S, CAT–3C and CAT–3X was assessed. The MIC (μg/ml) values were obtained and presented in Table

5.3–5.5. Lower the MIC values are indicative of higher antifungal activity. The antifungal study was conducted on the clinically collected samples. Most of the obtained clinical isolates were FLZ resistant *C. albicans* as shown in Table 5.3–5.5. For this reason MIC for FLZ in addition to 30 % v/v CLZ EtOH solution was obtained to gain better interpretation. In addition, to assess the interaction of BHA+BHT and CLZ within selected three formulations, 30% v/v EtOH CLZ solution was used. We hypothesized that hydroethanolic solution used for micellar solution preparation and afterward dispersed into the gel base probably could influence the antifungal activity. EtOH itself is known to have antimicrobial property so, surely could have impact on antifungal profile of the respective formulations. Interestingly, when examined EtOH did not responded below MIC 1024, however, was found evident to promote antifungal property of plain CLZ in combination. In comparison from the MIC values CAT–3S showed promising activity against the clinical isolates. In particular, the calculated MIC values for CAT–3S was found to lie within the range of 0.25 – 8.0 (μg/ml) against FLZ / MLZ resistant and FLZ susceptible *C. albicans* isolates. Moreover the activity was promising against *C. tropicalis* isolates. Surprisingly, all the three formulations were not found as active against *C. glabrata* clinical isolates.

Given the fact that results suggested an interaction between CLZ and micellar encapsulated BHA+BHT, the FIC was calculated to investigate whether the combination was synergistic. This was carried by FICI approach. Here, FICI represents the sum of FICs of each compound tested/ presented within the system (formulation), where, FIC is determined for each compound by dividing the MIC of each compound when used in combination by the MIC of each compound when used alone.

Considering that FICI value among three screened formulations, CAT–3S was found with maximum number of synergism against 30 clinical isolates (Table 5.3). With regard to the FICI calculated values, CAT–3S was found to be most promising against FLZ resistant PDI/MDL54 clinical isolate with FICI = 0.13, therefore, the latter studies were performed against this clinical isolate. Results found in this *in vitro* experiment suggested a clear and decisive role of the antioxidants as well as the micellar system. Moreover, MIC values revealed promising inhibition of the growth of *Candida* species at the concentration lower than the drug (CLZ). Therefore, *in vitro antifungal* activity showed CAT–3S was the best among others which was thereafter accounted for further analysis and studies.

Table 5.3: Antifungal activity (MIC μg/ml) of CAT–3S formulation against various *Candida* species clinical isolates.

S. No.	Clinical Isolates	Type	Species	CAT–3S	BHA	BHT	FLZ	CLZ	FICI	RESULT
1	PGI/DML14	R	*C. albicans*	0.50	>512	64	>512	2.0	0.26	SY
2	PGI/DML34	R	*C. albicans*	1.0	>512	128	>512	2.0	0.51	AD
3	PGI/DML41	R	*C. albicans*	0.25	256	64	32	1.0	0.26	SY
4	PGI/DML54	R	*C. albicans*	0.50	>512	128	>512	4.0	0.13	SY
5	PGI/DML61	R	*C. albicans*	8.0	>512	>512	128	32	0.28	SY
6	PGI/DML85	R	*C. albicans*	8.0	>512	>512	>512	32	0.28	SY
7	PGI/DML43A	R	*C. albicans*	2.0	256	256	64	8.0	0.27	SY
8	PGI/DML77A	R	*C. albicans*	2.0	>512	>512	>512	16	0.13	SY
9	PGI/DML94A	R	*C. albicans*	16	>512	>512	>512	32	0.56	AD
10	PGI/DML106A	R	*C. albicans*	0.50	128	32	16	2.0	0.27	SY
11	PGI/DML05C	R	*C. albicans*	4.0	>512	128	64	8.0	0.54	AD
12	PGI/DML83C	R	*C. albicans*	1.0	256	64	>512	4.0	0.27	SY
13	PGI/DML74E	R	*C. albicans*	0.25	256	64	32	2.0	0.13	SY
14	PGI/DML88E	R	*C. albicans*	1.0	>512	128	>512	4.0	0.26	SY
15	PGI/DML92E	R	*C. albicans*	0.50	>512	64	>512	4.0	0.13	SY
16	PGI/DSS103	S	*C. albicans*	0.25	256	128	128	4.0	0.07	SY
17	PGI/DSS114	S	*C. albicans*	0.50	>512	128	256	8.0	0.07	SY
18	PGI/DSS123	S	*C. albicans*	4.0	128	>512	>512	16	0.31	SY
19	IGMC/LM1/021	S	*C. tropicalis*	0.50	>512	128	64	1.0	0.51	AD
20	IGMC/LM1/025	S	*C. tropicalis*	0.50	>512	32	>512	4.0	0.15	SY
21	IGMC/LM1/044	S	*C. tropicalis*	2.0	>512	128	32	4.0	0.52	AD
22	IGMC/LM2/010	S	*C. tropicalis*	1.0	256	>512	128	2.0	0.51	AD
23	IGMC/LM2/004	S	*C. tropicalis*	4.0	>512	64	64	4.0	1.07	IN
24	IGMC/LM2/001	S	*C. tropicalis*	8.0	128	>512	256	16	0.58	AD
25	IGMC/LM2/033	S	*C. tropicalis*	2.0	>512	128	64	8.0	0.27	SY
26	IGMC/LM4A/05	S	*C. tropicalis*	4.0	256	32	256	4.0	1.14	IN
27	IGMC/LM1/070	S	*C. glabrata*	4.0	256	64	16	0.50	8.08	AN
28	IGMC/LM1/091	S	*C. glabrata*	8.0	>512	32	128	2.0	4.27	AN
29	IGMC/LM4A/12	S	*C. glabrata*	16	>512	>512	>512	8.0	2.06	IN
30	IGMC/LM4A/19	S	*C. glabrata*	8.0	128	256	256	2.0	4.09	AN

Table 5.4: Antifungal activity (MIC μg/ml) of CAT–3C formulation against various *Candida* species clinical isolates.

S. No.	Clinical Isolates	Type	Species	CAT–3C	BHA	BHT	FLZ	CLZ	FICI	RESULT
1	PGI/DML14	R	*C. albicans*	1.0	>512	64	>512	2.0	0.52	AD
2	PGI/DML34	R	*C. albicans*	1.0	>512	128	>512	2.0	0.51	AD
3	PGI/DML41	R	*C. albicans*	1.0	256	64	32	1.0	1.02	IN
4	PGI/DML54	R	*C. albicans*	1.0	>512	128	>512	4.0	0.26	SY
5	PGI/DML61	R	*C. albicans*	8.0	>512	>512	128	32	0.28	SY
6	PGI/DML85	R	*C. albicans*	16	>512	>512	>512	32	0.06	SY
7	PGI/DML43A	R	*C. albicans*	4.0	256	256	64	8.0	0.53	AD
8	PGI/DML77A	R	*C. albicans*	8.0	>512	>512	>512	16	0.53	AD
9	PGI/DML94A	R	*C. albicans*	16	>512	>512	>512	32	0.56	AD
10	PGI/DML106A	R	*C. albicans*	1.0	128	32	16	2.0	0.54	AD
11	PGI/DML05C	R	*C. albicans*	4.0	>512	128	64	8.0	0.54	AD
12	PGI/DML83C	R	*C. albicans*	1.0	256	64	>512	4.0	0.27	SY
13	PGI/DML74E	R	*C. albicans*	1.0	256	64	32	2.0	0.52	AD
14	PGI/DML88E	R	*C. albicans*	1.0	>512	128	>512	4.0	0.26	SY
15	PGI/DML92E	R	*C. albicans*	0.50	>512	64	>512	4.0	0.13	SY
16	PGI/DSS103	S	*C. albicans*	0.25	256	128	128	4.0	0.07	SY
17	PGI/DSS114	S	*C. albicans*	1.0	>512	128	256	8.0	0.14	SY
18	PGI/DSS123	S	*C. albicans*	4.0	128	>512	>512	16	0.29	SY
19	IGMC/LM1/021	S	*C. tropicalis*	0.50	>512	128	64	1.0	0.51	AD
20	IGMC/LM1/025	S	*C. tropicalis*	1.0	>512	32	>512	4.0	0.28	SY
21	IGMC/LM1/044	S	*C. tropicalis*	4.0	>512	128	32	4.0	1.04	IN
22	IGMC/LM2/010	S	*C. tropicalis*	2.0	256	>512	128	2.0	1.01	IN
23	IGMC/LM2/004	S	*C. tropicalis*	2.0	>512	64	64	4.0	0.54	AD
24	IGMC/LM2/001	S	*C. tropicalis*	8.0	128	>512	256	16	0.58	AD
25	IGMC/LM2/033	S	*C. tropicalis*	2.0	>512	128	64	8.0	0.27	SY
26	IGMC/LM4A/05	S	*C. tropicalis*	1.0	256	32	256	4.0	0.29	SY
27	IGMC/LM1/070	S	*C. glabrata*	1.0	256	64	16	0.50	2.02	IN
28	IGMC/LM1/091	S	*C. glabrata*	1.0	>512	32	128	2.0	0.54	AD
29	IGMC/LM4A/12	S	*C. glabrata*	8.0	>512	>512	>512	8.0	1.03	IN
30	IGMC/LM4A/19	S	*C. glabrata*	2.0	128	256	256	2.0	1.02	IN

Table 5.5: Antifungal activity (MIC μg/ml) of CAT–3X formulation against various *Candida* species clinical isolates.

S. No.	Clinical Isolates	Type	Species	CAT–3X	BHA	BHT	FLZ	CLZ	FICI	RESULT
1	PGI/DML14	R	*C. albicans*	0.50	>512	64	>512	2.0	0.26	SY
2	PGI/DML34	R	*C. albicans*	0.50	>512	128	>512	2.0	0.26	SY
3	PGI/DML41	R	*C. albicans*	0.25	256	64	32	1.0	0.26	SY
4	PGI/DML54	R	*C. albicans*	1.0	>512	128	>512	4.0	0.26	SY
5	PGI/DML61	R	*C. albicans*	8.0	>512	>512	128	32	0.28	SY
6	PGI/DML85	R	*C. albicans*	16	>512	>512	>512	32	0.56	AD
7	PGI/DML43A	R	*C. albicans*	2.0	256	256	64	8.0	0.27	SY
8	PGI/DML77A	R	*C. albicans*	4.0	>512	>512	>512	16	0.27	SY
9	PGI/DML94A	R	*C. albicans*	16	>512	>512	>512	32	0.56	AD
10	PGI/DML106A	R	*C. albicans*	0.50	128	32	16	2.0	0.27	SY
11	PGI/DML05C	R	*C. albicans*	2.0	>512	128	64	8.0	0.27	SY
12	PGI/DML83C	R	*C. albicans*	2.0	256	64	>512	4.0	0.54	AD
13	PGI/DML74E	R	*C. albicans*	1.0	256	64	32	2.0	0.52	AD
14	PGI/DML88E	R	*C. albicans*	2.0	>512	128	>512	4.0	0.52	AD
15	PGI/DML92E	R	*C. albicans*	1.0	>512	64	>512	4.0	0.27	SY
16	PGI/DSS103	S	*C. albicans*	0.50	256	128	128	4.0	0.13	SY
17	PGI/DSS114	S	*C. albicans*	2.0	>512	128	256	8.0	0.27	SY
18	PGI/DSS123	S	*C. albicans*	2.0	128	>512	>512	16	0.15	SY
19	IGMC/LM1/021	S	*C. tropicalis*	0.50	>512	128	64	1.0	0.51	AD
20	IGMC/LM1/025	S	*C. tropicalis*	1.0	>512	32	>512	4.0	0.28	SY
21	IGMC/LM1/044	S	*C. tropicalis*	2.0	>512	128	32	4.0	0.52	AD
22	IGMC/LM2/010	S	*C. tropicalis*	1.0	256	>512	128	2.0	0.51	AD
23	IGMC/LM2/004	S	*C. tropicalis*	4.0	>512	64	64	4.0	1.07	IN
24	IGMC/LM2/001	S	*C. tropicalis*	8.0	128	>512	256	16	0.58	AD
25	IGMC/LM2/033	S	*C. tropicalis*	2.0	>512	128	64	8.0	0.27	SY
26	IGMC/LM4A/05	S	*C. tropicalis*	1.0	256	32	256	4.0	0.29	SY
27	IGMC/LM1/070	S	*C. glabrata*	2.0	256	64	16	0.50	4.04	AN
28	IGMC/LM1/091	S	*C. glabrata*	1.0	>512	32	128	2.0	0.53	AD
29	IGMC/LM4A/12	S	*C. glabrata*	16	>512	>512	>512	8.0	2.06	IN
30	IGMC/LM4A/19	S	*C. glabrata*	8.0	128	256	256	2.0	4.13	AN

5.3 Morphological study

To gain more insight on the best scrutinized formulation i.e. CAT–3S, the morphological studies were performed. From the SEM images as presented in Figure 5.3(a,b,c), it was well observed that CAT–3S was homogeneous with no signs of precipitation. Milky white appearance with a colloidal system characteristic was visualized. However, nano – micellar bodies were also visualized with uniform distribution within the gel matrix system. In addition, the image was also taken after duration of 1 month (Figure 5.3b) and lately ~ 9 months (Figure 5.3c) in order to visualize any morphological changes within the formulation, suggesting stability of CAT–3S for a period of 9 month cycle. On the other hand, micellar structures were also characterized via SEM and TEM. Figure 5.4(a,b,c), depicting spherical micellar formation with no structural transition, which can occur sometime due to presence of EtOH caused by compensation between electrostatic interaction and hydrophobic hydration. From TEM images (Figure 5.4b,c) and physicochemical analysis, the size was found to be ~ 118 nm, with polydispersity index 0.17 ± 0.04 and zeta potential – 18.34 ± 2.43 mV suggesting narrow distribution and good stability of the micellar bodies within the system. In addition, it should be noted that carbomer molecule are negative charged with tightly coiled structure therefore provided greater stability, which was well observed in the formulation.

The mechanistic antifungal activity of CAT–3S was estimated using *C. albicans* (PGI/DML41) cell viability assay via TEM. To gain information with respect to contact activity and cytological damage caused by CAT–3S, the higher concentration i.e. 10 μg/ml was intentionally selected to avoid the budding of cells and cell adherence that are unaffected by the exposure. From the images (Figure 5.5a,b,c), the morphological changes of *C. albicans* induced by treatment were clearly revealed by TEM. Figure 5.5a of untreated *C. albicans* was well defined, intact shapes with smooth surface. After 15 min of treatment, a slight but considerable alteration was observed on fungal cell wall, whereas after 2 h and 6 h, well defined ultrastructural changes were noticed. Morphological cell wall deformation (peeling/ exfoliation) followed by shrinkage and complete cell damage was observed after 6 h (Figure 5.5d).

However, CLZ which is an imidazole derivative and known to act on fungal cell wall or membrane and binds to the heme part of cell wall leading to inhibition of ergosterol principally sterol in membrane and then destroys the integrity of the fungal membrane. In addition BHA and BHT do possess heme chelating property, so it is a speculation which

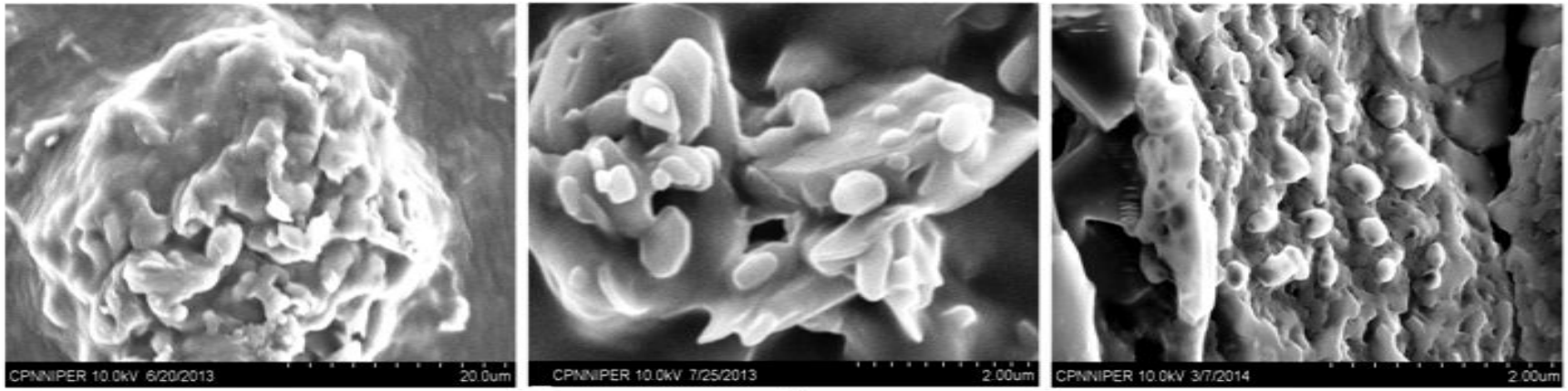

Figure 5.3: Scanning electron microscopy images of formulation (CAT–3S); (a) after preparation (b) after ~ 1 month, and (c) after ~ 9 months.

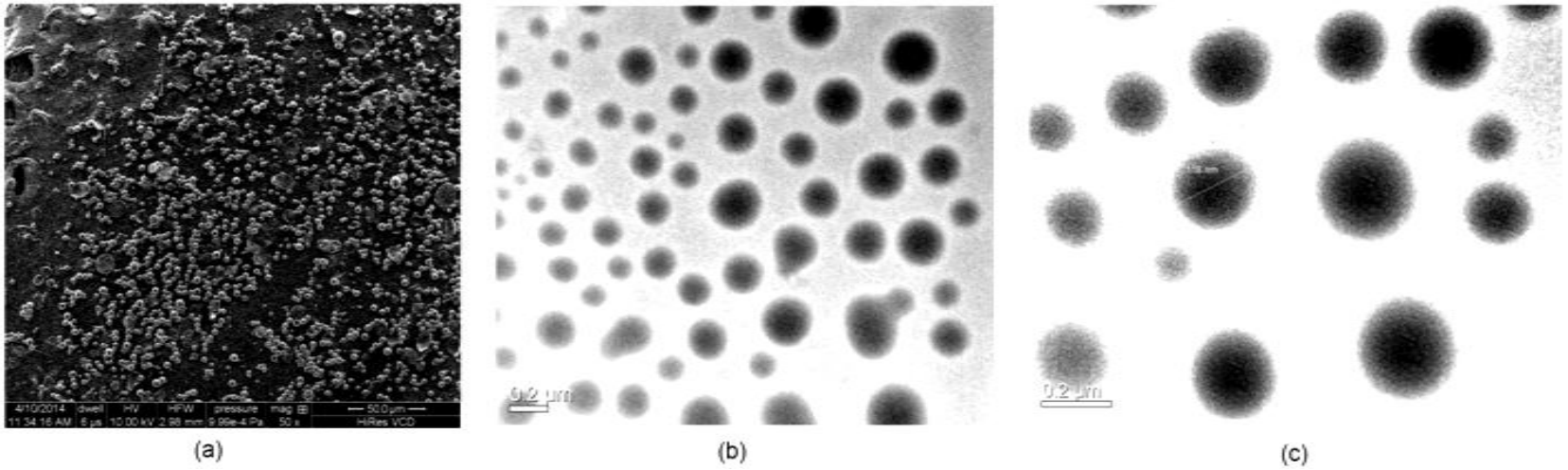

Figure 5.4: (a) Scanning electron microscopy image of prepared micelles, (b) and (c) transmission electron microscopy images of micelle dispersed within the formulation CAT-3S.

might be possible that they might have acted in a same manner and provided synergism in order to get better antifungal drug action.

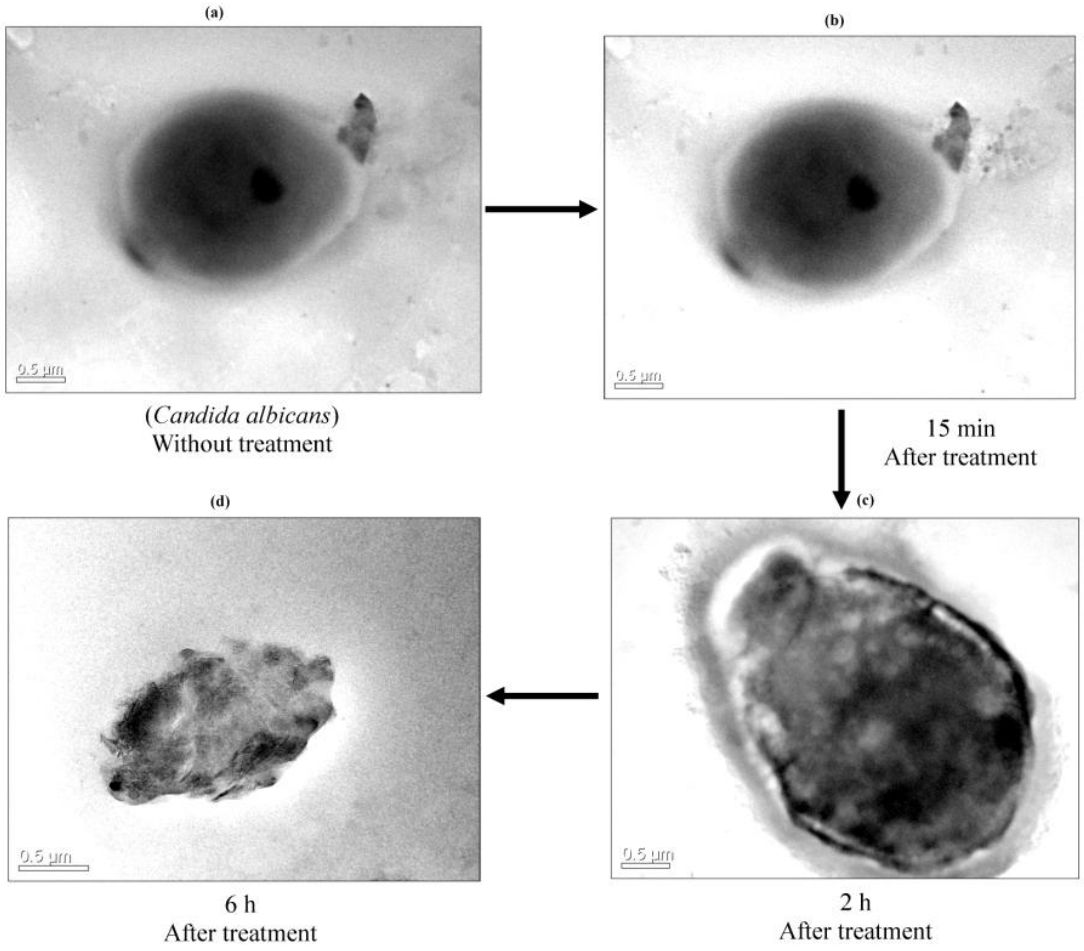

Figure 5.5: TEM images of an unexposed (control) cell and CAT–3S (10 μg/ml) treated cell of *C. albicans*.

5.4 Stability studies

5.4.1 Photo–stability study

In general, there are no such scientific reports suggesting that CLZ is photolabile, the United States Pharmacopoeia and very few articles from Santos et al. [44] recommends that photo protection of the drug during storage. In the present study, an examination was made of the ability of potential oxidation inhibitors (BHA/BHT) in prevention of CLZ photodegradation under UVC radiation. After the exposure of 14 h, the samples were analyzed for amount of remaining CLZ (% age). The presented Figure 5.6 shows the photodegradation of methanolic solution of CLZ and CAT–3S in comparison to the dark control of the CLZ. Form the results, the CLZ concentration of dark control was found almost 100%, whereas, methanolic CLZ

solution showed significant degradation of 76%. In comparison to dark control, the formulation (CAT–3S) resist with degradation of 22%. The result showed that antioxidants present in CAT–3S led to an increase of approximately 3.5 times of exposed methanolic solution of CLZ. The enhanced photostability is well attributed to the standard antioxidants. It can be explained as antioxidants might have prevented the degradation caused by UV exposure by absorbing the UV radiations or by trapping the free radicals generated during the process of oxidation.

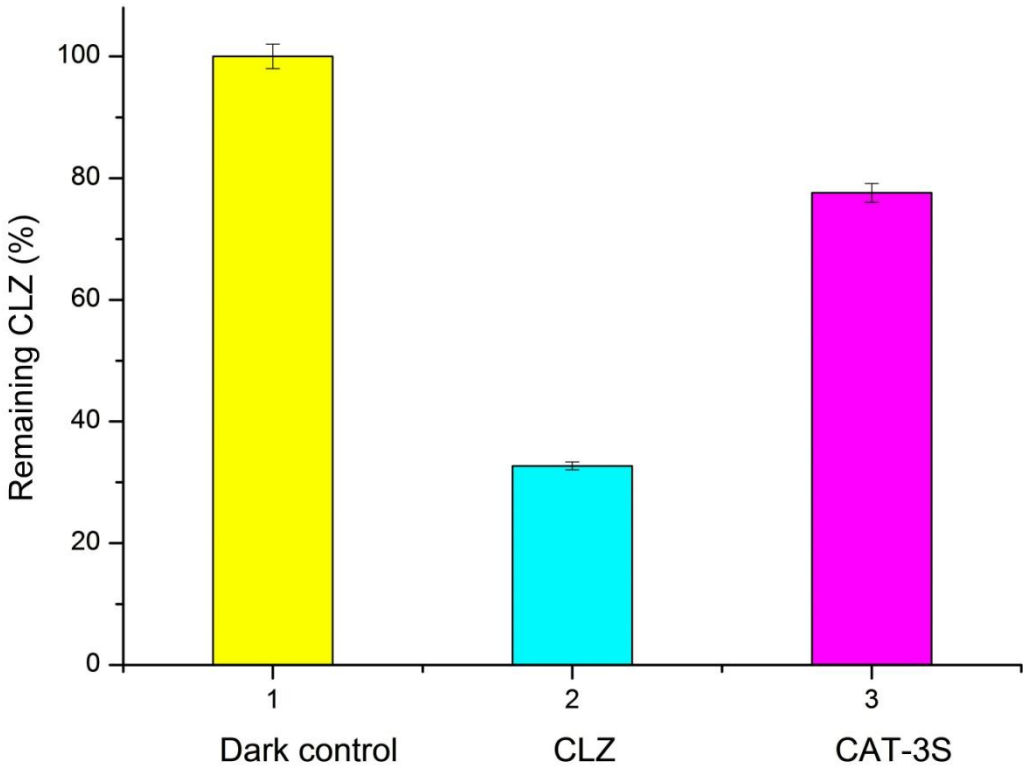

Figure 5.6: Plot representing clotrimazole (CLZ) content after 14 h exposure to UVC radiations.

5.4.2 Physical stability

In 9 month stability cycle at room temperature and light protected, no changes were observed in appearance, with no color change and without any kind of precipitation (Figure 5.3c). Whist in 60 days, marginal decrease was found in cumulative % drug release and pH. In addition, viscosity was also found to decrease marginally which might be because of EtOH presence in the formulation, thus, affecting the spreadability. With regard to BHA+BHT loaded micellar particle size and zeta potential, they were reasonably steady with slight increase in size and decrease in charge (Figure 5.7). In addition, polydispersity index was also found with marginal decrease.

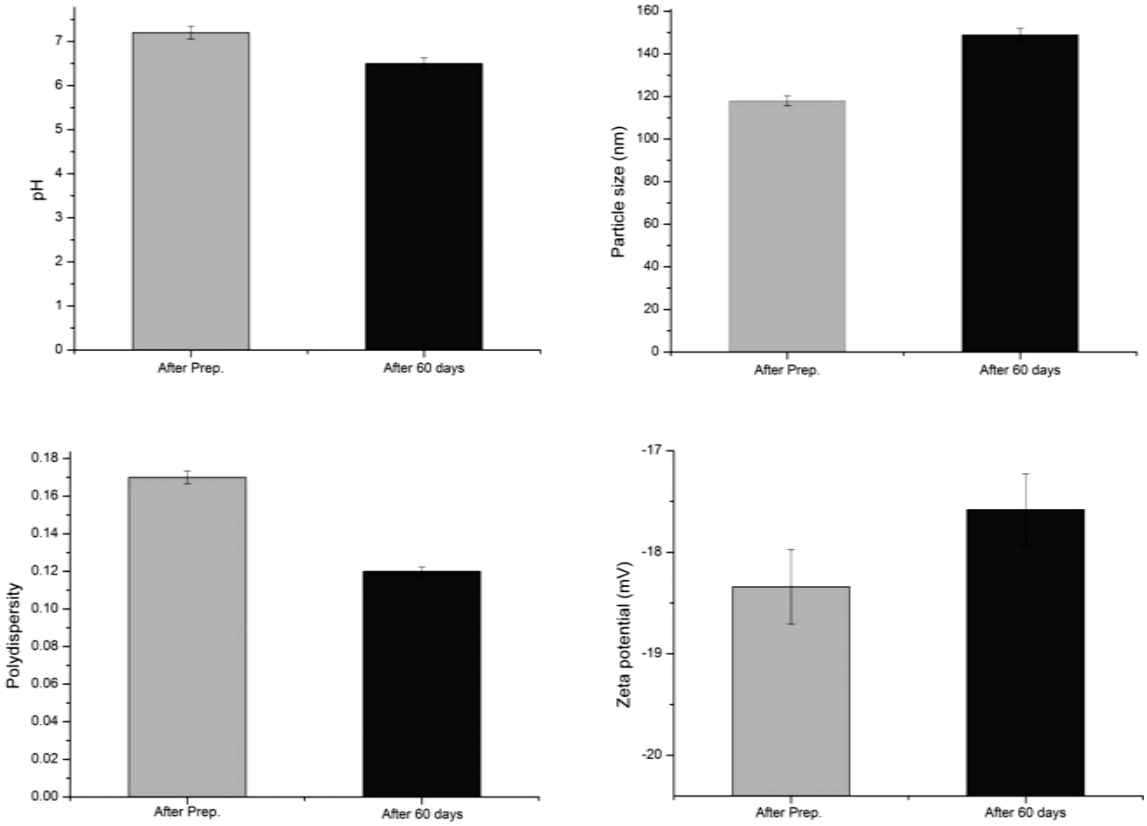

Figure 5.7: pH, particle size (nm), polydispersity and zeta potential (mV) of micellar structure, after preparation and after 60 days.

5.5 Skin irritation and *in vivo* toxicity study

Conventional therapy is associated with visual noticeable skin irritation check. If observed, it strongly restricts the applicability and acceptability of topical formulation by the patients. Ideally, the developed formulation should not cause any kind of irritation marks. In present investigation, skin irritation studies suggested that CAT–3S exhibited considerably no irritation. The primary irritation index (PII) was found to be 0.00, reflecting no irritation within the limited duration of studied time. In addition, no erythema or edema was observed on the abraded rat skin when compared with control (without treatment).

However, going beyond the conventional therapy evaluation and gain much clear perspective, we intended to examine the *in vivo* toxicity in major organs. The photo–micrographs of skin histological sections of treated and untreated animals are shown in Figure 5.8. H and E stained sections of control skin sample showed epidermis consisting of a cornified squamous layer and underlying germinative layer. No inflammatory infiltrate, granulomatous evidence of malignancy was visualized. The formulation CAT–3S did not show sign of inflammation such as inflammatory infiltrate or edema. Compared to the control,

no histopathological changes were visualized in other major organs (liver, kidney, and intestine) in treated animals. These results revealed that the developed surfactant aided antioxidants within CLZ gel system is safe for topical delivery.

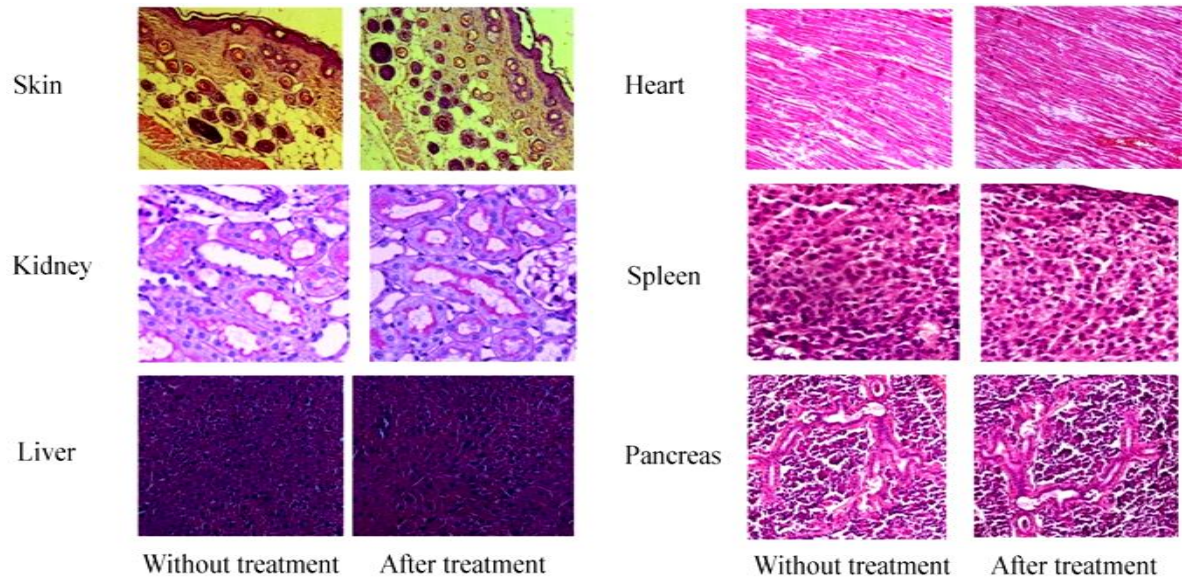

Figure 5.8: Histological images of major organs (A) untreated and (B) formulation (CAT–3S) treated, suggesting no toxicity, Scale 50μm.

5.6 Confocal laser scanning microscopy

Rhodamine B is an amphoteric dye, although usually listed as basic as it has an overall positive charge. On the other hand, carbopol polymer is anionic in nature, thus generates negative charges along their backbone and has the efficiency to bind with positively charged moiety via ion–ion interactions [45]. Employing CLSM of rat skin, the penetration of the dye within gel was investigated in order to assess the penetration range. The results of the study demonstrated that the penetration and accumulation within epidermis section of skin (Figure 5.9). It can be concluded that system having surfactant aided antioxidant micellar system provides an extra driving force to the molecules present in carbopol gel base, allowing better penetration by destabilizing the membrane whereas, ethanolic solution of drug was found to accumulate in the stratum corneum only. This study suggesting the relevance of residence time for drug on infected site offered by three dimensional polymeric gel system.

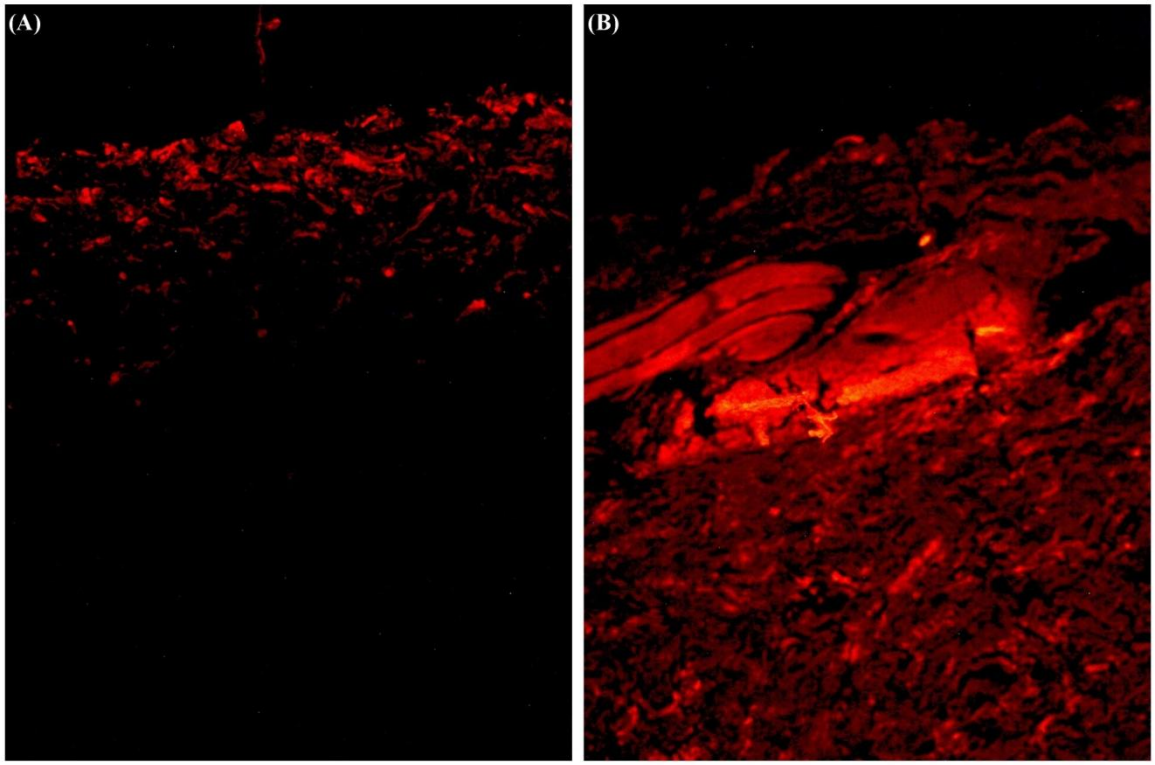

Figure 5.9: Confocal laser scanning micrograph of rat skin (A) treatment with hydroalcoholic solution of Rhodamine B, and (B) CAT–3S (Rhodamine B in polymeric system), Scale 50μm.

5.7 *In vivo* antifungal study (mouse model)

The *in vivo* antifungal activity of plain CLZ formulation and developed formulation CAT–3S (1 mg/cm^2 and 5 mg/cm^2) was determined by challenging the animals with FLZ resistant *C. albicans* (PGI/DML54) on 8 days mouse model. From Figure 5.10, it was found that infection in all animals was well established.

The efficacy of the formulation CAT–3S was assessed on the basis of viable CFU count at different time intervals after treatment. Results revealed that CAT–3S possessed significant therapeutic efficacy, as compared to plain drug. After three days both CAT–3S and plain CLZ formulation significantly reduced the growth of *C. albicans*. Interestingly, at dose level of 1 mg/cm^2 plain CLZ formulation exhibits somewhat higher efficacy than CAT–3S with 2.14 $\log_{10}$ reduction in viable CFU (**$p<0.01$; Figure) of *C. albicans* when compared with 48 h control. At the same time, formulation CAT–3S at dose level of 5 mg/cm^2 produced 2.28 $\log_{10}$ reduction in viable CFU (**$p<0.01$; Figure) of *C. albicans* when compared with 48 h control. However, this positive effect of plain CLZ formulation did not maintained throughout the experiment as increment in the viable CFUs was observed on day 5, 6, 7, and 8. In contrast to this, CAT–3S constantly reduced the burden of viable CFUs of infecting

organism and appreciated the longer term reduction of fungal infection in skin. In particular, CAT–3S induced 3.26, 3.58, 4.20, and 4.65 $\log_{10}$ reduction in viable CFUs of *C. albicans* on day 5, 6, 7, and 8 respectively when compared with 48 h control. Similarly, formulation at 5 mg/cm^2 decreased the burden of *C. albicans* by 4.52, 4.81, 5.38, and 5.73 $\log_{10}$ when growth was observed after 5, 6, 7, and 8 days respectively. It was further interesting to note that on day 8 numbers of viable CFUs was increased to 7.11 $\log_{10}$.

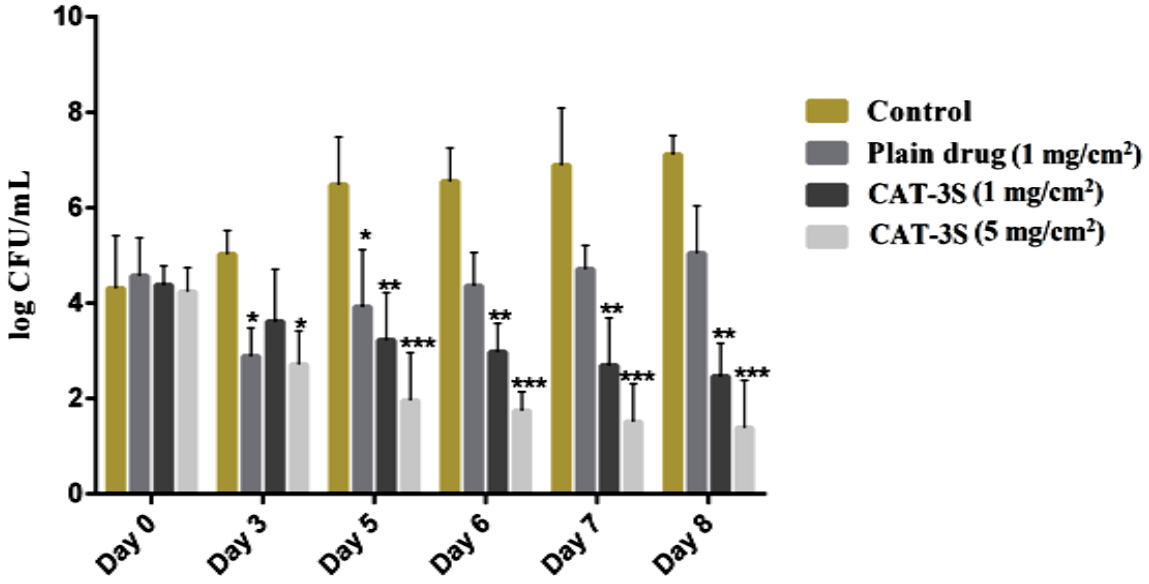

Figure 5.10: *In vivo* antifungal activity representing the infection burden in 8 days mouse model.

As it can be clearly stated that the animals treated with CAT–3S, demonstrated low fungal burden in skin with a colony count significantly less abundant than those treated with plain CLZ formulation. This impact of CAT–3S can be explained in term of presence of BHA and BHT within SDS hydroethanolic micellar system in bioadhesive gel, providing longer residence time, higher bioavailability with synergistic effect offered by antioxidants.

References

[1] V. Bhardwaj, S. Chauhan, K. Sharma, and P. Sharma, "Cosmeceutical active molecules and ethoxylated alkylphenol (Triton X-100) in hydroalcoholic solutions: Transport properties examination," *Thermochimica Acta*, vol. 577, pp. 66-78, 2014.

[2] V. Bhardwaj, P. Sharma, M. Chauhan, and S. Chauhan, "Thermodynamic, FTIR, ^{1}H-NMR, and acoustic studies of butylated hydroxyanisole and sodium dodecyl sulfate in ethanol, water rich and ethanol rich solutions," *Journal of Molecular Liquids*, vol. 180, pp. 192-199, 2013.

[3] V. Bhardwaj, S. Chauhan, and P. Sharma, "Probing effect of lipophilic butylated hydroxytoluene on anionic surfactant properties for potential food and pharmaceutical applications: Thermo-acoustic and spectroscopic study," *Fluid Phase Equilibria*, vol. 373, pp. 63-71, 2014.

[4] V. Bhardwaj, P. Sharma, and S. Chauhan, "Thermo-acoustic investigation in alcohol–water mixtures: Impact of lipophilic antioxidant on anionic surfactant properties for potential cosmeceutical application," *Thermochimica Acta*, vol. 566, pp. 155-161, 2013.

[5] P. Sharma, V. Bhardwaj, T. Chaudhary, I. Sharma, P. Kumar, and S. Chauhan, "Micellar interaction study of synthetic antioxidant (BHA) and sodium dodecyl sulfate (SDS) in aqueous solution for potential pharmaceutical/food applications," *Journal of Molecular Liquids*, vol. 187, pp. 287-293, 2013.

[6] V. Bhardwaj, P. Sharma, M. Chauhan, and S. Chauhan, "Micellization, interaction and thermodynamic study of butylated hydroxyanisole (synthetic antioxidant) and sodium dodecyl sulfate in aqueous-ethanol solution at 25, 30 and 35° C," *Journal of Saudi Chemical Society*, 2012. 10.1016/j.jscs.2012.09.008

[7] V. Bhardwaj, P. Sharma, S. Chauhan, and M. Chauhan, "Lipophilic Synthetic Antioxidants (BHA/BHT) and Sodium Dodecyl Sulfate (SDS) in Alcohol-Water Mixtures: A Thermodynamic Study," *Advanced Science, Engineering and Medicine*, vol. 5, pp. 971-978, 2013.

[8] R.-S. Juang, Y.-Y. Xu, and C.-L. Chen, "Separation and removal of metal ions from dilute solutions using micellar-enhanced ultrafiltration," *Journal of Membrane Science*, vol. 218, pp. 257-267, 2003.

[9] A. Modaressi, H. Sifaoui, B. Grzesiak, R. Solimando, U. Domanska, and M. Rogalski, "CTAB aggregation in aqueous solutions of ammonium based ionic liquids;

conductimetric studies," *Colloids and Surfaces A: Physicochemical and Engineering Aspects,* vol. 296, pp. 104-108, 2007.

[10] W. Zhou and L. Zhu, "Enhanced desorption of phenanthrene from contaminated soil using anionic/nonionic mixed surfactant," *Environmental Pollution,* vol. 147, pp. 350-357, 2007.

[11] M. Bakshi, S. Sachar, N. Mahajan, I. Kaur, G. Kaur, N. Singh, P. Sehgal, and H. Doe, "Mixed-micelle formation by strongly interacting surfactant binary mixtures: effect of head-group modification," *Colloid and Polymer Science,* vol. 280, pp. 990-1000, 2002.

[12] S. Chauhan and K. Sharma, "Effect of temperature and additives on the critical micelle concentration and thermodynamics of micelle formation of sodium dodecyl benzene sulfonate and dodecyltrimethylammonium bromide in aqueous solution: A conductometric study," *The Journal of Chemical Thermodynamics,* vol. 71, pp. 205-211, 2014.

[13] M. S. Akhter and S. M. Alawi, "The effect of organic additives on critical micelle concentration of non-aqueous micellar solutions," *Colloids and Surfaces A: Physicochemical and Engineering Aspects,* vol. 175, pp. 311-320, 2000.

[14] P. Sharma, S. Chauhan, M. Chauhan, and V. Syal, "Ultrasonic velocity and viscosity studies of tramacip and parvodex in binary mixtures of alcohol+ water," *Ind. J. Pure Appl. Phys,* vol. 46, pp. 839-843, 2008.

[15] R. Zana and Y. Talmon, "Dependence of aggregate morphology on structure of dimeric surfactants," *Nature,* vol. 362, pp. 228-230, 1993.

[16] M. Kahlweit, G. Busse, and J. Jen, "Adsorption of amphiphiles at water/air interfaces," *The Journal of Physical Chemistry,* vol. 95, pp. 5580-5586, 1991.

[17] S. Ghosh, A. Das Burman, G. C. De, and A. R. Das, "Interfacial and self-aggregation of binary mixtures of anionic and nonionic amphiphiles in aqueous medium," *The Journal of Physical Chemistry B,* vol. 115, pp. 11098-11112, 2011.

[18] M. A. Hoque, M. A. Khan, and M. D. Hossain, "Interaction of cefalexin monohydrate with cetyldimethylethylammonium bromide," *The Journal of Chemical Thermodynamics,* vol. 60, pp. 71-75, 2013.

[19] K. Mukherjee, S. Moulik, and D. Mukherjee, "Thermodynamics of micellization of Aerosol OT in polar and nonpolar solvents. A calorimetric study," *Langmuir,* vol. 9, pp. 1727-1730, 1993.

[20] P. Lianos, J. Lang, and R. Zana, "Fluorescence probe study of oil-in-water microemulsions. 2. Effect of the nature of alcohol, oil and surfactant on the surfactant aggregation number in the aggregates," *The Journal of Physical Chemistry,* vol. 86, pp. 4809-4814, 1982.

[21] B. Kumar, D. Tikariha, K. K. Ghosh, and P. Quagliotto, "Effect of short chain length alcohols on micellization behavior of cationic gemini and monomeric surfactants," *Journal of Molecular Liquids,* vol. 172, pp. 81-87, 2012.

[22] J. J. H. Nusselder and J. B. Engberts, "Toward a better understanding of the driving force for micelle formation and micellar growth," *Journal of Colloid and Interface Science,* vol. 148, pp. 353-361, 1992.

[23] S. K. Mehta, N. Jindal, and G. Kaur, "Quantitative investigation, stability and *in vitro* release studies of anti-TB drugs in Triton niosomes," *Colloids and Surfaces B: Biointerfaces,* vol. 87, pp. 173-179, 2011.

[24] C. J. Drummond and C. Fong, "Surfactant self-assembly objects as novel drug delivery vehicles," *Current Opinion in Colloid & Interface Science,* vol. 4, pp. 449-456, 1999.

[25] H. Zhang and O. Annunziata, "Modulation of drug transport properties by multicomponent diffusion in surfactant aqueous solutions," *Langmuir,* vol. 24, pp. 10680-10687, 2008.

[26] M. J. Schick, *Nonionic Surfactants: Physical Chemistry* vol. 23: CRC Press, 1987.

[27] C. C. Ruiz, J. Molina-Bolivar, J. Aguiar, G. MacIsaac, S. Moroze, and R. Palepu, "Thermodynamic and structural studies of Triton X-100 micelles in ethylene glycol-water mixed solvents," *Langmuir,* vol. 17, pp. 6831-6840, 2001.

[28] A. C. Williams and B. W. Barry, "Penetration enhancers," *Advanced Drug Delivery Reviews,* vol. 64, pp. 128-137, 2012.

[29] T. Kitano, S. Kawaguchi, N. Anazawa, and A. Minakata, "Dissociation behavior of an alternating copolymer of isobutylene and maleic acid by potentiometric titration and intrinsic viscosity," *Macromolecules,* vol. 20, pp. 2498-2506, 1987.

[30] S. Chauhan, V. Syal, M. Chauhan, and P. Sharma, "Viscosity studies of some narcotic–analgesic drugs in aqueous–alcoholic mixtures at 25° C," *Journal of Molecular Liquids,* vol. 136, pp. 161-164, 2007.

[31] A. D. Carswell, A. M. Lowe, X. Wei, and B. P. Grady, "CMC determination in the presence of surfactant-adsorbing inorganic particulates," *Colloids and Surfaces A: Physicochemical and Engineering Aspects,* vol. 212, pp. 147-153, 2003.

[32] L. Pikkarainen, "Densities and viscosities of binary mixtures of N, N-dimethylacetamide with aliphatic alcohols," *Journal of Chemical and Engineering Data*, vol. 28, pp. 344-347, 1983.

[33] N. Dharaiya and P. Bahadur, "Phenol induced growth in Triton X-100 micelles: Effect of pH and phenols' hydrophobicity," *Colloids and Surfaces A: Physicochemical and Engineering Aspects*, vol. 410, pp. 81-90, 2012.

[34] S. Chauhan, V. Sharma, and K. Sharma, "Maltodextrin–SDS interactions: Volumetric, viscometric and surface tension study," *Fluid Phase Equilibria*, vol. 354, pp. 236-244, 2013.

[35] U. Dash, J. Mahapatra, and B. Lal, "Ion association and solvation of Co (III) complexes in water+ alcohol mixtures at different temperatures," *Journal of Molecular Liquids*, vol. 124, pp. 13-18, 2006.

[36] R. Borbás, B. S. Murray, and É. Kiss, "Interfacial shear rheological behaviour of proteins in three-phase partitioning systems," *Colloids and Surfaces A: Physicochemical and Engineering Aspects*, vol. 213, pp. 93-103, 2003.

[37] K. Szymczyk and B. Jańczuk, "The adsorption at solution–air interface and volumetric properties of mixtures of cationic and nonionic surfactants," *Colloids and Surfaces A: Physicochemical and Engineering Aspects*, vol. 293, pp. 39-50, 2007.

[38] S. Chauhan, K. Sharma, K. Kumar, and G. Kumar, "A comparative study of micellization behavior of an ethoxylated alkylphenol in aqueous solutions of glycine and leucine," *Journal of Surfactants and Detergents*, vol. 17, pp. 161-168, 2014.

[39] F. Franks, "Water: a comprehensive treatise," Plenum Press, 1972.

[40] J. Krzaczkowska, E. Szcześniak, and S. Jurga, "Phase behaviour of dipalmitoylphosphatidylcholine/surfactant/water systems studied by infrared spectroscopy," *Journal of Molecular Structure*, vol. 794, pp. 168-172, 2006.

[41] K.-H. Kang, H.-U. Kim, and K.-H. Lim, "Effect of temperature on critical micelle concentration and thermodynamic potentials of micellization of anionic ammonium dodecyl sulfate and cationic octadecyl trimethyl ammonium chloride," *Colloids and Surfaces A: Physicochemical and Engineering Aspects*, vol. 189, pp. 113-121, 2001.

[42] S. Mehta, K. Bhasin, A. Kumar, and S. Dham, "Micellar behavior of dodecyldimethylethyl ammonium bromide and dodecyltrimethylammonium chloride in aqueous media in the presence of diclofenac sodium," *Colloids and Surfaces A: Physicochemical and Engineering Aspects*, vol. 278, pp. 17-25, 2006.

[43] D. Yu, X. Huang, M. Deng, Y. Lin, L. Jiang, J. Huang, and Y. Wang, "Effects of inorganic and organic salts on aggregation behavior of cationic gemini surfactants," *The Journal of Physical Chemistry B,* vol. 114, pp. 14955-14964, 2010.

[44] S. S. Santos, A. Lorenzoni, L. M. Ferreira, J. Mattiazzi, A. I. Adams, L. B. Denardi, S. H. Alves, S. R. Schaffazick, and L. Cruz, "Clotrimazole-loaded Eudragit® RS100 nanocapsules: Preparation, characterization and *in vitro* evaluation of antifungal activity against Candida species," *Materials Science and Engineering: C,* vol. 33, pp. 1389-1394, 2013.

[45] R. Barreiro-Iglesias, C. Alvarez-Lorenzo, and A. Concheiro, "Incorporation of small quantities of surfactants as a way to improve the rheological and diffusional behavior of carbopol gels," *Journal of Controlled Release,* vol. 77, pp. 59-75, 2001.

CHAPTER-6

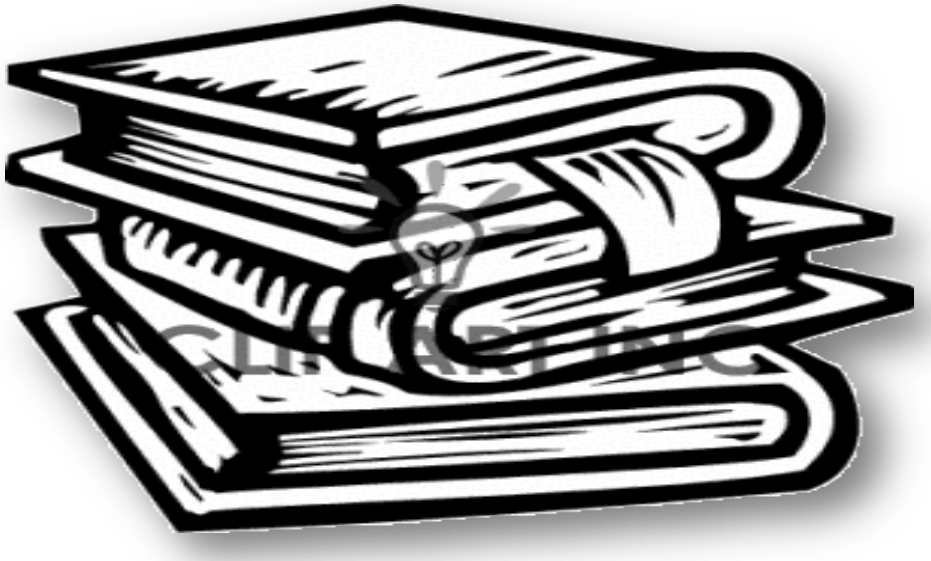

CONCLUSION

6. Conclusion

The focus of this dissertation was on the impact of antioxidant molecules on micellization, thermodynamic and transport properties of surfactant. Conclusively, in this context early micelle formation was observed with 30% v/v EtOH as the most feasible and thermodynamic stable system. The concentration dependence of apparent molal volume (ϕ_v) and apparent molar adiabatic compression (ϕ_k) calculated from density and speed of sound data shows evidence of interactions in hydroalcoholic or pure alcoholic solutions containing BHA and BHT. The positive values indicated the existence of hydrophobic interactions and solvation effect resulting association of molecules within the environment. Viscosity values were found to be in support of volumetric and compressibility measurements in terms of region of micellization. Spectroscopic analysis provided insight and understanding with regard of existing intermolecular interaction. The intermolecular interactions and the locus of BHA or BHT was determined in terms of chemical shift caused by the presence of antioxidant molecules. This marginal scale of shifting accounted for interactive forces of varying strength with no significant structural destruction. These observations guided antioxidant's micellar delivery in hydroalcoholic system. With eminence on the biological diversity of potential antioxidants and surfactants, further developments were made. For the first time, based on thermodynamic analysis the present study showed the feasibility and compatibility of utilizing antioxidant micellar system in combination of standard antifungal topical formulation. Conclusively, the developed formulation had satisfactory qualities. The results obtained in the present study show that the formulated gel holds good bioadhesive property, stability, prolonged residence time and higher penetration. In addition physicochemical studies directed the utilization of thermodynamically stable hydroethanolic antioxidant's micellar system, which showed potential synergism with better antifungal profile. From *in vitro* results, CAT-3S formulation was found to be the most promising one among all formulations. Biophysical morphology study revealed the mechanistic approach of CAT-3S via initial exfoliation causing drug accumulation and lastly cell damage. The fungal cell damage was well defined on the changes of morphology and biophysical properties. Photostability study suggested potential role of antioxidants to prevent the drug degradation caused by UV exposure. *In vivo* study demonstrated low fungal burden in skin with a colony count significantly less abundant with CAT-3S, than those treated with plain CLZ formulation.

Publications

[1] V. Bhardwaj, J. Monga, A. Sharma, S. Sharma, A. Sharma, and P. Sharma, "Novel surfactant immobilized micellar system of oxidation inhibitors in clotrimazole bio-adhesive gel formulation: Development, characterization, *in vitro* and *in vivo* antifungal evaluation on *Candida* clinical isolates," *RSC Advances*, vol. 4, pp. 47207–47221, 2014.

[2] V. Bhardwaj, K. Sharma, S. Chauhan, and P. Sharma, "Intermolecular Interactions of CTAB and Potential Oxidation Inhibitors: Physico–chemical Controlled Approach for Food/ Pharmaceutical Function," *RSC Advances*, vol. 4, pp. 49400–49414, 2014.

[3] V. Bhardwaj, S. Chauhan, and P. Sharma, "Probing effect of lipophilic butylated hydroxytoluene on anionic surfactant properties for potential food and pharmaceutical applications: Thermo-acoustic and spectroscopic study," *Fluid Phase Equilibria*, vol. 373, pp. 63-71, 2014.

[4] V. Bhardwaj, S. Chauhan, K. Sharma, and P. Sharma, "Cosmeceutical active molecules and ethoxylated alkylphenol (Triton X-100) in hydroalcoholic solutions: Transport properties examination," *Thermochimica Acta*, vol. 577, pp. 66-78, 2014.

[5] V. Bhardwaj, P. Sharma, and S. Chauhan, "Thermo-acoustic investigation in alcohol-water mixtures: Impact of lipophilic antioxidant on anionic surfactant properties for potential cosmeceutical application," *Thermochimica Acta*, vol. 566, pp. 155-161, 2013.

[6] V. Bhardwaj, P. Sharma, S. Chauhan, and M.S. Chauhan, "Thermodynamic, FTIR, ^{1}H-NMR, and acoustic studies of butylated hydroxyanisole and sodium dodecyl sulfate in ethanol, water rich and ethanol rich solutions. "*Journal of Molecular Liquids*, vol. 180, pp. 192-199, 2013.

[7] V. Bhardwaj, P. Sharma, S. Chauhan, and M.S. Chauhan, "Lipophilic synthetic antioxidants (BHA/BHT) and SDS in alcohol-water mixtures: A thermodynamic study," *Advanced Science Engineering and Medicine*, vol. 5, pp. 971-978, 2013.

[8] P. Sharma, V. Bhardwaj, Ishita Sharma, Tanvi Chaudhary, P. Kumar, and S. Chauhan, "Micellar interaction study of synthetic antioxidant (BHA) and sodium dodecyl sulfate (SDS) in aqueous solution for potential pharmaceutical/food applications," *Journal of Molecular Liquid*, vol. 187, pp. 287-293, 2013.

[9] V. Bhardwaj, P. Sharma, M.S. Chauhan, and S. Chauhan, "Micellization, interaction and thermodynamic study of butylated hydroxyanisole (synthetic antioxidant) and sodium dodecyl sulfate in aqueous-ethanol solution at 25, 30 and 35 °C," *In press-Journal of Saudi Chemical society*. (http://dx.doi.org/10.1016/j.jscs.2012.09.008)

[10] V. Bhardwaj, P. Sharma, and S. Chauhan, "Impact of BHA and SDS: A thermo-acoustic exploration for utilization in gel formulation," *Abstract*, ISBN: 978-986-89298-2-1.

Publications in DST Funded Project in Addition to PhD Thesis:

[1] V. Bhardwaj, T. Bhardwaj, K. Sharma, A. Gupta, S. Chauhan, S. S. Cameotra, S. Sharma, R. Gupta, and P. Sharma, "Drug – surfactant interaction: Thermo-acoustic investigation of sodium dodecyl sulfate and antimicrobial drug (Levofloxacin) for potential pharmaceutical application," *RSC Advances*, vol. 4, pp. 24935-24943, 2014.

[2] T. Bhardwaj, V. Bhardwaj, K. Sharma, A. Gupta, S. S. Cameotra, P. Sharma, "Thermo-acoustical analysis of sodium dodecyl sulfate – Fluconazole (antifungal drug) based micellar system in hydro-ethanol solutions for potential drug's topical application" *Journal of Chemical Thermodynamics*, vol. 78, pp. 1-6, 2014.

List of Conferences

1. APICENS-2013, "*Asia-Pacific Congress on Engineering and Natural Sciences*" held at Landmark, Thailand (16-18, April 2013). **ORAL PRESENTATION**

2. AICTE sponsored national conference on "*Advancement, Challenges & Opportunities in Pharmaceutical Research*" held at ASBASJSM College of Pharmacy, Bela, Ropar, Punjab, India. Poster Presentation (October 18-20, 2013)

3. GTU sponsored international conference on "*Emerging Trends in Drug Research and Development*" held at Shree Dhanvantary Pharmacy College, KIM, Surat, Gujarat, India (30-31, March 2013).

4. AICTE sponsored international conference on "*Recent Advances in Pharmaceutical Sciences*" held at Rayat Institute of Pharmacy, SBS Nagar, Punjab, India (21-23 March 2012)

5. National conference on "*Recent Trends in Materials science*" held at Jaypee University of Information Technology, Solan, Himachal Pradesh, India (8-10, October, 2011)

6. National conference "*Chemical Constellation Cheminar*" held at National Institute of Technology, Jalandhar, Punjab, India (20-21, August, 2011).

AWARDS

1. Young scientist International Travel Grant (DST) (March 10, 2013).

2. 1st Award for "Best Research-Poster Presentation" (March 31, 2013).

3. 3rd Award for "Best Research-Poster Presentation" (March 23, 2012).

APPENDICES


8.2231
8.2197
8.2033
8.1999
7.8404
7.8217
7.8218
7.8200
7.8169
7.8149
7.7981
7.7182
7.7011
7.7065
7.7039
7.7021
7.7022
7.5526
7.5057
7.4885
7.4848
7.3736
7.3733
7.3646
7.3632
7.2887
7.2854
6.6283
6.6238
6.6214
2.1726
0.0008
OBn
OBn
BnO
H
H
H
H
O
OBn
1.01
1.06
2.03
0.97
1.00
1.00
10
9
8
7
6
5
4
3
2
1
0

A1 Specific conductance (μS cm^{-1}) of SDS in presence of BHA (0.03 mol kg^{-1}) at temperature T = 25, 30 and 35 °C.

[SDS]	MeOH 100% (v/v)			MeOH 70% (v/v)			MeOH 30% (v/v)		
mmol kg^{-1}	25 °C	30 °C	35 °C	25 °C	30 °C	35 °C	25 °C	30 °C	35 °C
1.0	22.1	28.4	33.5	38.2	46.5	53.4	50.1	52.2	53.8
2.0	52.4	58.3	63.4	68.5	76.3	80.5	84.4	89.3	92.6
3.0	76.8	82.6	93.2	92.8	98.7	103.8	117.3	120.5	124.8
4.0	103.7	109.2	121.3	114.6	120.8	128.5	150.1	155.8	160.7
5.0	123.9	136.5	145.6	132.8	142.6	149.8	174.8	180.3	195.4
6.0	140.2	158.1	166.8	148.5	166.2	174.5	193.4	203	216
7.0	155.3	175.3	188.4	168.9	187.4	194.1	208	216	233
8.0	170.2	188.2	202	184.3	197.9	210	223	231	247
9.0	186.0	202	217	204	220	230	237	245	265
10.0	200	217	232	218	236	248	253	264	284
11.0	214	231	247	230	248	260	273	284	303
12.0	230	245	258	247	262	276	290	301	320
13.0	243	262	275	256	277	289	307	318	337
14.0	256	275	291	265	288	301	322	336	354
	EtOH 100% (v/v)			**EtOH 70% (v/v)**			**EtOH 30% (v/v)**		
1.0	18.3	21.4	23.5	23.2	25.3	27.1	31.8	34.6	36.5
2.0	34.2	37.5	40.3	43.1	46.6	49.4	55.8	65.5	69.5
3.0	52.1	54.3	56.7	56.4	65.1	71.2	79.6	83.4	88.2
4.0	65.7	70.1	75.6	70.4	80.3	87.7	96.4	107.2	112.2
5.0	78.3	84.4	88.9	85.1	96.6	104.3	116.6	125.4	132.1
6.0	90.1	96.7	102.3	103.5	114.2	121.7	129.5	144.0	155.2
7.0	101.5	112.3	114.5	113.2	127.7	139.3	146.6	161.2	173.3
8.0	107.4	119.2	124.6	124.5	136.3	152.8	159.1	174.7	189.6
9.0	117.3	130.1	135.6	135.2	147.7	166.3	178.4	195.5	210.3
10.0	127.5	139.2	144.3	146.7	161.5	179.2	198.3	218.2	234.6
11.0	137.5	151.4	156.4	156.4	171.2	193.7	216.6	238.6	255.4
12.0	148.4	162.6	170.1	166.6	183.4	206.3	226.3	250.3	270.2
13.0	154.2	170.1	179.6	177.2	197.1	219.8	236.2	259.3	282.6
14.0	165.3	179.8	190.3	185.5	208.2	234.3	250.6	274.7	298.3
	1-PrOH 100% (v/v)			**1-PrOH 70% (v/v)**			**1-PrOH 30% (v/v)**		
1.0	15.3	18.3	21.2	20.2	21.3	23.4	30.2	34.4	36.5
2.0	29.8	34.5	40.3	38.2	39.2	43.5	50.4	55.0	56.8
3.0	45.6	51.2	57.4	51.5	55.4	59.3	71.2	75.1	77.1
4.0	60.3	66.8	74.3	68.7	72.7	79.1	91.3	96.4	98.2
5.0	70.2	78.5	91.2	79.4	88.4	94.5	102.2	107.0	109.1
6.0	80.4	89.5	101.2	88.9	98.3	107.5	122.2	126.1	129.3
7.0	90.7	98.6	111.4	101.5	110.1	116.3	138.1	142.2	146.0
8.0	99.9	108.4	122.3	111.8	121.2	127.3	154.3	156.2	160.1
9.0	109.6	117.6	132.5	120.2	134.1	138.2	163.4	166.1	171.3
10.0	117.3	128.1	141.9	130.4	144.1	149.2	178.1	181.3	186.2
11.0	128.9	137.8	151.6	140.9	154.9	160.5	188.2	191.3	196.1
12.0	138.5	147.5	160.9	149.7	163.3	170.7	199.3	201	205
13.0	148.4	156.9	170.5	158.3	173.5	180.1	208	211	215
14.0	157.9	166.1	179.9	165.4	185.5	191.2	218	220	225

A2 Specific conductance (μS cm^{-1}) of SDS in presence of BHT (0.02 mol kg^{-1}) at temperature T = 25, 30 and 35 °C.

[SDS]	MeOH 100% (v/v)			MeOH 70% (v/v)			MeOH 30% (v/v)		
mmol kg^{-1}	25 °C	30 °C	35 °C	25 °C	30 °C	35 °C	25 °C	30 °C	35 °C
1.0	18.3	23.4	28.6	32.4	42.3	48.9	40.3	45.6	50.2
2.0	47.5	52.1	58.7	52.5	61.9	70.2	70.5	75.3	80.5
3.0	72.3	76.7	86.5	71.9	82.1	92.1	100.2	105.4	110.3
4.0	99.6	101.5	111.2	91.4	102.3	114.5	130.2	135.8	142.3
5.0	120.3	126.3	137.4	111.2	123.4	138.3	159.8	168.5	171.8
6.0	136.4	143.6	161.6	129.1	142.3	159.2	185.6	193.3	198.4
7.0	148.1	158.9	175.8	142.5	154.5	177.5	195.8	207	219
8.0	162.4	173.5	190.2	154.3	167.1	190.2	208	221	232
9.0	177.5	188.4	205	166.4	180.2	203	218	236	248
10.0	191.5	202	219	178.2	193.5	215	233	251	262
11.0	204	219	233	191.3	206	227	245	265	278
12.0	217	234	247	204	219	239	256	281	293
13.0	231	247	261	216	232	252	264	297	309
14.0	247	262	275	228	245	265	275	309	323
	EtOH 100% (v/v)			**EtOH 70% (v/v)**			**EtOH 30% (v/v)**		
1.0	18.6	18.8	19.1	22.1	27.5	31.2	29.4	33.3	37.2
2.0	28.8	30.8	32.2	38.3	44.3	50.1	56.5	59.4	66.8
3.0	42.6	44.8	48.5	52.6	58.4	65.3	79.2	83.5	93.2
4.0	55.5	57.1	58.4	64.5	71.1	78.9	98.5	108.5	115.1
5.0	64.2	65.3	69.6	79.4	85.4	93.1	114.3	129.9	138.6
6.0	70.5	75.2	79.4	91.5	97.5	106.3	133.2	145.3	156.5
7.0	90.2	92.2	97.1	100.2	109.2	123.4	147.5	164.3	174.7
8.0	99.7	103.4	106.6	109.3	117.9	133.2	162.1	178.1	190.5
9.0	103.1	106.5	112.8	120.1	127.5	145.3	174.2	188.3	201
10.0	108.6	114.4	119.6	129.8	138.1	155.5	184.4	201	215
11.0	114.5	118.9	124.5	141.5	147.9	168.6	192.6	215	228
12.0	118.5	124.8	130.7	152.4	158.2	179.3	207	229	245
13.0	124.2	130.9	136.2	163.5	172.5	188.3	217	241	258
14.0	130.2	136.9	142.5	172.4	180.5	197.6	227	252	271
	1-PrOH 100% (v/v)			**1-PrOH 70% (v/v)**			**1-PrOH 30% (v/v)**		
1.0	10.3	15.5	18.4	13.4	17.8	21.1	22.5	29.5	32.4
2.0	25.4	29.9	34.2	28.6	33.4	36.7	45.2	50.2	52.6
3.0	40.2	44.5	50.1	43.8	46.5	52.1	67.5	69.6	74.5
4.0	55.1	59.7	65.4	58.5	62.7	68.3	88.1	88.7	92.3
5.0	64.7	71.1	80.3	73.4	77.5	87.5	101.3	106.3	114.5
6.0	74.9	81.2	92.6	82.4	90.3	103.4	111.3	118.2	125.6
7.0	84.1	90.8	102.1	91.6	100.1	111.6	127.5	129.6	137.3
8.0	93.8	99.7	111.8	100.1	110.2	119.4	140.2	143.5	150.5
9.0	103.4	109.1	121.3	109.3	119.3	128.1	153.4	158.6	163.4
10.0	112.8	119.3	130.9	118.2	128.7	137.3	169.2	172.4	177.8
11.0	122.1	128.9	139.7	128.1	137.8	146.5	181.2	185.6	190.2
12.0	131.5	137.8	149.2	137.5	146.5	155.2	194.3	197.5	202
13.0	140.2	146.9	158.6	146.3	155.4	164.7	207	209	213
14.0	149.3	155.7	167.8	155.4	164.3	173.1	215	218	222

A3 Specific conductance (μS cm^{-1}) of CTAB in presence of BHA (0.03 mol kg^{-1}) at temperature T = 25, 30 and 35 °C.

[CTAB]	MeOH 100% (v/v)			MeOH 70% (v/v)			MeOH 30% (v/v)		
mmol kg^{-1}	25 °C	30 °C	35 °C	25 °C	30 °C	35 °C	25 °C	30 °C	35 °C
0.1	4.2	6.5	9.2	12.3	16.2	20.1	22.5	26.3	31.2
0.2	15.6	17.6	20.5	24.1	28.4	32.6	35.3	38.1	44.5
0.3	25.2	28.7	31.6	36.5	40.6	44.2	48.6	50.2	58.5
0.4	36.4	41.3	43.7	48.2	52.1	55.3	61.2	63.8	70.1
0.5	45.7	52.4	55.3	60.9	64.3	67.6	72.9	76.5	82.6
0.6	56.3	63.5	67.1	72.6	76.6	79.2	84.6	88.3	93.2
0.7	64.4	72.8	79.3	84.1	88.1	90.2	95.6	101.3	104.9
0.8	72.2	79.6	88.5	92.2	96.5	101.6	104.3	112.4	116.1
0.9	79.5	87.5	96.5	100.2	104.2	110.5	111.6	121.2	126.5
1.0	87.4	95.6	104.8	107.6	112.4	119.8	116.3	127.5	134.6
1.1	94.3	102.2	112.6	113.6	120.5	128.1	121.5	134.4	141.3
1.2	99.9	109.4	119.5	120.3	128.3	136.7	127.4	141.6	148.3
1.3	105.4	116.4	126.4	126.4	135.4	144.5	133.4	148.6	153.9
1.4	111.9	122.6	133.2	132.2	141.7	153.4	139.6	154.3	160.1
1.5	117.8	128.3	139.6	138.1	148.5	160.1	144.8	160.5	166.3
1.6	123.4	134.1	145.4	143.9	155.3	166.9	149.5	166.1	171.8
1.7	128.1	140.3	150.9	148.8	161.4	174.5	155.3	172.9	176.9
1.8	132.5	145.9	155.8	153.1	165.8	180.8	161.2	180.2	184.6
	EtOH 100% (v/v)			EtOH 70% (v/v)			EtOH 30% (v/v)		
0.1	10.6	13.7	17.8	22.3	26.7	30.5	40.8	43.4	47.2
0.2	20.8	24.9	27.1	34.2	38.6	43.4	50.4	53.3	57.2
0.3	30.2	35.4	39.6	45.6	48.9	55.2	60.1	65.7	69.0
0.4	40.7	46.9	50.0	56.8	60.4	65.9	70.8	76.2	80.3
0.5	50.6	57.1	62.3	67.4	72.6	77.5	80.0	87.3	92.8
0.6	61.3	67.4	72.7	77.3	83.3	89.2	90.6	98.4	103.8
0.7	70.5	78.0	84.0	86.1	93.4	100.3	100.1	109.1	115.3
0.8	78.8	88.1	95.4	94.7	103.5	112.4	109.4	118.8	127.4
0.9	85.8	97.6	105.9	102.8	111.4	122.6	115.9	126.4	138.2
1.0	92.8	104.9	112.2	110.8	120.6	131.3	121.7	132.5	144.7
1.1	98.9	110.4	119.7	116.9	129.5	138.7	128.4	140.4	152.2
1.2	105.7	117.8	127.2	123.1	137.9	145.8	135.3	148.2	159.8
1.3	111.6	123.5	132.8	129.8	144.2	153.1	141.8	156.2	168.4
1.4	117.3	128.1	140.4	135.7	151.3	160.4	149.3	164.6	177.2
1.5	123.8	134.7	146.0	142.3	158.7	167.7	158.2	174.3	186.1
1.6	127.4	140.8	151.4	148.2	165.1	175.7	167.9	183.2	195.4
1.7	132.7	145.4	157.1	154.1	172.6	182.6	176.6	191.2	203.1
1.8	138.5	150.3	163.6	160.3	179.4	189.3	185.7	200.9	211.2
	1-PrOH 100% (v/v)			1-PrOH 70% (v/v)			1-PrOH 30% (v/v)		
0.1	4.1	5.2	7.9	7.2	10.5	13.6	9.5	13.4	15.9
0.2	12.3	13.2	15.9	15.3	18.5	21.5	18.2	21.4	24.5
0.3	20.4	22.1	25.1	23.5	26.3	29.5	27.5	30.2	33.7
0.4	28.6	29.8	33.2	30.5	33.4	37.8	36.4	39.1	42.6
0.5	36.4	38.1	42.5	38.9	41.5	46.6	45.3	47.8	51.8
0.6	44.2	46.2	51.3	47.1	50.2	54.8	54.6	56.6	61.1
0.7	50.1	52.3	58.2	55.4	58.4	63.5	63.1	65.8	70.7
0.8	55.4	58.5	64.5	61.3	63.9	70.8	69.4	73.2	79.5
0.9	60.6	63.6	70.2	67.4	70.2	76.4	75.6	79.1	86.4
1.0	65.3	69.1	76.8	73.5	76.4	82.6	81.3	85.6	93.6
1.1	69.9	75.1	82.5	79.5	81.6	88.5	87.4	91.2	99.5
1.2	75.6	80.6	88.6	86.4	89.1	94.3	93.5	98.2	106.2
1.3	80.1	85.3	94.5	92.4	95.4	101.0	99.1	103.9	112.3
1.4	84.9	91.1	100.2	98.8	101.6	107.3	105.2	109.5	118.5
1.5	89.8	95.9	106.5	104.6	107.1	113.6	111.4	115.1	124.1
1.6	95.2	101	111.4	110.5	113.4	118.9	116.8	121.5	129.9
1.7	100.6	106.2	116.3	116.4	119.5	125.3	122.3	126.9	136.5
1.8	105.2	111.0	121.2	122.3	125.8	131.4	128.2	131.6	142.1

A4 Specific conductance (μS cm^{-1}) of CTAB in presence of BHT (0.02 mol kg^{-1}) at temperature T = 25, 30 and 35 °C.

[CTAB]	MeOH 100% (v/v)			MeOH 70% (v/v)			MeOH 30% (v/v)		
mmol kg^{-1}	25 °C	30 °C	35 °C	25 °C	30 °C	35 °C	25 °C	30 °C	35 °C
0.1	2.25	3.95	8.16	7.36	11.3	15.2	16.2	19.1	25.3
0.2	11.25	13.26	18.26	18.4	22.3	27.1	28.4	30.8	37.2
0.3	20.32	23.4	27.99	29.1	34.5	38.8	41.1	42.9	49.5
0.4	29.98	33.46	38.1	40.3	45.8	49.6	53.6	55.9	61.4
0.5	39.26	44.1	48.62	51.6	56.9	60.5	64.5	69.5	72.5
0.6	48.99	54.62	58.17	61.9	67.1	71.2	75.3	81.2	83.9
0.7	59.65	64.35	69.1	72.3	78.6	82.5	86.4	93.4	97.6
0.8	67.56	71.89	79.2	80.6	87.1	92.1	95.3	103.3	107.8
0.9	74.32	79.84	86.34	88.2	95.3	100.1	103.4	111.5	115.6
1.0	80.36	86.45	93.15	96.3	103.2	107.5	110.2	119.4	122.2
1.1	86.49	91.99	99.91	102.4	110.5	114.7	116.7	127.6	131.9
1.2	92.31	98.1	106.3	109.6	117.4	121.4	122.1	134.5	138.2
1.3	97.98	105.1	113.4	116.4	124.2	128.3	128.3	141.9	146.5
1.4	104.2	112.3	120.2	122.9	131.1	135.6	134.5	148.8	152.2
1.5	110.3	119.5	126.8	130.1	138.6	141.9	140.3	154.7	160.3
1.6	115.8	126.2	133.1	137.2	145.1	149.2	146.1	160.4	166.9
1.7	122.1	133.4	139.8	144.6	152.3	156.1	150.9	165.8	173.1
1.8	128.3	140.2	147.2	151.8	159.5	162.4	155.8	171.9	178.8
	EtOH 100% (v/v)			**EtOH 70% (v/v)**			**EtOH 30% (v/v)**		
0.1	6.35	9.35	12.3	9.25	13.5	16.6	12.3	16.8	20.3
0.2	16.3	18.8	22.3	19.3	23.3	28.1	26.3	30.6	34.0
0.3	25.3	29.1	32.5	30.6	34.6	39.8	38.6	44.3	48.3
0.4	35.4	38.9	43.1	41.3	44.5	50.3	50.3	55.6	61.2
0.5	46.1	48.4	54.6	51.6	54.8	61.8	62.6	67.3	73.5
0.6	56.3	58.5	65.4	60.5	65.1	73.1	73.7	79.4	85.3
0.7	63.3	68.1	75.6	68.6	73.2	83.5	83.6	90.3	96.1
0.8	69.4	76.1	85.3	76.2	81.2	91.5	91.3	98.6	107.1
0.9	75.1	82.9	92.3	83.4	88.8	99.5	101.3	107.3	117.2
1.0	81.6	88.2	99.6	89.9	94.5	107.4	110.3	115.9	125.3
1.1	87.1	94.6	106.1	96.7	100.9	114.6	118.9	123.1	133.4
1.2	92.5	100.0	112.6	103.5	106.4	121.1	127.6	132.9	141.5
1.3	97.1	106.3	118.5	110.6	113.1	128.3	134.3	140.3	149.3
1.4	102.6	112.4	124.2	116.3	120.3	134.7	141.4	148.1	157.5
1.5	107.4	118.3	130.2	122.6	126.4	142.3	146.9	155.9	163.9
1.6	113.2	123.8	135.4	127.9	131.9	148.1	153.1	162.7	170.7
1.7	119.1	129.9	140.2	132.8	137.1	153.8	160.2	169.5	177.4
1.8	124.8	135.6	145.9	137.7	142.8	159.6	165.8	176.4	184.6
	1-PrOH 100% (v/v)			**1-PrOH 70% (v/v)**			**1-PrOH 30% (v/v)**		
0.1	2.12	3.91	5.82	3.23	5.16	8.35	7.83	10.6	12.5
0.2	9.5	11.2	12.7	10.3	13.4	16.6	16.5	19.1	21.4
0.3	17.6	19.1	20.6	18.5	22.1	24.3	25.6	28.4	30.2
0.4	25.8	27.6	28.6	26.1	31.3	34.1	33.9	37.4	39.4
0.5	33.7	35.2	36.8	34.6	40.2	43.7	43.1	45.9	48.5
0.6	41.9	42.7	44.6	42.8	49.2	52.1	52.4	54.3	57.4
0.7	47.3	49.8	52.7	48.2	56.3	61.6	61.3	63.4	66.4
0.8	53.1	55.2	59.8	54.6	62.4	69.5	68.4	71.5	74.6
0.9	58.3	60.8	65.1	60.2	68.6	75.4	73.1	77.6	80.4
1.0	63.8	65.9	70.1	66.3	74.5	80.9	79.5	83.4	87.6
1.1	68.9	71.5	75.9	72.1	79.7	86.4	84.9	89.5	93.5
1.2	73.2	76.8	81.6	78.3	85.6	92.6	90.3	95.4	99.4
1.3	78.5	81.3	86.8	83.9	91.4	99.5	96.4	101.3	105.6
1.4	82.3	86.5	91.3	90.1	97.5	105.7	101.2	107.8	111.5
1.5	86.8	91.3	96.9	96.2	103.2	111.1	107.6	113.4	117.6
1.6	91.2	96.4	102.3	102.3	109.1	116.8	113.2	119.5	123.1
1.7	96.5	101.3	108.6	108.4	115.6	122.3	119.5	124.8	129.2
1.8	99.9	105.9	114.1	113.9	121.4	129.1	124.9	130.4	135.8

A5 Specific conductance ($\mu S\ cm^{-1}$) of TX 100 in presence of BHA (0.03 mol kg^{-1}) at temperature T = 25, 30 and 35 °C.

[TX100]	MeOH 100% (v/v)			MeOH 70% (v/v)			MeOH 30% (v/v)		
mmol kg^{-1}	25 °C	30 °C	35 °C	25 °C	30 °C	35 °C	25 °C	30 °C	35 °C
0.050	10.4	11.2	12.4	14.5	16.1	18.2	19.8	21.9	23.2
0.075	15.6	16.5	17.4	20.7	22.6	24.8	26.5	28.6	30.6
0.100	20.3	22.1	23.4	26.8	28.2	30.7	33.5	35.6	37.8
0.125	25.5	27.1	28.8	32.4	34.1	37.1	40.4	42.4	44.7
0.150	30.1	32.9	34.1	38.5	40.3	43.6	46.9	49.5	51.6
0.175	33.3	36.4	38.5	42.1	44.6	49.5	54.1	56.4	58.5
0.200	36.1	39.6	42.4	46.2	48.5	53.8	60.5	62.2	64.6
0.225	38.7	42.1	45.5	49.5	51.6	56.7	64.6	66.4	69.5
0.250	41.3	45.1	48.2	52.3	54.3	59.5	68.5	70.4	73.6
0.275	43.4	48.3	51.6	55.4	58.3	62.4	72.3	74.5	77.5
0.300	46.1	51.4	54.5	58.9	61.4	65.3	76.1	78.5	81.2
0.325	48.8	54.2	57.1	62.1	64.2	68.4	80.4	82.3	85.4
0.350	50.8	56.8	60.3	65.6	67.5	71.6	84.3	86.4	89.2
0.375	53.1	58.9	63.1	68.4	70.6	74.5	88.2	90.1	93.1
0.400	55.4	61.4	65.9	71.8	73.3	78.1	92.1	93.9	97.4
0.425	58.3	64.1	69.1	74.9	76.4	81.9	96.4	98	101.6
0.450	60.2	66.3	71.8	78.1	79.1	84.6	100.1	102.3	104.8
0.475	62.4	68.4	74.7	81.2	82.6	87.5	103.9	105.9	108.1
	EtOH 100% (v/v)			EtOH 70% (v/v)			EtOH 30% (v/v)		
0.050	3.6	4.5	5.1	7.5	9.4	11.2	10.2	13.6	16.1
0.075	8.5	9.4	10.6	13.6	16.1	18.3	16.5	19.8	23.7
0.100	13.7	14.6	15.4	19.7	22.6	24.6	22.3	25.7	29.5
0.125	18.6	19.5	20.6	25.8	28.6	30.7	28.4	31.5	36.4
0.150	22.8	23.4	25.5	31.6	34.7	36.5	34.6	37.6	43.5
0.175	26.4	27.6	30.3	36.4	39.7	42.3	40.5	43.4	50.2
0.200	28.7	30.1	34.6	40.5	44.2	47.4	46.5	49.6	56.4
0.225	31.2	33.2	37.7	43.6	47.5	51.3	50.2	53.7	62.5
0.250	33.1	36.5	40.2	46.9	50.3	54.6	54.3	56.4	65.6
0.275	36.4	39.4	43.1	49.5	53.6	57.5	58.1	60.4	68.5
0.300	38.9	43.2	46.2	52.4	56.4	60.3	61.9	64.5	73.1
0.325	42.5	45.9	48.9	55.6	59.1	63.4	65.7	68.4	76.5
0.350	44.9	48.6	52.1	58.3	62.5	66.5	69.5	72.6	79.6
0.375	46.7	50.6	55.2	61.2	65.4	69.4	72.8	75.4	82.4
0.400	48.8	52.8	57.8	64.3	68.1	72.5	75.9	78.7	85.7
0.425	50.5	54.7	60	67.1	71.2	75.5	78.7	81.3	89.6
0.450	52.4	56.9	62.7	70.3	73.9	78.1	81.6	84.2	92.3
0.475	54.2	58.6	64.8	73.2	76.8	81.2	84.7	87.9	95.4
	1-PrOH 100% (v/v)			1-PrOH 70% (v/v)			1-PrOH 30% (v/v)		
0.050	0.44	0.54	0.55	0.78	0.91	1.14	1.28	1.65	2.26
0.075	1.43	1.56	1.58	1.81	1.93	2.18	2.31	2.68	3.31
0.100	2.46	2.52	2.63	2.79	2.92	3.21	3.34	3.71	4.32
0.125	3.39	3.48	3.58	3.77	3.89	4.22	4.41	4.74	5.36
0.150	4.34	4.44	4.56	4.76	4.86	5.24	5.46	5.77	6.41
0.175	4.78	5.12	5.32	5.52	5.68	6.06	6.48	6.79	7.42
0.200	5.16	5.53	5.74	5.96	6.32	6.86	7.34	7.68	8.23
0.225	5.53	5.92	6.21	6.38	6.75	7.35	8.10	8.42	9.08
0.250	5.91	6.35	6.62	6.77	7.12	7.71	8.62	8.93	9.56
0.275	6.32	6.72	7.06	7.06	7.53	8.05	9.12	9.34	10.05
0.300	6.73	7.13	7.46	7.41	7.91	8.41	9.51	9.76	10.57
0.325	7.11	7.51	7.85	7.71	8.32	8.84	9.99	10.25	11.01
0.350	7.48	7.93	8.23	8.03	8.73	9.21	10.48	10.67	11.52
0.375	7.86	8.35	8.67	8.35	9.12	9.56	10.97	11.21	11.99
0.400	8.17	8.71	9.06	8.68	9.39	9.92	11.45	11.69	12.49
0.425	8.55	9.14	9.49	8.99	9.78	10.31	11.92	12.18	12.98
0.450	8.93	9.46	9.98	9.34	10.02	10.66	12.39	12.63	13.47
0.475	9.26	9.76	10.4	9.62	10.33	11.01	12.88	13.12	13.92

A6 Specific conductance (μS cm^{-1}) of TX 100 in presence of BHT (0.02 mol kg^{-1}) at temperature T = 25, 30 and 35 °C.

[TX100]	MeOH 100% (v/v)			MeOH 70% (v/v)			MeOH 30% (v/v)		
mmol kg^{-1}	25 °C	30 °C	35 °C	25 °C	30 °C	35 °C	25 °C	30 °C	35 °C
0.050	7.51	9.83	11.4	10.6	13.5	16.1	15.5	17.6	20.3
0.075	12.9	15.2	16.5	16.7	19.4	22.1	22.2	24.5	27.4
0.100	17.6	20.3	21.6	22.8	25.6	28.5	29.5	31.5	34.5
0.125	22.4	25.4	26.7	28.6	31.2	34.6	36.8	38.6	41.2
0.150	27.6	30.5	31.8	34.7	37.5	40.2	43.2	45.7	48.5
0.175	31.2	34.6	36.6	40.8	42.8	46.2	48.9	52.4	55.5
0.200	33.8	38.4	40.5	44.6	46.8	50.9	54.5	59.6	62.8
0.225	36.6	41.2	43.2	47.9	50.2	54.7	58.4	63.5	67.8
0.250	39.4	44.3	46.8	50.5	53.1	57.9	62.1	67.8	71.5
0.275	42.2	47.1	49.6	53.2	56.2	60.4	66.1	71.8	75.5
0.300	44.6	49.8	52.5	56.4	59.4	63.8	70.5	75.6	79.6
0.325	46.8	51.9	55.8	59.6	62.6	66.5	74.4	79.4	83.4
0.350	49.2	54.1	58.6	62.3	65.3	69.4	78.3	83.5	87.7
0.375	51.8	57.2	61.5	65.1	68.5	72.3	82.5	87.2	91.8
0.400	54.2	59.5	64.2	68.4	71.2	75.2	86.7	91.1	95.7
0.425	56.7	62.2	67	71.2	74.6	78.1	90.8	95.5	99.6
0.450	58.9	64.7	69.5	74.6	77.2	80.2	94.5	99.2	103.2
0.475	60.8	66.9	72.1	77.2	80.1	83.5	98.7	103.1	106.5
	EtOH 100% (v/v)			EtOH 70% (v/v)			EtOH 30% (v/v)		
0.050	2.59	3.26	4.15	3.82	7.62	9.85	7.81	11.22	14.5
0.075	7.51	8.15	8.63	10.2	13.8	16.5	14.1	18.1	20.7
0.100	12.3	12.3	13.4	17.4	19.5	23.1	21.4	24.2	26.7
0.125	16.9	17.5	19.1	23.6	26.4	29.5	27.5	30.5	33.2
0.150	21.3	22.1	24.4	30.2	33.2	35.4	33.1	36.5	40.1
0.175	24.2	25.6	29.2	34.9	38.1	41.6	38.8	42.1	46.7
0.200	26.8	28.4	32.7	38.5	42.1	45.8	44.9	47.9	52.3
0.225	29.5	31.5	35.9	41.8	45.8	49.6	48.9	52.5	58.5
0.250	32.3	34.6	38.7	44.4	48.9	52.7	52.1	55.6	62.4
0.275	34.6	37.4	41.7	47.1	51.1	55.3	56.3	59.5	66.7
0.300	36.8	40.1	44.3	50.2	54.2	58.4	59.8	63.4	70.6
0.325	38.9	43.2	47.1	53.4	57.4	61.6	63.5	67.1	73.5
0.350	41.1	46.4	50.3	55.9	60.2	64.7	66.1	70.5	77.1
0.375	43.2	48.8	53.6	59.2	63.4	67.5	68.9	73.2	80.1
0.400	45.4	50.9	56.1	61.8	66.2	70.4	71.8	76.1	83.6
0.425	47.6	53.8	58.9	63.7	68.8	73.2	74.5	79.5	86.7
0.450	49.3	55.9	61.1	66.1	71.7	76.5	78.2	82.4	89.9
0.475	51.4	57.9	63.5	69.4	73.9	79.1	81.2	85.5	92.5
	1-PrOH 100% (v/v)			1-PrOH 70% (v/v)			1-PrOH 30% (v/v)		
0.050	0.31	0.42	0.49	0.51	0.76	0.81	0.89	1.45	1.96
0.075	1.21	1.32	1.39	1.63	1.81	1.89	1.85	2.39	2.88
0.100	2.12	2.36	2.51	2.58	2.83	2.91	2.91	3.35	3.85
0.125	3.03	3.25	3.45	3.59	3.72	3.93	3.88	4.31	4.83
0.150	3.96	4.25	4.39	4.55	4.71	4.86	4.83	5.28	5.79
0.175	4.61	4.91	5.14	5.33	5.55	5.79	5.79	6.27	6.74
0.200	5.04	5.28	5.67	5.78	6.21	6.68	6.58	7.25	7.77
0.225	5.39	5.71	6.01	6.16	6.62	7.12	7.12	7.91	8.69
0.250	5.81	6.14	6.43	6.51	7.01	7.51	7.53	8.39	9.11
0.275	6.15	6.49	6.82	6.83	7.42	7.92	8.01	8.79	9.42
0.300	6.57	6.91	7.21	7.18	7.79	8.29	8.51	9.22	9.86
0.325	6.95	7.28	7.63	7.48	8.14	8.66	9.02	9.63	10.39
0.350	7.31	7.73	7.99	7.79	8.52	9.03	9.49	10.02	10.84
0.375	7.68	8.08	8.43	8.08	8.94	9.39	9.98	10.45	11.26
0.400	7.98	8.47	8.82	8.47	9.24	9.75	10.46	10.87	11.65
0.425	8.31	8.89	9.24	8.76	9.63	10.11	10.92	11.35	12.02
0.450	8.75	9.18	9.68	9.05	9.91	10.49	11.41	11.77	12.41
0.475	9.09	9.49	10.06	9.43	10.19	10.91	11.89	12.28	12.84

A7 Density, ρ (kgm^{-3}), ultrasonic velocity, u (ms^{-1}) and Isentropic Compressibility, κ_S (TPa^{-1}) of SDS (2.0–14.0 mmol kg^{-1}) in water-methanol compositions (% v/v) of 0.03 mol kg^{-1} BHA over three different temperatures.

[SDS] mmol kg^{-1}	100% Methanol			70% Methanol			30% Methanol		
	25 °C	30 °C	35 °C	25 °C	30 °C	35 °C	25 °C	30 °C	35 °C
				ρ (kgm^{-3})					
2.0	802.515	798.169	794.008	876.382	870.158	864.505	927.781	921.568	917.201
4.0	803.201	798.850	794.766	877.432	871.554	865.758	928.654	922.483	918.584
6.0	802.994	798.634	794.450	877.348	871.304	865.548	928.848	922.754	918.794
8.0	803.074	798.664	794.756	877.526	871.355	865.405	928.491	922.468	918.395
10.0	802.281	798.216	794.104	877.018	870.991	865.398	928.355	922.485	918.265
12.0	801.821	797.789	793.705	877.181	870.979	865.284	928.351	922.499	918.146
14.0	801.825	797.770	793.682	877.032	870.977	865.286	928.255	922.399	918.218
				u (ms^{-1})					
2.0	1211.54	1194.52	1179.51	1304.70	1282.68	1262.55	1553.89	1547.65	1541.51
4.0	1209.49	1192.70	1175.75	1304.78	1282.99	1262.68	1553.75	1547.85	1541.61
6.0	1209.75	1192.75	1175.78	1304.91	1283.10	1262.75	1553.68	1547.98	1541.78
8.0	1209.42	1192.49	1175.53	1305.08	1283.16	1262.84	1553.64	1548.18	1541.89
10.0	1213.25	1196.23	1179.20	1305.12	1283.14	1262.79	1553.75	1548.20	1541.84
12.0	1208.84	1191.89	1174.89	1306.03	1283.19	1262.80	1553.71	1548.16	1541.86
14.0	1209.22	1192.22	1175.21	1306.01	1283.17	1262.83	1553.78	1548.22	1541.91
				κ_S TPa^{-1} × 10^{-10}					
2.0	8.489	8.780	9.052	6.703	6.984	7.256	4.464	4.530	4.588
4.0	8.510	8.799	9.101	6.694	6.970	7.245	4.461	4.525	4.581
6.0	8.509	8.801	9.105	6.693	6.971	7.245	4.460	4.523	4.578
8.0	8.513	8.804	9.105	6.691	6.971	7.246	4.461	4.522	4.580
10.0	8.467	8.754	9.056	6.694	6.973	7.246	4.461	4.522	4.581
12.0	8.534	8.823	9.127	6.683	6.972	7.247	4.462	4.522	4.581
14.0	8.529	8.818	9.122	6.684	6.973	7.246	4.462	4.522	4.580

Standard uncertainties in ρ, u and κ_S are ± 4×10^{-3} kgm^{-3}, ± 0.5 ms^{-1} and ±0.02× 10^{-10} TPa^{-1}.

A8 Density, ρ (kgm^{-3}), ultrasonic velocity, u (ms^{-1}) and Isentropic Compressibility, K_S (TPa^{-1}) of SDS (2.0–14.0 mmol kg^{-1}) in water-methanol compositions (% v/v) of 0.02 mol kg^{-1} BHT over three different temperatures.

[SDS] mmol kg^{-1}	100% Methanol			70% Methanol			30% Methanol		
	25 °C	30 °C	35 °C	25 °C	30 °C	35 °C	25 °C	30 °C	35 °C
				ρ (kgm^{-3})					
2.0	806.645	802.913	795.644	886.748	874.543	869.494	934.232	928.444	922.994
4.0	805.324	802.783	795.356	886.382	874.293	869.384	933.938	928.384	922.884
6.0	804.867	802.564	795.212	885.892	873.949	869.192	933.863	928.236	922.763
8.0	804.123	802.231	795.033	885.734	873.854	868.784	933.677	928.093	922.664
10.0	804.324	801.783	794.893	885.342	873.674	868.557	933.454	927.847	922.493
12.0	803.797	801.436	794.564	885.222	873.442	868.432	933.253	927.732	922.228
14.0	803.656	801.122	794.342	885.074	873.282	868.226	933.075	927.646	922.112
				u (ms^{-1})					
2.0	1236.74	1214.68	1196.39	1321.89	1288.32	1268.45	1586.54	1555.11	1545.34
4.0	1236.88	1214.82	1196.44	1321.98	1288.64	1268.56	1586.68	1555.34	1545.42
6.0	1236.99	1215.23	1196.63	1322.14	1288.78	1268.76	1586.79	1555.53	1545.57
8.0	1237.14	1215.36	1196.82	1322.24	1288.83	1268.84	1586.94	1555.67	1545.66
10.0	1237.32	1215.48	1197.14	1322.43	1288.93	1268.99	1587.06	1555.74	1545.78
12.0	1237.56	1215.66	1197.35	1322.65	1288.98	1269.34	1587.25	1555.89	1545.89
14.0	1237.88	1215.82	1197.59	1322.87	1289.09	1269.35	1587.39	1555.96	1545.96
				K_S TPa^{-1} × 10^{-10}					
2.0	8.645	8.807	9.222	6.921	7.143	7.422	4.556	4.643	4.730
4.0	8.653	8.812	9.231	6.924	7.146	7.428	4.558	4.646	4.734
6.0	8.667	8.814	9.235	6.927	7.157	7.430	4.559	4.649	4.738
8.0	8.679	8.817	9.239	6.934	7.164	7.433	4.562	4.653	4.742
10.0	8.683	8.822	9.243	6.937	7.176	7.434	4.564	4.656	4.746
12.0	8.688	8.826	9.246	6.942	7.184	7.438	4.568	4.558	4.754
14.0	8.694	8.834	9.248	6.951	7.185	7.440	4.570	4.562	4.757

Standard uncertainties in ρ, u and K_S are ± 4×10^{-3} kgm^{-3}, ± 0.5 ms^{-1} and ±0.02× 10^{-10} TPa^{-1}.

A9 Density, ρ (kgm^{-3}), ultrasonic velocity, u (ms^{-1}) and Isentropic Compressibility, κ_S (TPa^{-1}) of SDS (2.0–14.0 mmol kg^{-1}) in water-ethanol compositions (% v/v) of 0.03 mol kg^{-1} BHA over three different temperatures.

[SDS] mmol kg^{-1}	100% Ethanol			70% Ethanol			30% Ethanol		
	25 °C	30 °C	35 °C	25 °C	30 °C	35 °C	25 °C	30 °C	35 °C
				ρ (kgm^{-3})					
2.0	788.996	784.327	780.362	878.828	874.804	870.589	955.658	953.109	950.183
4.0	788.845	784.274	779.812	878.495	874.230	869.906	956.883	954.291	951.253
6.0	788.789	784.178	779.747	877.660	873.394	869.067	957.921	954.961	951.868
8.0	788.512	784.169	779.680	877.026	872.758	868.428	957.998	955.044	952.036
10.0	788.488	784.142	779.625	876.370	872.096	867.764	958.679	955.341	952.586
12.0	788.420	784.140	779.512	875.816	871.672	867.062	958.495	955.345	952.995
14.0	788.334	784.111	779.450	875.808	871.539	867.208	958.245	955.494	952.998
				u (ms^{-1})					
2.0	1151.30	1134.68	1117.52	1391.55	1376.88	1358.92	1613.22	1603.80	1594.11
4.0	1150.75	1134.34	1116.90	1386.99	1372.17	1357.14	1614.47	1604.55	1595.23
6.0	1149.30	1133.84	1116.41	1384.67	1369.86	1354.79	1614.69	1604.59	1595.28
8.0	1149.22	1133.65	1116.40	1382.90	1368.05	1352.97	1614.75	1604.86	1595.33
10.0	1149.11	1133.58	1116.38	1381.08	1366.22	1351.13	1614.77	1604.99	1595.88
12.0	1149.05	1133.49	1116.31	1381.09	1364.01	1350.02	1614.99	1605.08	1595.94
14.0	1148.99	1133.32	1116.32	1381.06	1364.02	1350.04	1615.02	1605.13	1595.97
				κ_S TPa^{-1} × 10^{-10}					
2.0	9.562	9.902	10.260	5.876	6.029	6.220	4.020	4.079	4.141
4.0	9.573	9.909	10.270	5.917	6.075	6.241	4.009	4.070	4.131
6.0	9.597	9.919	10.280	5.942	6.101	6.269	4.003	4.067	4.128
8.0	9.602	9.922	10.290	5.962	6.122	6.290	4.003	4.065	4.127
10.0	9.604	9.924	10.290	5.982	6.143	6.312	4.000	4.063	4.121
12.0	9.606	9.925	10.290	5.986	6.166	6.328	4.000	4.063	4.119
14.0	9.608	9.929	10.290	5.986	6.166	6.326	4.000	4.062	4.119

Standard uncertainties in ρ, u and κ_S are ± 4×10^{-3} kgm^{-3}, ± 0.5 ms^{-1} and ±0.02× 10^{-10} TPa^{-1}.

A10 Density, ρ (kgm^{-3}), ultrasonic velocity, u (ms^{-1}) and Isentropic Compressibility, K_S (TPa^{-1}) of SDS (2.0–14.0 mmol kg^{-1}) in water-ethanol compositions (% v/v) of 0.02 mol kg^{-1} BHT over three different temperatures.

[SDS] mmol kg^{-1}	100% Ethanol			70% Ethanol			30% Ethanol		
	25 °C	30 °C	35 °C	25 °C	30 °C	35 °C	25 °C	30 °C	35 °C
				ρ (kgm^{-3})					
2.0	789.446	785.134	780.879	876.501	872.162	867.750	960.928	958.180	955.288
4.0	789.711	785.396	781.249	876.418	872.149	867.821	960.599	957.807	954.867
6.0	789.792	785.465	781.404	876.767	872.520	868.202	960.791	957.856	954.678
8.0	790.623	786.607	782.656	876.961	872.806	868.287	961.062	958.441	955.206
10.0	791.553	787.268	782.742	876.532	872.505	867.969	960.785	958.002	955.058
12.0	791.285	787.369	782.617	876.543	872.382	868.051	960.455	957.652	954.684
14.0	790.709	786.387	781.733	876.422	872.101	867.610	960.410	957.602	954.424
				u (ms^{-1})					
2.0	1147.91	1131.06	1114.19	1381.17	1368.52	1358.53	1618.54	1610.26	1601.72
4.0	1148.36	1131.53	1114.20	1381.38	1366.57	1351.50	1617.85	1609.36	1600.60
6.0	1150.66	1133.80	1115.70	1381.59	1366.88	1351.82	1616.16	1607.53	1598.60
8.0	1150.08	1133.25	1115.92	1381.85	1367.07	1352.00	1617.20	1608.68	1599.97
10.0	1150.88	1133.85	1116.40	1379.49	1364.71	1349.63	1616.75	1608.39	1599.69
12.0	1149.82	1132.93	1117.60	1381.76	1364.11	1352.06	1616.64	1607.47	1598.63
14.0	1151.04	1134.06	1117.17	1382.66	1359.01	1352.80	1616.00	1607.02	1598.60
				K_S $TPa^{-1} \times 10^{-10}$					
2.0	9.613	9.956	10.315	5.980	6.122	6.198	3.972	4.024	4.080
4.0	9.602	9.944	10.310	5.979	6.139	6.170	3.977	4.031	4.087
6.0	9.563	9.904	10.280	5.975	6.134	6.164	3.984	4.040	4.098
8.0	9.562	9.899	10.260	5.971	6.130	6.162	3.978	4.031	4.089
10.0	9.538	9.880	10.250	5.995	6.153	6.186	3.981	4.035	4.091
12.0	9.558	9.895	10.230	5.975	6.160	6.163	3.983	4.041	4.098
14.0	9.545	9.888	10.249	5.968	6.208	6.240	3.987	4.043	4.100

Standard uncertainties in ρ, u and K_S are $\pm 4\times10^{-3}$ kgm^{-3}, $\pm$ 0.5 ms^{-1} and $\pm0.02\times 10^{-10}$ TPa^{-1}.

A11 Density, ρ (kgm^{-3}), ultrasonic velocity, u (ms^{-1}) and Isentropic Compressibility, K_S (TPa^{-1}) of SDS (2.0–14.0 mmol kg^{-1}) in water-1-propanol compositions (% v/v) of 0.03 mol kg^{-1} BHA over three different temperatures.

[SDS] mmol kg^{-1}	100% v/v 1-propanol			70% v/v 1-propanol			30% v/v 1-propanol		
	25 °C	**30 °C**	**35 °C**	**25 °C**	**30 °C**	**35 °C**	**25 °C**	**30 °C**	35 °C
				ρ (kgm^{-3})					
2.0	822.394	813.284	805.675	892.885	882.466	877.479	983.229	977.249	970.349
4.0	822.637	813.783	805.993	892.428	882.107	877.134	983.268	977.248	970.358
6.0	821.894	813.394	805.783	892.854	882.354	877.554	983.556	977.501	970.659
8.0	821.784	813.213	805.702	892.848	882.454	877.595	983.601	977.481	970.556
10.0	821.294	813.145	805.678	892.694	882.169	877.469	983.267	977.354	970.486
12.0	820.120	813.078	805.573	892.668	882.107	877.348	983.169	977.287	970.399
14.0	820.024	812.998	805.403	892.647	882.105	877.338	983.101	977.183	970.302
				u (ms^{-1})					
2.0	1382.43	1294.34	1227.67	1454.47	1446.37	1440.54	1724.96	1718.64	1711.95
4.0	1382.65	1294.45	1227.79	1454.56	1446.54	1440.64	1725.11	1718.62	1711.99
6.0	1382.89	1294.63	1227.94	1454.68	1446.65	1440.55	1725.26	1718.69	1712.19
8.0	1383.14	1294.74	1228.23	1454.79	1446.78	1440.71	1725.33	1718.78	1712.35
10.0	1383.32	1294.85	1228.43	1454.76	1446.77	1440.88	1725.31	1718.86	1712.28
12.0	1383.45	1295.12	1228.58	1454.86	1446.85	1440.93	1725.38	1718.95	1712.30
14.0	1383.61	1295.25	1228.59	1454.83	1446.91	1440.91	1725.37	1718.92	1712.36
				K_S TPa^{-1} × 10^{-10}					
2.0	6.362	7.339	8.235	5.294	5.416	5.491	3.418	3.464	3.516
4.0	6.358	7.333	8.230	5.296	5.417	5.493	3.417	3.464	3.516
6.0	6.362	7.335	8.230	5.293	5.415	5.491	3.415	3.463	3.514
8.0	6.360	7.335	8.227	5.292	5.414	5.489	3.415	3.462	3.513
10.0	6.362	7.334	8.225	5.293	5.415	5.489	3.416	3.463	3.514
12.0	6.370	7.332	8.224	5.293	5.415	5.490	3.416	3.462	3.515
14.0	6.370	7.331	8.225	5.293	5.415	5.490	3.416	3.463	3.515

Standard uncertainties in ρ, u and K_S are ± 4×10^{-3} kgm^{-3}, ± 0.5 ms^{-1} and ±0.02× 10^{-10} TPa^{-1}.

A12 Density, ρ (kgm^{-3}), ultrasonic velocity, u (ms^{-1}) and Isentropic Compressibility, K_S (TPa^{-1}) of SDS (2.0–14.0 mmol kg^{-1}) in water-1-propanol compositions (% v/v) of 0.02 mol kg^{-1} BHT over three different temperatures.

[SDS] mmol kg^{-1}	100% v/v 1-propanol			70% v/v 1-propanol			30% v/v 1-propanol		
	25 °C	30 °C	35 °C	25 °C	30 °C	35 °C	25 °C	30 °C	35 °C
				ρ (kgm^{-3})					
2.0	828.044	818.814	810.344	897.354	888.232	879.784	988.173	980.843	973.565
4.0	828.673	819.363	810.826	897.892	888.763	880.228	988.874	981.326	973.893
6.0	827.983	818.762	810.254	897.212	888.542	879.893	988.264	980.899	973.648
8.0	827.881	818.653	810.142	897.083	888.433	879.748	988.208	980.746	973.577
10.0	827.744	818.564	810.073	896.872	888.354	879.662	988.162	980.665	973.440
12.0	827.682	818.352	809.983	896.674	888.302	879.473	988.115	980.534	973.385
14.0	827.562	818.210	809.837	896.562	888.221	879.293	988.083	980.435	973.294
				u (ms^{-1})					
2.0	1394.87	1310.54	1238.10	1468.04	1455.29	1448.80	1740.09	1727.46	1720.08
4.0	1394.92	1310.67	1238.26	1468.26	1455.47	1448.87	1740.25	1727.53	1720.34
6.0	1394.97	1310.83	1238.48	1468.48	1455.65	1448.93	1740.39	1727.67	1720.43
8.0	1395.05	1310.95	1238.64	1468.71	1455.78	1448.96	1740.48	1727.74	1720.47
10.0	1395.18	1311.10	1238.82	1468.99	1455.89	1448.99	1740.57	1727.80	1720.58
12.0	1395.38	1311.19	1238.98	1469.15	1455.94	1449.23	1740.66	1727.88	1720.66
14.0	1395.57	1311.24	1239.01	1469.24	1455.99	1449.48	1740.85	1727.92	1720.72
				K_S TPa^{-1} × 10^{-10}					
2.0	6.464	7.356	8.243	5.344	5.436	5.452	3.426	3.586	3.663
4.0	6.466	7.358	8.244	5.346	5.437	5.453	3.427	3.587	3.664
6.0	6.468	7.357	8.246	5.345	5.438	5.454	3.428	3.588	3.665
8.0	6.469	7.359	8.248	5.347	5.440	5.456	3.430	3.590	3.667
10.0	6.472	7.362	8.249	5.348	5.442	5.458	3.431	3.592	3.666
12.0	6.474	7.364	8.252	5.349	5.443	5.459	3.432	3.593	3.668
14.0	6.476	7.366	8.254	5.350	5.444	5.460	3.432	3.594	3.669

Standard uncertainties in ρ, u and K_S are ± 4×10^{-3} kgm^{-3}, ± 0.5 ms^{-1} and ±0.02× 10^{-10} TPa^{-1}.

A13 Density, ρ (kgm^{-3}), ultrasonic velocity, u (ms^{-1}) and Isentropic Compressibility, K_S (TPa^{-1}) of CTAB (0.2–1.8 mmol kg^{-1}) in water-methanol compositions (% v/v) of 0.03 mol kg^{-1} BHA over three different temperatures.

[CTAB] mmol kg^{-1}	100% v/v Methanol			70% v/v Methanol			30% v/v Methanol		
	25 °C	30 °C	35 °C	25 °C	30 °C	35 °C	25 °C	30 °C	35 °C
				ρ (Kgm^{-3})					
0.2	778.984	774.584	761.424	832.938	821.464	811.839	875.944	864.345	853.294
0.4	777.132	773.132	759.353	831.012	820.147	810.783	875.111	863.673	852.455
0.6	775.484	772.484	758.011	831.084	819.574	809.995	874.374	862.789	851.566
0.8	778.158	774.158	761.845	832.993	821.577	811.892	875.905	864.312	853.275
1.0	778.545	774.545	761.794	832.912	821.503	811.815	875.835	864.293	853.196
1.2	777.901	774.901	761.705	832.854	821.475	811.763	875.778	864.231	853.099
1.4	777.865	774.865	761.663	832.794	821.414	811.712	875.723	864.187	853.012
1.6	777.796	774.796	761.597	832.722	821.354	811.665	875.686	864.146	852.934
1.8	777.743	774.743	761.513	832.646	821.288	811.599	875.615	864.094	852.901
				u (ms^{-1})					
0.2	1137.54	1124.54	1111.32	1284.83	1272.43	1257.93	1512.83	1503.74	1487.22
0.4	1137.67	1124.68	1111.45	1284.89	1272.64	1258.12	1512.98	1503.93	1487.38
0.6	1137.84	1124.79	1111.53	1284.95	1272.85	1258.37	1513.22	1504.07	1487.51
0.8	1137.99	1124.88	1111.66	1285.09	1272.91	1258.59	1513.45	1504.18	1487.66
1.0	1138.34	1124.97	1111.78	1285.17	1273.11	1258.74	1513.62	1504.35	1487.79
1.2	1138.51	1125.14	1111.89	1285.18	1273.15	1258.86	1513.75	1504.49	1487.92
1.4	1138.75	1125.29	1112.02	1285.31	1273.28	1258.97	1513.82	1504.62	1488.14
1.6	1138.88	1125.42	1112.17	1285.57	1273.29	1258.99	1513.86	1504.78	1488.39
1.8	1138.89	1125.51	1112.26	1285.66	1273.33	1259.04	1513.98	1504.93	1488.55
				K_S TPa^{-1} × 10^{-10}					
0.2	9.921	1.021*	1.063*	7.272	7.518	7.784	4.988	5.116	5.298
0.4	9.942	1.023	1.066	7.288	7.528	7.792	4.992	5.119	5.303
0.6	9.960	1.023	1.068	7.287	7.531	7.797	4.995	5.123	5.307
0.8	9.923	1.021	1.062	7.269	7.512	7.776	4.984	5.114	5.295
1.0	9.912	1.020	1.062	7.269	7.510	7.774	4.984	5.113	5.295
1.2	9.917	1.019	1.062	7.269	7.510	7.773	4.983	5.112	5.295
1.4	9.914	1.019	1.062	7.268	7.509	7.773	4.983	5.111	5.294
1.6	9.912	1.019	1.062	7.266	7.509	7.773	4.983	5.111	5.292
1.8	9.913	1.019	1.061	7.265	7.509	7.773	4.982	5.110	5.291

* K_S TPa^{-1} × 10^{-9}. Standard uncertainties in ρ , u and K_S are ± 4×10^{-3} kgm^{-3}, ± 0.5 ms^{-1} and ±0.01× 10^{-10} TPa^{-1}.

A14 Density, ρ (kgm^{-3}), ultrasonic velocity, u (ms^{-1}) and Isentropic Compressibility, K_S (TPa^{-1}) of CTAB (0.2–1.8 mmol kg^{-1}) in water-methanol compositions (% v/v) of 0.02 mol kg^{-1} BHT over three different temperatures.

[CTAB] mmol kg^{-1}	**100% v/v Methanol**			**70% v/v Methanol**			**30% v/v Methanol**		
	25 °C	**30 °C**	**35 °C**	**25 °C**	**30 °C**	**35 °C**	**25 °C**	**30 °C**	**35 °C**
				ρ (Kgm^{-3})					
0.2	785.353	778.439	768.345	845.632	830.292	821.293	882.839	870.754	857.353
0.4	783.704	777.839	767.548	844.458	829.499	820.995	880.148	869.994	857.278
0.6	782.003	777.014	766.832	843.623	829.238	820.748	880.036	869.748	857.248
0.8	782.249	776.949	766.786	843.784	829.112	820.292	880.374	869.685	856.984
1.0	784.186	776.894	766.711	843.825	829.084	820.218	880.343	869.643	856.891
1.2	784.102	776.827	766.679	843.784	829.003	820.184	880.295	869.579	856.824
1.4	784.058	776.764	766.607	843.766	828.974	820.132	880.211	869.515	856.776
1.6	783.975	776.701	766.563	843.791	828.904	820.099	880.184	869.483	856.713
1.8	783.958	776.678	766.521	843.747	828.881	820.001	880.132	869.421	856.701
				u (ms^{-1})					
0.2	1164.24	1146.83	1125.23	1284.83	1280.45	1272.89	1526.44	1515.49	1503.24
0.4	1164.39	1146.98	1125.39	1284.89	1280.68	1272.93	1526.48	1515.64	1503.45
0.6	1164.66	1147.13	1125.46	1284.95	1280.69	1273.14	1526.69	1515.75	1503.57
0.8	1164.74	1147.32	1125.75	1285.09	1280.78	1273.29	1526.85	1515.83	1503.73
1.0	1164.76	1147.48	1125.96	1285.17	1280.91	1273.37	1527.12	1515.99	1503.94
1.2	1164.89	1147.61	1126.03	1285.18	1281.05	1273.46	1527.24	1516.15	1504.06
1.4	1164.98	1147.74	1126.26	1285.31	1281.23	1273.74	1527.29	1516.26	1504.28
1.6	1165.05	1147.78	1126.54	1285.57	1281.39	1273.88	1527.38	1516.32	1504.39
1.8	1165.27	1147.93	1126.73	1285.66	1281.55	1273.97	1527.41	1516.33	1504.44
				K_S TPa^{-1} × 10^{-10}					
0.2	9.394	9.767	1.027*	7.164	7.346	7.515	4.861	5.000	5.162
0.4	9.411	9.772	1.028	7.173	7.350	7.517	4.876	5.003	5.161
0.6	9.427	9.780	1.029	7.179	7.352	7.517	4.875	5.004	5.161
0.8	9.423	9.778	1.029	7.176	7.353	7.519	4.872	5.004	5.160
1.0	9.400	9.776	1.028	7.175	7.351	7.519	4.870	5.003	5.160
1.2	9.398	9.774	1.028	7.175	7.350	7.518	4.870	5.002	5.159
1.4	9.398	9.773	1.028	7.174	7.349	7.515	4.870	5.002	5.158
1.6	9.397	9.773	1.027	7.171	7.347	7.514	4.870	5.002	5.158
1.8	9.394	9.771	1.027	7.170	7.346	7.514	4.870	5.002	5.157

* K_S TPa^{-1} × 10^{-9}. Standard uncertainties in ρ, u and K_S are ± 3×10^{-3} kgm^{-3}, ± 0.3 ms^{-1} and ± 0.02 × 10^{-10} TPa^{-1}.

A15 Density, ρ (kgm^{-3}), ultrasonic velocity, u (ms^{-1}) and Isentropic Compressibility, κ_S (TPa^{-1}) of CTAB (0.2–1.8) mmol kg^{-1} in water-ethanol compositions (v/v %) of 0.03 mol kg^{-1} BHA over three different temperatures.

[CTAB] mmol kg^{-1}	100% v/v Ethanol			70% v/v Ethanol			30% v/v Ethanol		
	25 °C	30 °C	35 °C	25 °C	30 °C	35 °C	25 °C	30 °C	35 °C
				ρ (Kgm^{-3})					
0.2	781.841	776.522	764.291	839.832	828.914	816.732	882.670	873.384	864.442
0.4	780.271	775.885	764.192	838.615	827.889	816.003	881.193	872.142	863.438
0.6	781.152	776.171	764.182	838.884	827.992	816.005	881.024	872.003	863.399
0.8	782.529	777.318	765.608	839.788	828.878	817.154	882.663	873.332	864.392
1.0	782.317	777.343	765.542	839.715	828.804	817.096	882.616	873.312	864.316
1.2	782.263	777.310	765.471	839.656	828.735	817.004	882.574	873.256	864.278
1.4	782.165	777.262	765.401	839.601	828.697	816.985	882.492	873.184	864.224
1.6	782.002	777.182	765.337	839.534	828.622	816.889	882.403	873.102	864.169
1.8	781.994	777.095	765.283	839.473	828.584	816.815	882.378	873.047	864.116
				u (ms^{-1})					
0.2	1155.88	1138.55	1114.17	1291.14	1276.38	1261.28	1523.44	1510.73	1494.62
0.4	1156.11	1138.72	1114.84	1291.32	1276.51	1261.35	1523.58	1510.88	1494.84
0.6	1156.37	1138.97	1114.99	1291.45	1276.79	1261.44	1523.76	1510.96	1494.99
0.8	1156.72	1139.19	1115.23	1291.66	1276.94	1261.65	1523.97	1511.14	1495.16
1.0	1156.92	1139.36	1115.56	1291.79	1277.33	1261.79	1524.16	1511.25	1495.37
1.2	1157.34	1139.78	1115.85	1291.88	1277.58	1261.93	1524.45	1511.39	1495.52
1.4	1157.63	1140.02	1116.11	1291.97	1277.62	1262.09	1524.69	1511.54	1495.77
1.6	1157.84	1140.18	1116.35	1292.06	1277.73	1262.24	1524.84	1511.68	1495.88
1.8	1158.08	1140.32	1116.62	1292.15	1277.81	1262.38	1524.92	1511.77	1495.91
				κ_S TPa^{-1} × 10^{-10}					
0.2	9.573	9.934	1.054*	7.143	7.405	7.697	4.881	5.017	5.178
0.4	9.589	9.940	1.052	7.151	7.413	7.703	4.889	5.023	5.183
0.6	9.574	9.932	1.052	7.147	7.409	7.701	4.889	5.023	5.182
0.8	9.551	9.910	1.050	7.137	7.399	7.688	4.878	5.014	5.175
1.0	9.550	9.910	1.049	7.136	7.395	7.687	4.877	5.014	5.174
1.2	9.544	9.903	1.049	7.136	7.393	7.686	4.876	5.013	5.173
1.4	9.540	9.899	1.048	7.135	7.393	7.684	4.874	5.013	5.172
1.6	9.539	9.898	1.048	7.135	7.392	7.683	4.874	5.012	5.171
1.8	9.535	9.896	1.048	7.135	7.391	7.682	4.874	5.012	5.172

* κ_S TPa^{-1} × 10^{-9}. Standard uncertainties in ρ, u and κ_S are ± 4×10^{-3} kgm^{-3}, ± 0.3 ms^{-1} and ±0.02×10^{-10} TPa^{-1}.

A16 Density, ρ (kgm^{-3}), ultrasonic velocity, u (ms^{-1}) and Isentropic Compressibility, κ_S (TPa^{-1}) of CTAB (0.2–1.8) mmol kg^{-1} in water-ethanol compositions (% v/v) of 0.02 mol kg^{-1} BHT over three different temperatures.

[CTAB] mmol kg^{-1}	100% v/v Ethanol			70% v/v Ethanol			30% v/v Ethanol		
	25 °C	30 °C	35 °C	25 °C	30 °C	35 °C	25 °C	30 °C	35 °C
				ρ (Kgm^{-3})					
0.2	789.644	782.943	773.495	847.844	837.728	829.744	892.183	882.848	871.848
0.4	788.345	781.323	772.748	846.263	836.985	828.893	891.747	881.999	870.993
0.6	788.013	780.044	772.003	846.145	836.294	828.381	891.043	881.384	870.283
0.8	788.003	780.928	771.937	847.858	836.193	828.316	891.994	881.371	870.225
1.0	788.038	780.902	771.911	847.713	836.187	828.274	891.916	881.354	870.184
1.2	788.002	780.884	771.891	847.685	836.132	828.222	891.894	881.312	870.121
1.4	787.994	780.845	771.874	847.627	836.096	828.184	891.843	881.274	870.094
1.6	787.952	780.843	771.818	847.583	836.001	828.113	891.804	881.233	870.023
1.8	787.915	780.815	771.794	847.517	835.986	828.082	891.799	881.195	870.007
				u (ms^{-1})					
0.2	1171.23	1164.22	1152.43	1310.35	1294.43	1272.14	1548.84	1538.85	1518.84
0.4	1171.39	1164.34	1152.47	1310.64	1294.75	1272.47	1548.92	1538.98	1519.35
0.6	1171.54	1164.58	1152.64	1310.87	1294.81	1272.69	1549.26	1539.15	1519.44
0.8	1171.73	1164.74	1152.72	1310.98	1294.99	1272.83	1549.43	1539.32	1519.61
1.0	1171.94	1164.89	1152.88	1311.34	1295.12	1273.14	1549.64	1539.48	1519.74
1.2	1172.28	1165.03	1152.95	1311.49	1295.35	1273.32	1549.82	1539.64	1519.85
1.4	1172.43	1165.25	1153.05	1311.58	1295.54	1273.58	1549.98	1539.79	1519.97
1.6	1172.64	1165.48	1153.24	1311.74	1295.71	1273.93	1550.04	1539.85	1520.05
1.8	1172.88	1165.49	1153.28	1311.83	1295.79	1273.99	1550.11	1539.92	1520.16
				κ_S TPa^{-1} × 10^{-10}					
0.2	9.232	9.423	9.734	6.869	7.124	7.447	4.672	4.783	4.972
0.4	9.244	9.441	9.743	6.879	7.127	7.451	4.674	4.787	4.974
0.6	9.246	9.452	9.749	6.878	7.132	7.453	4.676	4.789	4.977
0.8	9.243	9.439	9.749	6.863	7.131	7.452	4.670	4.788	4.976
1.0	9.239	9.437	9.746	6.860	7.130	7.449	4.669	4.787	4.976
1.2	9.234	9.435	9.745	6.859	7.128	7.447	4.668	4.787	4.975
1.4	9.232	9.432	9.744	6.858	7.126	7.444	4.667	4.786	4.975
1.6	9.229	9.428	9.741	6.857	7.125	7.441	4.667	4.786	4.975
1.8	9.226	9.428	9.741	6.856	7.124	7.440	4.667	4.786	4.974

* κ_S TPa^{-1} × 10^{-9}. Standard uncertainties in ρ, u and κ_S are ± 4×10^{-3} kgm^{-3}, ± 0.5 ms^{-1} and ± 0.25 10^{-10} TPa^{-1}.

A17 Density, ρ (kgm^{-3}), ultrasonic velocity, u (ms^{-1}) and Isentropic Compressibility, κ_S (TPa^{-1}) of CTAB (0.2–1.8) mmol kg^{-1} in water-1-propanol compositions (v/v %) of 0.03 mol kg^{-1} BHA over three different temperatures.

[CTAB] mmol kg^{-1}	100% v/v 1-propanol			70% v/v 1-propanol			30% v/v 1-propanol		
	25 °C	30 °C	35 °C	25 °C	30 °C	35 °C	25 °C	30 °C	35 °C
				ρ (Kgm^{-3})					
0.2	810.024	806.543	798.786	848.223	839.348	829.744	880.323	866.948	858.778
0.4	808.915	805.455	797.834	847.938	839.124	829.712	879.857	866.933	858.723
0.6	807.564	804.684	796.459	847.893	839.094	829.675	879.548	866.675	858.699
0.8	810.876	806.588	798.658	847.812	839.573	829.616	880.304	866.649	858.747
1.0	810.816	806.504	798.586	847.238	839.515	829.688	880.275	866.592	858.683
1.2	810.776	806.449	798.512	847.189	839.456	829.594	880.237	866.535	858.624
1.4	810.558	806.398	798.442	847.095	839.398	829.535	880.183	866.489	858.598
1.6	810.495	806.315	798.388	846.993	839.332	829.489	880.116	866.435	858.556
1.8	810.435	806.264	798.311	846.924	839.284	829.444	880.078	866.408	858.525
				u (ms^{-1})					
0.2	1221.76	1214.34	1193.43	1361.48	1348.39	1339.39	1569.84	1552.43	1543.03
0.4	1221.84	1214.55	1193.54	1361.59	1348.48	1339.43	1569.97	1552.58	1543.28
0.6	1221.98	1214.68	1193.65	1361.84	1348.62	1339.68	1570.06	1552.69	1543.37
0.8	1222.12	1214.82	1193.78	1361.96	1348.85	1339.74	1570.28	1552.75	1543.48
1.0	1222.31	1215.04	1193.92	1362.15	1348.91	1339.87	1570.44	1552.84	1543.65
1.2	1222.42	1215.22	1194.09	1362.39	1349.06	1340.03	1570.68	1552.96	1543.78
1.4	1222.55	1215.39	1194.21	1362.54	1349.08	1340.16	1570.74	1553.12	1543.87
1.6	1222.56	1215.44	1194.35	1362.66	1349.17	1340.32	1570.81	1552.28	1543.98
1.8	1222.69	1215.45	1194.38	1362.69	1349.26	1340.34	1570.83	1552.35	1544.04
				κ_S TPa^{-1} × 10^{-10}					
0.2	8.270	8.408	8.790	6.360	6.553	6.718	4.609	4.786	4.891
0.4	8.281	8.416	8.799	6.361	6.554	6.718	4.611	4.785	4.889
0.6	8.293	8.422	8.812	6.359	6.553	6.716	4.612	4.786	4.889
0.8	8.257	8.401	8.786	6.359	6.547	6.716	4.607	4.786	4.888
1.0	8.255	8.398	8.785	6.361	6.546	6.714	4.606	4.786	4.887
1.2	8.254	8.396	8.783	6.359	6.545	6.713	4.605	4.785	4.887
1.4	8.254	8.395	8.782	6.359	6.546	6.712	4.605	4.784	4.886
1.6	8.255	8.395	8.781	6.358	6.545	6.711	4.605	4.790	4.886
1.8	8.254	8.395	8.781	6.359	6.545	6.711	4.605	4.790	4.886

* κ_S TPa^{-1} × 10^{-9}. Standard uncertainties in ρ, u and κ_S are ± 3×10^{-3} kgm^{-3}, ± 0.4 ms^{-1} and ± 0.15×10^{-10} TPa^{-1}.

A18 Density, ρ (kgm^{-3}), ultrasonic velocity, u (ms^{-1}) and Isentropic Compressibility, K_S (TPa^{-1}) of CTAB (0.2–1.8) mmol kg^{-1}) in water-1-propanol compositions (% v/v) of 0.02 mol kg^{-1} BHT over three different temperatures.

[CTAB] mmol kg^{-1}	100% v/v 1-propanol			70% v/v 1-propanol			30% v/v 1-propanol		
	25 °C	30 °C	35 °C	25 °C	30 °C	35 °C	25 °C	30 °C	35 °C
				ρ (Kgm^{-3})					
0.2	825.658	815.365	803.265	865.748	848.254	833.265	901.965	884.328	866.768
0.4	824.748	814.354	802.369	865.455	848.176	833.658	900.258	883.195	865.847
0.6	823.198	813.582	801.472	865.158	848.119	833.614	900.005	882.759	864.995
0.8	825.554	815.654	803.546	864.996	848.075	833.547	901.856	884.584	865.688
1.0	825.494	815.598	803.502	864.935	848.006	833.468	901.782	884.507	865.824
1.2	825.422	815.542	803.476	864.886	847.984	833.405	901.716	884.468	865.775
1.4	825.381	815.488	803.434	864.812	847.967	833.364	901.649	884.408	865.711
1.6	825.313	815.426	803.384	864.759	847.914	833.318	901.601	884.356	865.666
1.8	825.276	815.395	803.335	864.711	847.863	833.286	901.579	884.297	865.613
				u (ms^{-1})					
0.2	1241.25	1228.35	1204.65	1386.98	1371.65	1359.65	1586.95	1570.26	1562.95
0.4	1241.31	1228.51	1204.86	1387.16	1371.83	1359.87	1587.06	1570.39	1563.14
0.6	1241.49	1228.62	1204.99	1387.36	1371.96	1360.15	1587.29	1570.47	1563.36
0.8	1241.68	1228.77	1205.16	1387.47	1372.19	1360.39	1587.48	1570.62	1563.58
1.0	1241.85	1228.94	1205.48	1387.59	1372.38	1360.52	1587.62	1570.77	1563.72
1.2	1242.01	1229.28	1205.64	1387.78	1372.49	1360.68	1587.83	1570.91	1563.8
1.4	1242.27	1229.37	1205.81	1387.86	1372.64	1360.83	1588.01	1571.09	1563.97
1.6	1242.33	1229.49	1206.03	1387.91	1372.77	1360.91	1588.28	1571.22	1564.08
1.8	1242.36	1229.51	1206.09	1387.98	1372.81	1360.99	1588.33	1571.34	1564.11
				K_S TPa^{-1} × 10^{-10}					
0.2	7.861	8.128	8.579	6.004	6.266	6.491	4.402	4.586	4.722
0.4	7.869	8.136	8.585	6.004	6.264	6.486	4.410	4.591	4.726
0.6	7.882	8.143	8.593	6.005	6.264	6.484	4.410	4.593	4.730
0.8	7.857	8.120	8.568	6.005	6.262	6.482	4.399	4.582	4.725
1.0	7.855	8.118	8.564	6.004	6.261	6.482	4.399	4.582	4.723
1.2	7.854	8.114	8.562	6.003	6.260	6.480	4.398	4.581	4.723
1.4	7.851	8.114	8.560	6.003	6.259	6.479	4.398	4.580	4.722
1.6	7.851	8.113	8.558	6.003	6.258	6.479	4.396	4.580	4.722
1.8	7.851	8.113	8.557	6.002	6.258	6.478	4.396	4.580	4.722

* K_S TPa^{-1} × 10^{-9}. Standard uncertainties in ρ , u and K_S are ± 5×10^{-3} kgm^{-3}, ± 0.4 ms^{-1} and ± 0.20×10^{-10} TPa^{-1}.

A19 Density, ρ (kgm^{-3}), ultrasonic velocity, u (ms^{-1}) and Isentropic Compressibility, K_S (TPa^{-1}) of TX100 (0.05–0.45 mmol kg^{-1}) in water-methanol compositions (% v/v) of 0.03 mol kg^{-1} BHA over three different temperatures.

[TX100] mmol kg^{-1}	100% v/v Methanol			70% v/v Methanol			30% v/v Methanol		
	25 °C	30 °C	35 °C	25 °C	30 °C	35 °C	25 °C	30 °C	35 °C
					ρ (kgm^{-3})				
0.05	790.992	787.168	782.502	835.482	830.283	826.394	880.832	875.393	870.889
0.10	791.521	787.689	783.405	836.329	830.937	826.948	880.783	875.555	871.323
0.15	792.582	788.408	784.104	837.738	831.538	827.843	881.604	876.432	871.912
0.20	792.608	788.683	784.607	837.702	831.479	827.738	881.564	876.336	871.888
0.25	792.342	788.735	784.503	837.658	831.413	827.645	881.498	876.276	871.758
0.30	791.971	787.975	784.432	837.672	831.357	827.588	881.484	876.222	871.673
0.35	791.801	787.905	784.426	837.573	831.307	827.523	881.387	876.179	871.615
0.40	791.749	787.883	784.347	837.512	831.263	827.475	881.322	876.135	871.567
0.45	791.648	787.802	784.289	837.457	831.211	827.422	881.288	876.068	871.492
					u (ms^{-1})				
0.05	1118.17	1105.36	1082.40	1289.24	1278.49	1269.87	1554.27	1540.43	1530.49
0.10	1118.84	1105.26	1084.34	1289.48	1278.39	1270.17	1554.62	1540.58	1530.77
0.15	1118.99	1106.04	1084.03	1290.76	1279.22	1270.32	1554.59	1540.83	1530.91
0.20	1118.99	1106.83	1084.82	1290.78	1279.35	1270.66	1554.83	1540.99	1531.32
0.25	1119.56	1108.43	1085.45	1290.99	1279.53	1270.78	1555.12	1541.17	1531.54
0.30	1120.15	1109.57	1085.77	1291.05	1279.67	1270.94	1555.35	1541.39	1531.66
0.35	1120.61	1109.64	1085.79	1291.23	1279.93	1271.25	1555.39	1541.83	1531.78
0.40	1121.03	1109.83	1085.83	1291.31	1280.11	1271.37	1555.53	1542.01	1531.95
0.45	1121.31	1109.89	1085.94	1291.55	1280.15	1271.44	1555.61	1542.09	1532.11
					K_S TPa^{-1} × 10^{-10}				
0.05	1.011*	1.039*	1.090*	7.201	7.504	7.504	4.699	4.902	4.902
0.10	1.009	1.039	1.085	7.191	7.495	7.495	4.697	4.897	4.897
0.15	1.007	1.036	1.085	7.164	7.485	7.485	4.693	4.893	4.893
0.20	1.007	1.034	1.083	7.164	7.482	7.482	4.692	4.891	4.891
0.25	1.006	1.031	1.081	7.162	7.481	7.481	4.690	4.890	4.890
0.30	1.006	1.030	1.081	7.162	7.480	7.480	4.689	4.890	4.890
0.35	1.005	1.030	1.081	7.160	7.477	7.477	4.689	4.889	4.889
0.40	1.005	1.030	1.081	7.160	7.476	7.476	4.689	4.888	4.888
0.45	1.004	1.030	1.081	7.158	7.476	7.476	4.689	4.888	4.888

* K_S TPa^{-1} × 10^{-9}. Standard uncertainties in ρ , u and K_S are ± 4×10^{-3} kgm^{-3}, ± 0.4 ms^{-1} and ± 0.10×10^{-10} TPa^{-1}.

A20 Density, ρ (kgm^{-3}), ultrasonic velocity, u (ms^{-1}) and Isentropic Compressibility, K_S (TPa^{-1}) of TX100 (0.05–0.45 mmol kg^{-1}) in water-methanol compositions (% v/v) of 0.02 mol kg^{-1} BHT over three different temperatures.

[TX100] mmol kg^{-1}	100% v/v Methanol			70% v/v Methanol			30% v/v Methanol		
	25 °C	30 °C	35 °C	25 °C	30 °C	35 °C	25 °C	30 °C	35 °C
				ρ (Kgm^{-3})					
0.05	795.278	791.150	786.541	856.003	850.242	844.921	883.432	878.895	871.994
0.10	796.484	792.213	787.390	856.242	850.511	845.232	883.583	879.253	872.483
0.15	797.382	793.106	788.546	856.598	850.783	845.498	883.948	879.563	872.749
0.20	797.689	793.518	788.755	856.583	850.701	845.701	883.874	879.452	872.701
0.25	797.636	793.412	788.656	856.512	850.632	845.640	883.756	879.340	872.631
0.30	797.545	793.381	788.585	856.469	850.579	845.572	883.677	879.289	872.568
0.35	797.401	793.242	788.409	856.388	850.497	845.482	883.601	879.213	872.685
0.40	797.359	793.084	788.378	856.301	850.406	845.414	883.534	879.139	872.604
0.45	797.342	792.801	788.193	856.247	850.355	845.381	883.487	879.069	872.549
				u (ms^{-1})					
0.05	1121.66	1105.74	1089.81	1303.23	1294.78	1277.35	1588.59	1574.11	1560.68
0.10	1122.64	1107.01	1091.04	1303.43	1294.84	1277.54	1588.62	1574.39	1560.83
0.15	1124.64	1118.40	1102.57	1303.32	1295.11	1277.49	1588.75	1574.29	1560.93
0.20	1130.56	1114.66	1110.23	1303.56	1295.45	1277.68	1589.02	1574.44	1561.14
0.25	1133.34	1119.42	1113.14	1303.89	1295.62	1277.83	1589.15	1574.63	1561.22
0.30	1134.97	1120.31	1114.36	1304.12	1295.71	1277.94	1589.33	1574.87	1561.49
0.35	1135.53	1121.11	1115.87	1304.77	1295.68	1278.25	1589.46	1574.98	1561.84
0.40	1135.75	1121.32	1115.92	1304.91	1295.82	1278.39	1589.68	1575.12	1561.79
0.45	1135.83	1121.38	1115.91	1305.21	1295.95	1278.54	1589.59	1575.05	1561.88
				K_S TPa^{-1} × 10^{-10}					
0.05	9.994	1.033*	1.070*	6.878	7.016	7.254	4.485	4.592	4.708
0.10	9.961	1.030	1.066	6.874	7.013	7.249	4.484	4.588	4.705
0.15	9.915	1.008	1.043	6.873	7.008	7.247	4.482	4.587	4.703
0.20	9.808	1.014	1.028	6.870	7.005	7.243	4.481	4.587	4.702
0.25	9.760	1.005	1.023	6.867	7.003	7.242	4.481	4.587	4.702
0.30	9.733	1.004	1.021	6.865	7.003	7.241	4.480	4.585	4.701
0.35	9.725	1.002	1.018	6.859	7.004	7.239	4.480	4.585	4.698
0.40	9.722	1.002	1.018	6.858	7.003	7.238	4.479	4.585	4.698
0.45	9.721	1.003	1.018	6.856	7.002	7.236	4.479	4.586	4.698

* K_S TPa^{-1} × 10^{-9}. Standard uncertainties in ρ , u and K_S are ± 4×10^{-3} kgm^{-3}, ± 0.4 ms^{-1} and ± 0.10×10^{-10} TPa^{-1}.

A21 Density, ρ (kgm^{-3}), ultrasonic velocity, u (ms^{-1}) and Isentropic Compressibility, K_S (TPa^{-1}) of TX100 (0.05–0.45 mmol kg^{-1} in water-ethanol compositions (v/v %) of 0.03 mol kg^{-1} BHA over three different temperatures.

[TX100] mmol kg^{-1}	100% v/v Ethanol			70% v/v Ethanol			30% v/v Ethanol		
	25 °C	30 °C	35 °C	25 °C	30 °C	35 °C	25 °C	30 °C	35 °C
				ρ (Kgm^{-3})					
0.05	784.943	780.421	773.094	856.483	850.768	845.324	887.384	881.329	872.424
0.10	785.532	780.932	773.383	856.522	850.843	845.384	886.895	881.204	872.532
0.15	786.146	781.557	774.158	856.754	850.942	845.555	887.385	881.338	872.613
0.20	786.893	782.703	774.661	857.843	851.586	846.214	888.124	881.513	872.944
0.25	786.784	782.693	774.618	858.534	851.839	846.675	888.576	882.674	873.453
0.30	786.703	782.612	774.564	858.502	851.733	846.598	888.502	882.602	873.378
0.35	786.655	782.585	774.499	858.467	851.654	846.512	888.434	882.596	873.302
0.40	786.576	782.534	774.402	858.329	851.595	846.445	888.394	882.525	873.274
0.45	786.515	782.495	774.387	858.244	851.502	846.382	888.302	882.481	873.215
				u (ms^{-1})					
0.05	1138.59	1132.48	1116.84	1216.45	1200.23	1173.24	1460.23	1443.53	1435.03
0.10	1138.95	1132.74	1116.97	1216.66	1200.34	1173.32	1460.38	1443.75	1435.22
0.15	1139.28	1132.89	1117.43	1216.94	1200.53	1173.41	1460.69	1443.88	1435.35
0.20	1139.44	1133.14	1117.84	1217.12	1200.76	1173.58	1460.71	1443.82	1435.59
0.25	1139.47	1133.38	1117.89	1217.25	1200.91	1173.74	1460.92	1443.98	1435.77
0.30	1139.68	1133.76	1118.11	1217.49	1201.14	1173.89	1461.21	1444.14	1435.82
0.35	1139.72	1133.84	1118.17	1217.48	1201.43	1174.03	1461.42	1444.25	1435.99
0.40	1139.85	1134.12	1118.34	1217.77	1201.65	1174.15	1461.58	1444.37	1435.98
0.45	1139.94	1134.11	1118.48	1217.95	1201.71	1174.28	1461.59	1444.54	1436.03
				K_S TPa^{-1} × 10^{-10}					
0.05	9.827	9.991	1.037*	7.890	8.159	8.594	5.285	5.445	5.566
0.10	9.813	9.979	1.036	7.887	8.157	8.592	5.287	5.444	5.564
0.15	9.800	9.969	1.034	7.881	8.154	8.589	5.282	5.442	5.562
0.20	9.788	9.950	1.033	7.869	8.144	8.580	5.277	5.442	5.558
0.25	9.789	9.946	1.033	7.861	8.140	8.573	5.273	5.433	5.554
0.30	9.786	9.940	1.032	7.858	8.138	8.572	5.271	5.433	5.554
0.35	9.786	9.939	1.032	7.859	8.135	8.571	5.270	5.432	5.553
0.40	9.785	9.935	1.032	7.856	8.132	8.569	5.269	5.431	5.553
0.45	9.784	9.935	1.032	7.855	8.132	8.568	5.269	5.430	5.553

* K_S TPa^{-1} × 10^{-9}. Standard uncertainties in ρ , u and K_S are ± 4×10^{-3} kgm^{-3}, ± 0.4 ms^{-1} and ± 0.10×10^{-10} TPa^{-1}.

A22 Density, ρ (kgm^{-3}), ultrasonic velocity, u (ms^{-1}) and Isentropic Compressibility, κ_S (TPa^{-1}) of TX100 (0.05–0.45 mmol kg^{-1}) in water-ethanol compositions (% v/v) of 0.02 mol kg^{-1} BHT over three different temperatures.

[TX100] mmol kg^{-1}	100% v/v Ethanol			70% v/v Ethanol			30% v/v Ethanol		
	25 °C	30 °C	35 °C	25 °C	30 °C	35 °C	25 °C	30 °C	35 °C
				ρ (Kgm^{-3})					
0.05	785.551	781.573	776.240	863.001	860.323	855.504	896.053	891.232	887.282
0.10	786.541	782.384	775.091	863.241	860.744	856.072	896.209	891.284	887.302
0.15	790.333	785.521	779.788	864.333	861.494	856.817	896.743	891.895	888.004
0.20	794.660	787.420	781.115	865.515	862.642	857.801	897.869	892.748	888.353
0.25	793.304	787.050	780.712	865.904	862.602	857.712	897.784	892.684	888.297
0.30	792.141	786.857	780.529	865.524	862.692	857.683	897.687	892.581	888.205
0.35	790.353	786.191	778.789	865.253	862.649	857.643	897.594	892.515	888.157
0.40	790.458	786.143	778.649	865.210	862.546	857.638	897.502	892.468	888.098
0.45	790.236	786.004	778.603	865.189	862.532	857.599	897.462	892.352	887.945
				u (ms^{-1})					
0.05	1158.65	1141.92	1125.29	1221.43	1204.24	1187.05	1466.67	1452.53	1444.25
0.10	1159.84	1141.21	1125.42	1222.21	1204.76	1187.82	1466.69	1452.64	1444.53
0.15	1158.66	1142.16	1125.43	1222.94	1205.34	1188.49	1466.85	1452.83	1444.89
0.20	1163.92	1143.34	1126.68	1223.52	1205.99	1189.43	1467.03	1453.23	1445.14
0.25	1163.46	1144.01	1127.32	1224.54	1206.48	1189.98	1467.13	1453.34	1445.53
0.30	1165.22	1144.52	1128.03	1224.17	1208.39	1190.34	1467.09	1453.46	1445.35
0.35	1166.34	1144.31	1128.04	1225.89	1208.59	1190.06	1467.16	1454.16	1445.73
0.40	1166.05	1145.45	1128.68	1226.35	1209.32	1191.43	1467.28	1454.34	1445.81
0.45	1167.19	1145.71	1129.43	1226.56	1209.95	1191.67	1467.3	1454.25	1446.01
				κ_S TPa^{-1} × 10^{-10}					
0.05	9.482	9.812	1.017*	7.766	8.015	8.295	5.188	5.318	5.403
0.10	9.451	9.814	1.018	7.754	8.004	8.279	5.187	5.317	5.401
0.15	9.424	9.758	1.012	7.735	7.990	8.262	5.183	5.312	5.394
0.20	9.289	9.715	1.008	7.717	7.971	8.240	5.175	5.304	5.390
0.25	9.312	9.708	1.007	7.701	7.964	8.233	5.175	5.304	5.388
0.30	9.297	9.701	1.006	7.709	7.938	8.228	5.176	5.303	5.389
0.35	9.301	9.713	1.009	7.690	7.936	8.233	5.176	5.299	5.387
0.40	9.304	9.695	1.008	7.685	7.927	8.214	5.175	5.298	5.387
0.45	9.288	9.692	1.006	7.682	7.919	8.211	5.175	5.299	5.386

* κ_S TPa^{-1} × 10^{-9}. Standard uncertainties in ρ , u and κ_S are ± 4×10^{-3} kgm^{-3}, ± 0.4 ms^{-1} and ± 0.10×10^{-10} TPa^{-1}.

A23 Density, ρ (kgm^{-3}), ultrasonic velocity, u (ms^{-1}) and Isentropic Compressibility, K_S (TPa^{-1}) of TX100 (0.05–0.45 mmol kg^{-1}) in water-1-propanol compositions (v/v %) of 0.03 mol kg^{-1} BHA over three different temperatures.

[TX100] mmol kg^{-1}	100% v/v 1-propanol			70% v/v 1-propanol			30% v/v 1-propanol		
	25 °C	30 °C	35 °C	25 °C	30 °C	35 °C	25 °C	30 °C	35 °C
				ρ (Kgm^{-3})					
0.05	801.232	793.248	781.859	861.093	850.234	839.752	903.243	896.353	888.384
0.10	801.847	793.933	782.536	861.958	850.826	840.483	903.803	896.994	888.944
0.15	801.803	793.874	782.485	861.861	850.785	840.378	903.754	896.748	888.854
0.20	801.763	793.739	782.368	861.803	850.659	840.302	903.683	896.681	888.786
0.25	801.694	793.674	782.219	861.758	850.606	840.275	903.602	896.602	888.692
0.30	801.615	793.612	782.159	861.699	850.594	840.211	903.534	896.532	888.614
0.35	801.559	793.574	782.102	861.645	850.525	840.157	903.482	896.493	888.584
0.40	801.512	793.523	782.084	861.598	850.472	840.095	903.374	896.417	888.502
0.45	801.478	793.465	782.002	861.572	850.396	840.004	903.294	896.357	888.438
				u (ms^{-1})					
0.05	1212.42	1185.39	1142.42	1412.34	1383.52	1358.34	1573.65	1550.23	1533.52
0.10	1212.53	1185.43	1142.57	1412.43	1383.75	1358.39	1573.84	1550.46	1533.64
0.15	1212.56	1185.85	1142.75	1412.65	1383.84	1358.68	1573.98	1550.73	1533.85
0.20	1212.74	1185.93	1142.89	1412.74	1384.07	1358.82	1574.17	1550.89	1533.99
0.25	1212.99	1186.34	1143.23	1412.93	1384.35	1359.14	1574.33	1551.24	1534.26
0.30	1213.15	1186.52	1143.47	1413.15	1384.59	1359.34	1574.57	1551.45	1534.35
0.35	1213.34	1186.68	1143.65	1413.24	1384.88	1359.57	1574.72	1551.78	1534.68
0.40	1213.55	1186.85	1143.83	1413.27	1384.94	1359.74	1574.94	1551.91	1534.72
0.45	1213.73	1186.98	1144.01	1413.46	1385.08	1359.92	1575.13	1552.28	1534.75
				K_S TPa^{-1} × 10^{-10}					
0.05	8.491	8.972	9.800	5.822	6.144	6.454	4.471	4.642	4.787
0.10	8.482	8.963	9.789	5.815	6.138	6.448	4.467	4.638	4.783
0.15	8.483	8.958	9.786	5.814	6.137	6.446	4.466	4.637	4.782
0.20	8.480	8.958	9.785	5.814	6.136	6.445	4.466	4.637	4.781
0.25	8.478	8.952	9.781	5.813	6.134	6.442	4.465	4.635	4.780
0.30	8.476	8.950	9.778	5.811	6.132	6.441	4.464	4.634	4.780
0.35	8.474	8.948	9.776	5.811	6.130	6.439	4.463	4.632	4.778
0.40	8.472	8.946	9.773	5.811	6.130	6.438	4.463	4.632	4.778
0.45	8.470	8.945	9.771	5.810	6.129	6.437	4.462	4.630	4.779

Standard uncertainties in ρ , u and K_S are ± 4×10^{-3} kgm^{-3}, ± 0.4 ms^{-1} and ± 0.10×10^{-10} TPa^{-1}.

A24 Density, ρ (kgm^{-3}), ultrasonic velocity, u (ms^{-1}) and Isentropic Compressibility, K_S (TPa^{-1}) of TX100 (0.05–0.45 mmol kg^{-1}) in water-1-propanol compositions (% v/v) of 0.02 mol kg^{-1} BHT over three different temperatures.

[TX100] mmol kg^{-1}	100% v/v 1-propanol			70% v/v 1-propanol			30% v/v 1-propanol		
	25 °C	30 °C	35 °C	25 °C	30 °C	35 °C	25 °C	30 °C	35 °C
				ρ (Kgm^{-3})					
0.05	819.102	811.333	795.197	868.129	861.584	849.383	915.299	910.785	902.492
0.10	819.713	811.931	796.283	868.948	862.29	849.783	915.841	911.393	903.264
0.15	820.964	812.913	796.574	868.883	862.585	850.249	916.248	911.849	903.753
0.20	820.715	812.641	796.710	868.480	862.517	850.237	916.223	911.832	903.679
0.25	820.693	812.532	796.424	868.429	862.472	850.178	916.168	911.736	903.593
0.30	820.392	812.407	796.299	868.378	862.389	850.132	916.129	911.692	903.537
0.35	820.143	812.276	796.556	868.305	862.394	850.089	916.087	911.626	903.478
0.40	820.098	812.178	796.438	868.268	862.315	849.993	915.993	911.538	903.394
0.45	820.005	812.067	796.332	868.211	862.265	849.978	915.984	911.486	903.335
				u (ms^{-1})					
0.05	1230.20	1198.53	1155.29	1421.67	1391.24	1356.34	1581.45	1560.32	1543.64
0.10	1230.93	1198.78	1155.42	1422.01	1391.45	1356.56	1581.39	1560.56	1543.87
0.15	1231.13	1198.69	1155.43	1422.34	1391.64	1356.75	1581.40	1560.43	1544.24
0.20	1231.05	1198.98	1155.68	1422.39	1391.61	1356.76	1581.69	1560.75	1544.55
0.25	1231.37	1199.12	1155.32	1422.38	1391.78	1356.93	1581.84	1560.93	1544.63
0.30	1231.51	1199.24	1156.03	1422.54	1391.92	1357.15	1582.32	1561.24	1544.83
0.35	1232.20	1199.48	1156.04	1422.67	1392.04	1357.24	1582.54	1561.35	1544.87
0.40	1232.57	1199.85	1156.11	1422.78	1392.22	1357.37	1582.62	1561.56	1545.03
0.45	1232.79	1199.83	1156.15	1422.82	1392.31	1357.42	1582.73	1561.67	1545.21
				K_S TPa^{-1} × 10^{-10}					
0.05	8.067	8.580	9.422	5.699	5.996	6.399	4.368	4.510	4.650
0.10	8.051	8.570	9.407	5.691	5.989	6.394	4.366	4.505	4.645
0.15	8.036	8.561	9.403	5.688	5.986	6.389	4.364	4.504	4.640
0.20	8.040	8.560	9.397	5.691	5.986	6.389	4.363	4.502	4.639
0.25	8.035	8.559	9.407	5.691	5.985	6.388	4.362	4.502	4.639
0.30	8.037	8.558	9.396	5.690	5.985	6.386	4.360	4.501	4.638
0.35	8.030	8.556	9.393	5.690	5.984	6.385	4.359	4.500	4.638
0.40	8.026	8.552	9.394	5.689	5.983	6.385	4.359	4.499	4.637
0.45	8.024	8.554	9.394	5.689	5.982	6.385	4.358	4.499	4.636

Standard uncertainties in ρ , u and K_S are ± 4×10^{-3} kgm^{-3}, ± 0.4 ms^{-1} and ± 0.10×10^{-10} TPa^{-1}.

FTIR spectrum of Butylatedhydroxy anisole; BHA (A)

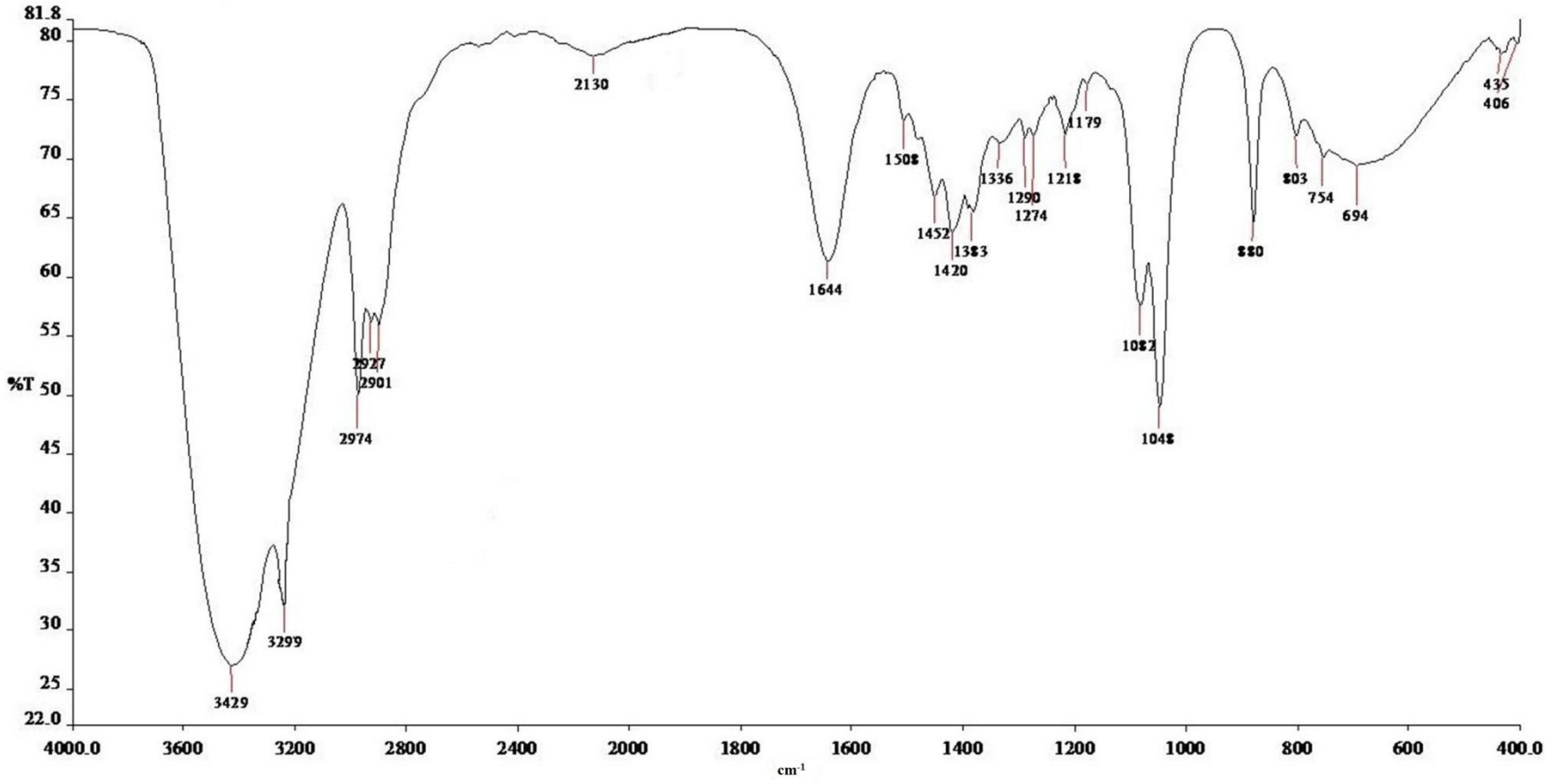

FTIR spectrum of Butylatedhydroxy toluene; BHT (T)

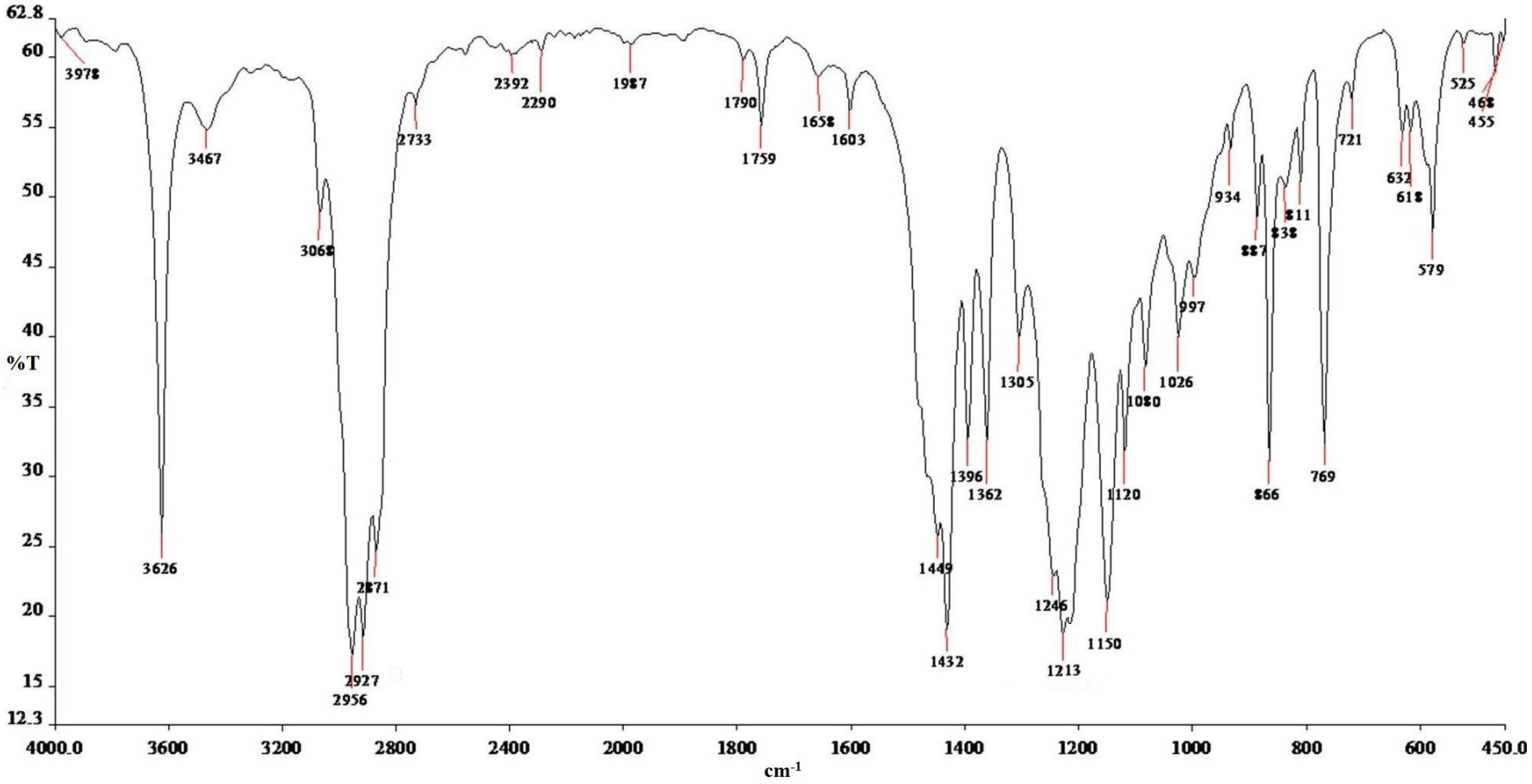

FTIR spectrum of Sodium dodecyl sulfate; SDS (S)

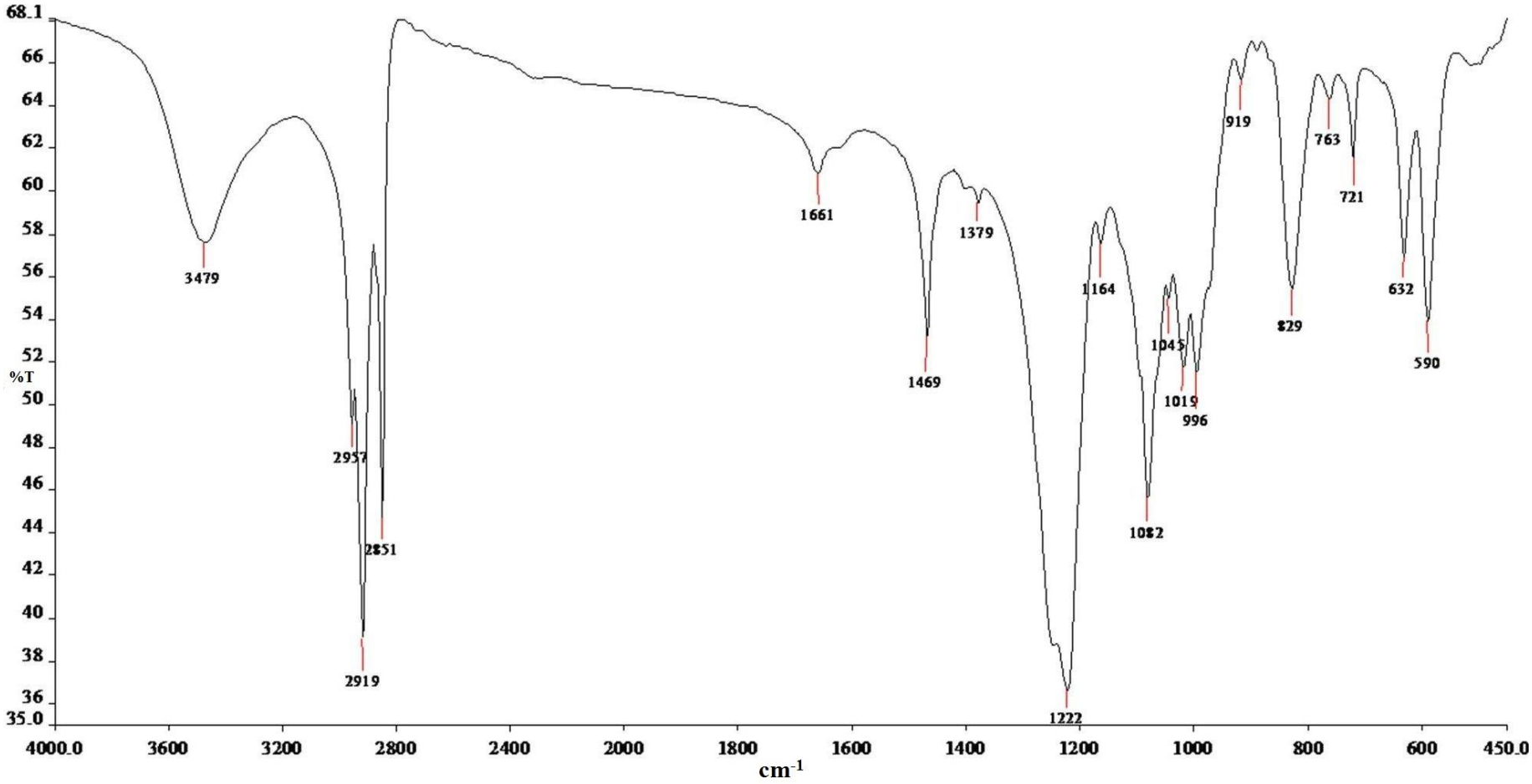

FTIR spectrum of SAM (M; MeOH)

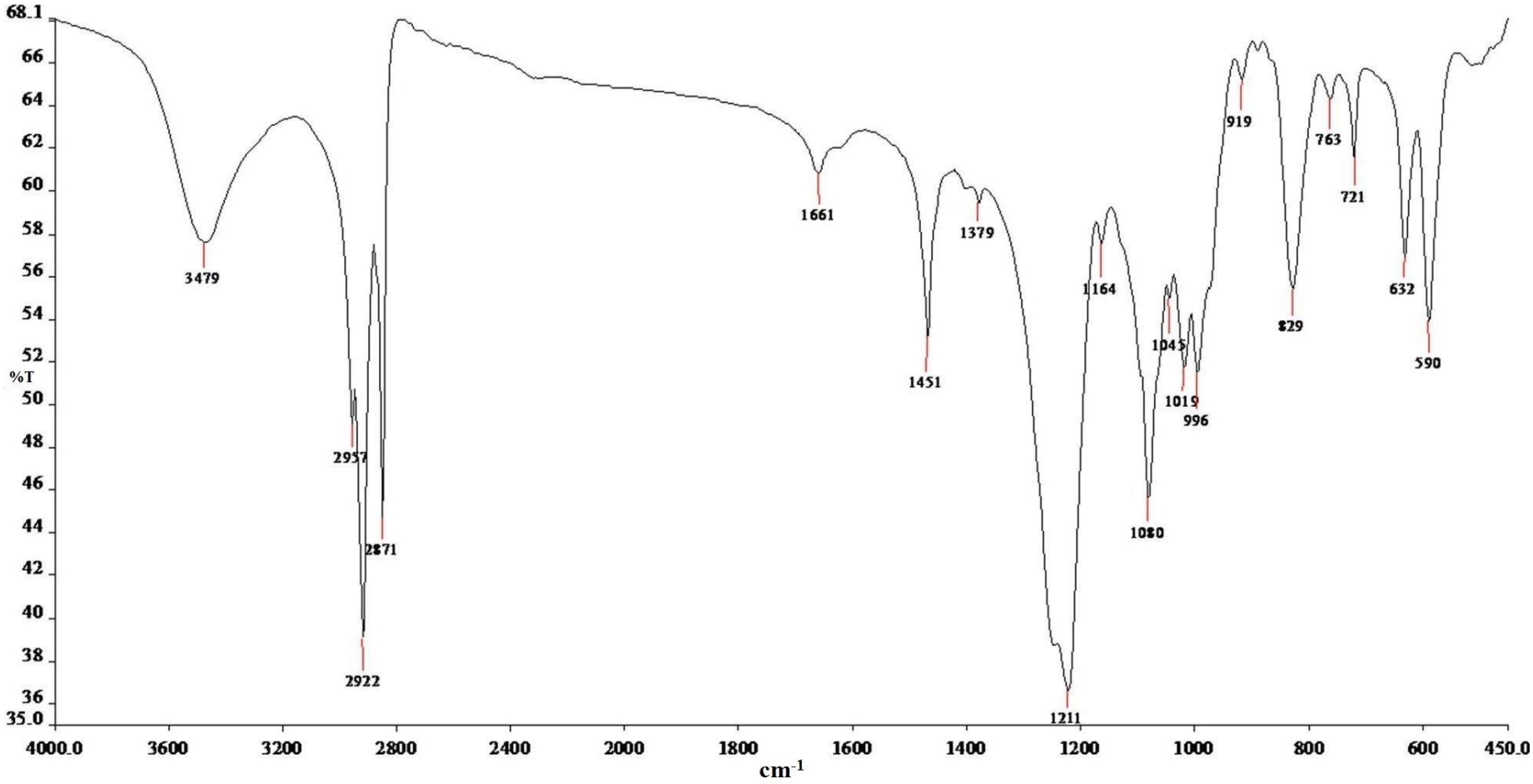

FTIR spectrum of SAE (E; EtOH)

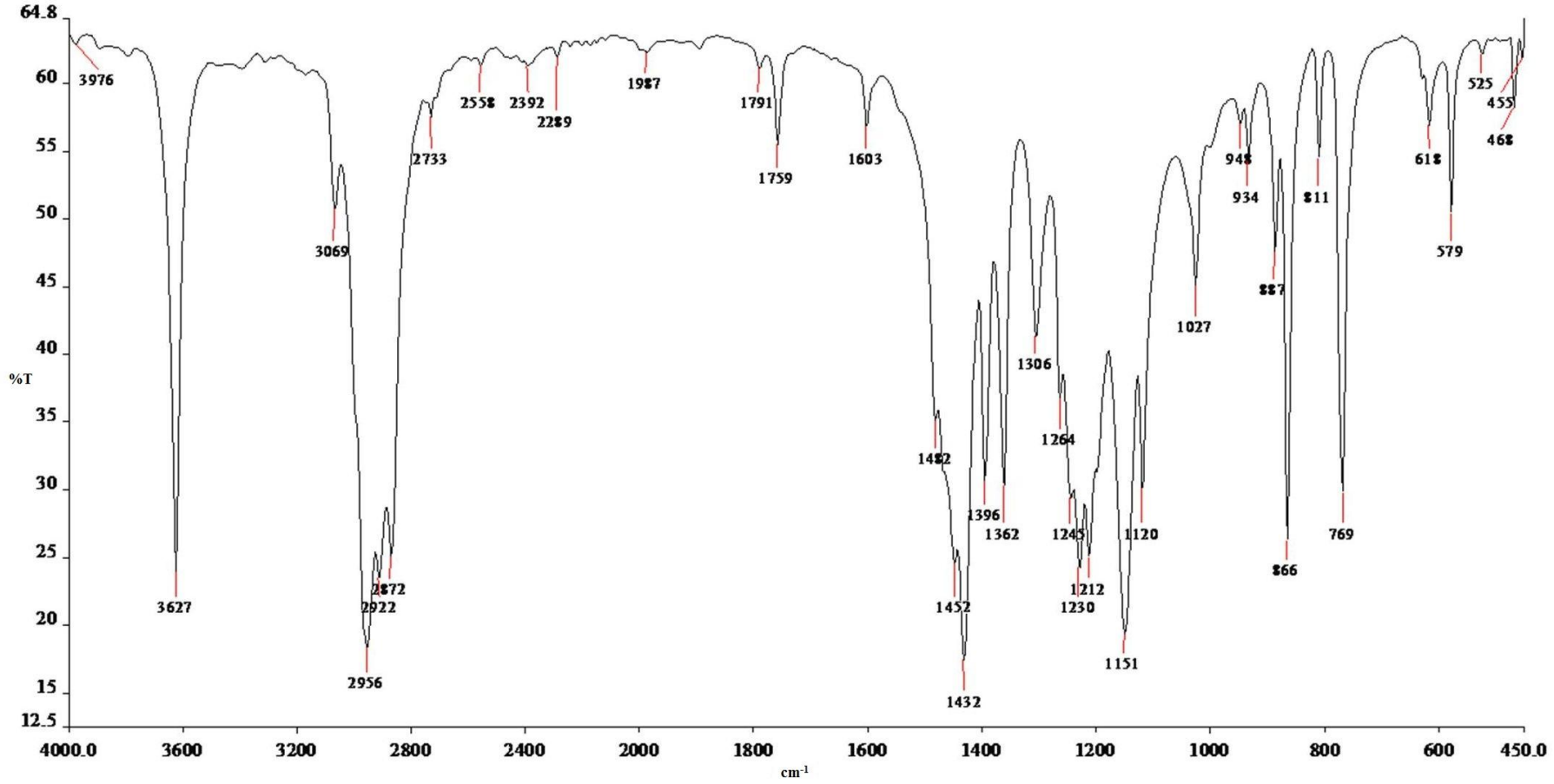

FTIR spectrum of SAP (P; 1-PrOH)

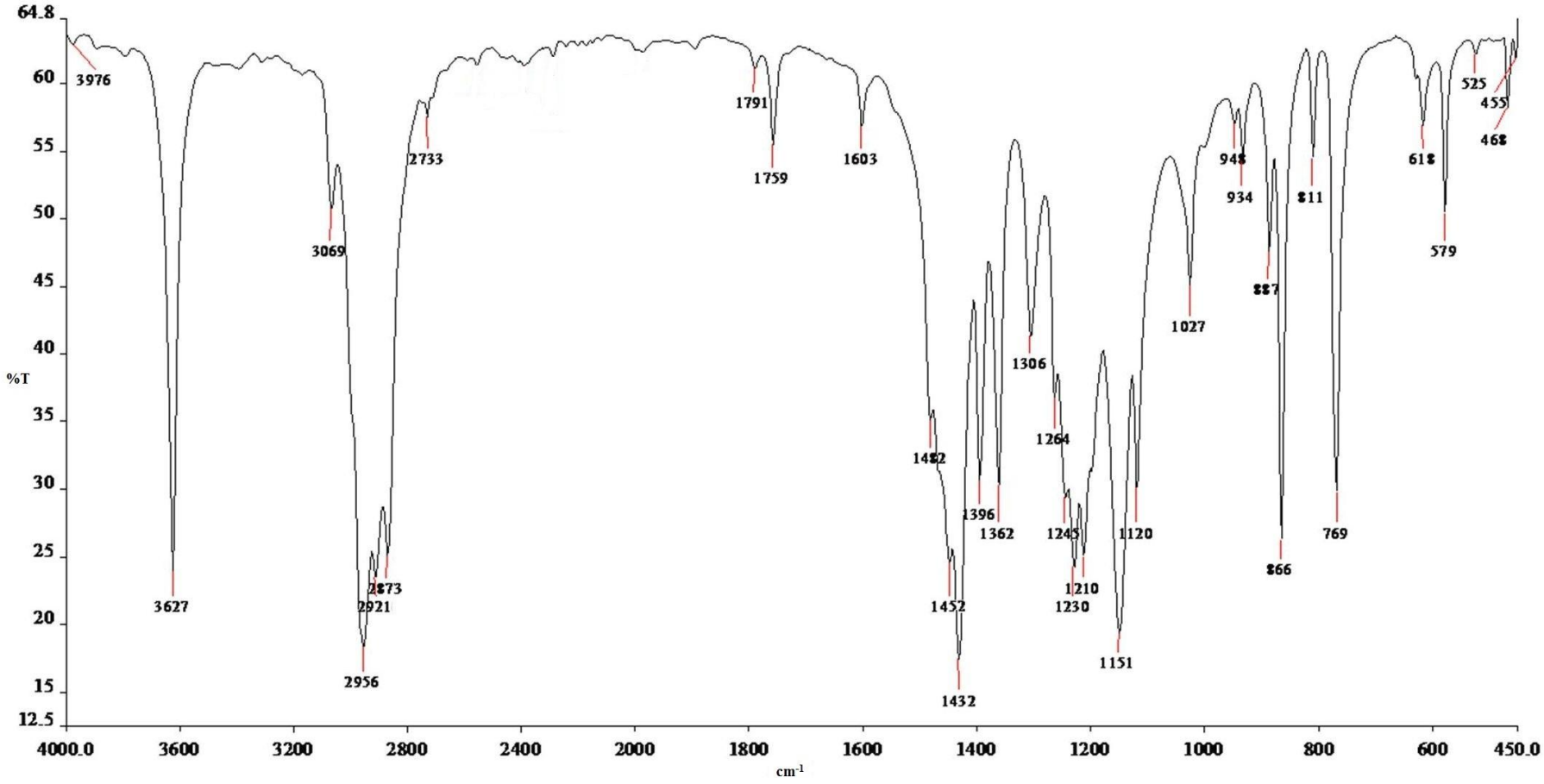

FTIR spectrum of STM (M; MeOH)

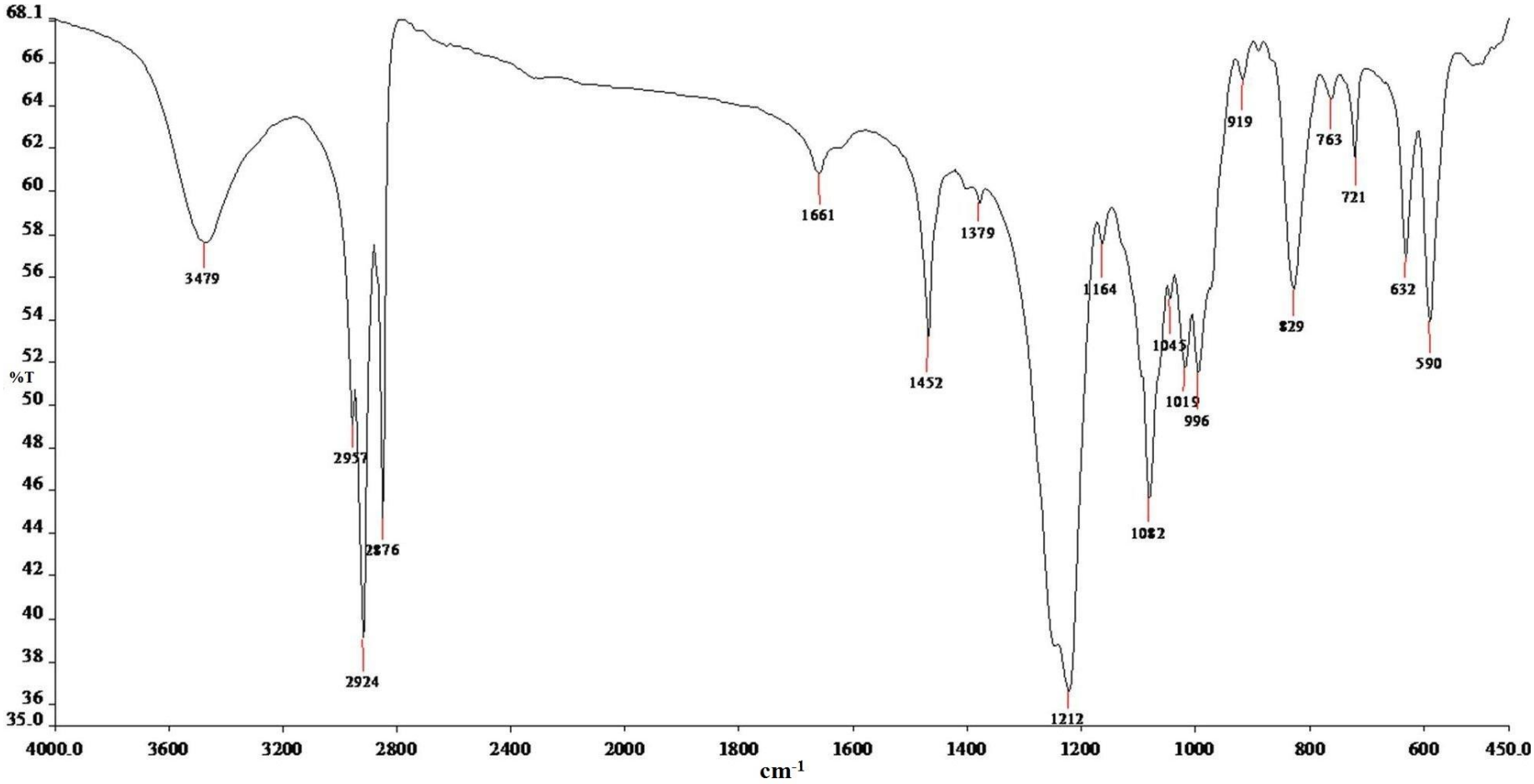

FTIR spectrum of STE (E; EtOH)

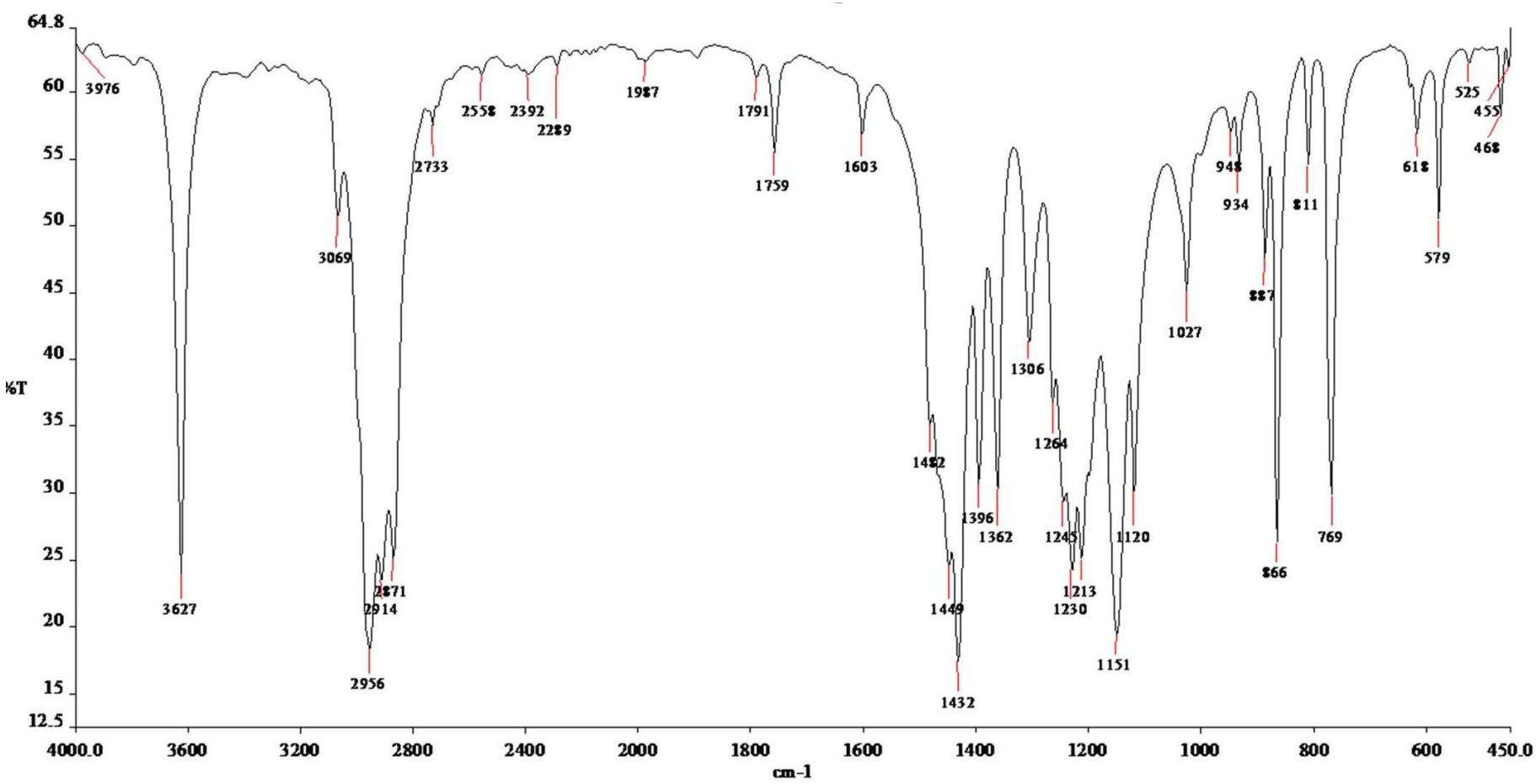

FTIR spectrum of STP (P; 1-PrOH)

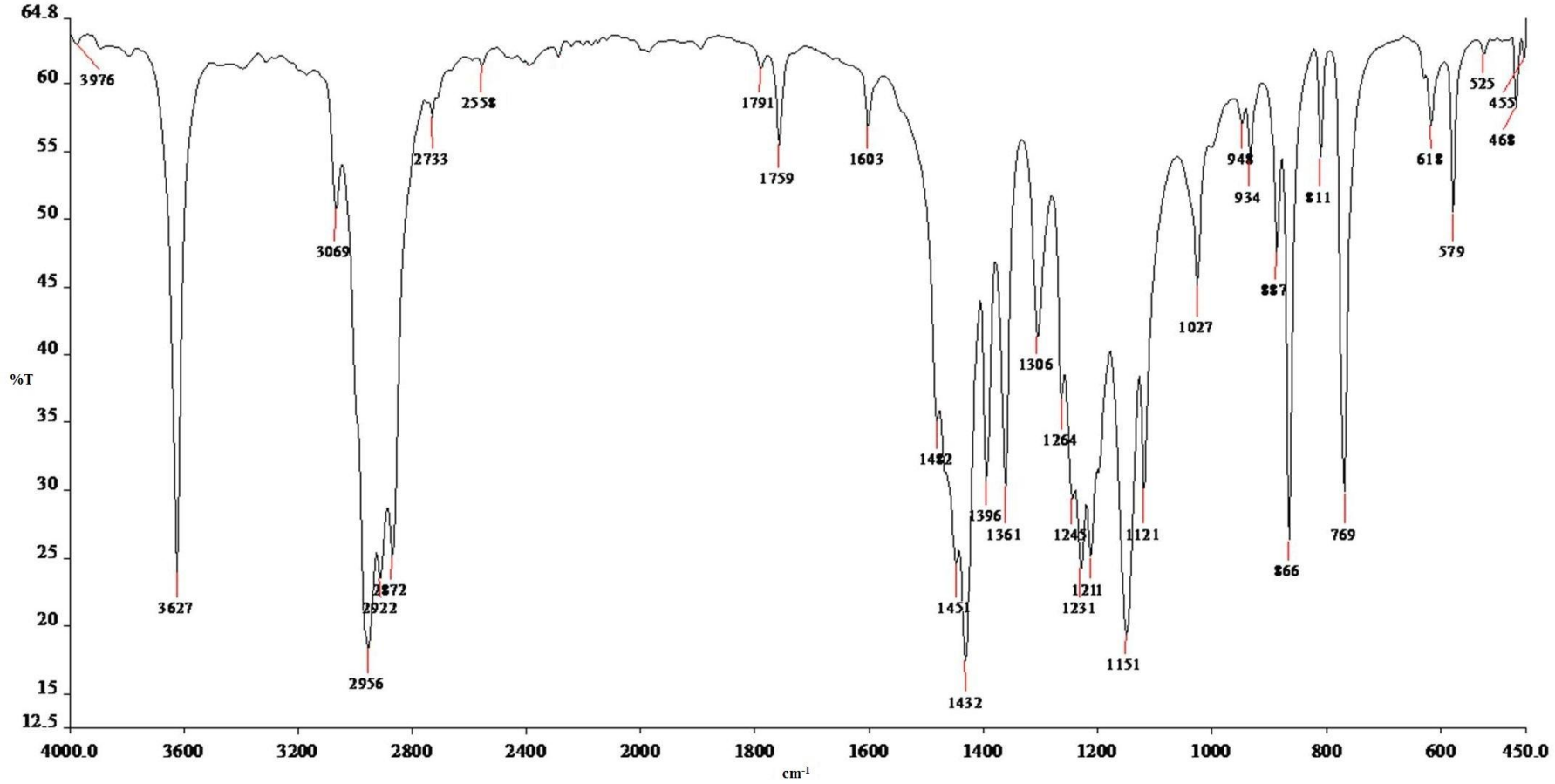

FTIR spectrum of Cetyltrimethylammonium bromide; CTAB (C)

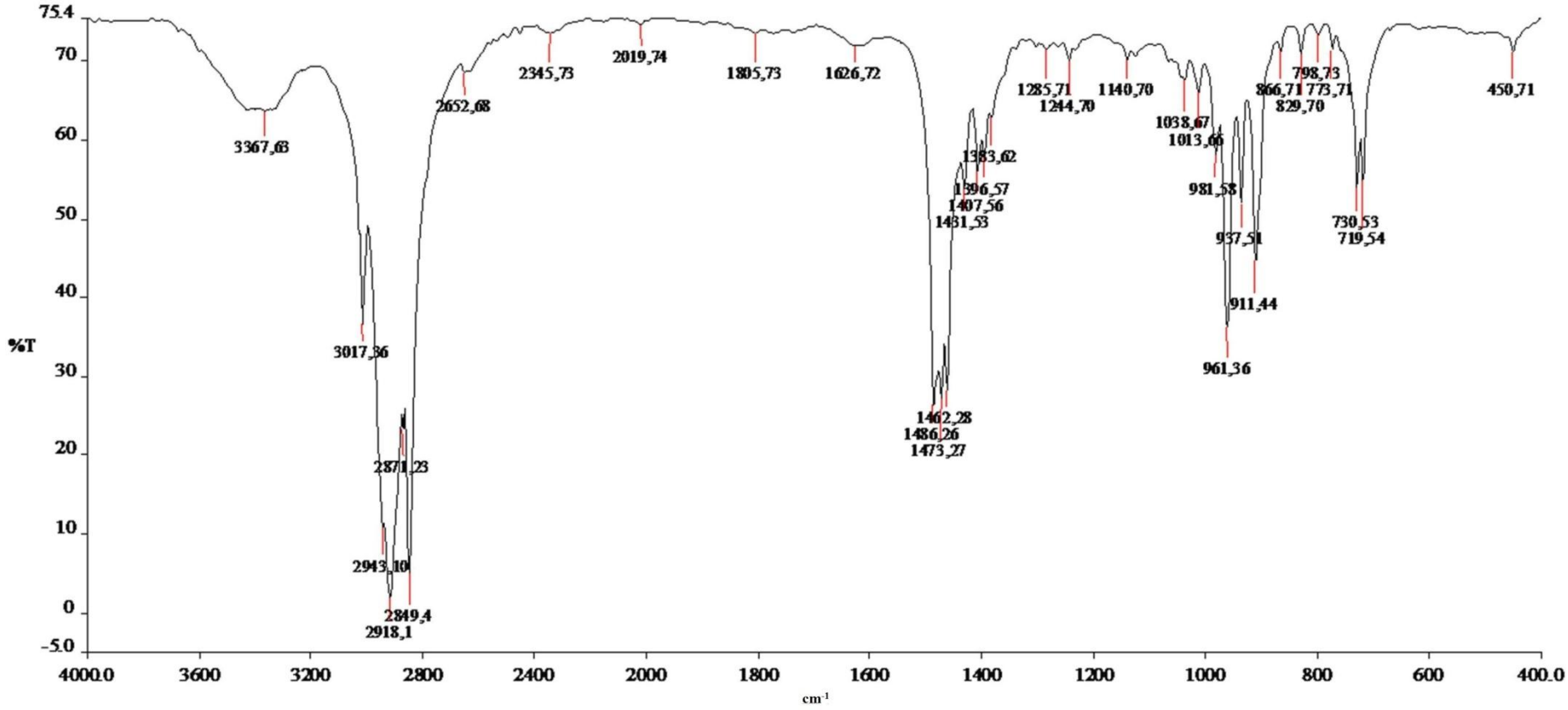

FTIR spectrum of CAM (M; MeOH)

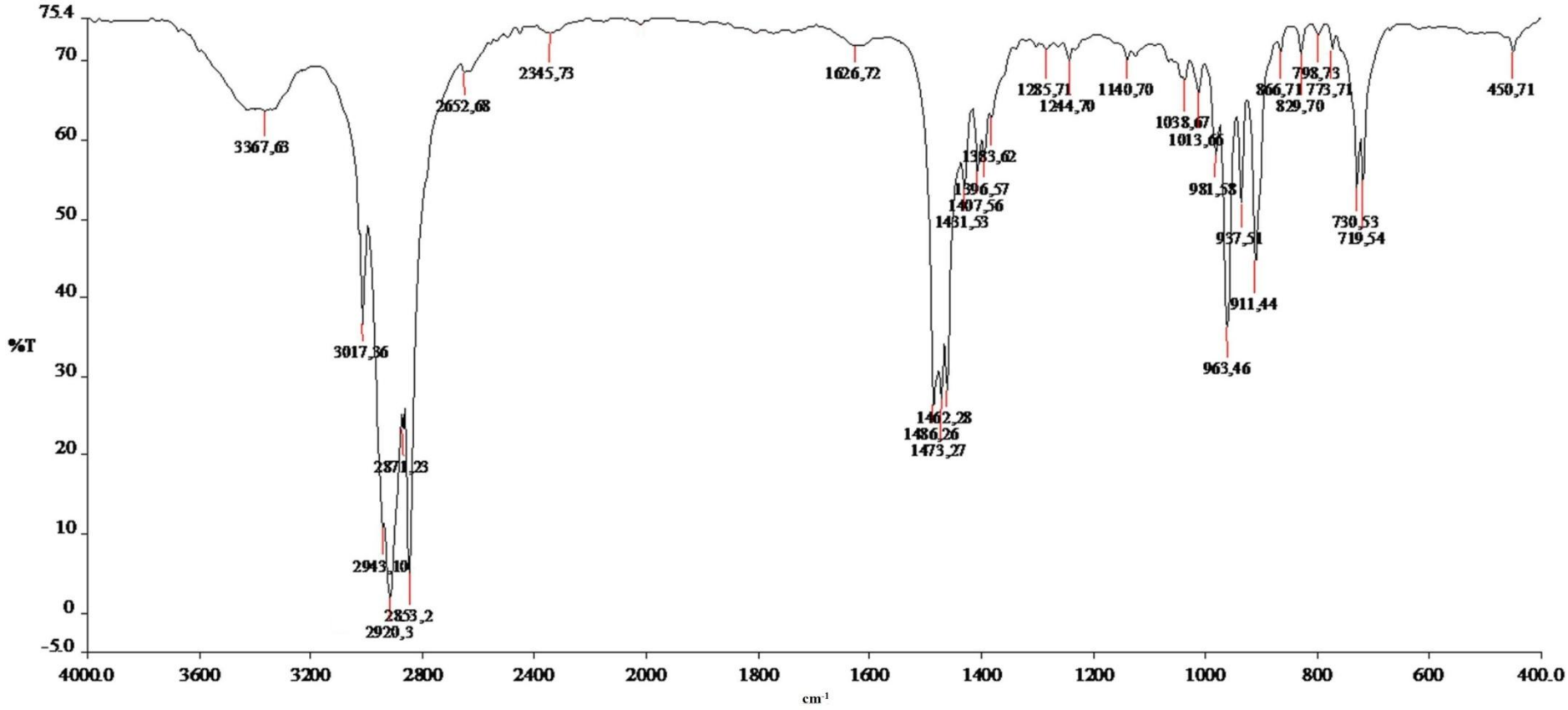

FTIR spectrum of CAE (E; EtOH)

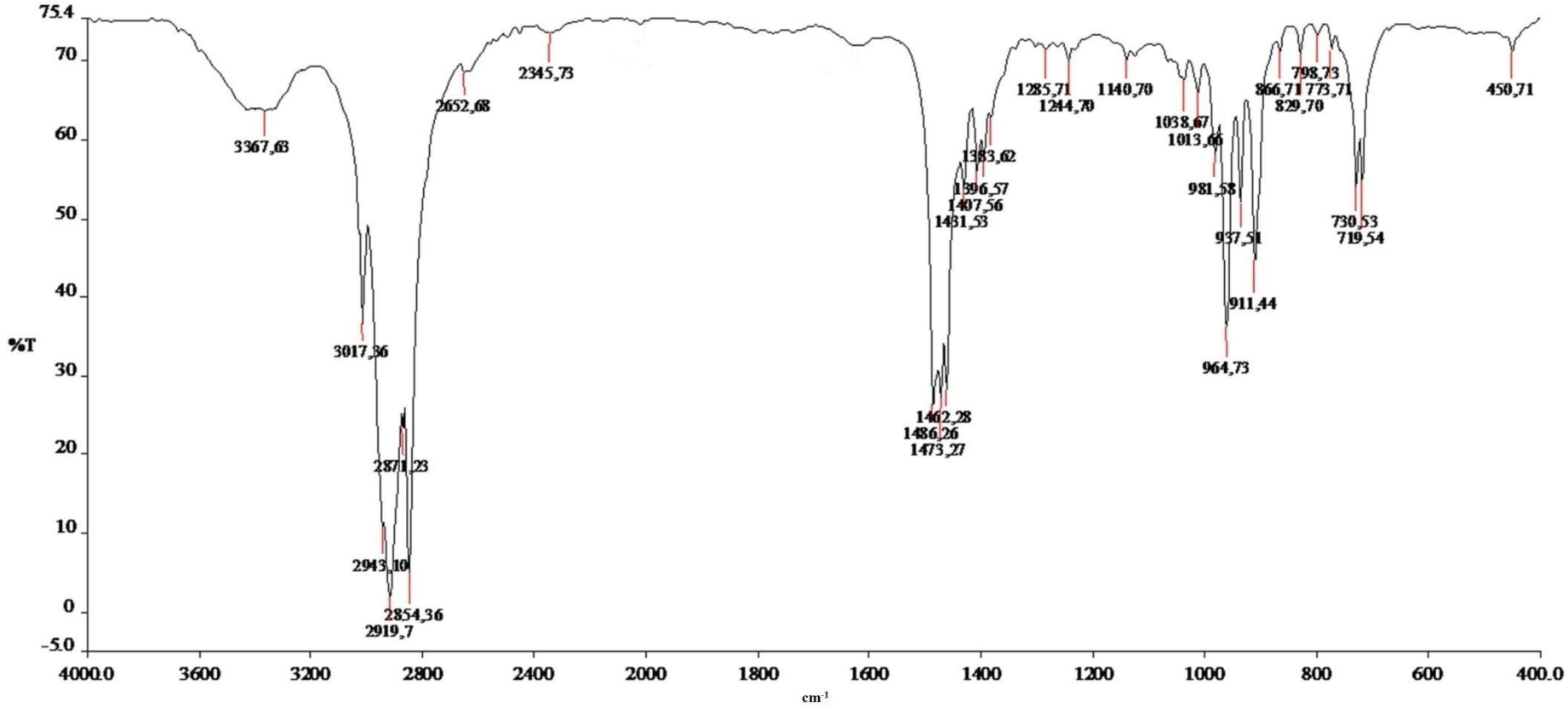

FTIR spectrum of CAP (P; 1-PrOH)

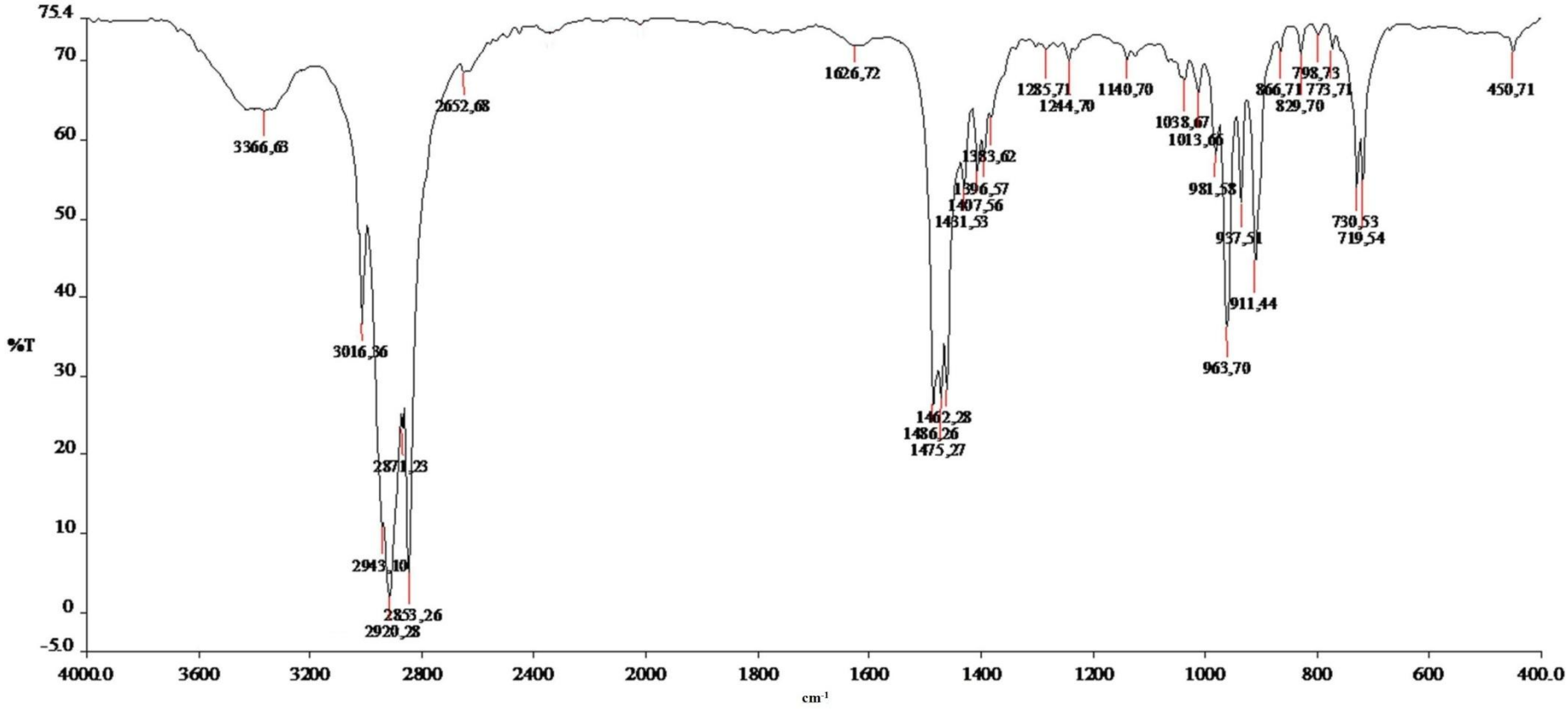

FTIR spectrum of CTM (M; MeOH)

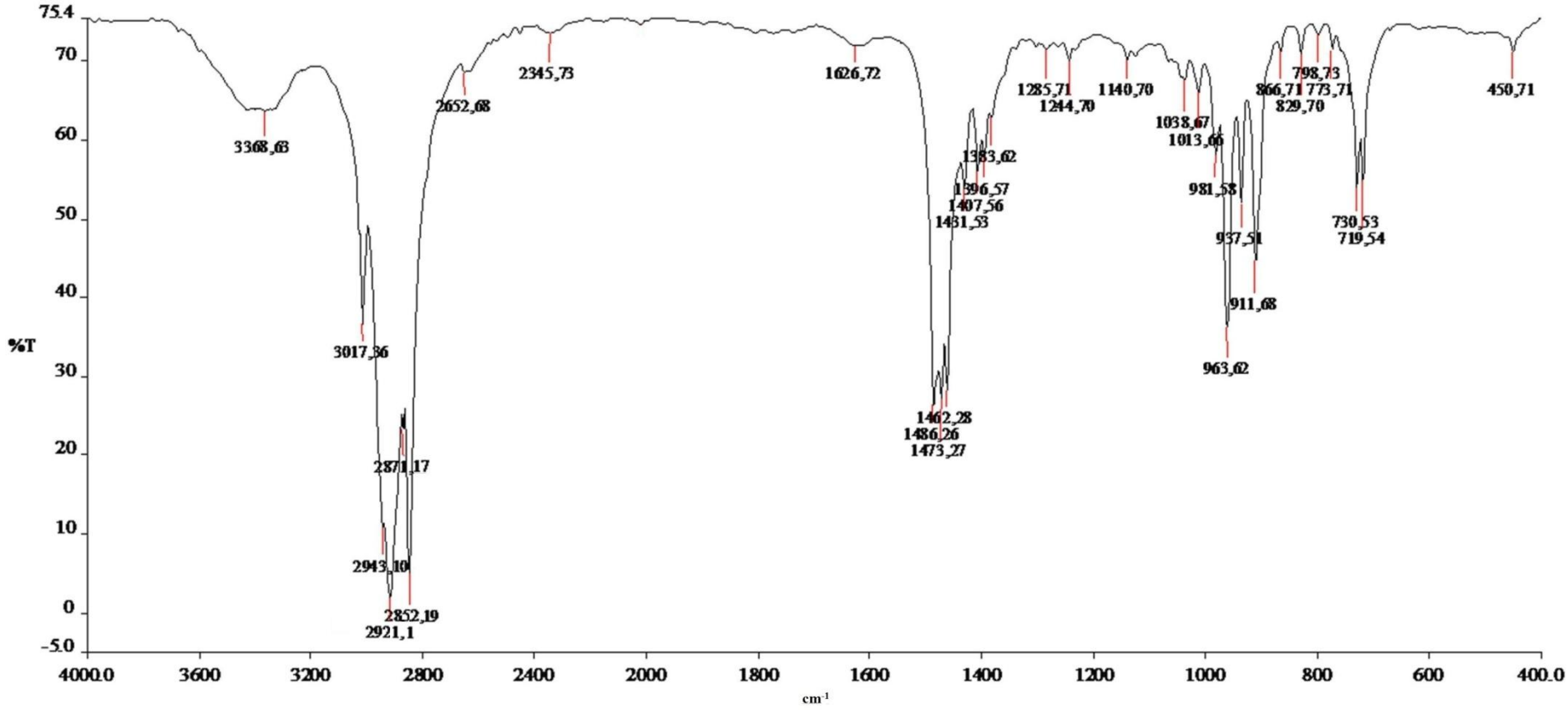

FTIR spectrum of CTE (E; EtOH)

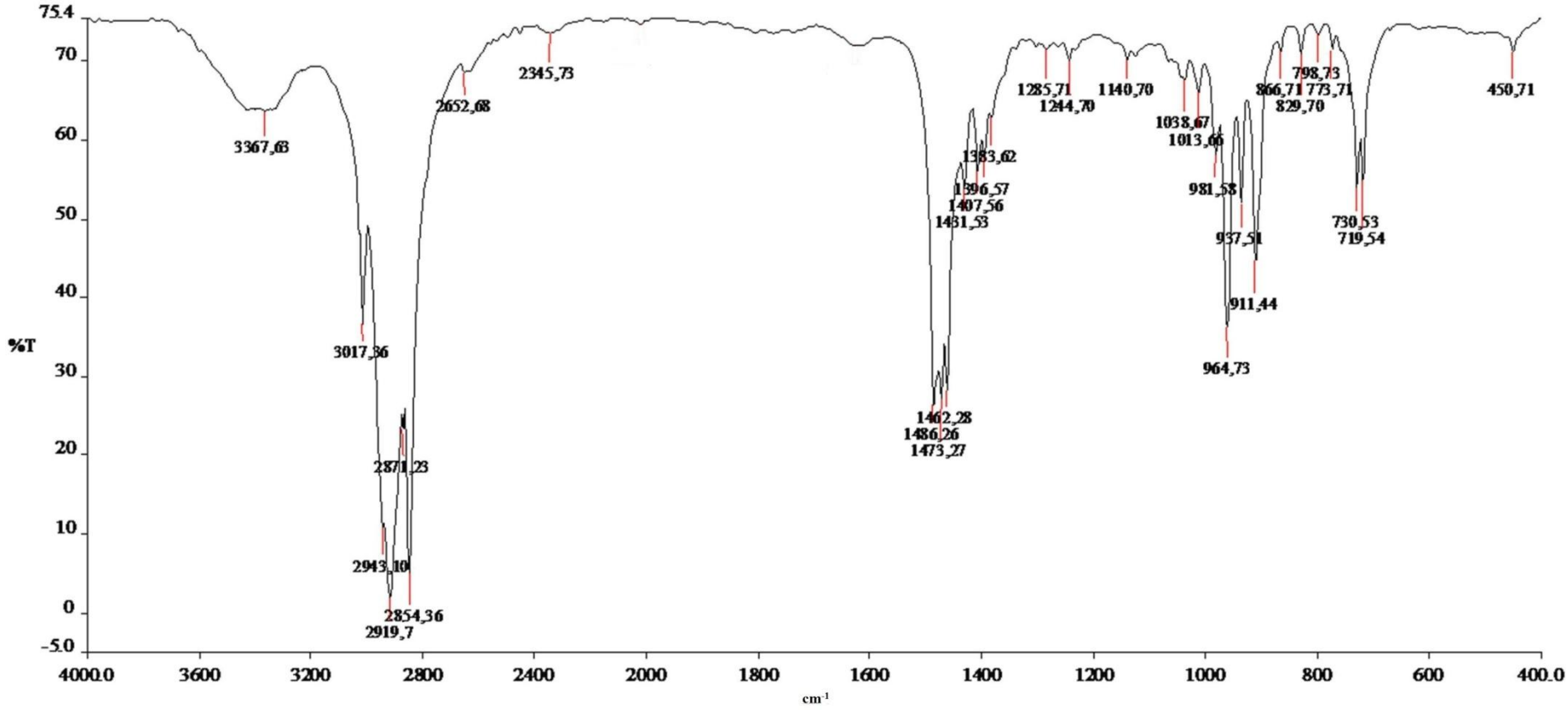

FTIR spectrum of CTP (P; 1-PrOH)

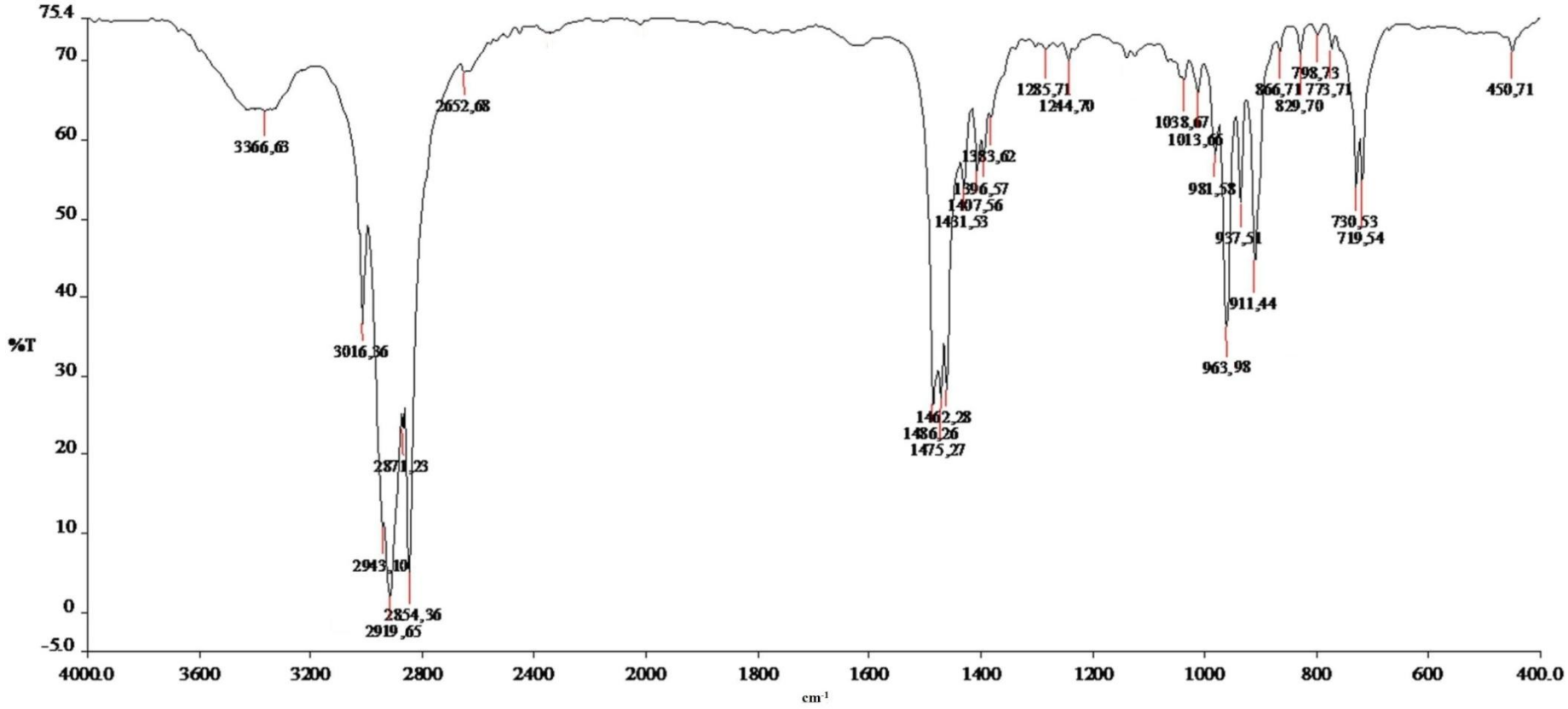

FTIR spectrum of *tert*-octylphenol ethoxylate; TX100 (X)

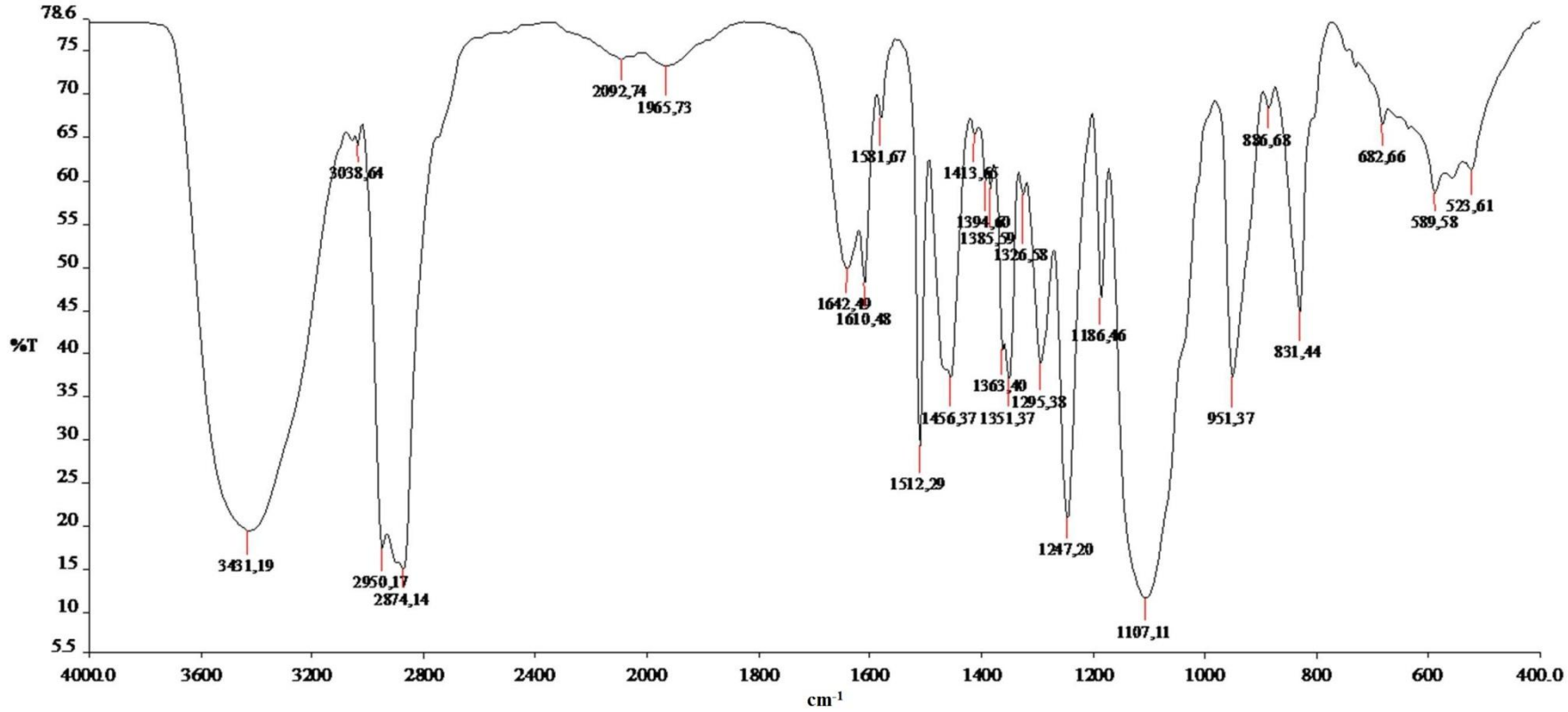

FTIR spectrum of XAM (M; MeOH)

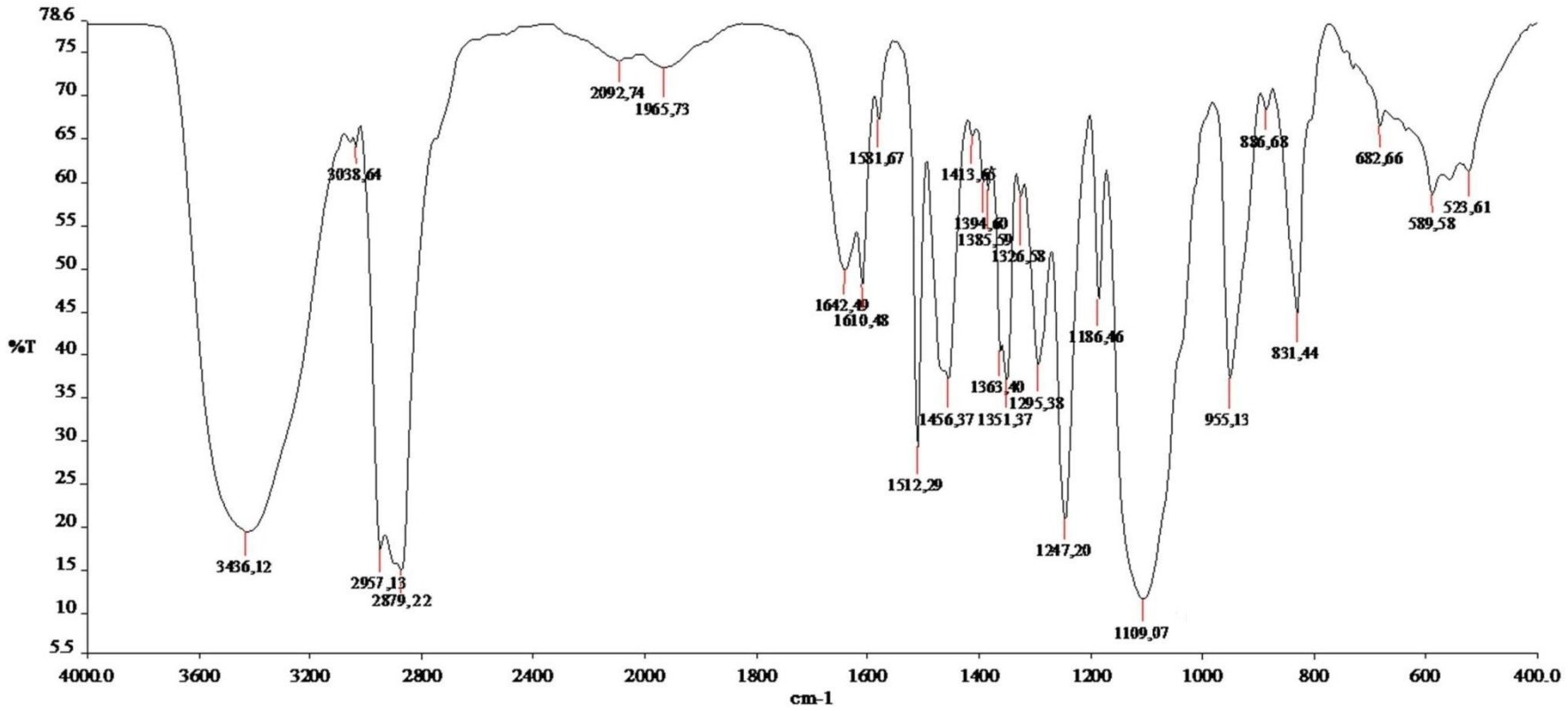

FTIR spectrum of XAE (E; EtOH)

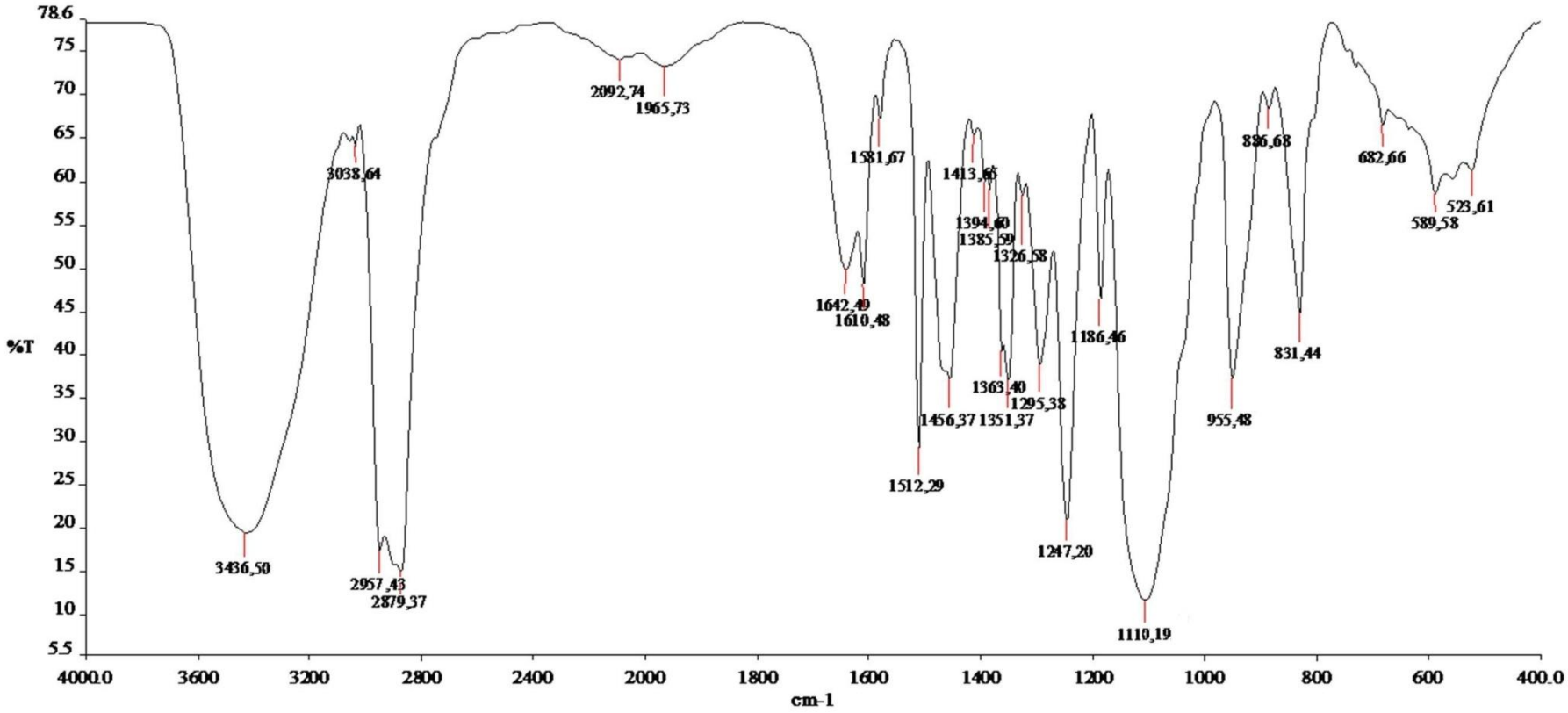

FTIR spectrum of XAP (P; 1-PrOH)

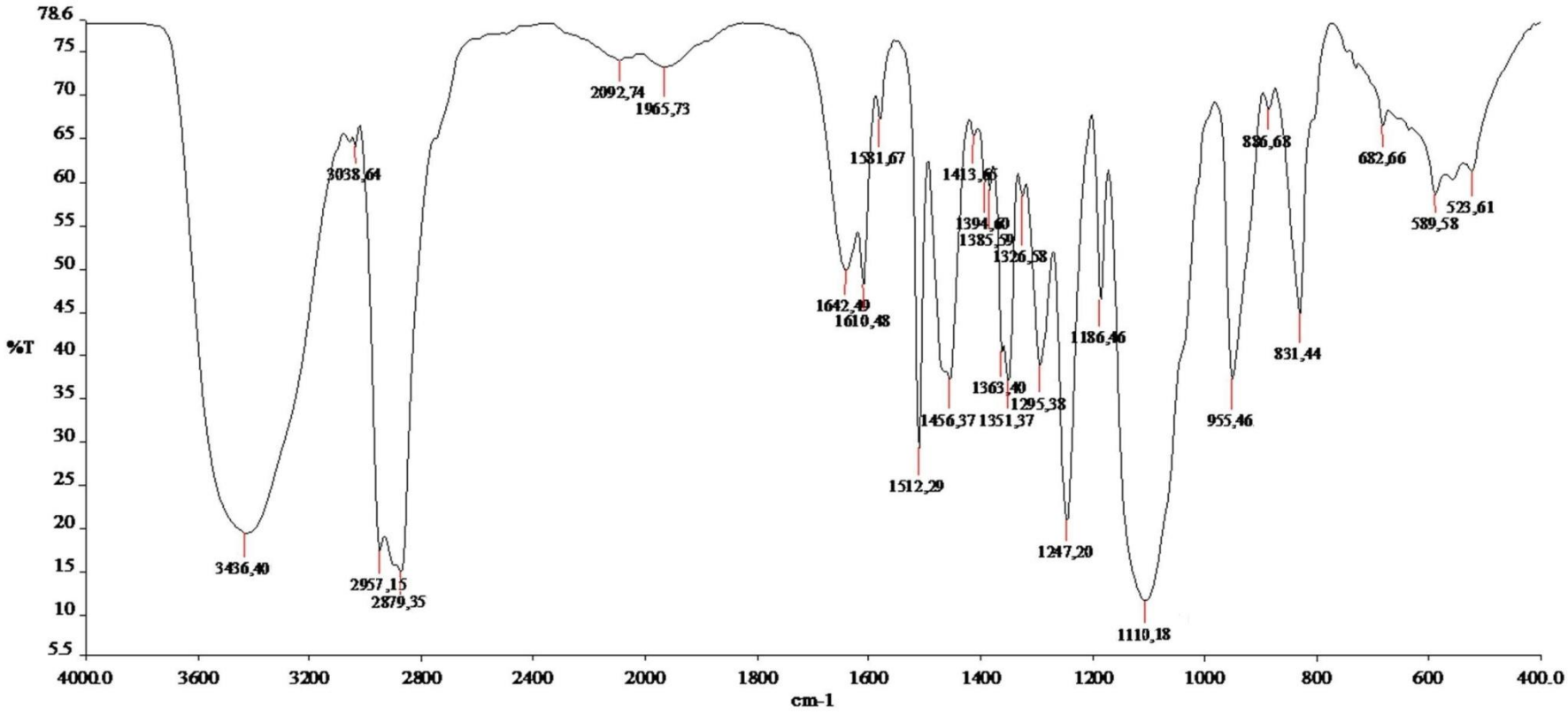

FTIR spectrum of XTM (M; MeOH)

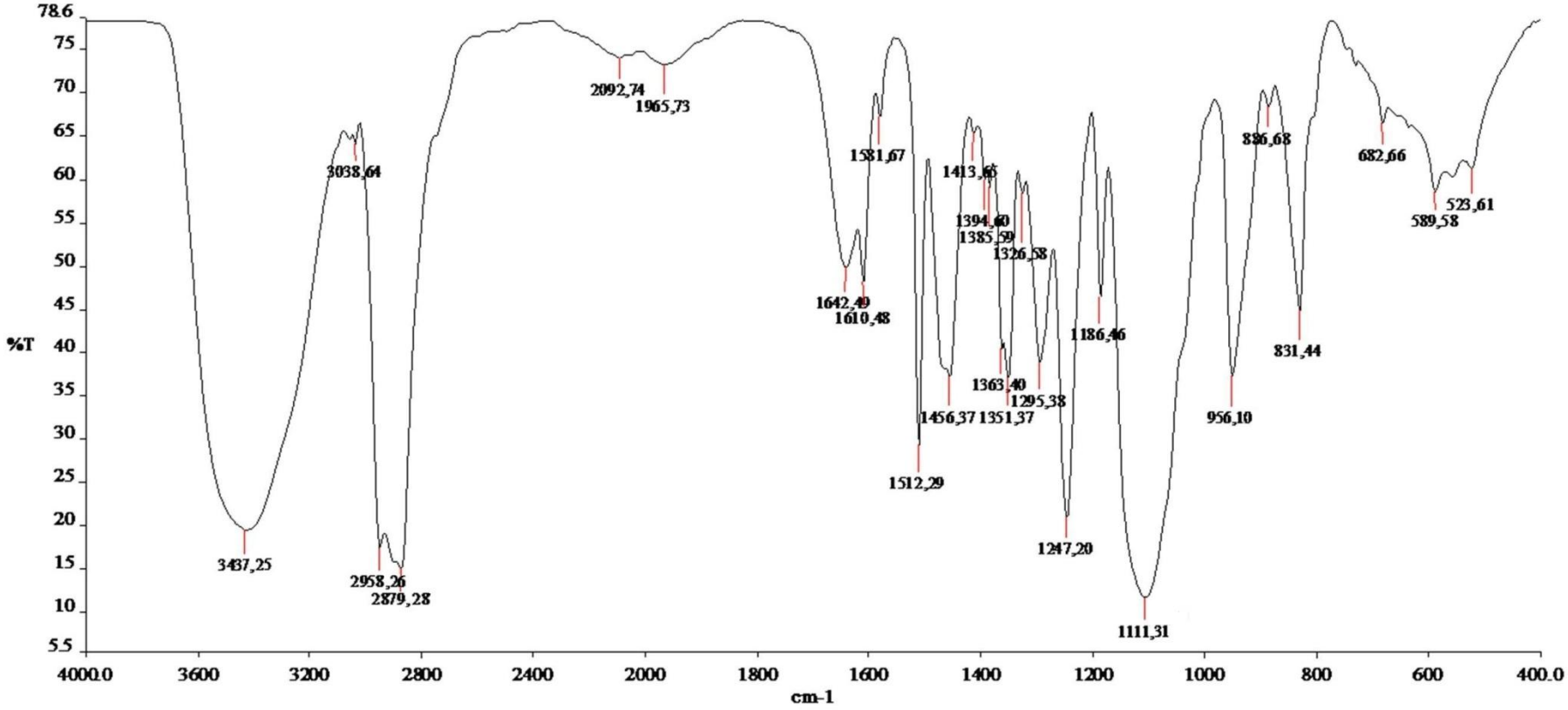

FTIR spectrum of XTE (E; EtOH)

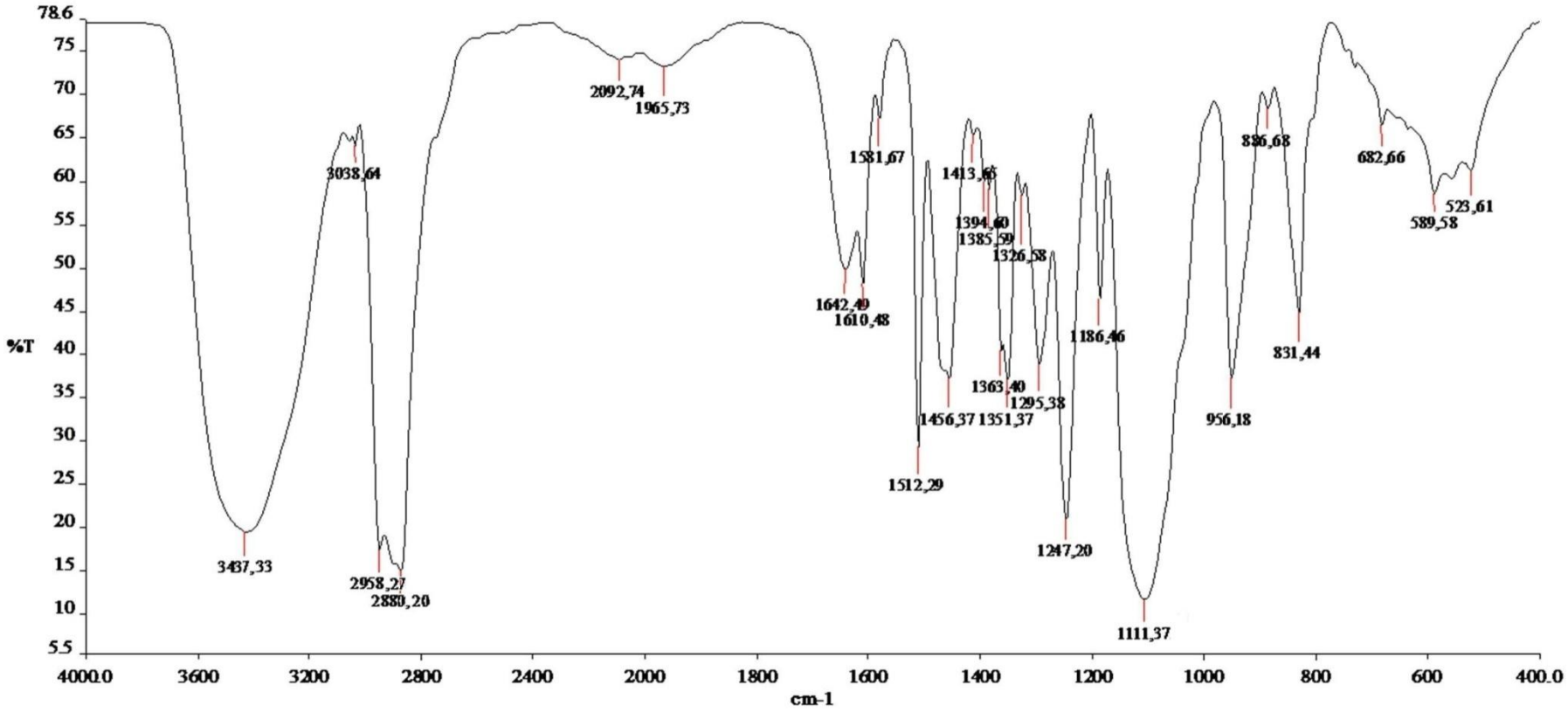

FTIR spectrum of XTP (P; 1-PrOH)

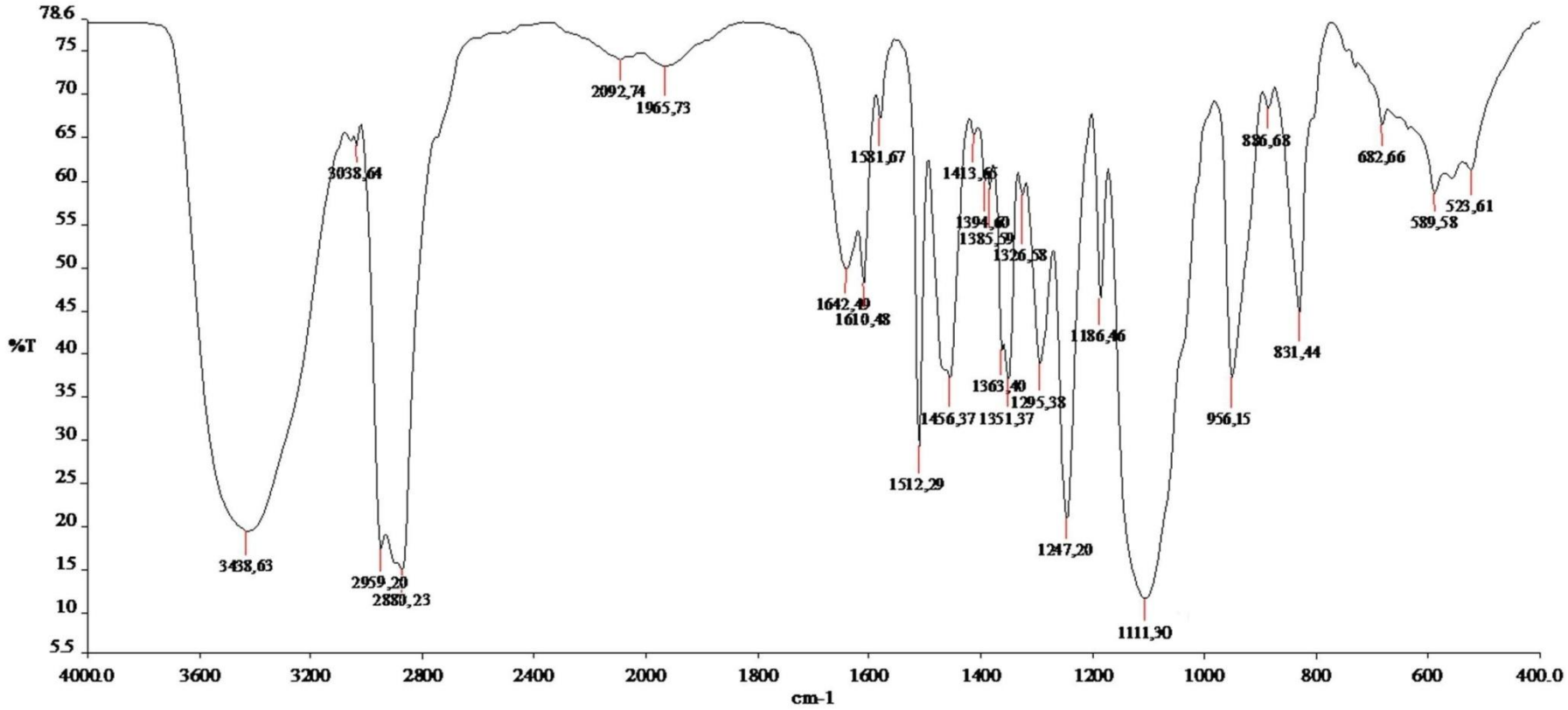

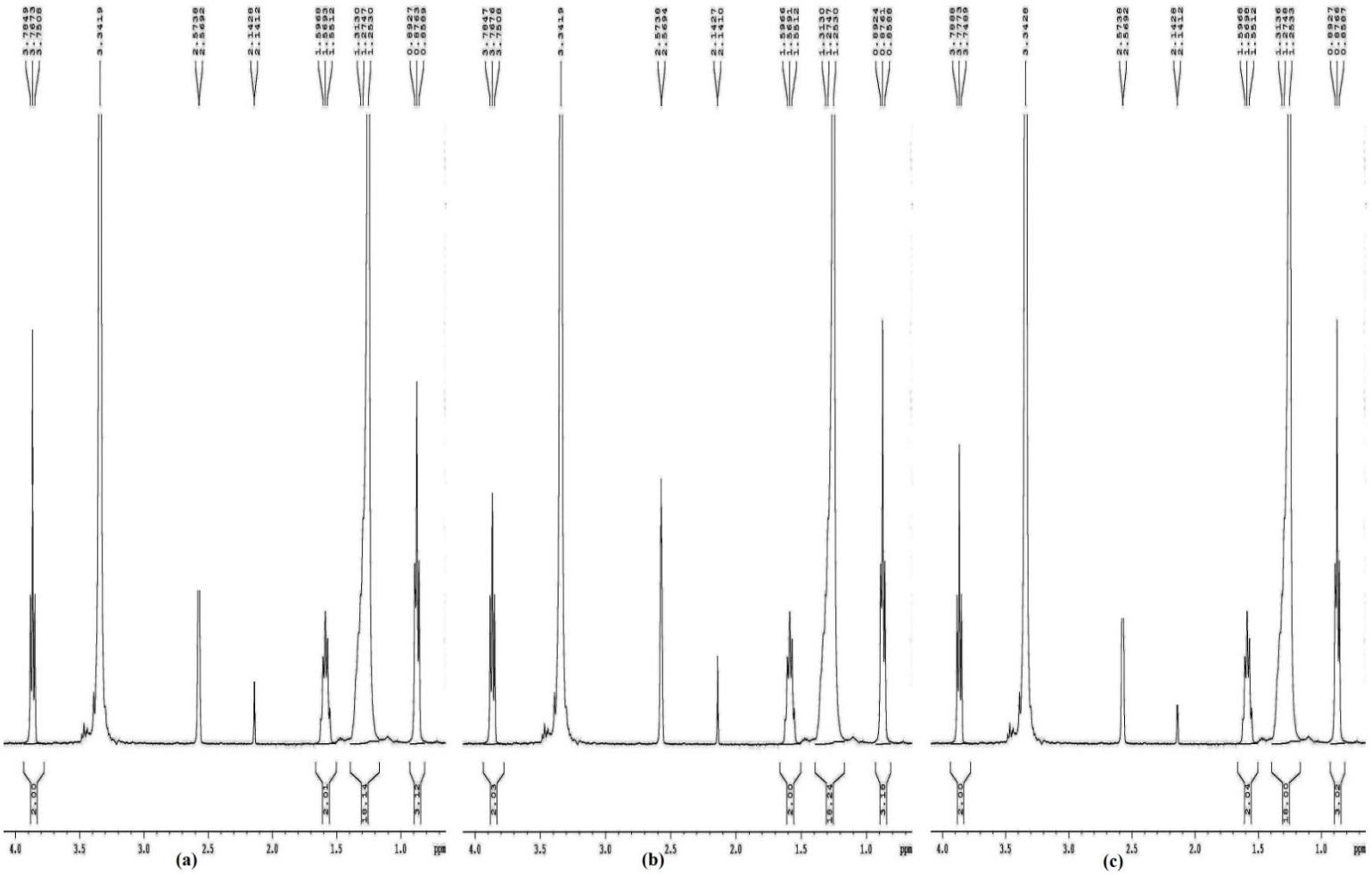

B1 ^{1}H NMR spectra of SDS molecule prepared in (a) water-methanol mixture (b) water-ethanol mixture (c) water-1-propanol mixture containing BHA (0.03 mmol kg^{-1}).

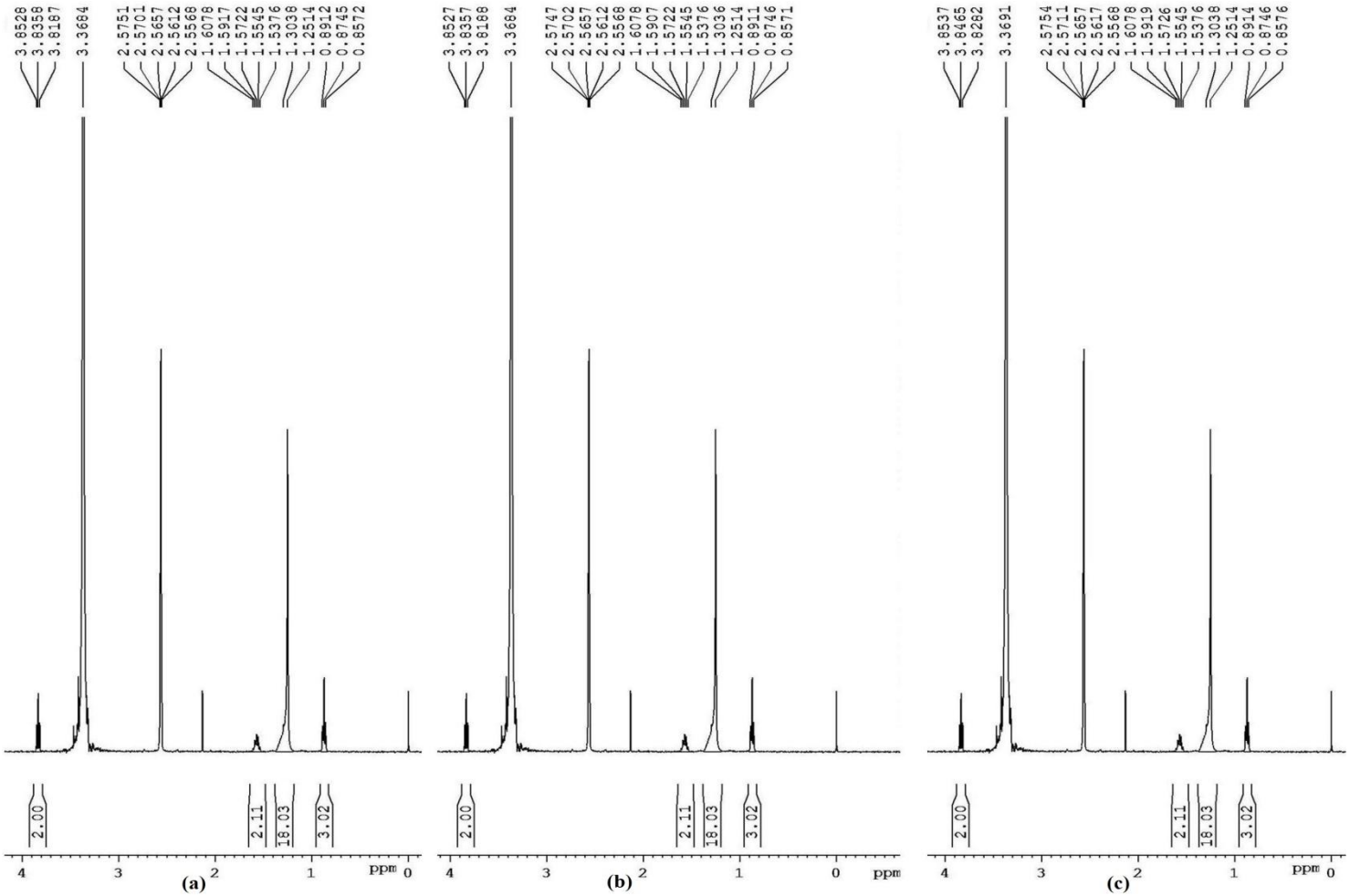

B2 ^{1}H NMR spectra of SDS molecule prepared in (a) water-methanol mixture (b) water-ethanol mixture (c) water-1-propanol mixture containing BHT (0.02 mmol kg^{-1}).

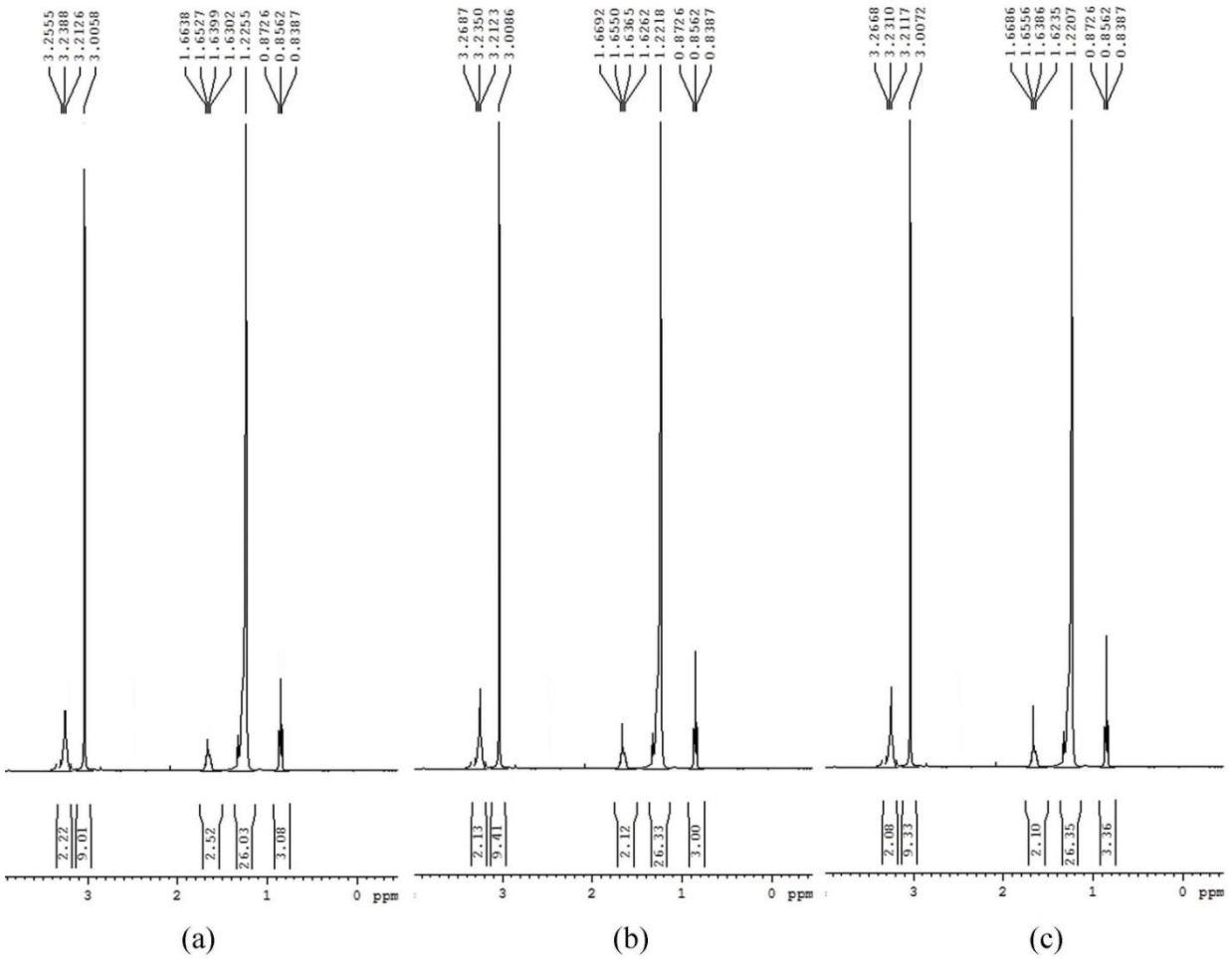

B3 ^{1}H NMR spectra of CTAB molecule prepared in (a) water-methanol mixture (b) water-ethanol mixture (c) water-1-propanol mixture containing BHA (0.03 mmol kg^{-1}).

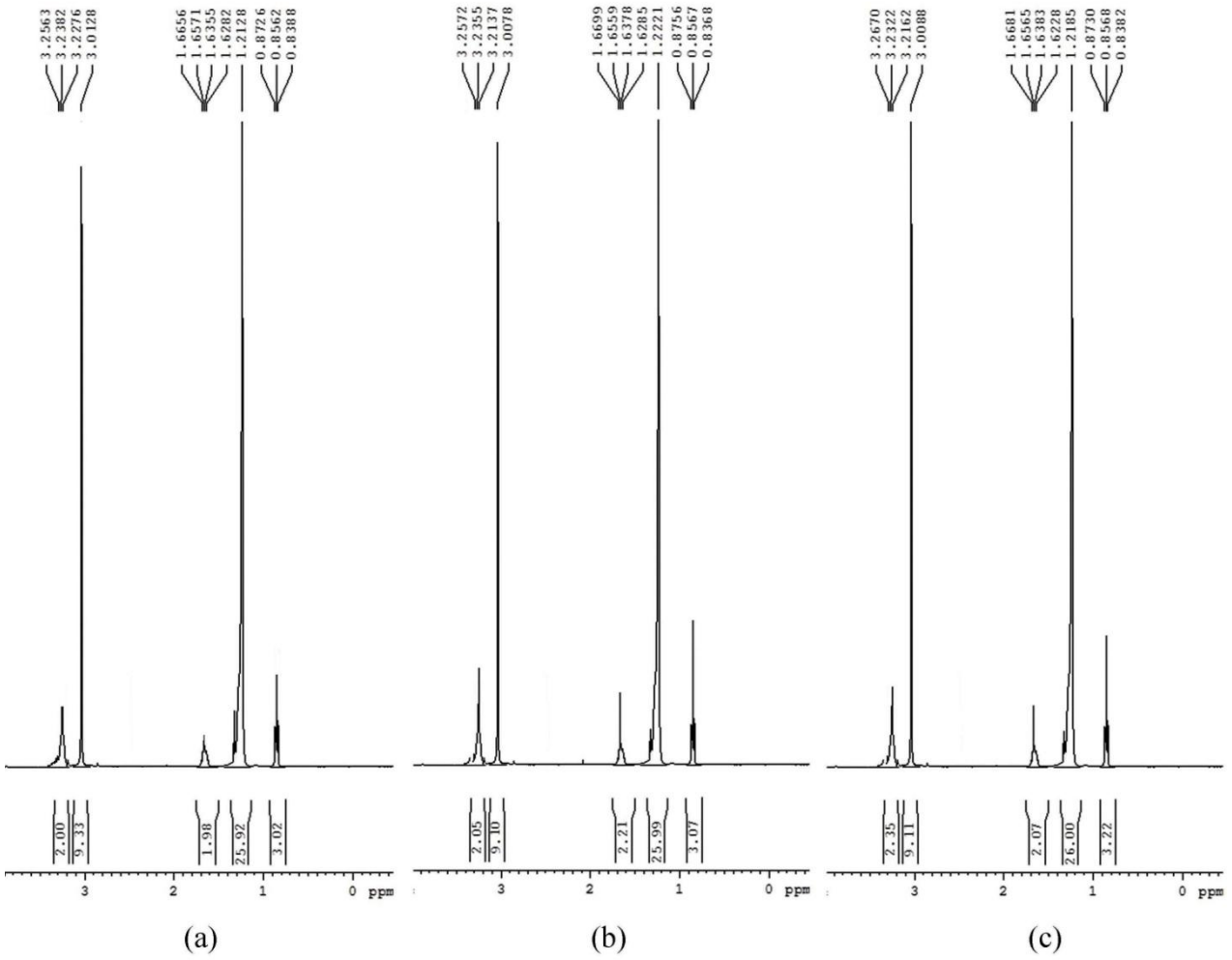

B4 ^{1}H NMR spectra of CTAB molecule prepared in (a) water-methanol mixture (b) water-ethanol mixture (c) water-1-propanol mixture containing BHT (0.02 mmol kg^{-1}).

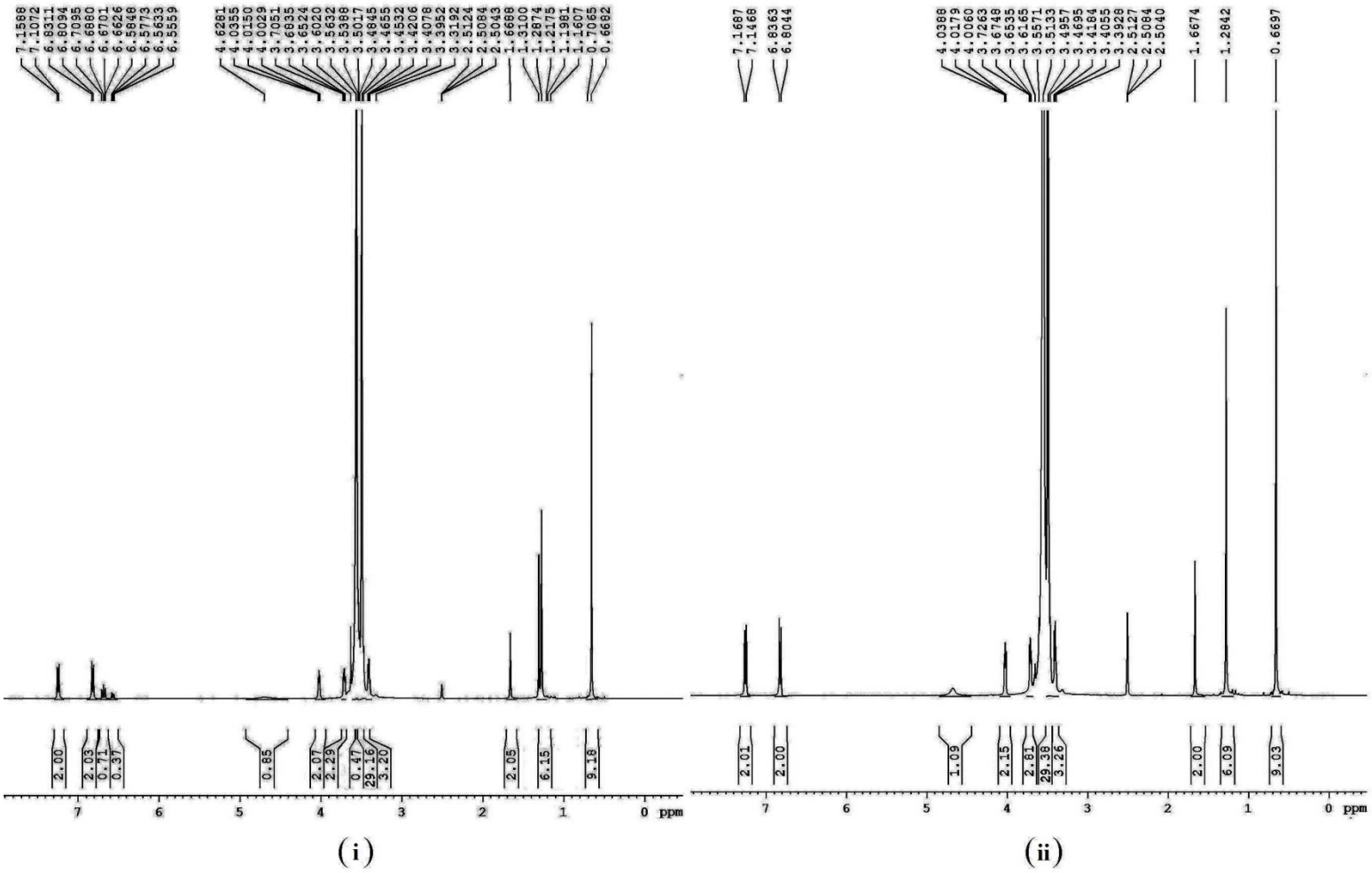

B5 The ^{1}H NMR spectra of TX100 molecule prepared in water-methanol mixture containing; i) BHA and ii) BHT.

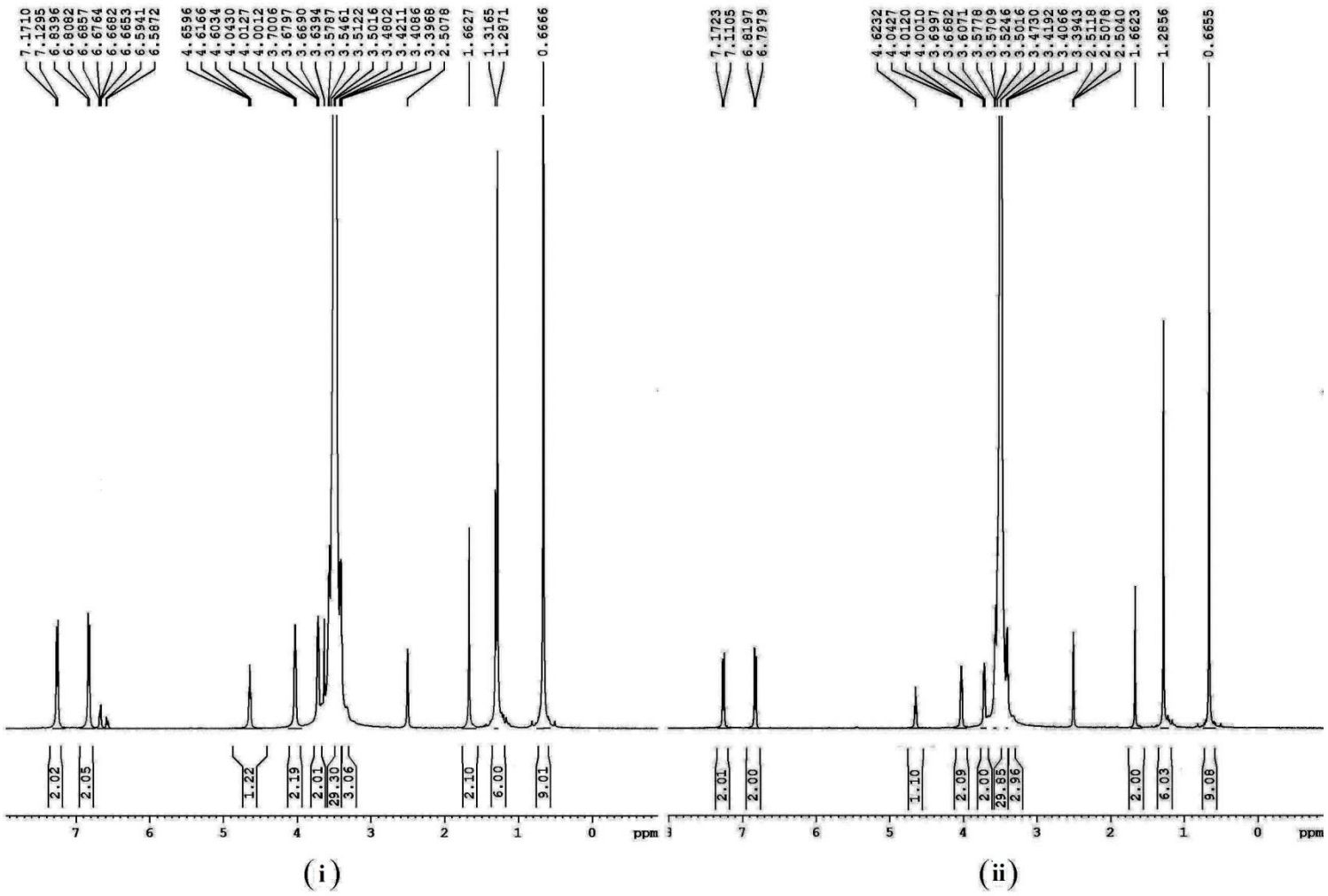

B6 The ^{1}H NMR spectra of TX100 molecule prepared in water-ethanol mixture containing; i) BHA and ii) BHT.

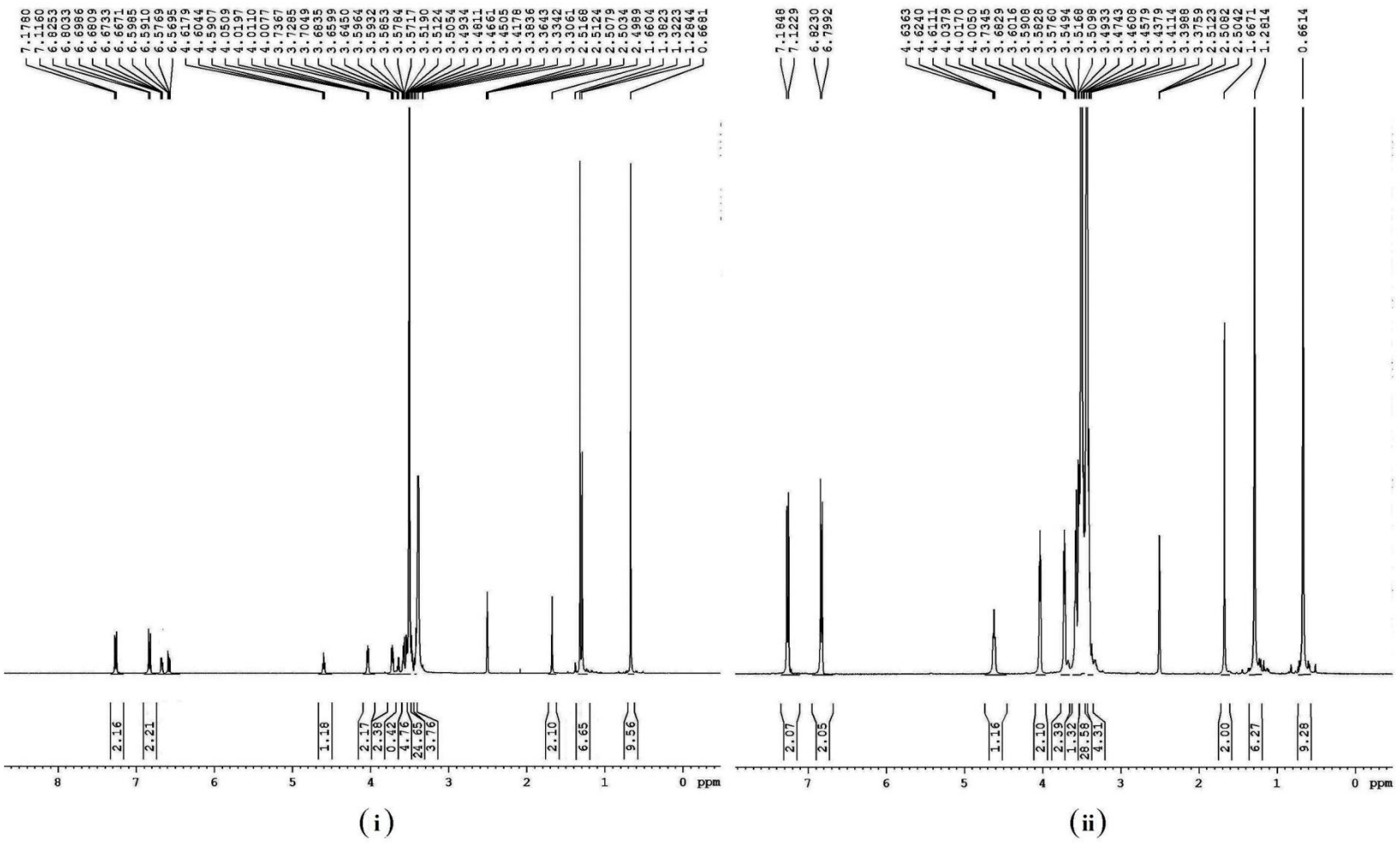

B7 ^{1}H NMR spectra of TX100 molecule prepared in water-1-propanol mixture containing; i) BHA and ii) BHT.

B8 *In vitro* release rate profile with model kinetics for all formulations.

Formulations	Zero order		First order		Higuchi		Korsmeyer–Peppas	
	R^2	K	R^2	K	R^2	K	R^2	n
CA-1S	0.998	0.222	0.711	0.001303	0.929	4.546	0.992	0.325
CA-2S	0.998	0.235	0.699	0.001302	0.930	4.805	0.994	0.328
CA-3S	0.996	0.252	0.665	0.001302	0.937	5.186	0.995	0.330
CT-1S	0.998	0.223	0.710	0.001303	0.929	4.559	0.992	0.325
CT-2S	0.998	0.236	0.698	0.001303	0.914	10.05	0.994	0.328
CT-3S	0.991	0.248	0.705	0.006513	0.909	10.38	0.994	0.330
CAT-1S	0.996	0.225	0.661	0.001303	0.911	10.53	0.995	0.331
CAT-2S	0.998	0.237	0.695	0.001303	0.931	4.860	0.994	0.328
CAT-3S	0.956	0.231	0.506	0.001303	0.986	4.637	0.972	0.326
CA-1C	0.998	0.215	0.632	0.001737	0.918	4.371	0.985	0.324
CA-2C	0.998	0.220	0.728	0.001303	0.916	9.674	0.988	0.324
CA-3C	0.997	0.224	0.698	0.001303	0.928	4.583	0.993	0.323
CT-1C	0.998	0.216	0.737	0.001303	0.918	4.393	0.986	0.324
CT-2C	0.998	0.221	0.727	0.001303	0.921	4.495	0.989	0.325
CT-3C	0.997	0.225	0.695	0.001303	0.912	9.863	0.993	0.323
CAT-1C	0.997	0.217	0.712	0.001303	0.913	9.649	0.992	0.322
CAT-2C	0.998	0.220	0.715	0.001303	0.923	4.486	0.991	0.323
CAT-3C	0.997	0.227	0.693	0.001303	0.929	4.637	0.994	0.324
CA-1X	0.997	0.230	0.683	0.001303	0.912	9.962	0.995	0.356
CA-2X	0.997	0.237	0.682	0.001303	0.713	45.17	0.995	0.327
CA-3X	0.995	0.250	0.655	0.001303	0.706	47.01	0.996	0.330
CT-1X	0.997	0.230	0.715	0.006947	0.912	9.971	0.995	0.325
CT-2X	0.997	0.237	0.712	0.006513	0.663	33.01	0.995	0.327
CT-3X	0.995	0.250	0.796	0.006513	0.911	10.43	0.995	0.330
CAT-1X	0.997	0.231	0.678	0.001303	0.935	4.750	0.995	0.325
CAT-2X	0.997	0.238	0.678	0.001303	0.911	10.15	0.995	0.327
CAT-3X	0.995	0.252	0.653	0.001303	0.942	5.207	0.995	0.330
PLAIN	0.997	0.161	0.730	0.001303	0.946	3.324	0.984	0.307